Dynamic Combinatorial Mass Spectrometry for 2-oxoglutarate oxygenase inhibition

A thesis submitted to the Board of the Faculty of Physical Sciences of the University of Oxford in partial fulfilment of the requirements for the degree of Doctor of Philosophy

Marina Demetriades

St. Peter's College

Trinity Term 2013

Abstract

In the last decade, dynamic combinatorial mass spectrometry (DCMS) with protein targets has emerged as a promising method for the identification of enzyme-inhibitors. 2-Oxoglutarate (2OG) oxygenases are involved in important biological processes related to many diseases; several human 2OG oxygenases are targeted for pharmaceutical intervention. This thesis describes inhibition studies on three 2OG oxygenases using DCMS and structure activity relation (SAR) studies.

Disulphide based DCMS was used for the identification of *N*-oxalyl based lead inhibitors for the 2OG oxygenase AlkB from *Escherichia coli.* Crystallographic analyses of AlkB with a lead inhibitor assisted in the design of a second generation of inhibitors using *N*-oxalyl, pyridyl and quinolinyl scaffolds. Crystallographic and kinetic data of three potent and selective AlkB inhibitors validates the DCMS approach for the development of 2OG oxygenase inhibitors.

The hypoxia inducible factor hydroxylase, prolyl hydroxylase domain 2 (PHD2), was then used as the model enzyme for the development of a novel DCMS approach employing the reversible reaction of boronic acids with diols to form boronate esters. The 'boronate' DCMS method was used to identify pyridyl- substituted lead compounds. Further modification of the pyridine scaffold, based on structural analyses, led to the development of highly potent and selective PHD2 inhibitors.

To identify inhibitors for the fat mass and obesity associated protein (FTO), another 2OG oxygenase, an inhibition assay was developed. The inhibition assay was used in conjunction with a differential scanning fluorimetry (DSF) binding assay to identify isoquinolinyl and pyridyl inhibitor scaffolds, related to those used in the DCMS studies. FTO complexed structures of these compounds, and with a natural product anthraquinone, enabled the design and synthesis of new inhibitors that are both co-substrate and substrate competitors of FTO. One such compound proved to be a potent FTO inhibitor with improved selectivity over other 2OG oxygenases.

Overall, the work validates the use of DCMS methods for the development of potent and selective inhibitors for 2OG oxygenases, and by implication of other enzyme families.

Table of contents

Acknowledgements

Firstly, I should like to thank Prof. Chris Schofield for allowing me the freedom to pursue my ideas and the opportunity to get involved in a variety of projects, for extensive proof-reading and for his invaluable advice.

I'd like to thank everyone in the Schofield group for their help and advice over the past few years and for keeping the friendly atmosphere in the group. Many thanks to Dr Sander van Berkel, Dr Martin Münzel, Katherine England, Duncan Hay, Dr Luc Henry, Dr Richard Hopkinson, Cyrille Thinnes and Dr Esther Woon for advice on organic synthesis; Dr James McCullagh, Dr James Wickens and Lingzhi Gong for help with mass spectrometry. I am also indebted to Dr Rashed Chowdhury, Dr Mike McDonough and Wei Shen Aik for their help and advice on protein crystallography and modelling; Dr Ivanhoe Leung and Dr Tim Claridge for NMR especially Ivan for his support and contribution to the boronate DCMS project; Dr Adam Hardy, Dr Rashed Chowdhury, Dr Ruben Castellanos, Ivan and WeiShen for their help and advice regarding enzymology. Many thanks to Wendy Sobey for keeping the lab running smoothly, Dr Adam Hardy for looking after the computers and printers in the lab and all of the CRL support staff. My thanks also go to Andrew Mun Chan, Tzu-Lan Yeh, Antony Tumber, Svetlana Krylova, Dr Eleanor Bagg, Kamilin Hamdan and Caitlin Clunie-O'Connor for fruitful collaborations.

A special thank you to Wei Shen Aik for introducing me to the amazing world of FTO and for providing me with everything needed for the inhibition project. Moreover, I should thank Dr Esther Woon for initiating the DCMS project and for her helpful advice.

A big thanks goes to the people who have proof-read this thesis, Richard, Greg McSweeney, Andrea Szollossi, Katherine, Cyrille, Ivan and Mike. Also many thanks to Rashed and WeiShen for their help in generating crystallography figures.

I should also like to thank Cyrille, Jake, Rob, Martin, Greg, Duncan and Sander for making LG1 the greatest work place ever; also Richard, Ivan, Andrea, Ruben, Greg and Cyrille for being precious friends during my time in the lab. Outside the lab, I'd like to thank all of my friends for the enjoyable escapes from science; more specifically Vasileia, Kimon, Angelos and Giannis for giving me a taste of home and for the regular board game sessions.

I am eternally grateful to the Bodossaki foundation and St. Peter's College for giving me the opportunity to pursue my degree in Oxford; especially Bodossaki for funding. Last but not

least, I would like to express my gratitude to my family for their unconditional support and love. Also thanks to my father for being a source of inspiration!

Abbreviations

2OG	2-oxoglutarate
1MeA	1-methyladenine
3MeC	3-methylcytocine
3MeT	3-methylthymidine
6MeA	6-methyladenine
AlkB	alkylation repair enzyme B
AlkBH	human alkylation repair enzyme
BBOX	γ-butyrobetaine hydroxylase
BEH	ethylene bridged hybrid
Bn	benzyl
CA	carbonic anhydrase
CAD	*C*- terminal transactivation domain
CODD	*C*- terminal oxygen-dependent degradation domain
CE	capillary electrophoresis
CV	column volume
CC	combinatorial chemistry
Da	Dalton
DCC	dynamic combinatorial chemistry
DCL	dynamic combinatorial library
DCMS	dynamic combinatorial mass spectrometry
DMF	dimethylformamide
DNA	deoxyribonucleic acid
dppf	1,1'-bis(diphenylphosphino)ferrocene.
DIPEA	diisopropylethylamine
DMSO	dimethylsulfoxide
DMSO-d_6	deuterated dimethylsulfoxide
DSF	differential scanning fluorimetry
E. coli	*Escherichia coli*
EDCI	1-ethyl-3-(3-dimethylaminopropyl) carbodiimide
EDTA	ethylenediaminetetraacetic acid

EPO	erythropoietin
ESI-MS	electrospray ionization mass spectrometry
Et	ethyl
EtOAc	ethyl acetate
FAD	flavin adenine dinucleotide
FDH	formaldehyde dehydrogenase
FI	field ionisation
FIH	factor inhibiting hypoxia inducible factor
FPLC	fast protein liquid chromatography
FTO	fat mass and obesity protein;
HATU	1-[Bis(dimethylamino)methylene]-1H-1,2,3-triazolo[4,5-b]pyridinium 3-oxid hexafluorophosphate
HIF	hypoxia inducible factor
HOBT	Hydroxybenzotriazole
HPLC	high performance liquid chromatography
HRE	hypoxia response elements
HRMS	high resolution mass spectrometry
IR	infrared
K_D	binding constant
KDM	histone demethylase
KOAc	potassium acetate
LC	liquid chromatography
LCMS	liquid chromatography mass spectrometry
LSDs	lysine specific demethylases
MALDI	matrix assisted laser desorption ionisation mass spectrometry
Me	methyl
MES	2-(*N*-Morpholino)ethanesulfonic acid
mp	melting point
MS	mass spectrometry
mw	microwave irradiation
NAOXs	nucleic acid oxygenases
NBS	*N*-bromosuccinimide
NMR	nuclear magnetic resonance
NODD	*N*-terminal oxygen-dependent degradation domain

NOG	*N*-oxalylglycine
PDB	protein databank
PEG	polyethylene glycol
PHF8	plant homeodomain finger protein 8
PHD2	prolyl hydroxylase domain 2
$(PinB)_2$	bispinacolatodiboron,
PTM	post-transcriptional modification
PyBOP	benzotriazol-1-yl-oxytripyrrolidinophosphonium hexafluorophosphate
Q-TOF	quadrupole-time of flight
RNA	ribonucleic acid
SAR	structure-activity relation
r.t	room temperature
T3P	propylphosphonic anhydride
TET	Ten-Eleven-Translocation
THF	tetrahydrofuran
TMSCl	trimethylsilylchloride
TLC	thin layer chromatography
T_m	melting temperature
TOF	time of flight
Tris	tris(hydroxymethyl)aminomethane
Ts	tosyl
VEGF	vascular endothelial growth factor
UV	ultraviolet
V_{max}	maximal speed

Chapter 1. Introduction

1.1 Fe(II) and 2-oxoglutarate dependent dioxygenases

Fe(II) and 2-oxoglutarate dependent dioxygenases (2OG oxygenases) are non-haem enzymes which depend on 2-oxoglutarate (2OG) and iron for their catalytic activity (Figure 1. 1).[1-4] 2OG oxygenase family enzymes are present in plants, microorganisms and animals where they catalyse a wide variety of biologically important reactions. In humans about 60 members of the family are predicted by genomic studies; however, there is limited information regarding the function(s) of some 2OG oxygenases.[5, 6] In humans, 2OG oxygenases catalyse hydroxylation and hydroxylation mediated demethylation of a number of diverse substrates. Through this catalytic mechanism they are involved in important biological processes including oxygen sensing, modification of nucleic acid alkylation repair and epigenetic modifications (Figure 1. 2).[7, 8]

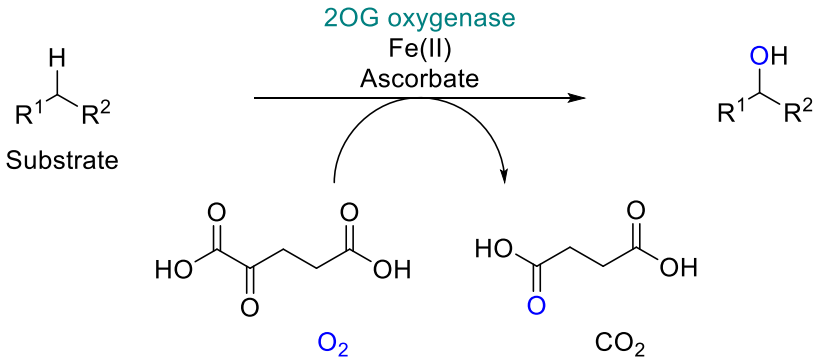

Figure 1. 1 *General reaction catalysed by 2OG oxygenases.*

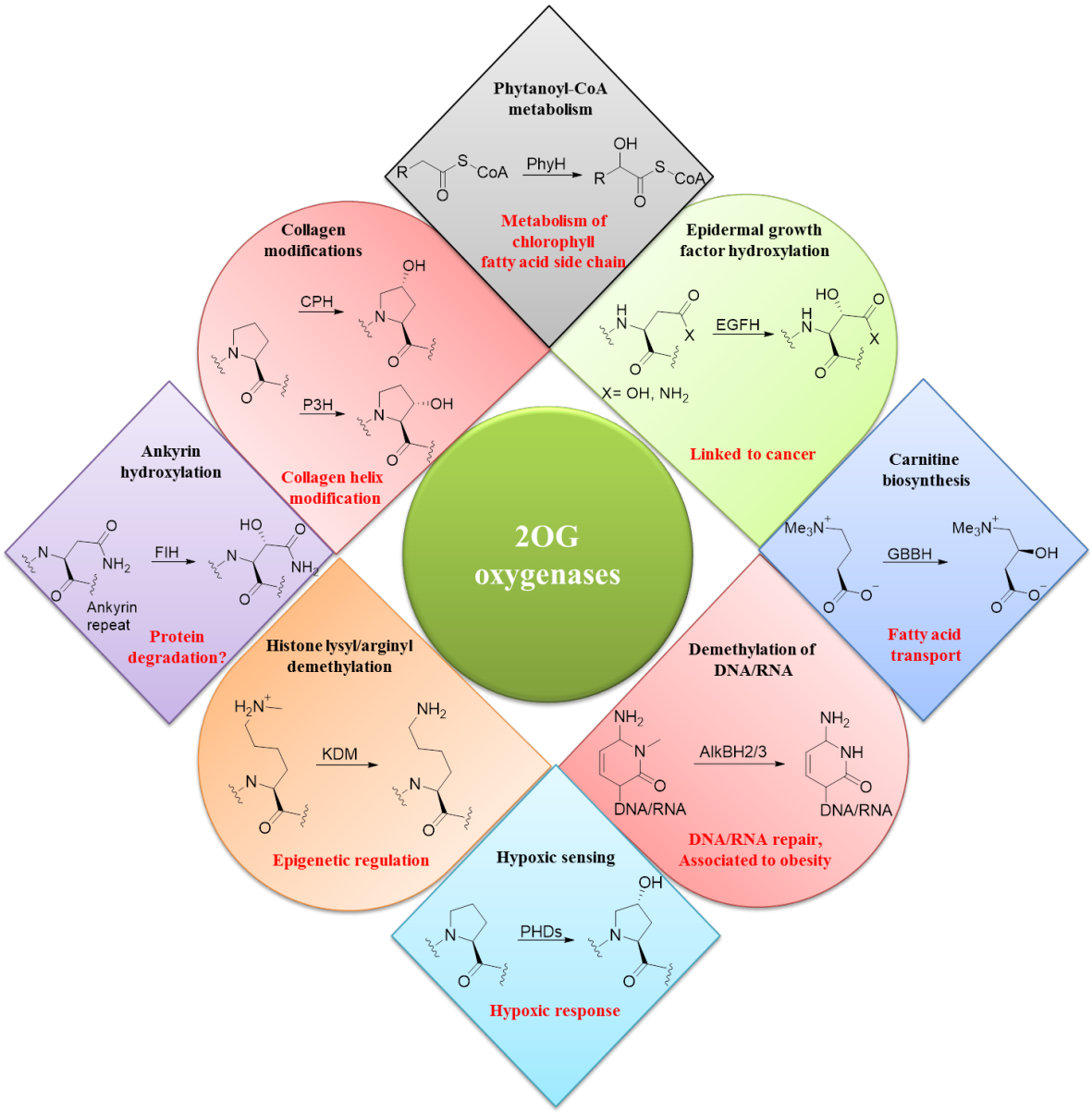

Figure 1. 2 *Outline summary of reactions catalysed by human 2OG oxygenases. Assigned or potential roles of these reactions are in red.*

1.1.1 Mechanism of 2OG oxygenases

Work to date indicates that most, if not all, 2OG oxygenases share a substantially common catalytic mechanism. This has been extensively studied using crystallographic and spectroscopic analyses.[3, 9-11] Fe(II) is normally chelated in the active site of 2OG oxygenases through interactions with three residues, usually two histidines and one aspartic or glutamic

acid (Figure 1. 3 A).[2, 12, 13] The other three ligand binding sites around the iron (which is bound in an octahedral coordination) are filled by 2-3 water molecules when the enzyme is in the 'resting state', Figure 1. 4).

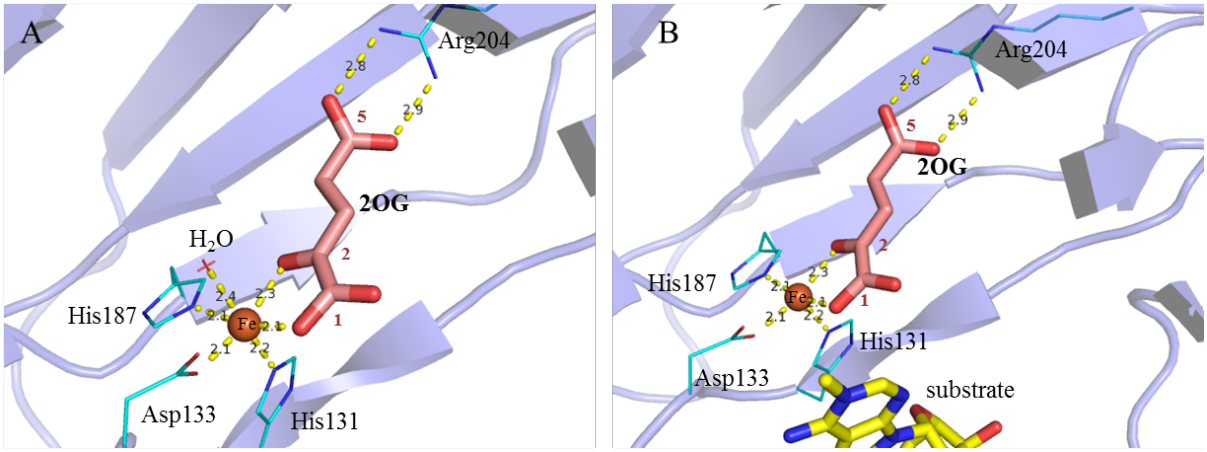

Figure 1. 3 *View from the crystal structure of a representative 2OG oxygenase (E. coli AlkB) with Fe(III) and A) 2OG, B) 2OG and substrate (3-methylthymidine) complexes (PDB ID: 3I2O, 1.7 A resolution).*[14] *The figure was generated using Pymol.*

Once bound, 2OG chelates the iron *via* the oxalyl group with the C-2 carbonyl positioned *trans* to the aspartyl/glutamyl residue (Figure 1. 3 B). The C-1 carboxylate chelation position varies within members of the family; it is usually positioned to enable the C-5 carboxylate to adopt electrostatic interactions with basic residues in the active site (Figure 1. 3 B).[1] Binding of the 'prime' substrate in the active site displaces, or weakens binding of, the remaining iron-bound water molecule, allowing dioxygen to bind at the position vacated by the water (**1**, Figure 1. 4).[3, 11, 15] A key step in the catalytic cycle is the oxidative reaction of 2OG and dioxygen at the iron centre, which results in the formation of a reactive Fe(IV)-oxo intermediate, with concomitant decarboxylation of 2OG to form succinate and CO_2. It is believed that the dioxygen forms a peroxide containing six membered ring with 2OG and iron (**2**, Figure 1. 4), which then reacts to form succinate, CO_2 and the Fe(IV)=O (ferryl) species (**3**, Figure 1. 4). The ferryl group is sufficiently reactive to abstract a hydrogen from the prime substrate to generate Fe(III)-OH and $R^1R^2CH\cdot$ (**4**, Figure 1. 4). These two species then react together to form the hydroxylated product and regenerating Fe(II).[16-20] The

hydroxylated substrate and succinate can leave the active site, either returning the enzyme to the 'resting state' (*via* water binding) or allowing another molecule of 2OG to bind the iron, thus beginning a new catalytic cycle.[21] It should be noted that even though this catalytic cycle is conserved, variations in the rate determining step,[22] formation of intermediates or product release[23] have been observed for different members of the 2OG oxygenase family.

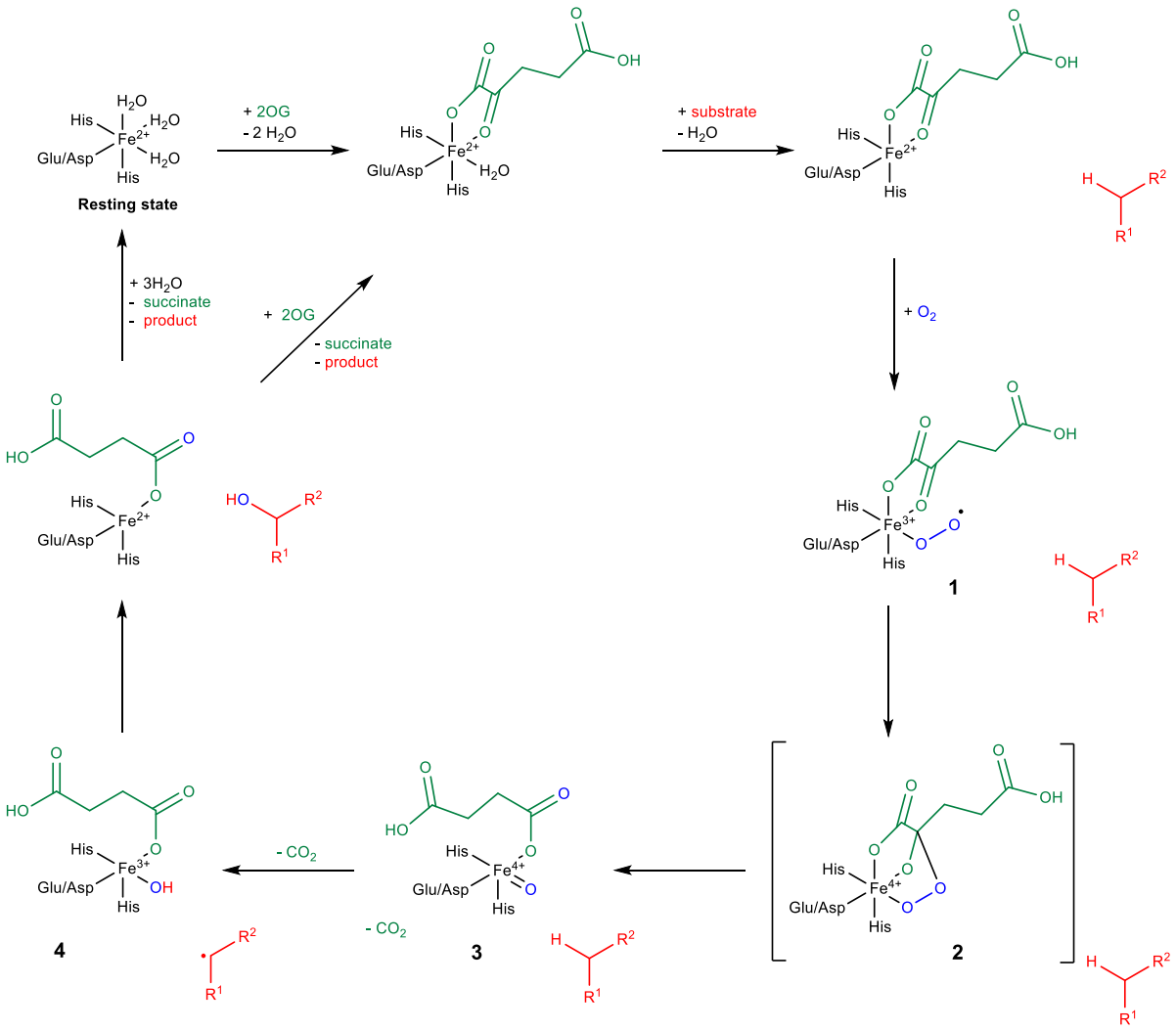

Figure 1. 4 *Consensus mechanism for 2OG oxygenase catalysed oxidation.*

1.2 Biological roles of 2OG oxygenases

1.2.1 Oxygen sensing

2OG oxygenases have been shown to play roles in oxygen sensing and hypoxia adaptation mechanisms in animals. In humans, four 2OG oxygenases (PHD1-3, FIH) are involved in regulation of the hypoxia inducible factor (HIF) in an oxygen dependent way. HIF is a heterodimeric transcription factor that activates the transcription of genes that are associated to the hypoxia response elements (HRE), including vascular endothelial growth factor (VEGF), erythropoietin (EPO) and glycolytic enzymes (Figure 1. 5).[24-26] Both subunits of heterodimeric HIF (α, β) belong to the basic helix-loop-helix (bHLH) PAS protein family and are constantly produced in cells (Figure 1. 5). Human HIFα exists in three isoforms HIF1α, HIF2α and HIF3α;[27, 28] while HIF1α is produced in most tissues, HIF2α and HIF3α have more restricted expression patterns.[29-34] In hypoxic conditions ($[O_2] < 1$ %) the PHD and FIH activity is reduced, stabilising HIF1α/2α which is transported to the nucleus where it dimerises with HIFβ and binds the transcription cofactor p300/CBP (Figure 1. 5). It has been demonstrated that stabilisation of HIF1α and HIF2α protects against acute cardiac ischemia[35-37] and results in cardioprotection.[38] Moreover, upregulation of HIFα can be used in the treatment of anaemia.[39, 40]

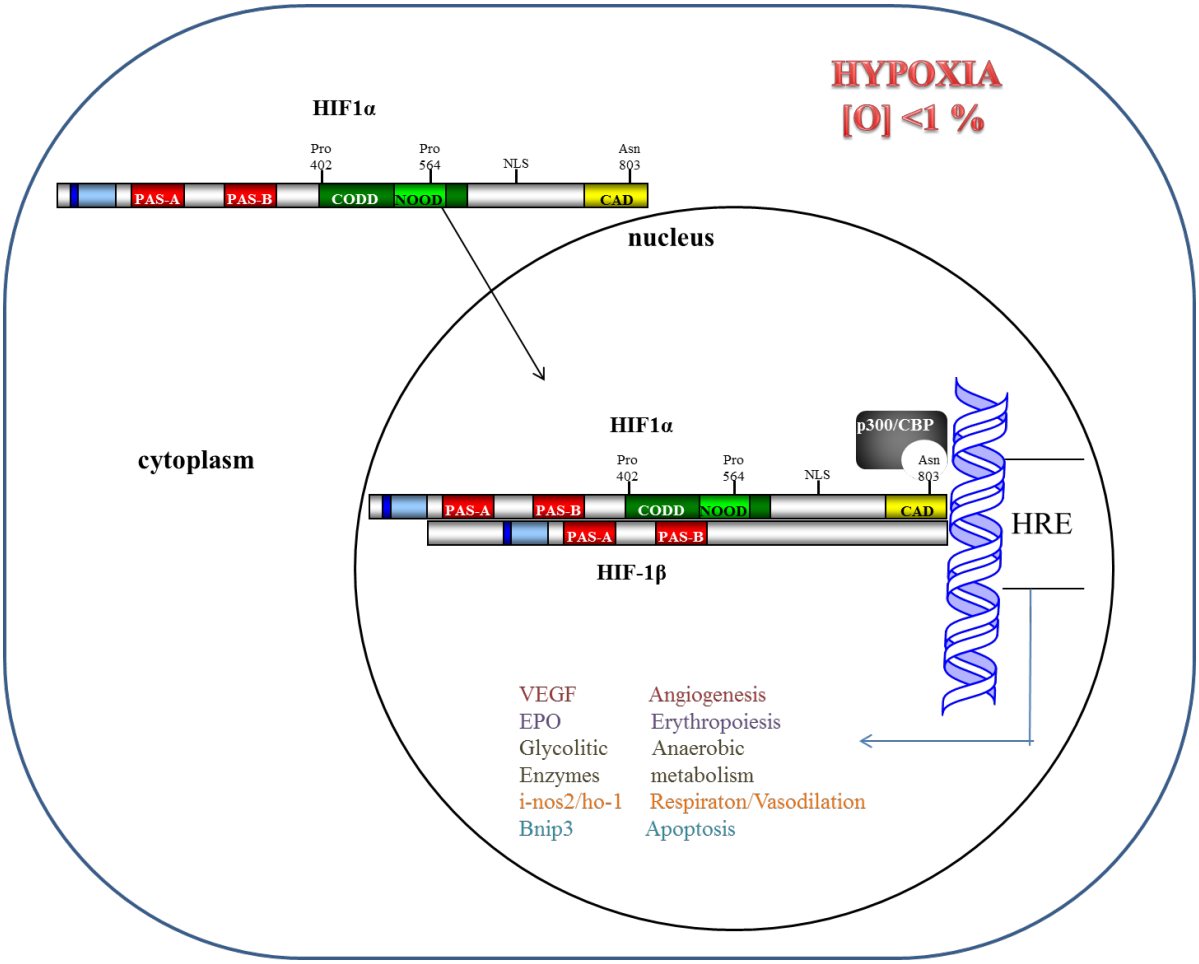

Figure 1. 5 *Increased transcription of genes with hypoxia response elements is mediated by HIF under hypoxic controls.*

Under normal physiological oxygen levels (normoxia), HIFα, which is present in the cytoplasm, undergoes proline hydroxylation by the Fe(II) and 2OG dependent HIF prolyl hydroxylases (PHD1-3) at the *N*- and *C*- terminal oxygen-dependent degradation domains (NODD and CODD, Figure 1. 6) in an oxygen dependent manner.[41] In an apparently complimentary mechanism, another 2OG oxygenase, factor inhibiting HIF (FIH), catalyses hydroxylation of an asparagyl residue in the *C*- terminal transactivation domain (CAD) of HIFα (Figure 1. 6).[1, 5] Hydroxylation at this position blocks binding of the transcriptional activator p300/CBP to the HIFα/β heterodimer, negating transcriptional activation of HIF target genes (Figure 1. 6). FIH catalysis is dependent on oxygen, enabling oxygen dependent regulation of p300/CBP binding.[42-45] However, FIH appears to be less sensitive to oxygen

levels than the PHD's, suggesting that the two regulatory mechanisms respond differently to oxygen stress.[46]

Proline-residue hydroxylation, which is catalysed by PHD1-3 leads to increased binding of HIFα isoforms to the von Hippel-Lindau complex, resulting in ubiquitination and degradation of HIFα *via* the proteasome pathway (Figure 1. 6). PHD1-3 share homology in the *C*-terminal catalytic domains, but differ in their *N*-terminal sequences[47] and functionally in terms of their expression, cellular localisation, tissue distribution, and catalytic activity.[48-50] Several lines of evidence have shown that PHD2, out of the three human isoforms (PHD1-3), is the most important in humans.[48, 51] siRNA studies indicate that decreased levels of PHD2 are sufficient for HIF1α upregulation (at least in some contexts),[52] whereas low expression of PHD1 and PHD3 results in upregulation of HIF2α.[53] Another siRNA study has also shown that PHD2 suppression is enough for HRE transcription even when FIH is still active.[52] Other studies imply that PHD2 has a more important role in normoxia and modest hypoxia, whereas FIH is a more important regulator of HIFα in severe hypoxia.[54] Overall, PHD2 is considered the key regulator of HIF1α levels under most conditions.[47, 52, 55] There are likely many more regulatory mechanisms that control HIF function. However, its hydroxylation by the PHDs, and especially PHD2 in the case of HIF1α, appears to be a fundamental regulatory mechanism. As a consequence, PHD2 has been targeted for pharmaceutical intervention.

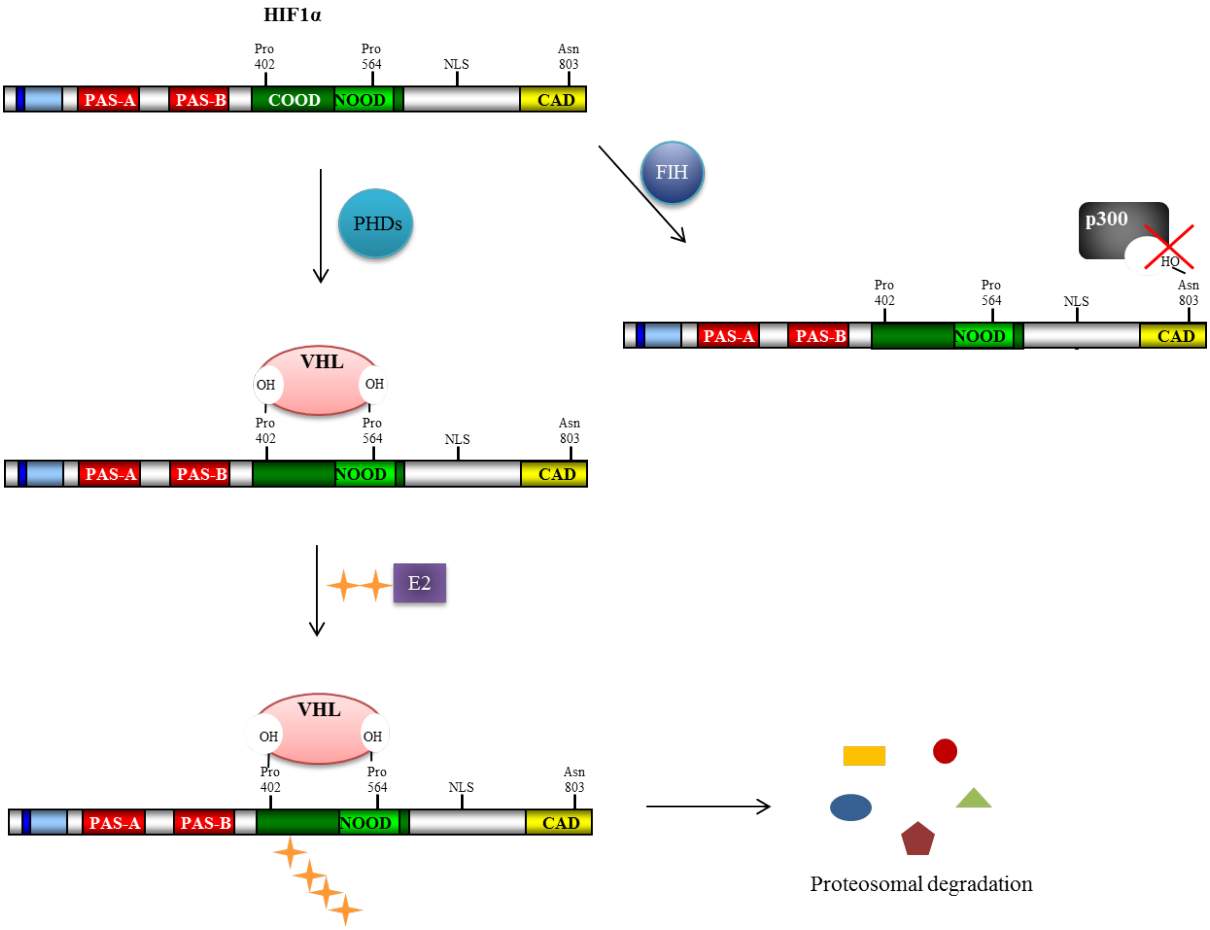

Figure 1. 6 *Oxygen dependent regulation of HIF1α by FIH and the PHDs.*

1.2.2 DNA/RNA modification

Modifications of nucleic acid bases can cause cytotoxic/mutagenic DNA damage which has been associated with cancer, neurological disease and developmental defects.[56, 57] Post-transcriptional modifications (PTMs) to RNA (mRNA, tRNA etc.) are also critical for proper RNA folding, stability, and function.[58] These RNA and DNA modifications include alkylation of the sugar or the base of the nucleoside by an alkylating agent and more complex modifications occurring after multiple enzymatic steps.[59-61] Base methylation is the most common modification observed.[59, 60] The repair mechanisms include excision of methylated DNA bases from glycosylases and transfer of alkyl groups from other lesions onto a cysteine residue by DNA methyltransferases in order to repair alkylated DNA.[62-64] A third repair mechanism identified is the oxidative demethylation of bases by nucleic acid oxygenases

(NAOXs), that are members of the 2OG oxygenase superfamily.[65] The *E. coli* demethylase AlkB,[57] the human AlkB homologues (AlkBH 1-8), the fat mass and obesity protein (FTO) and the ten-eleven translocation enzymes (TETs1-3) are members of this family.[66-68] NAOXs initially hydroxylate nucleic acid bases. In the case of *N*-methylated bases, hydroxylation forms unstable hemiaminals which degrade to the demethylated base and formaldehyde (Figure 1. 7).

AlkB demethylates 1-methyladenine and 3-methylcytosine in single stranded DNA and RNA (ssDNA and ssRNA). AlkBH3 has been found to catalyse demethylation on a similar set of substrates as AlkB in humans. Another human analogue of AlkB, AlkBH2 demethylates 1-methyladenine and 3-methylcytosine nucleosides on double stranded DNA (dsDNA) but apparently has no activity on RNA.[69] Another member of AlkBH family, AlkBH8 has no demethylase activity; it instead hydroxylates 5-methoxycarbonylmethyluridine on tRNA to form 5-methoxycarbonylhydroxymethyl uridine.[66] The differentiated function of AlkBH8 compared to AlkBH2-3 implies that other members of the AlkBHs may have diverse roles.[61] FTO catalyses demethylation of 3-methylthymidine in ssDNA and 3-methyluracil and 6-methyladenine in ssRNA (Chapter 3). Recently the TET enzymes have been reported to catalyse hydroxylation of 5-methylcytosine to give 5-hydroxymethylcytosine[70] and 5-carbonylcytosine analogues (Figure 1. 7).[71]

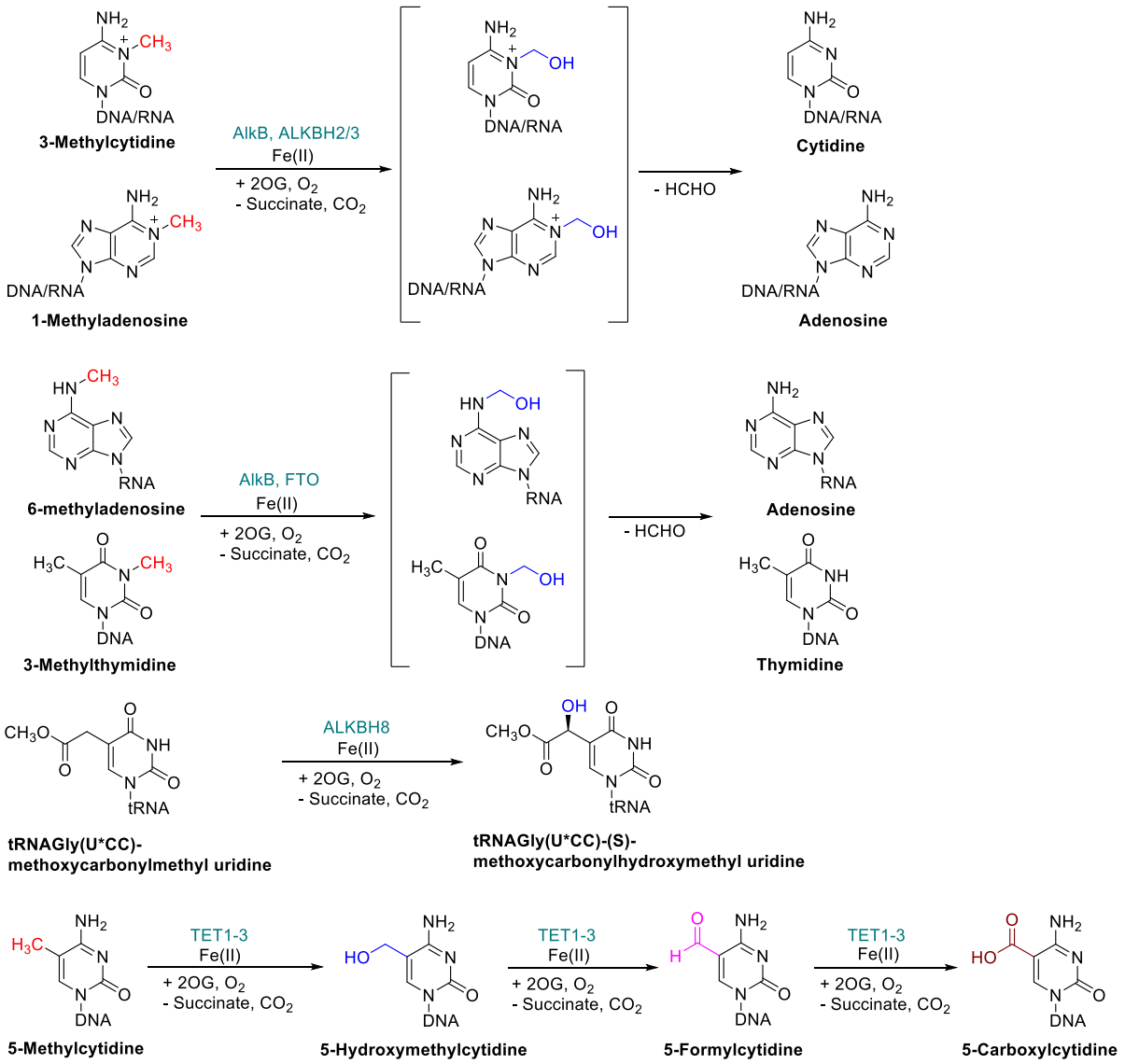

Figure 1. *7 Exemplary modifications of nucleic acid bases by NAOXs and outline demethylation mechanisms.*

1.2.3 Epigenetic regulation

The field of epigenetics can be defined as 'the study of heritable phenotypes resulting from changes in a chromosome without alterations in the 'ATGC' DNA sequence'.[72, 73] DNA (~160 base pairs) is wrapped around 8 histones to form nucleosomes.[74] The modifications of amino acid residues on histone proteins are in part involved in epigenetic regulation of gene expression, and are currently of considerable interest. The *N*-terminal regions on histones have multiple basic and nucleophilic residues such as lysines and arginines that undergo

PTMs.[75-77] Methylation, which can occur on both lysines and arginines, has been identified on multiple sites on histones and is linked transcriptional activation and repression as well as the DNA damage response.[72, 78] The first class of histone demethylase (KDM) was discovered in 2004 followed by the identification of several KDMs.[79] This class, the lysine specific demethylases (LSDs), employ a flavin cofactor and catalyse removal of the methyl group *via* concomitant reduction of flavin adenine dinucleotide (FAD, Figure 1. 8).[80] The precise mechanism for this redox reaction is unclear, although it is likely to involve a hydride transfer process from the methyl group onto FAD (Figure 1. 8). The larger class of KDMs, the JmjC demethylases, are 2OG oxygenases; demethylation by these enzymes proceeds *via* an analogous mechanism to NAOX catalysis (Figure 1. 8). About 15 human 2OG dependent demethylases have been identified to date; they catalyse demethylation of different modification sites and can also accept mono-, di-, and trimethylated lysines as substrates (Table 1. 1).

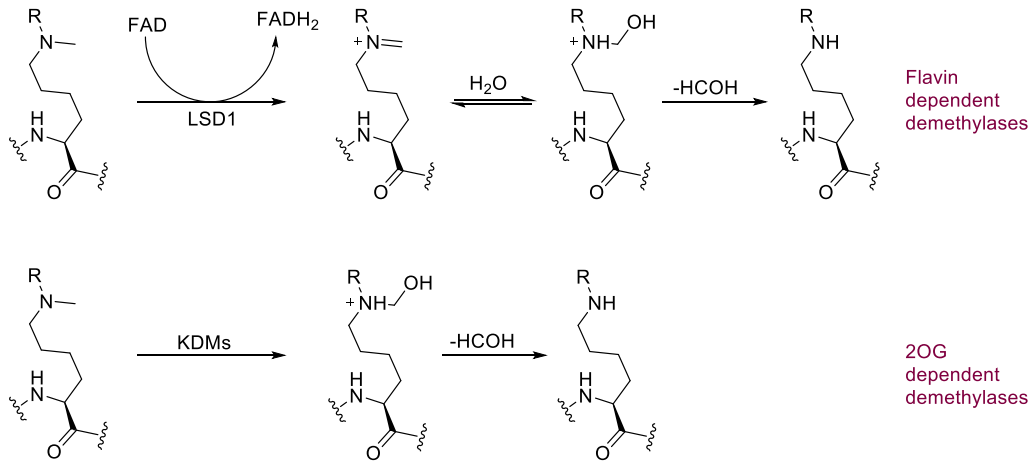

Figure 1. 8 *Lysine demethylation by LSD (top) and JmjC (bottom) demethylases.*

Table 1. 1 *JmjC demethylases and some of their substrates.*

Lysine demethylases (KDMs)	Substrate
FBXL10/FBXL11	H3K36Me_2/Me
JMJD1A/JMJD1B	H3K9Me_2/Me
JMJD2A/JMJD2B/JMJD2C	H3K9Me_3/Me_2, H3K36Me_3/Me_2
JMJD2D/JMJD2E	H3K9Me_3/Me_2
JARID1A/JARID1B/JARID1C/JARID1D	H3K4Me_3/Me_2
JMJD3/UTX	H3K27Me_3/Me_2

1.3 Non Denaturing Electrospray Ionisation Mass Spectrometry

Electrospray Ionisation Mass Spectrometry (ESI-MS) is a well-established mild ionisation technique wherein sample protonation occurs at atmospheric pressure.[81] Samples flow through a capillary with an electrostatic charge at the tip, which enables charge separation in solution since molecules with the opposite charge to the capillary are withheld in the capillary while molecules with the same charge as the capillary are slowly released in the form of droplets (Figure 1. 9 A). These droplets, after traveling through a gradient of pressure and potential under desolvation gas (N_2), decrease in size until the electrostatic repulsion within the droplets results in a coulombic explosion, during which formation of smaller droplets of multiple (different) charges occurs (Figure 1. 9 A). A big advantage of this technique is that the use of acidic solutions is often not necessary for the protonation of the sample because of the charge applied on the capillary.[82, 83] The ability to generate protonated species under physiological pH makes ESI-MS applicable to biomolecules and especially proteins. Usually protein mass spectrometry occurs in 1:1 water/organic solvent (MeOH, CH_3CN) solution in the presence of 0.1-0.2% formic acid (to provide the required protonation for mass spectrometry) which results in partial and some cases complete denaturation of the protein. ESI-MS samples can be prepared in buffers; most buffers however (as salts) interfere with the

ionisation of the sample and broaden the MS peaks, and are therefore not compatible with mass spectrometry.

Ammonium acetate and ammonium bicarbonate are volatile buffers that can often be used in ESI-MS without interfering with the ionisation/desolvation procedure. These buffers are not very commonly used in chemical biology; protein samples thus have to be desalted and buffer exchanged into a volatile buffer prior to MS experiments.

The development of nanospray ESI sources has further advanced non denaturing ESI-MS further. In the nanospray technique, the rate of sample flow is decreased thus forming smaller droplets from the capillary, reducing sample consumption (Figure 1. 9 B). Sample signal is also improved even in the presence of small amounts of non-volatile cations such as salts.[84] Protonation of samples can take place in ESI-MS without extensive unfolding of the protein. The mass of the protein, as well as the mass of bound species, can be calculated using appropriate software from the pattern of charged states observed. Since proteins under these conditions maintain most of their tertiary structure, the observation of non-covalent interactions of a protein with small molecules, metals, peptides and other proteins is possible, as observed by mass difference.[85-89] Optimisation of the sample desolvation process may be required in order for these interactions to survive.[90, 91]

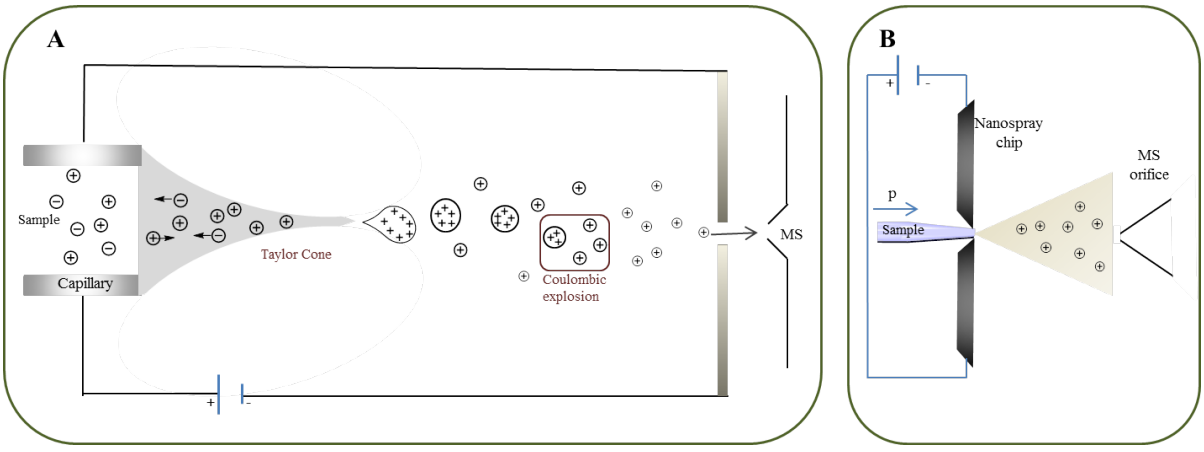

Figure 1. 9 *Schematic representation of A) electrospray ionisation (ESI) source and B) chip based nanospray ESI source.*

1.4 Dynamic Combinatorial Chemistry

1.4.1 History and principles of dynamic combinatorial chemistry

Combinatorial Chemistry (CC) was first used in 1988 for the parallel one pot syntheses of multiple compounds.[92, 93] The libraries formed were then tested against biological targets to provide quick screening of inhibitors. The method immediately attracted the attention of the pharmaceutical industry for its ability to decrease compound preparation time.

A new form of CC, dynamic combinatorial chemistry (DCC) was subsequently introduced. In DCC, the reacting compounds in a single vessel contain functional groups that take part in reversible reactions and are in dynamic equilibrium. These dynamic systems are substantially under thermodynamic control; by changing conditions the composition of the products in the library changes with the more energetically favourable products being stabilized and amplified.[94-97] Therefore, the content of the equilibrating systems is liable to external influences such as pressure, temperature, light, pH and the presence of templates.[94, 97, 98] The presence of a template, such as a metal[99] and a biomolecule[100] (such as a protein target) can bias equilibrium by stabilising dynamic species that bind the template (Figure 1. 10). DCC, in principle can be utilised to identify template binders from complex mixtures of building blocks.[101, 102] To be considered appropriate for DCC, reactions must be reversible on a reasonable time scale for assays (typically minutes to a day). Further, under the conditions used (such as solvent, pH, temperature), library members and products should be soluble and of similar energy for the reaction equilibrium not to be too biased before the addition of template.[101] When using a biomolecule target the conditions need to be compatible with the template. Over the years, several reactions that meet these conditions have been found.

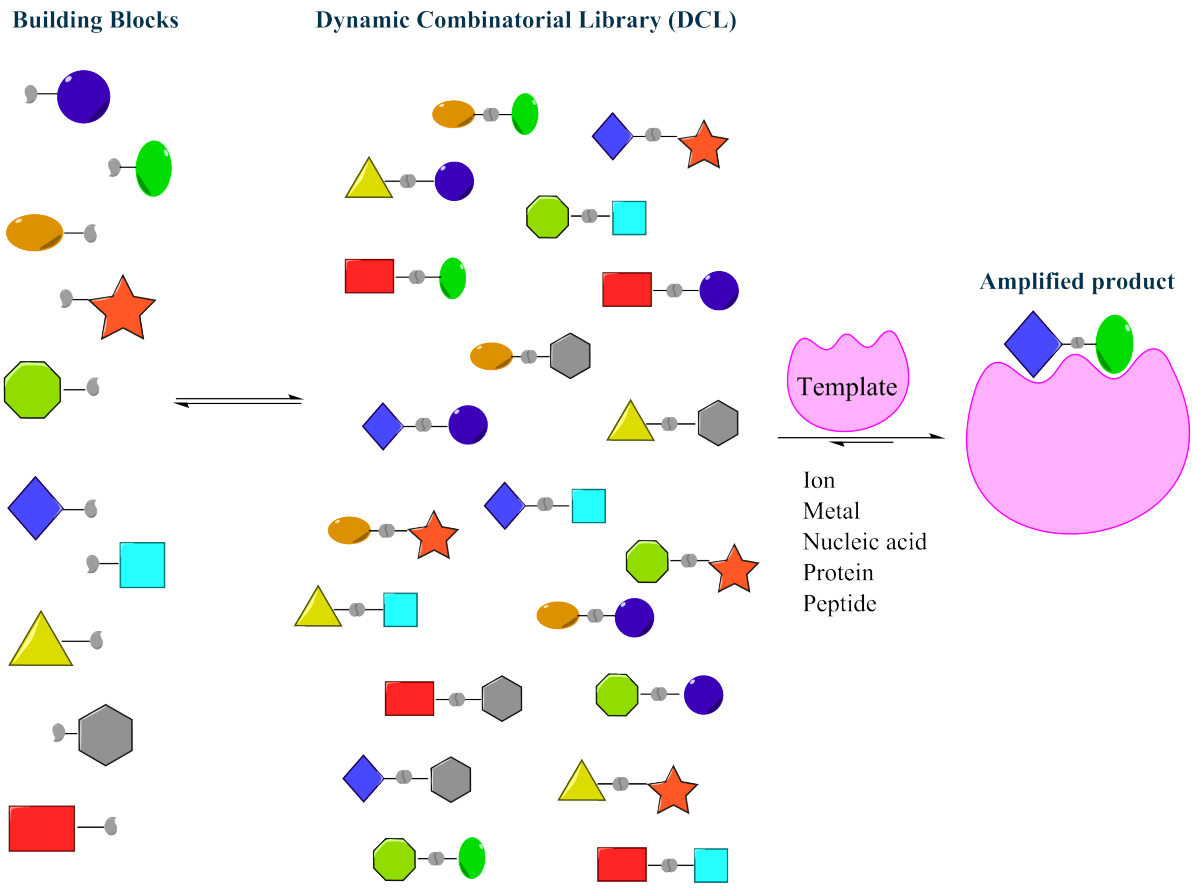

Figure 1. 10 *Principle of the dynamic combinatorial chemistry.*

1.4.2 Reversible reactions used in dynamic combinatorial chemistry

Amide exchange[103, 104] was one of the first reactions to be applied in DCC experiments (Figure 1. 11). The presence of amide bonds in peptides led to the use of small peptide libraries in DCC.[103] For the use of these mixtures, however, proteolytic enzymes had to be used to cleave the amide bonds to form the reacting oligopeptides, which often led to the formation of biased libraries.[105, 106]

Thioester exchange has been recently used in DCC.[107] The reaction between thiols and thioesters can take place in water and does not require an activation step to initiate and propagate the reaction.[101] Thus, thioester exchange is a DCC reaction amenable for studies using biomolecules.[108] Hydrazone exchange is another reaction widely used in DCC; it has been successfully used with ions,[109] nucleic acids,[110] peptides[111] and proteins as

templates.[108, 112] The relative stability of product hydrazones derived from electron rich carbonyls precludes their use in DCC however; libraries can only be derived, in most cases, using electron poor carbonyls such as acylated derivatives.

Imine exchange is also often used in DCC (Figure 1. 11).[100, 113] The imine bond is formed by reaction of carbonyl containing compounds with amines. The reactions of amines with aldehydes has been widely used.[114] The stability of the products is dependent on the substitution pattern and stereoelectronic effects; for this reason only amines of similar reactivity should be used to ensure formation of non-biased libraries.[115, 116] The analytical detection of imines is complicated by hydrolysis, which can occur under the acidic conditions of high performance liquid chromatography (HPLC) used for library analysis.[101] To overcome this problem, imines can be reduced to form stable amines under the incubation of the dynamic combinatorial library (DCL) with the template.

Disulphide exchange reactions may take place in aqueous solution at physiological pH. As a consequence disulphide exchange has found application in DCC with many biological templates,[117-119] including metallo-enzymes.[120, 121] Other DCC systems have been reported, but their use is uncommon, either because the reactions need catalysts to ensure reversibility or are temperature and/or, organic solvent dependent.[101, 122]

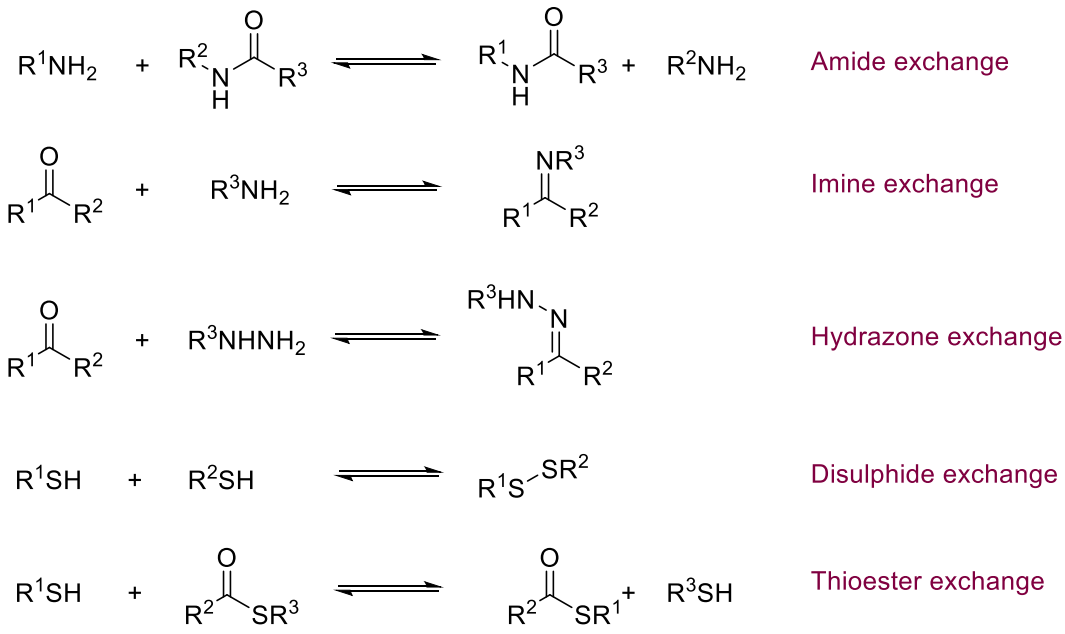

Figure 1. 11 *Examples of reversible reactions used in DCC studies.*

1.4.3 Protein directed dynamic combinatorial chemistry

1.4.3.1 Reversible reactions

The use of DCC with protein templates is highly attractive because the method potentially allows for fast and efficient identification of protein binders/inhibitors that may help to enable medicinal chemistry efforts.[117, 123-125] The sensitivity of proteins to pH, temperature and organic reagents/solvents, however, restricts the chemical reactions that may be used in protein directed DCC.[122] As described in the previous section, many of the reactions used in DCC take place in organic solvents or need an organic or biological catalyst.

One of first applications of DCC with proteins involved the use of imine formation for the identification of binders of carbonic anhydrase (CA).[126] The aldehyde/amine reaction was pre-equilibrated in the absence of enzyme to give a dynamic combinatorial library (DCL). The DCL was then incubated with CA for two weeks in order for dynamic equilibrium to be reached and the amplified ligands to be detected.[126] This reaction has since been used with other protein targets such as neuraminidase and galactosyl-transferases.[100, 126-131] An acyl hydrazone library was also developed to identify inhibitors of acetyl choline esterase; this reaction later found use with CA and concanavalin A (ConA) proteins.[108, 112, 132-134] The reaction of acyl hydrazones occurs at acidic pH and is therefore not applicable for use with enzymes. The libraries are usually pre-equilibrated at acidic pH and after equilibrium they are incubated with the protein target under physiological conditions.[122, 132] The formation of disulphides by thiols was initially used in protein directed DCC for the identification of ligands for Con A.[118, 119] The thiol/disulphide DCC has been applied for the identification of ligands and 'hit' structures for inhibitor development of other enzymes such as aurora A kinase, metallo-β-lactamases and CA.[120, 121, 135]

1.4.3.2 Analytical techniques

The analytical method used is vital to the success of DCC. Multiple analytical techniques have been used to detect amplified products from protein directed DCC. The most widely used technique is HPLC coupled with mass[136] or UV detection.[126, 137] This method is based on the analysis of the compound library set before and after incubation with the template; therefore it is independent from the protein target used. Both disulphide[136, 138] and imine[130, 139] containing DCLs have been screened with HPLC in experiments involving different templates. Another analytical technique for library analysis in DCC is NMR.[140] More recently, methods that directly investigate protein-ligand complexes have been developed. X-ray crystallography[141] has provided significant structural information; however it typically requires large amounts of enzyme and is applicable only for studies with readily crystallisable enzymes.[122]

Non-denaturing mass spectrometry of the template ligand complexes was introduced for DCC analyses in order to overcome the high sample consumption and the laborious and expensive analyses/processing required by the aforementioned techniques. Fourier transform mass spectrometry (ESI-FTMS) and quadrupole-time of flight mass spectrometry (QTOF/ESI-MS) have been used for hydrazine/hydrazone and thiol/disulphide reactions respectively against different protein targets [120, 121, 133, 134, 142, 143] The application of ESI-MS is further discussed in Chapter 2.

1.5 Aims of work detailed in this thesis

The overall aims of the studies outlined in this thesis were to:

- Explore the use of non-denaturing ESI-MS in DCC and binding studies to identify inhibitors of the 2OG oxygenases AlkB and PHD2.
- Develop and utilisation of new assay methods, crystallographic studies, and inhibitor design for the development of FTO inhibitors.

1.6 References

1. Clifton, I.J., McDonough, M.A., Ehrismann, D., Kershaw, N.J., Granatino, N., and Schofield, C.J., Structural studies on 2-oxoglutarate oxygenases and related double-stranded beta-helix fold proteins. *J Inorg Biochem*, **2006**, 100, 644-69.

2. Costas, M., Mehn, M.P., Jensen, M.P., and Que, L., Dioxygen activation at mononuclear nonheme iron active sites: Enzymes, models, and intermediates. *Chem Rev*, **2004**, 104, 939-86.

3. Hausinger, R.P., Fe(II)/alpha-ketoglutarate-dependent hydroxylases and related enzymes. *Crit Rev Biochem Mol*, **2004**, 39, 21-68.

4. Schofield, C.J. and Zhang, Z.H., Structural and mechanistic studies on 2-oxoglutarate-dependent oxygenases and related enzymes. *Curr Opin Struc Biol*, **1999**, 9, 722-31.

5. Loenarz, C. and Schofield, C.J., Expanding chemical biology of 2-oxoglutarate oxygenases. *Nat Chem Biol*, **2008**, 4, 152-6.

6. Rose, N.R., McDonough, M.A., King, O.N.F., Kawamura, A., and Schofield, C.J., Inhibition of 2-oxoglutarate dependent oxygenases. *Chem Soc Rev*, **2011**, 40, 4364-97.

7. Prescott, A.G. and Lloyd, M.D., The iron(II) and 2-oxoacid-dependent dioxygenases and their role in metabolism. *Nat Prod Rep*, **2000**, 17, 367-83.

8. Ryle, M.J. and Hausinger, R.P., Non-heme iron oxygenases. *Curr Opin Chem Biol*, **2002**, 6, 193-201.

9. Pavel, E.G., Zhou, J., Busby, R.W., Gunsior, M., Townsend, C.A., and Solomon, E.I., Circular dichroism and magnetic circular dichroism spectroscopic studies of the non-heme ferrous active site in clavaminate synthase and its interaction with alpha-ketoglutarate cosubstrate. *J Am Chem Soc*, **1998**, 120, 743-53.

10. Price, J.C., Barr, E.W., Tirupati, B., Bollinger, J.M., and Krebs, C., The first direct characterization of a high-valent iron intermediate in the reaction of an alpha-ketoglutarate-dependent dioxygenase: A high-spin Fe(IV) complex in taurine/alpha-ketoglutarate dioxygenase (TauD) from Escherichia coli. *Biochemistry-Us*, **2003**, 42, 7497-508.

11. Zhou, J., Kelly, W.L., Bachmann, B.O., Gunsior, M., Townsend, C.A., and Solomon, E.I., Spectroscopic studies of substrate interactions with clavaminate synthase 2, a multifunctional alpha-KG-dependent non-heme iron enzyme: Correlation with mechanisms and reactivities. *J Am Chem Soc*, **2001**, 123, 7388-98.

12. Roach, P.L., Clifton, I.J., Fulop, V., Harlos, K., Barton, G.J., Hajdu, J., Andersson, I., Schofield, C.J., and Baldwin, J.E., Crystal-Structure of Isopenicillin N-Synthase Is the First from a New Structural Family of Enzymes. *Nature*, **1995**, 375, 700-4.

13. Valegard, K., van Scheltinga, A.C.T., Lloyd, M.D., Hara, T., Ramaswamy, S., Perrakis, A., Thompson, A., Lee, H.J., Baldwin, J.E., Schofield, C.J., Hajdu, J., and Andersson, I., Structure of a cephalosporin synthase. *Nature*, **1998**, 394, 805-9.

14. Yu, B. and Hunt, J.F., Enzymological and structural studies of the mechanism of promiscuous substrate recognition by the oxidative DNA repair enzyme AlkB. *P Natl Acad Sci USA*, **2009**, 106, 14315-20.

15. Zhang, Z.H., Ren, J.S., Stammers, D.K., Baldwin, J.E., Harlos, K., and Schofield, C.J., Structural origins of the selectivity of the trifunctional oxygenase clavaminic acid synthase. *Nat Struct Biol*, **2000**, 7, 127-33.

16. Majamaa, K., Hanauskeabel, H.M., Gunzler, V., and Kivirikko, K.I., The 2-Oxoglutarate Binding-Site of Prolyl 4-Hydroxylase - Identification of Distinct Subsites and Evidence for 2-Oxoglutarate Decarboxylation in a Ligand Reaction at the Enzyme-Bound Ferrous Ion. *Eur J Biochem*, **1984**, 138, 239-45.

17. Proshlyakov, D.A., Henshaw, T.F., Monterosso, G.R., Ryle, M.J., and Hausinger, R.P., Direct detection of oxygen intermediates in the non-heme Fe enzyme taurine/alpha-ketoglutarate dioxygenase. *J Am Chem Soc*, **2004**, 126, 1022-3.

18. Price, J.C., Barr, E.W., Glass, T.E., Krebs, C., and Bollinger, J.M., Evidence for hydrogen abstraction from C1 of taurine by the high-spin Fe(IV) intermediate detected during oxygen activation by taurine :alpha-ketoglutarate dioxygenase (TauD). *J Am Chem Soc*, **2003**, 125, 13008-9.

19. Sinnecker, S., Svensen, N., Barr, E.W., Ye, S., Bollinger, J.M., Neese, F., and Krebs, C., Spectroscopic and computational evaluation of the structure of the high-spin Fe(IV)-oxo

intermediates in taurine: alpha-Ketoglutarate dioxygenase from Escherichia coli and its His99Ala ligand variant. *J Am Chem Soc*, **2007**, 129, 6168-79.

20. Hanauskeabel, H.M. and Gunzler, V., A Stereochemical Concept for the Catalytic Mechanism of Prolylhydroxylase - Applicability to Classification and Design of Inhibitors. *J Theor Biol*, **1982**, 94, 421-55.

21. Hewitson, K.S., Lienard, B.M.R., McDonough, M.A., Clifton, I.J., Butler, D., Soares, A.S., Oldham, N.J., McNeill, L.A., and Schofield, C.J., Structural and mechanistic studies on the inhibition of the hypoxia-inducible transcription factor hydroxylases by tricarboxylic acid cycle intermediates. *J Biol Chem*, **2007**, 282, 3293-301.

22. Flashman, E., Hoffart, L.M., Hamed, R.B., Bollinger, J.M., Krebs, C., and Schofield, C.J., Evidence for the slow reaction of hypoxia-inducible factor prolyl hydroxylase 2 with oxygen. *Febs J*, **2010**, 277, 4089-99.

23. Price, J.C., Barr, E.W., Hoffart, L.M., Krebs, C., and Bollinger, J.M., Kinetic dissection of the catalytic mechanism of taurine: alpha-ketoglutarate dioxygenase (TauD) from Escherichia coli. *Biochemistry-Us*, **2005**, 44, 8138-47.

24. Pescador, N., Cuevas, Y., Naranjo, S., Alcaide, M., Villar, D., Landazuri, M., and Del Peso, L., Identification of a functional hypoxia-responsive element that regulates the expression of the egl nine homologue 3 (egln3/phd3) gene. *Biochem J*, **2005**, 390, 189-97.

25. Wenger, R.H. and Gassmann, M., Oxygen(es) and the hypoxia-inducible factor-1. *Biol Chem*, **1997**, 378, 609-16.

26. Semenza, G.L., Signal transduction to hypoxia-inducible factor 1. *Biochem Pharmacol*, **2002**, 64, 993-8.

27. Wenger, R.H., Cellular adaptation to hypoxia: O-2-sensing protein hydroxylases, hypoxia-inducible transcription factors, and O-2-regulated gene expression. *Faseb J*, **2002**, 16.

28. Pereira, T., Okamoto, K., and Poellinger, L., Hypoxia-inducible transcription factors and regulation of angiogenesis. *Toxicology*, **2001**, 164, 11-2.

29. Ema, M., Taya, S., Yokotani, N., Sogawa, K., Matsuda, Y., and FujiiKuriyama, Y., A novel bHLH-PAS factor with close sequence similarity to hypoxia-inducible factor 1 alpha

regulates the VEGF expression and is potentially involved in lung and vascular development. *P Natl Acad Sci USA*, **1997**, 94, 4273-8.

30. Stroka, D.M., Burkhardt, T., Desbaillets, I., Wenger, R.H., Neil, D.A.H., Bauer, C., Gassmann, M., and Candinas, D., HIF-1 is expressed in normoxic tissue and displays an organ-specific regulation under systemic hypoxia. *Faseb J*, **2001**, 15, 2445-53.

31. Talks, K.L., Turley, H., Gatter, K.C., Maxwell, P.H., Pugh, C.W., Ratcliffe, P.J., and Harris, A.L., The expression and distribution of the hypoxia-inducible factors HIF-1 alpha and HIF-2 alpha in normal human tissues, cancers, and tumor-associated macrophages. *Am J Pathol*, **2000**, 157, 411-21.

32. Hara, S., Hamada, J., Kobayashi, C., Kondo, Y., and Imura, N., Expression and characterization of hypoxia-inducible factor (HIF)-3 alpha in human kidney: Suppression of HIF-mediated gene expression by HIF-3 alpha. *Biochem Bioph Res Co*, **2001**, 287, 808-13.

33. Maxwell, P.H., Wiesener, M.S., Chang, G.W., Clifford, S.C., Vaux, E.C., Cockman, M.E., Wykoff, C.C., Pugh, C.W., Maher, E.R., and Ratcliffe, P.J., The tumour suppressor protein VHL targets hypoxia-inducible factors for oxygen-dependent proteolysis. *Nature*, **1999**, 399, 271-5.

34. Maynard, M.A., Qi, H., Chung, J., Lee, E.H.L., Kondo, Y., Hara, S., Conaway, R.C., Conaway, J.W., and Ohh, M., Multiple splice variants of the human HIF-3 alpha locus are targets of the von Hippel-Lindau E3 uhiquitin ligase complex. *J Biol Chem*, **2003**, 278, 11032-40.

35. Eckle, T., Kohler, D., Lehmann, R., El Kasmi, K.C., and Eltzschig, H.K., Hypoxia-inducible factor-1 is central to cardioprotection - A new paradigm for ischemic preconditioning. *Circulation*, **2008**, 118, 166-75.

36. Holscher, M., Silter, M., Krull, S., von Ahlen, M., Hesse, A., Schwartz, P., Wielockx, B., Breier, G., Katschinski, D.M., and Zieseniss, A., Cardiomyocyte-specific Prolyl-4-hydroxylase Domain 2 Knock Out Protects from Acute Myocardial Ischemic Injury. *J Biol Chem*, **2011**, 286, 11185-94.

37. Hyvarinen, J., Hassinen, I.E., Sormunen, R., Maki, J.M., Kivirikko, K.I., Koivunen, P., and Myllyharju, J., Hearts of Hypoxia-inducible Factor Prolyl 4-Hydroxylase-2

Hypomorphic Mice Show Protection against Acute Ischemia-Reperfusion Injury. *J Biol Chem*, **2010**, 285, 13646-57.

38. Myllyharju, J., HIF Prolyl 4-Hydroxylases and their Potential as Drug Targets. *Curr Pharm Design*, **2009**, 15, 3878-85.

39. Muchnik, E. and Kaplan, J., HIF prolyl hydroxylase inhibitors for anemia. *Expert Opin Inv Drug*, **2011**, 20, 645-56.

40. Yan, L., Colandrea, V.J., and Hale, J.J., Prolyl hydroxylase domain-containing protein inhibitors as stabilizers of hypoxia-inducible factor: small molecule-based therapeutics for anemia. *Expert Opinion on Therapeutic Patents*, **2010**, 20, 1219-45.

41. Epstein, A.C.R., Gleadle, J.M., McNeill, L.A., Hewitson, K.S., O'Rourke, J., Mole, D.R., Mukherji, M., Metzen, E., Wilson, M.I., Dhanda, A., Tian, Y.M., Masson, N., Hamilton, D.L., Jaakkola, P., Barstead, R., Hodgkin, J., Maxwell, P.H., Pugh, C.W., Schofield, C.J., and Ratcliffe, P.J., C-elegans EGL-9 and mammalian homologs define a family of dioxygenases that regulate HIF by prolyl hydroxylation. *Cell*, **2001**, 107, 43-54.

42. Hewitson, K.S., McNeill, L.A., Riordan, M.V., Tian, Y.M., Bullock, A.N., Welford, R.W., Elkins, J.M., Oldham, N.J., Bhattacharya, S., Gleadle, J.M., Ratcliffe, P.J., Pugh, C.W., and Schofield, C.J., Hypoxia-inducible factor (HIF) asparagine hydroxylase is identical to factor inhibiting HIF (FIH) and is related to the cupin structural family. *J Biol Chem*, **2002**, 277, 26351-5.

43. Dames, S.A., Martinez-Yamout, M., De Guzman, R.N., Dyson, H.J., and Wright, P.E., Structural basis for Hif-1 alpha/CBP recognition in the cellular hypoxic response. *P Natl Acad Sci USA*, **2002**, 99, 5271-6.

44. Dann, C.E., Bruick, R.K., and Deisenhofer, J., Structure of factor-inhibiting hypoxia-inducible factor 1: An asparaginyl hydroxylase involved in the hypoxic response pathway. *P Natl Acad Sci USA*, **2002**, 99, 15351-6.

45. Elkins, J.M., Hewitson, K.S., McNeill, L.A., Seibel, J.F., Schlemminger, I., Pugh, C.W., Ratcliffe, P.J., and Schofield, C.J., Structure of factor-inhibiting hypoxia-inducible factor (HIF) reveals mechanism of oxidative modification of HIF-1 alpha. *J Biol Chem*, **2003**, 278, 1802-6.

46. Huang, L.E., Gu, J., Schau, M., and Bunn, H.F., Regulation of hypoxia-inducible factor 1 alpha is mediated by an O-2-dependent degradation domain via the ubiquitin-proteasome pathway. *P Natl Acad Sci USA*, **1998**, 95, 7987-92.

47. Huang, J.H., Zhao, Q., Mooney, S.M., and Lee, F.S., Sequence determinants in hypoxia-inducible factor-1 alpha for hydroxylation by the prolyl hydroxylases PHD1, PHD2, and PHD3. *J Biol Chem*, **2002**, 277, 39792-800.

48. Appelhoff, R.J., Tian, Y.M., Raval, R.R., Turley, H., Harris, A.L., Pugh, C.W., Ratcliffe, P.J., and Gleadle, J.M., Differential function of the prolyl hydroxylases PHD1, PHD2, and PHD3 in the regulation of hypoxia-inducible factor. *J Biol Chem*, **2004**, 279, 38458-65.

49. Karuppagounder, S.S. and Ratan, R.R., Hypoxia-inducible factor prolyl hydroxylase inhibition: robust new target or another big bust for stroke therapeutics? *J Cerebr Blood F Met*, **2012**, 32, 1347-61.

50. Siddiq, A., Aminova, L.R., and Ratan, R.R., Hypoxia inducible factor prolyl 4-hydroxylase enzymes: Center stage in the battle against hypoxia, metabolic compromise and oxidative stress. *Neurochem Res*, **2007**, 32, 931-46.

51. Fong, G.H. and Takeda, K., Role and regulation of prolyl hydroxylase domain proteins. *Cell Death Differ*, **2008**, 15, 635-41.

52. Berra, E., Benizri, E., Ginouves, A., Volmat, V., Roux, D., and Pouyssegur, J., HIF prolyl-hydroxylase 2 is the key oxygen sensor setting low steady-state levels of HIF-1 alpha in normoxia. *Embo J*, **2003**, 22, 4082-90.

53. Kojima, I., Tanaka, T., Inagi, R., Kato, H., Yamashita, T., Sakiyama, A., Ohneda, O., Takeda, N., Sata, M., Miyata, T., Fujita, T., and Nangaku, M., Protective role of hypoxia-inducible factor-2 alpha against ischemic damage and oxidative stress in the kidney. *J Am Soc Nephrol*, **2007**, 18, 1218-26.

54. Stolze, I.P., Tian, Y.M., Appelhoff, R.J., Turley, H., Wykoff, C.C., Gleadle, J.M., and Ratcliffe, P.J., Genetic analysis of the role of the asparaginyl hydroxylase factor inhibiting hypoxia-inducible factor (FIH) in regulating hypoxia-inducible factor (HIF) transcriptional target genes. (vol 279, pg 42719, 2004). *J Biol Chem*, **2004**, 279, 54974-.

55. Tuckerman, J.R., Zhao, Y.G., Hewitson, K.S., Tian, Y.M., Pugh, C.W., Ratcliffe, P.J., and Mole, D.R., Determination and comparison of specific activity of the HIF-prolyl hydroxylases. *Febs Lett*, **2004**, 576, 145-50.

56. Yu, B., Edstrom, W.C., Benach, J., Hamuro, Y., Weber, P.C., Gibney, B.R., and Hunt, J.F., Crystal structures of catalytic complexes of the oxidative DNA/RNA repair enzyme AlkB. *Nature*, **2006**, 439, 879-84.

57. Trewick, S.C., Henshaw, T.F., Hausinger, R.P., Lindahl, T., and Sedgwick, B., Oxidative demethylation by Escherichia coli AlkB directly reverts DNA base damage. *Nature*, **2002**, 419, 174-8.

58. Grosjean, H., *Fine-tuning of RNA functions by modification and editing*. 2005, Germany: Springer.

59. Czerwoniec, A., Dunin-Horkawicz, S., Purta, E., Kaminska, K.H., Kasprzak, J.M., Bujnicki, J.M., Grosjean, H., and Rother, K., MODOMICS: a database of RNA modification pathways. 2008 update. *Nucleic Acids Res*, **2009**, 37, D118-D21.

60. Grosjean, H., *DNA and RNA modification enzymes: structure, mechanism, function, and evolution*. 2009, Austin: Landes Bioscience.

61. Fu, D., Brophy, J.A.N., Chan, C.T.Y., Atmore, K.A., Begley, U., Paules, R.S., Dedon, P.C., Begley, T.J., and Samson, L.D., Human AlkB Homolog ABH8 Is a tRNA Methyltransferase Required for Wobble Uridine Modification and DNA Damage Survival. *Mol Cell Biol*, **2010**, 30, 2449-59.

62. Lindahl, T., Sedgwick, B., Sekiguchi, M., and Nakabeppu, Y., Regulation and Expression of the Adaptive Response to Alkylating-Agents. *Annu Rev Biochem*, **1988**, 57, 133-57.

63. Seeberg, E. and Berdal, K.G., in *Base Excision Repair of DNA Damage*, I.D. Hickson, Editor. 1999, Landes Bioscience. p. 151–68

64. Gehring, M., Reik, W., and Henikoff, S., DNA demethylation by DNA repair. *Trends Genet*, **2009**, 25, 82-90.

65. Falnes, P.O., Johansen, R.F., and Seeberg, E., AlkB-mediated oxidative demethylation reverses DNA damage in Escherichia coli. *Nature*, **2002**, 419, 178-82.

66. Fu, Y., Dai, Q., Zhang, W., Ren, J., Pan, T., and He, C.A., The AlkB Domain of Mammalian ABH8 Catalyzes Hydroxylation of 5-Methoxycarbonylmethyluridine at the Wobble Position of tRNA. *Angew Chem Int Edit*, **2010**, 49, 8885-8.

67. Fu, Y. and He, C.A., Nucleic acid modifications with epigenetic significance. *Curr Opin Chem Biol*, **2012**, 16, 516-24.

68. van den Born, E., Vagbo, C.B., Songe-Moller, L., Leihne, V., Lien, G.F., Leszczynska, G., Malkiewicz, A., Krokan, H.E., Kirpekar, F., Klungland, A., and Falnes, P.O., ALKBH8-mediated formation of a novel diastereomeric pair of wobble nucleosides in mammalian tRNA. *Nat Commun*, **2011**, 2.

69. Falnes, P.O., Bjoras, M., Aas, P.A., Sundheim, O., and Seeberg, E., Substrate specificities of bacterial and human AlkB proteins. *Nucleic Acids Res*, **2004**, 32, 3456-61.

70. Tahiliani, M., Koh, K.P., Shen, Y.H., Pastor, W.A., Bandukwala, H., Brudno, Y., Agarwal, S., Iyer, L.M., Liu, D.R., Aravind, L., and Rao, A., Conversion of 5-Methylcytosine to 5-Hydroxymethylcytosine in Mammalian DNA by MLL Partner TET1. *Science*, **2009**, 324, 930-5.

71. Ito, S., Shen, L., Dai, Q., Wu, S.C., Collins, L.B., Swenberg, J.A., He, C., and Zhang, Y., Tet Proteins Can Convert 5-Methylcytosine to 5-Formylcytosine and 5-Carboxylcytosine. *Science*, **2011**, 333, 1300-3.

72. Tian, X.Q. and Fang, J.Y., Current perspectives on histone demethylases. *Acta Bioch Bioph Sin*, **2007**, 39, 81-8.

73. Berger, S.L., Kouzarides, T., Shiekhattar, R., and Shilatifard, A., An operational definition of epigenetics. *Gene Dev*, **2009**, 23, 781-3.

74. Kornberg, R.D. and Lorch, Y.L., Twenty-five years of the nucleosome, fundamental particle of the eukaryote chromosome. *Cell*, **1999**, 98, 285-94.

75. Allfrey, V.G., Faulkner, R., and Mirsky, A.E., Acetylation + Methylation of Histones + Their Possible Role in Regulation of Rna Synthesis. *P Natl Acad Sci USA*, **1964**, 51, 786-&.

76. Zhang, K.L., Siino, J.S., Jones, P.R., Yau, P.M., and Bradbury, E.M., A mass spectrometric "western blot" to evaluate the correlations between histone methylation and histone acetylation. *Proteomics*, **2004**, 4, 3765-75.

77. Zhang, L.W., Eugeni, E.E., Parthun, M.R., and Freitas, M.A., Identification of novel histone post-translational modifications by peptide mass fingerprinting. *Chromosoma*, **2003**, 112, 77-86.

78. Martin, C. and Zhang, Y., The diverse functions of histone lysine methylation. *Nat Rev Mol Cell Bio*, **2005**, 6, 838-49.

79. Shi, Y.J., Lan, F., Matson, C., Mulligan, P., Whetstine, J.R., Cole, P.A., Casero, R.A., and Shi, Y., Histone demethylation mediated by the nuclear arnine oxidase homolog LSD1. *Cell*, **2004**, 119, 941-53.

80. Karytinos, A., Forneris, F., Profumo, A., Ciossani, G., Battaglioli, E., Binda, C., and Mattevi, A., A Novel Mammalian Flavin-dependent Histone Demethylase. *J Biol Chem*, **2009**, 284, 17775-82.

81. Wanner, K. and Hofner, G., *Mass spectrometry in medicinal chemistry. Applications in drug discovery*. Vol. 36. 2007: Wiley-VCH.

82. Kebarle, P., A brief overview of the present status of the mechanisms involved in electrospray mass spectrometry. *J Mass Spectrom*, **2000**, 35, 804-17.

83. Sharon, M. and Robinson, C.V., The role of mass Spectrometry in structure elucidation of dynamic protein complexes. *Annu Rev Biochem*, **2007**, 76, 167-93.

84. Benkestock, K., Sundqvist, G., Edlund, P.O., and Roeraade, J., Influence of droplet size, capillary-cone distance and selected instrumental parameters for the analysis of noncovalent protein-ligand complexes by nano-electrospray ionization mass spectrometry. *J Mass Spectrom*, **2004**, 39, 1059-67.

85. Daniel, J.M., McCombie, G., Wendt, S., and Zenobi, R., Mass spectrometric determination of association constants of adenylate kinase with two noncovalent inhibitors. *J Am Soc Mass Spectr*, **2003**, 14, 442-8.

86. Gabelica, V., Galic, N., Rosu, F., Houssier, C., and De Pauw, E., Influence of response factors on determining equilibrium association constants of non-covalent complexes by electrospray ionization mass spectrometry. *J Mass Spectrom*, **2003**, 38, 491-501.

87. Ganem, B., Li, Y.T., and Henion, J.D., Observation of Noncovalent Enzyme Substrate and Enzyme Product Complexes by Ion-Spray Mass-Spectrometry. *J Am Chem Soc*, **1991**, 113, 7818-9.

88. Loo, J.A., Studying noncovalent protein complexes by electrospray ionization mass spectrometry. *Mass Spectrom Rev*, **1997**, 16, 1-23.

89. McNeill, L.A., Flashman, E., Buck, M.R.G., Hewitson, K.S., Clifton, I.J., Jeschke, G., Claridge, T.D.W., Ehrismann, D., Oldham, N.J., and Schofield, C.J., Hypoxia-inducible factor prolyl hydroxylase 2 has a high affinity for ferrous iron and 2-oxoglutarate. *Mol Biosyst*, **2005**, 1, 321-4.

90. Ashcroft, A.E., Recent developments in electrospray ionisation mass spectrometry: noncovalently bound protein complexes. *Nat Prod Rep*, **2005**, 22, 452-64.

91. Heck, A.J.R., Native mass spectrometry: a bridge between interactomics and structural biology. *Nat Methods*, **2008**, 5, 927-33.

92. Furka, A., Sebestyen, F., Asgedom, M., and Dibo, G., General-Method for Rapid Synthesis of Multicomponent Peptide Mixtures. *Int J Pept Prot Res*, **1991**, 37, 487-93.

93. Houghten, R.A., Pinilla, C., Blondelle, S.E., Appel, J.R., Dooley, C.T., and Cuervo, J.H., Generation and Use of Synthetic Peptide Combinatorial Libraries for Basic Research and Drug Discovery. *Nature*, **1991**, 354, 84-6.

94. Anderson, S., Anderson, H.L., and Sanders, J.K.M., Expanding Roles for Templates in Synthesis. *Accounts Chem Res*, **1993**, 26, 469-75.

95. Anderson, S., Anderson, H.L., and Sanders, J.K.M., Template-Directed Synthesis of Linear and Cyclic Butadiyne-Linked Porphyrin Oligomers up to a Linear Octamer. *J Chem Soc Perk T 1*, **1995**, 2247-54.

96. Busch, D.H., Structural Definition of Chemical Templates and the Prediction of New and Unusual Materials. *J Inclus Phenom Mol*, **1992**, 12, 389-95.

97. Busch, D.H. and Stephenson, N.A., Molecular-Organization, Portal to Supramolecular Chemistry - Structural-Analysis of the Factors Associated with Molecular-Organization in Coordination and Inclusion Chemistry, Including the Coordination Template Effect. *Coordin Chem Rev*, **1990**, 100, 119-54.

98. Hoss, R. and Vogtle, F., Template Syntheses. *Angewandte Chemie-International Edition in English*, **1994**, 33, 375-84.

99. Thompson, M.C. and Busch, D.H., Reactions of Coordinated Ligands .2. Nickel(Ii) Complexes of Some Novel Tetradentate Ligands. *J Am Chem Soc*, **1962**, 84, 1762-&.

100. Goodwin, J.T. and Lynn, D.G., Template-Directed Synthesis - Use of a Reversible-Reaction. *J Am Chem Soc*, **1992**, 114, 9197-8.

101. Corbett, P.T., Leclaire, J., Vial, L., West, K.R., Wietor, J.L., Sanders, J.K.M., and Otto, S., Dynamic combinatorial chemistry. *Chem Rev*, **2006**, 106, 3652-711.

102. Huc, I. and Nguyen, R., Dynamic combinatorial chemistry. *Comb Chem High T Scr*, **2001**, 4, 53-74.

103. Swann, P.G., Casanova, R.A., Desai, A., Frauenhoff, M.M., Urbancic, M., Slomczynska, U., Hopfinger, A.J., LeBreton, G.C., and Venton, D.L., Nonspecific protease-catalyzed hydrolysis synthesis of a mixture of peptides: Product diversity and ligand amplification by a molecular trap. *Biopolymers*, **1996**, 40, 617-25.

104. Ulijn, R.V., De Martin, L., Gardossi, L., and Halling, P.J., Biocatalysis in reaction mixtures with undissolved solid substrates and products. *Curr Org Chem*, **2003**, 7, 1333-46.

105. Erbeldinger, M., Ni, X.W., and Halling, P.J., Effect of water and enzyme concentration on thermolysin-catalyzed solid-to-solid peptide synthesis. *Biotechnol Bioeng*, **1998**, 59, 68-72.

106. Kitaguchi, H. and Klibanov, A.M., Enzymatic Peptide-Synthesis Via Segment Condensation in the Presence of Water Mimics. *J Am Chem Soc*, **1989**, 111, 9272-3.

107. Woll, M.G. and Gellman, S.H., Backbone thioester exchange: A new approach to evaluating higher order structural stability in polypeptides. *J Am Chem Soc*, **2004**, 126, 11172-4.

108. Ramstrom, O., Lohmann, S., Bunyapaiboonsri, T., and Lehn, J.M., Dynamic combinatorial carbohydrate libraries: Probing the binding site of the concanavalin A lectin. *Chem-Eur J*, **2004**, 10, 1711-5.

109. Bornaghi, L.F., Wilkinson, B.L., Kiefel, M.J., and Poulsen, S.A., Synthesis of cyclic oligomers of a modified sugar amino acid utilising dynamic combinatorial chemistry. *Tetrahedron Lett*, **2004**, 45, 9281-4.

110. Eckardt, L.H., Naumann, K., Pankau, W.M., Rein, M., Schweitzer, M., Windhab, N., and von Kiedrowski, G., DNA nanotechnology: Chemical copying of connectivity. *Nature*, **2002**, 420, 286-.

111. Nguyen, R. and Huc, I., Optimizing the reversibility of hydrazone formation for dynamic combinatorial chemistry. *Chem Commun*, **2003**, 942-3.

112. Bunyapaiboonsri, T., Ramstrom, O., Lohmann, S., Lehn, J.M., Peng, L., and Goeldner, M., Dynamic deconvolution of a pre-equilibrated dynamic combinatorial library of acetylcholinesterase inhibitors. *Chembiochem*, **2001**, 2, 438-44.

113. Huc, I. and Lehn, J.M., Virtual combinatorial libraries: Dynamic generation of molecular and supramolecular diversity by self-assembly (vol 94, pg 2106, 1997). *P Natl Acad Sci USA*, **1997**, 94, 8272-.

114. Hochgurtel, M., Biesinger, R., Kroth, H., Piecha, D., Hofmann, M.W., Krause, S., Schaaf, O., Nicolau, C., and Eliseev, A.V., Ketones as building blocks for dynamic combinatorial libraries: Highly active neuraminidase inhibitors generated via selection pressure of the biological target. *Journal of Medicinal Chemistry*, **2003**, 46, 356-8.

115. Moffett, R.B. and Hoehn, W.M., Analgesics .2. The Grignard Reaction with Schiff Bases. *J Am Chem Soc*, **1947**, 69, 1792-4.

116. Freifeld.M, Selective Hydrogenolysis . Dehalogenation in Presence of N-Benzyl Linkage. *J Org Chem*, **1966**, 31, 3875-&.

117. Otto, S., Furlan, R.L.E., and Sanders, J.K.M., Dynamic combinatorial libraries of macrocyclic disulfides in water. *J Am Chem Soc*, **2000**, 122, 12063-4.

118. Ramstrom, O. and Lehn, J.M., In situ generation and screening of a dynamic combinatorial carbohydrate library against concanavalin A. *Chembiochem*, **2000**, 1, 41-8.

119. Sando, S., Narita, A., and Aoyama, Y., A facile route to dynamic glycopeptide libraries based on disulfide-linked sugar-peptide coupling. *Bioorg Med Chem Lett*, **2004**, 14, 2835-8.

120. Lienard, B.M.R., Hueting, R., Lassaux, P., Galleni, M., Frere, J.M., and Schofield, C.J., Dynamic combinatorial mass spectrometry leads to metallo-beta-lactamase inhibitors. *Journal of Medicinal Chemistry*, **2008**, 51, 684-8.

121. Lienard, B.M.R., Selevsek, N., Oldham, N.J., and Schofield, C.J., Combined mass spectrometry and dynamic chemistry approach to identify metalloenzyme inhibitors. *Chemmedchem*, **2007**, 2, 175-+.

122. Miller, B.L., *Dynamic Combinatorial Chemistry: In Drug Discovery, Bioorganic Chemistry, and Materials Science*. 2010: Wiley. 265.

123. Furlan, R.L.E., Otto, S., and Sanders, J.K.M., Supramolecular templating in thermodynamically controlled synthesis. *P Natl Acad Sci USA*, **2002**, 99, 4801-4.

124. Karan, C. and Miller, B.L., Dynamic diversity in drug discovery: Putting small-molecule evolution to work. *Drug Discov Today*, **2000**, 5, 67-75.

125. Ramstrom, O., Bunyapaiboonsri, T., Lohmann, S., and Lehn, J.M., Chemical biology of dynamic combinatorial libraries. *Bba-Gen Subjects*, **2002**, 1572, 178-86.

126. Huc, I. and Lehn, J.M., Virtual combinatorial libraries: Dynamic generation of molecular and supramolecular diversity by self-assembly. *P Natl Acad Sci USA*, **1997**, 94, 2106-10.

127. Bugaut, A., Toulme, J.J., and Rayner, B., Use of dynamic combinatorial chemistry for the identification of covalently appended residues that stabilize oligonucleotide complexes. *Angew Chem Int Edit*, **2004**, 43, 3144-7.

128. Klekota, B., Hammond, M.H., and Miller, B.L., Generation of novel DNA-binding compounds by selection and amplification from self-assembled combinatorial libraries. *Tetrahedron Lett*, **1997**, 38, 8639-42.

129. Gerber-Lemaire, S., Popowycz, F., Rodriguez-Garcia, E., Asenjo, A.T.C., Robina, I., and Vogel, P., An efficient combinatorial method for the discovery of glycosidase inhibitors. *Chembiochem*, **2002**, 3, 466-70.

130. Valade, A., Urban, D., and Beau, J.M., Two galactosyltransferases' selection of different binders from the same uridine-based dynamic combinatorial library. *J Comb Chem*, **2007**, 9, 1-4.

131. Zameo, S., Vauzeilles, B., and Beau, J.M., Dynamic combinatorial chemistry: Lysozyme selects an aromatic motif that mimics a carbohydrate residue. *Angew Chem Int Edit*, **2005**, 44, 965-9.

132. Cousins, G.R.L., Poulsen, S.A., and Sanders, J.K.M., Dynamic combinatorial libraries of pseudo-peptide hydrazone macrocycles. *Chem Commun*, **1999**, 1575-6.

133. Poulsen, S.A., Direct screening of a dynamic combinatorial library using mass spectrometry. *J Am Soc Mass Spectr*, **2006**, 17, 1074-80.

134. Poulsen, S.A., Davis, R.A., and Keys, T.G., Screening a natural product-based combinatorial library using FTICR mass spectrometry. *Bioorgan Med Chem*, **2006**, 14, 510-5.

135. Cancilla, M.T., He, M.M., Viswanathan, N., Simmons, R.L., Taylor, M., Fung, A.D., Cao, K., and Erlanson, D.A., Discovery of an Aurora kinase inhibitor through site-specific dynamic combinatorial chemistry. *Bioorg Med Chem Lett*, **2008**, 18, 3978-81.

136. Danieli, B., Giardini, A., Lesma, G., Passarella, D., Peretto, B., Sacchetti, A., Silvani, A., Pratesi, G., and Zunino, F., Thiocolchicine-podophyllotoxin conjugates: Dynamic libraries based on disulfide exchange reaction. *J Org Chem*, **2006**, 71, 2848-53.

137. Hochgurtel, M., Kroth, H., Piecha, D., Hofmann, M.W., Nicolau, C., Krause, S., Schaaf, O., Sonnenmoser, G., and Eliseev, A.V., Target-induced formation of neuraminidase inhibitors from in vitro virtual combinatorial libraries. *P Natl Acad Sci USA*, **2002**, 99, 3382-7.

138. Milanesi, L., Hunter, C.A., Sedelnikova, S.E., and Waltho, J.P., Amplification of bifunctional ligands for calmodulin from a dynamic combinatorial library. *Chem-Eur J*, **2006**, 12, 1081-7.

139. Valade, A., Urban, D., and Beau, J.M., Target-assisted selection of galactosyltransferase binders from dynamic combinatorial libraries. An unexpected solution with restricted amounts of the enzyme. *Chembiochem*, **2006**, 7, 1023-7.

140. Scott, D.E., Dawes, G.J., Ando, M., Abell, C., and Ciulli, A., A Fragment-Based Approach to Probing Adenosine Recognition Sites by Using Dynamic Combinatorial Chemistry. *Chembiochem*, **2009**, 10, 2772-9.

141. Congreve, M.S., Davis, D.J., Devine, L., Granata, C., O'Reilly, M., Wyatt, P.G., and Jhoti, H., Detection of ligands from a dynamic combinatorial library by X-ray crystallography. *Angew Chem Int Edit*, **2003**, 42, 4479-82.

142. Rose, N.R., Woon, E.C.Y., Kingham, G.L., King, O.N.F., Mecinovic, J., Clifton, I.J., Ng, S.S., Talib-Hardy, J., Oppermann, U., McDonough, M.A., and Schofield, C.J., Selective Inhibitors of the JMJD2 Histone Demethylases: Combined Nondenaturing Mass Spectrometric Screening and Crystallographic Approaches. *Journal of Medicinal Chemistry*, **2010**, 53, 1810-8.

143. Woon, E.C.Y., Demetriades, M., Bagg, E.A.L., Aik, W., Krylova, S.M., Ma, J.H.Y., Chan, M.C., Walport, L.J., Wegman, D.W., Dack, K.N., McDonough, M.A., Krylov, S.N., and Schofield, C.J., Dynamic Combinatorial Mass Spectrometry Leads to Inhibitors of a 2-Oxoglutarate-Dependent Nucleic Acid Demethylase. *Journal of Medicinal Chemistry*, **2012**, 55, 2173-84.

Chapter 2. Dynamic Combinatorial Mass Spectrometry for the identification of AlkB inhibitors

2.1 Introduction

2.1.1 AlkB

AlkB is a bacterial (*Escherichia coli*) 2-oxoglutarate and Fe(II) dependent oxygenase that is involved in the repair of alkylated DNA and RNA bases.[1, 2] To date 9 homologues of AlkB have been found in humans: AlkBH1-8 (ABH1-8) and FTO.[3-5] AlkBH2 and AlkBH3 are the most similar to prokaryotic AlkB: they catalyse *N*-demethylation of nucleic bases including 1-methyladenine and 3-methylcytosine.[2] Oxidative demethylation as catalysed by *E. coli* AlkB directly reverses DNA base damage, caused by S_N2 type alkylating reagents. It is proposed that AlkBH2/AlkBH3 act in DNA repair *in vivo*, however, roles in the regulation of gene-expression are also possible for AlkBH1-8 and FTO.[2, 6-8] Recently it has been shown that AlkBH2 has a preference for double stranded DNA (dsDNA) with little activity on RNA, while AlkBH3 and AlkB demethylate nucleosides on single stranded DNA (ssDNA) and RNA.[1, 7] While AlkB is not a human protein, the ease of production and purification compared to the human analogues and its structural similarity to AlkBH2 and AlkBH3, makes it a useful model for pioneering studies on AlkBH inhibition.

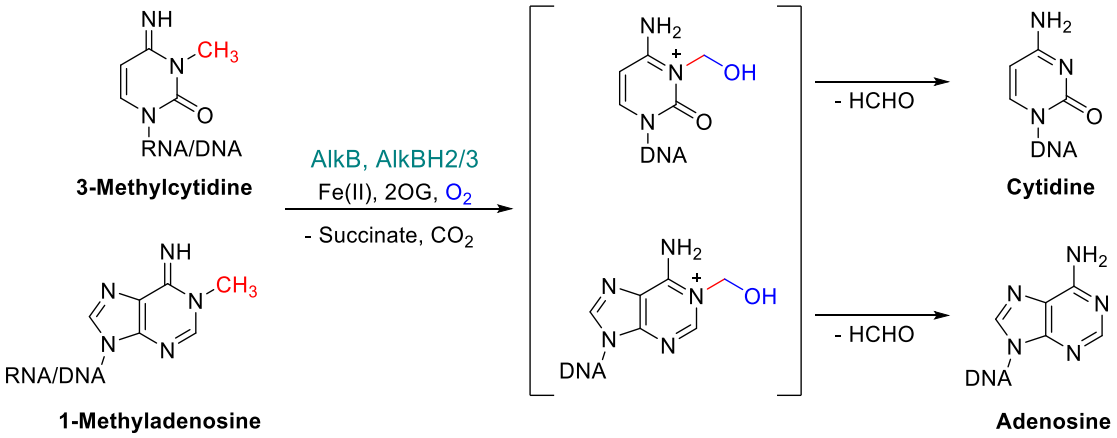

Figure 2. 1 *Demethylations catalysed by AlkB and the human analogues AlkBH2, AlkBH3.*

2.1.2 Dynamic combinatorial mass spectrometry

The applicability of dynamic combinatorial methods is determined by the reversible reaction(s) used for the study, the target and the analytical method(s) used (Chapter 1). The potential advantage of DCC as a single vessel method for synthesis and screening is often over-shadowed by the long and sometimes costly analysis.[9] Traditional analytical techniques for dynamic combinatorial methods include HPLC[10, 11] and NMR,[12] which require separate analysis of the library with and without the target to identify potentially amplified products. These compounds are then synthesised and individually tested to validate the screen, often resulting in time and labour intensive analyses. Further, some binders in the mixtures may not be detected due to, for example, structural instability (in the case of HPLC analysis) or poor resolution.

To overcome the problems of sample analysis using conventional methods, mass spectrometry (MS) has been investigated as an analytical method for DCC. MS is a quick and sensitive technique that requires relatively little sample, making it attractive for resolving complex mixtures of compounds.[13] For protein-directed DCC, it was envisaged that non-denaturing MS methods could be used for the direct analysis of non-covalent native protein-ligand interactions by observation of mass shift relative to the uncomplexed protein. Poulsen was the first to report the use of mass spectrometry for analysis of dynamic combinatorial libraries;[14] earlier work had shown that non denaturing ESI-MS can be used to select

peptides binding to proteases from mixtures. [15] Subsequently, the DCC-MS method had been applied to metallo-β-lactamases, using the thiol/disulphide exchange systems.[16-19] In our lab there was great interest in applying the DCC linked MS approach (termed DCMS) to identify inhibitors of 2OG oxygenases, including AlkB. Work on the development of the DCMS method and its use for the design of AlkB inhibitors is described in this chapter.

2.2 ESI-MS binding of *N*-oxalyl amino acids to AlkB

Initial experiments focused on identifying a suitable AlkB template ligand for use in DCMS analyses. This ligand must bind to AlkB with reasonable affinity and must also possess (a) suitable reactive group(s) to allow reversible reactions with other fragments in the mixtures. It was envisaged that an appropriate functionalised analogue of the broad spectrum 2OG oxygenase inhibitor *N*-oxalyl glycine (**NOG**, **202a**)[20] might be suitable. To investigate this hypothesis, various D and L *N*-oxalyl amino acids were synthesised and their ability to bind to recombinant AlkB was tested using non-denaturing electrospray ionisation mass spectrometry (ESI-MS). *N*-Oxalyl amino acids were synthesised from the corresponding amino acid methyl esters and monomethyl oxalyl chloride followed by saponification (Scheme 2. 1).

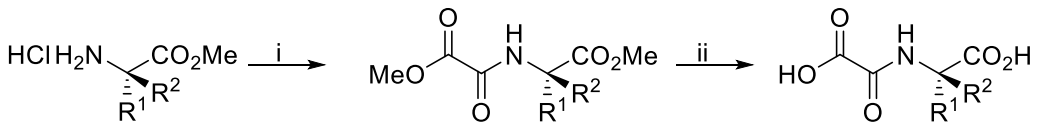

R^1, R^2= H	**201a**	**202a**
R^1= CH_2SH, R^2= H	**201b**	**202b**
R^1= CH_3, R^2= H	**201c**	**202c**
R^1= $CH(CH_3)_2$, R^2= H	**201d**	**202d**
R^1= CH_2Ph, R^2= H	**201e**	**202e**
R^1= H, R^2= CH_2SH	**201f**	**202f**
R^1= H, R^2= CH_3	**201g**	**202g**
R^1= H, R^2= $CH(CH_3)_2$	**201h**	**202h**
R^1= H, R^2= CH_2Ph	**201i**	**202i**

Scheme 2. 1 *Synthesis of N-oxalyl amino acids.*

Reagents and Conditions i) monomethyl oxalyl chloride, Et_3N, CH_2Cl_2, r.t; ii) 1M NaOH, MeOH, r.t.

*Compounds **201c-201i** and **202c-i** were synthesised by Dr. Jasmin Mecinovic.*

Apo-AlkB was used for the non-denaturing electrospray ionisation mass spectrometry (nd ESI-MS) binding experiments. For complete formation of the AlkB·Fe complex, which is required for inhibitor binding,[21] five equivalents of Fe(II) were found to be required. This also resulted in partial formation of AlkB·2Fe and AlkB·3Fe species (Figure 2. 2). The binding experiments were then carried out using one equivalent of the appropriate *N*-oxalyl amino acids without pre-incubation. The binding of *N*-oxalyl amino acids with small side-chains (alanine and cysteine) was observed to be strong with small differences in binding between the L and D isomers (Figure 2. 2). For analogues with larger side-chains (valine and phenylalanine), the L isoforms bound stronger to AlkB, implying that AlkB has selectivity for the L-amino acid derivatives (Figure 2. 2).

Apo-AlkB was produced and purified by Dr. Eleanor A. L. Bagg.

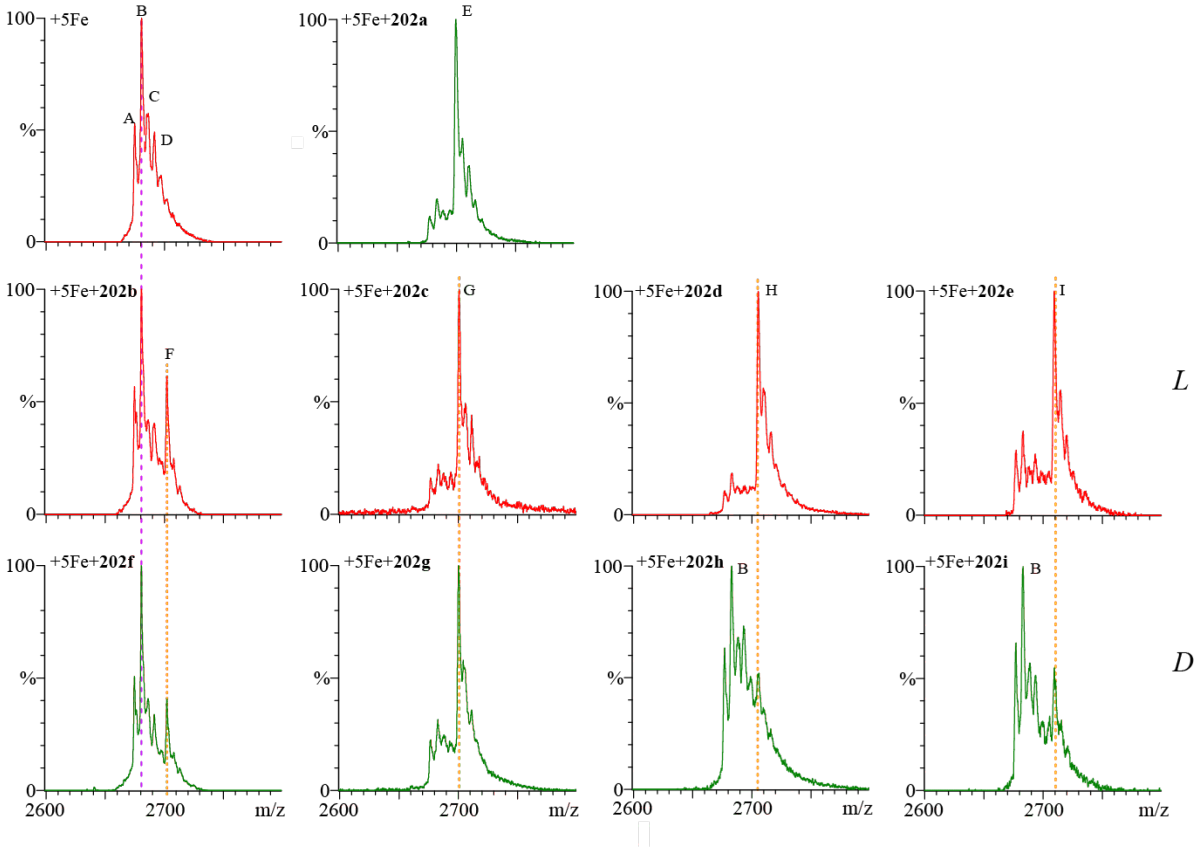

Figure 2. 2 *Non denaturing ESI-MS of AlkB·Fe(II) with* ***202a-i*** *at cone voltage 50V. A: AlkB, B: AlkB·Fe, C: AlkB·2Fe, D: AlkB·3Fe, E: AkB·Fe·****202a****, F: AkB·Fe·****202b/f****, G: AkB·Fe·****202c/g****, H: AkB·Fe·****202d/h****, I: AkB·Fe·****202e/i****.*

The results obtained from the ESI-MS experiments were supported by those from differential scanning fluorimetry assays (DSF, for description of this method see Chapter 4).[22] AlkB displayed higher melting temperatures in the presence of the L-amino acid analogues compared to the D-isomers implying that *N*-oxalyl-L-amino acids significantly stabilize the enzyme, presumably due to stronger binding in the active site (Table 2. 1). Modelling of the compounds into the active site of AlkB (based on an AlkB-2OG·trinucleoside crystal structure PDB ID: 3I20)[23] suggest that there is more space surrounding the side-chains of the L-amino acid derivatives, whereas the D-amino acid derivatives have less space to expand in the active site (Figure 2. 3). Therefore, *N*-oxalyl-L-cysteine was selected as the template ligand due to its relatively high binding efficiency and its potential to form disulfides with fragments that may exploit that binding pocket.

Table 2. 1 *Melting temperatures of AlkB and inhibition results with N-oxalyl amino acids.*

Compound	ΔTm (°C)	IC_{50} (μM)
202a	2.9	32
202b	-1.2	>1000
202c	3.8	35
202e	4.3	75
202f	-1.1	>1000
202h	2.9	149
202i	1.0	260

ESI-MS binding assays with N-oxalyl amino acids were carried out by Dr. Esther Woon.

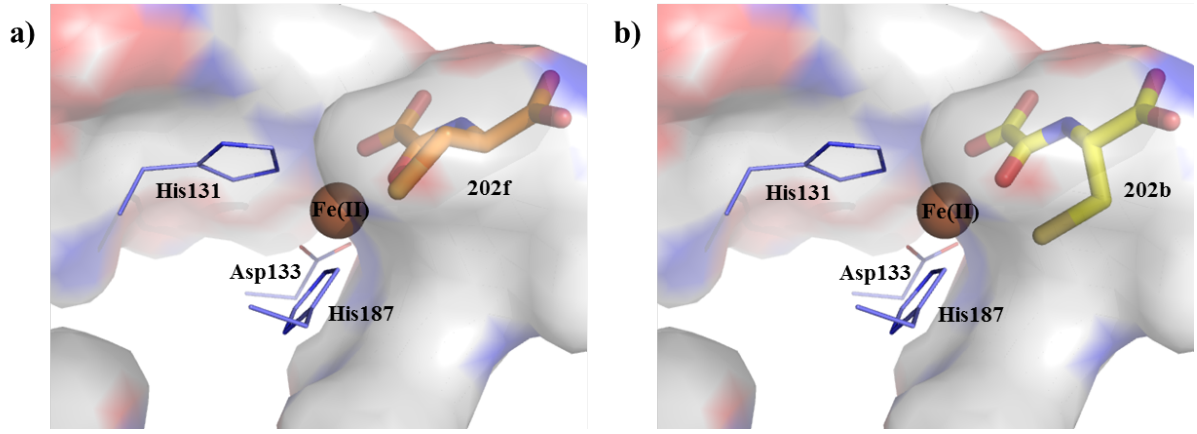

Figure 2. 3 *Modelling of N-oxalyl cysteine into the active site pocket of AlkB·Fe(II)·2OG (gray surface, PDB ID: 3I20).*[23] *a) The cysteinyl thiol of N-oxalyl-D-cysteine appears sterically hindered; b) the thiol of N-oxalyl-L-cysteine appears to be positioned towards the extended pocket, implying that disulphides at this position bind with improved efficacy.*

2.3 Non-denaturing ESI-MS using a disulphide dynamic combinatorial library

To explore the AlkB active site using the DCMS approach, a library containing a variety of aliphatic, aromatic and heteroaromatic thiols was incubated with **202b** (Figure 2. 4) and

AlkB·Fe in a 1:1:1 ratio. Non-denaturing ESI-MS assays were carried out at different time points to investigate the equilibrium state of the reaction.

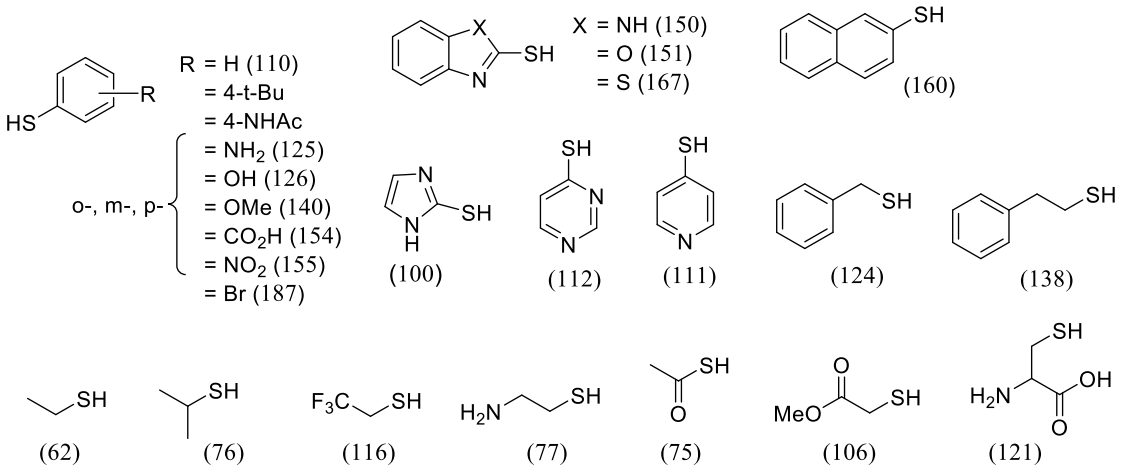

Figure 2. 4 *Thiols used in the dynamic combinatorial library. The mass of each compound is shown in parentheses (in Da).*

Without incubation (t= 0 h) the AlkB·Fe·**202b** complex (peak E) was the only adduct observed, presumably because disulphides were either not yet formed, or because any disulphides formed in solution did not bind to the protein. After 1 hour of incubation a species was observed at 17182 Da (peak F, + 124 Da relative to E). An additional peak appeared at 17211 Da (peak G, E + 153 Da) after 2 hours. In time the intensity of peak E decreased, giving higher intensity for the disulphide adduct peaks (F and G). This indicates the formation/binding of the same thiols over time (Figure 2. 5). Accordingly, *N*-oxalyl-D-cysteine (**202f**) and the thiol library were mixed with AlkB·Fe and tested for binding after 2 h. No AlkB disulphide complex peak was observed, demonstrating that disulphides formed with **202f** did not bind to AlkB·Fe (Figure 2. 5 g). This demonstrates that the adducts identified by non-denaturing ESI-MS occur from binding of disulfides formed from the L-enantiomer **202b** and thiols of masses 124 and 153 Da.

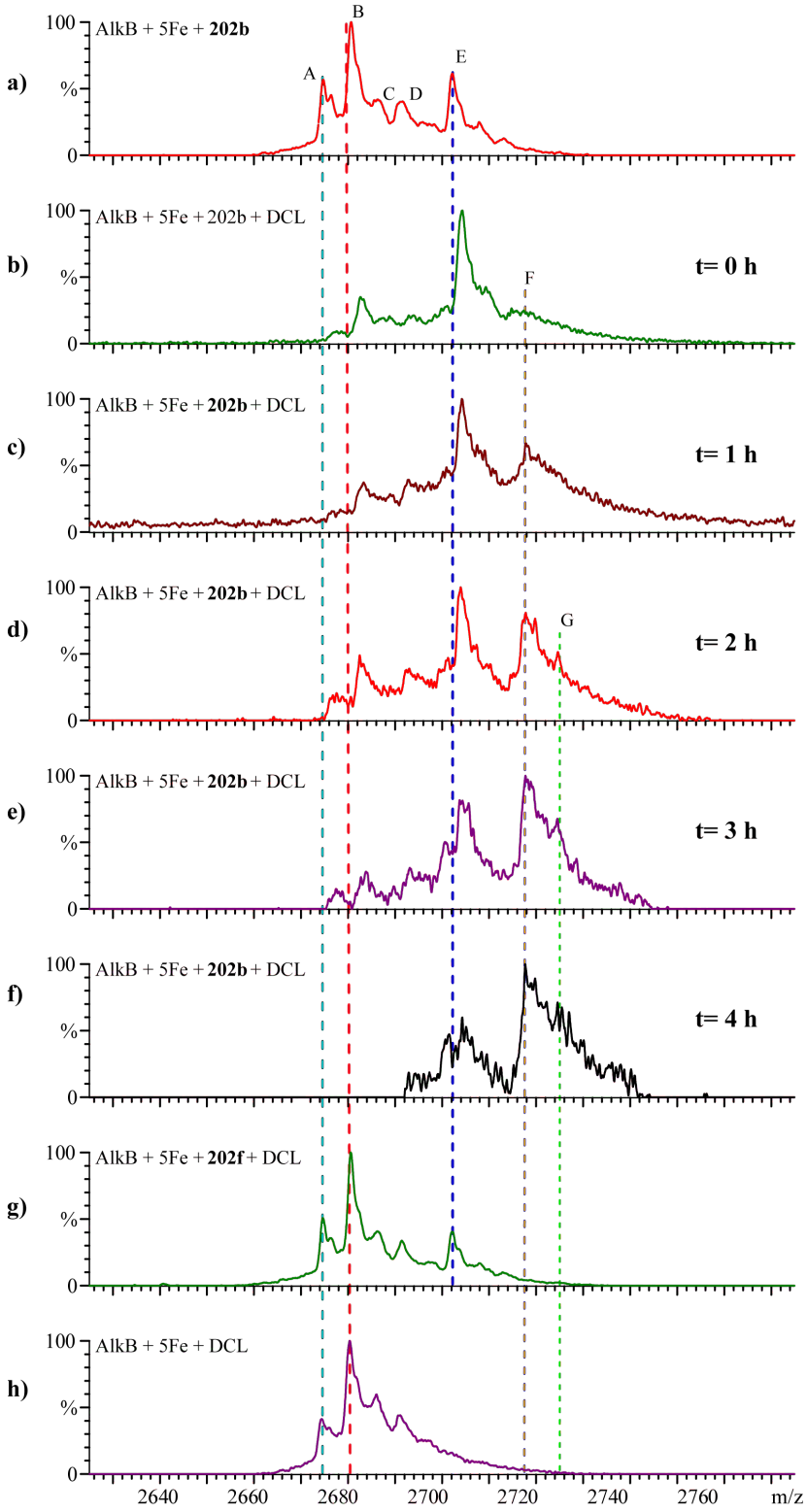

Figure 2. 5 *Non denaturing ESI-MS spectra of AlkB·Fe(II) (5 equiv.) with* ***202b*** *(1 equiv.) and the DCL (1 equiv.) at a cone voltage of 40V showing z=10. A: AlkB, B: AlkB·Fe,C: AlkB·2Fe, D: AlkB·3Fe, E: AlkB·Fe·****202b****, F,G: AlkGB·Fe·[****202b****disulphide].*

Within the library, 16 thiols with masses near 124 or 153 (±3 Da) were found and individually tested for binding with AlkB·Fe·**202b** by ESI-MS (after 10 min, Figure 2. 6a). Of these, three disulfides formed by **202b** and 2-hydroxybenzothiol (**1**), 3-hydroxybenzothiol (**2**) and 3-nitrobenzothiol (**3**) were observed to bind to AlkB·Fe (Figure 2. 6 b). These results show a preference for binding of the *ortho*- and *meta*- substituted thiols with **202b** and AlkB·Fe.

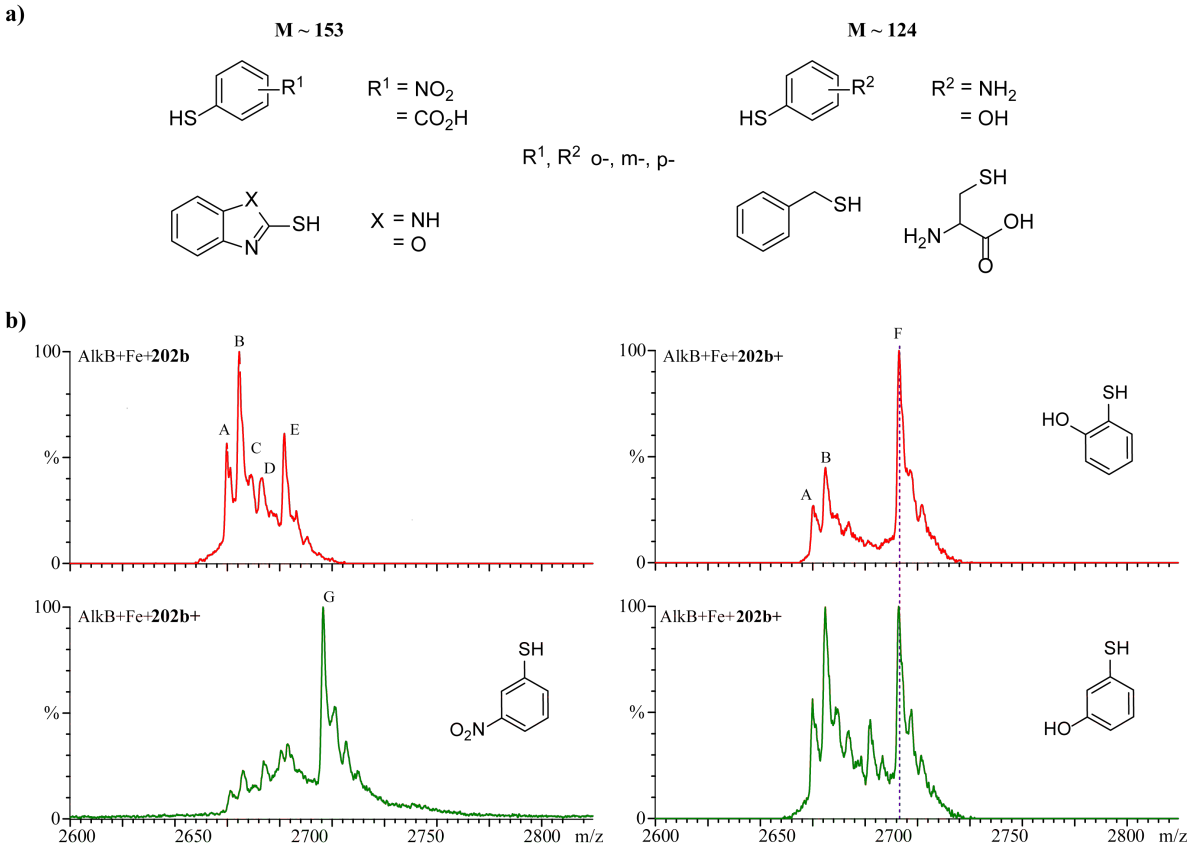

Figure 2. 6. *a) Thiols with molar masses of 153 ±3 Da and 124 ± 3 Da. b) Non denaturing ESI-MS spectra of AlkB·Fe(II) with* ***202b*** *and individual diols at a cone voltage of 40V. A: AlkB, B: AlkB·Fe, C: AlkB·2Fe, C: AlkB·3Fe, E: AlkB·Fe·****202b****, F: AlkB·Fe·(****1****,****2****), G: AlkB·Fe·****3****.*

DCMS with ***202b*** *and further controls were carried out by Dr. Esther Woon.*

2.4 Synthesis of stable *N*-oxalyl analogues

Following the identification of 'hits' from DCMS inhibitors; analogues of the disulphides which lack the cleavable disulphide (S-S) bond were synthesised (*via* nucleophilic substitution reactions on the cysteinyl thiol, Scheme 2. 2). *N*-oxalyl thioethers were initially synthesised from **201b** and tested against AlkB (**208**-**210**, Scheme 2. 2). The DSF assay (see Chapter 4) was first used to evaluate the effect of the potential inhibitors on the stability of AlkB. A capillary electrophoresis-based assay was then used to measure IC_{50} values for derivatives **208**-**210**.[24, 25] The nitro containing compound **208** displayed the strongest binding and best inhibitory activity against AlkB (ΔT_m= 4 ºC, IC_{50}= 5.2 μM) compared to the hydroxyl analogues **209** (ΔT_m= 1.3 ºC, IC_{50}= 50.4 μM) and **210** (ΔT_m= 1.8 ºC, IC_{50}= 48 μM).

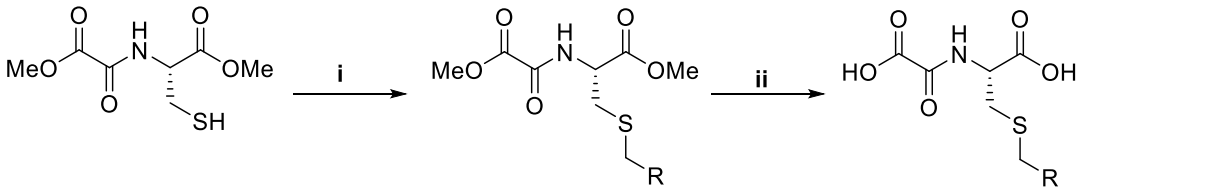

203		**208**	R = 3-nitrophenyl
204	R = 2-benzoyloxybenzyl	**209**	R = 2-hydroxybenzyl
205	R = 3-benzoyloxybenzyl	**210**	R = 3-hydroxybenzyl
206		**211**	R = 1-naphthyl
207		**212**	R = 2-naphthyl

Scheme 2. 2 *Syntheses of N-oxalyl inhibitors.*
Reagents and *Conditions*: i) RCH_2Br, Et_3N, CH_2Cl_2, r.t; ii) 1M LiOH, 1,4-dioxane, r.t.

*Synthesis of compounds **203-205** and **208-210** was performed by Dr. Esther Woon. Dr. S.M. Krylova and Dr. Eleanor Bagg carried out IC_{50} measurements and the DSF assay respectively.*

2.5 Crystallography of *N*-oxalylcysteine derivatives

The good inhibitory activity of **208** against AlkB and the small difference in activity between the 3-hydroxy thioether and the 2-hydroxy thioether suggests the presence of interactions

(presumably electrostatic and/or hydrogen bonding interactions) between the *meta*- position and side-chains in the AlkB active site.

To investigate this hypothesis, and also to aid further optimisation of the inhibitor series, crystallographic analyses were undertaken. A crystal structure of AlkB complexed with Fe(III) and **208** was obtained (PDB ID 3T4H, Figure 2. 7, 1.65 Å); the structure reveals the active site iron is coordinated by the side chains of His131, Asp133, His187 and a putative water molecule located *trans* to His131, as observed with most other AlkB structures.[26] The iron is coordinated by the oxalyl group of **208** in a bidentate manner, with the carboxamide oxygen positioned *trans* to Asp133 (2.2Å) and one of the carboxylate oxygens of **208** (2.6Å) *trans* to His187. This arrangement has been observed in other structures of 2OG oxygenases in complex with *N*-oxalylglycine and derivatives. The C-1 carboxylate oxygen not chelating the iron is positioned to form hydrogen-bonds with the side chain NH_2 of Arg210 (3.3Å) and the side chain oxygen of Asn120 (3.2Å). The carboxylic acid of **208** is positioned to form a salt bridge to Arg204 (2.9Å and 3.0Å), hydrogen-bonds with the hydroxyl group of Tyr122 (2.7Å), and to the side-chain oxygen of Asn206 (2.7Å).

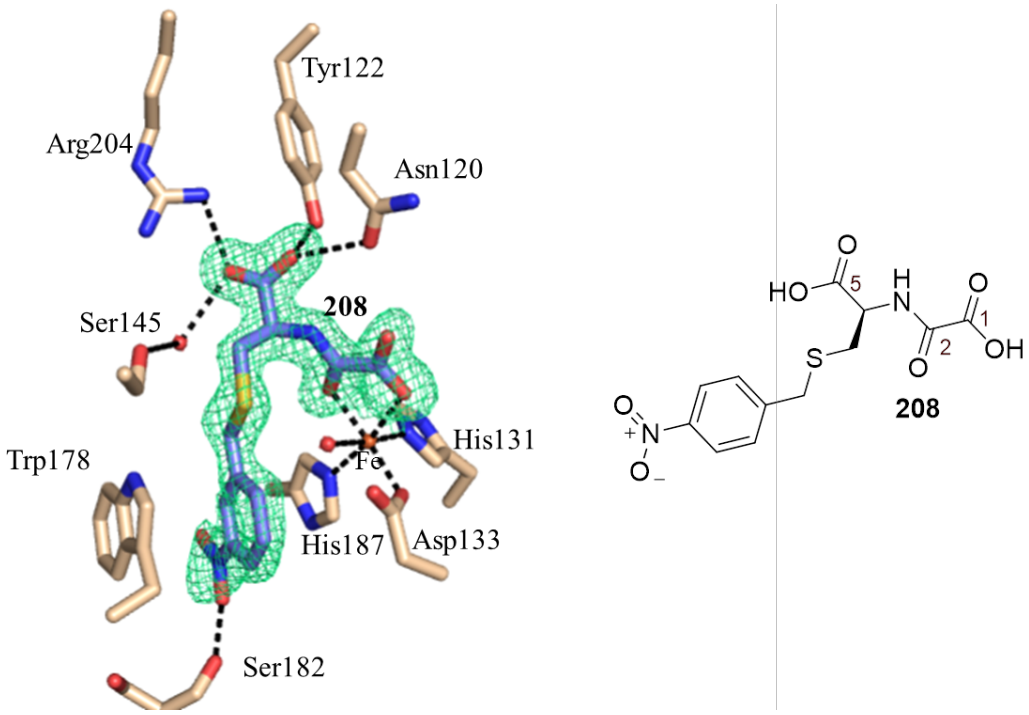

Figure 2. *7 View from the crystal structure of AlkB·Fe (beige) complexed with* ***208*** *(lilac). The image shows the salt bridge and hydrogen bonds of the carboxylic acid of* ***208*** *with amino acids side-chains and apparent π-π stacking of the 3-nitrophenol with the side chain of Trp178 in the hydrophobic pocket (contoured to 1.5σ).*

An overlay of this structure with that of AlkB·Mn in complex with 2OG (PDB ID 3I3Q)[27] reveals little difference in the overall conformation of the active site residues except for the side chain of Trp178, which is rotated slightly with respect to its position in the 2OG complex structure, to enable an apparent π-stacking interaction between the phenyl ring of **208** and the side chains of His187 and Trp178 (Figure 2. 8). The navigation of the phenyl ring of **208** into the hydrophobic sub-pocket defined by Ile143, Phe154, Trp178, Ser182 and His187 is apparently made possible through the presence of the relatively flexible modified cysteinyl linker. The complex is further stabilized by apparent hydrogen-bonding interactions between the 3-nitro group of **208** and the backbone carbonyl oxygen of Ser182 (3.3Å) (Figure 2. 7). Modelling studies suggest that similar interactions are not possible when the 3-nitro group is replaced with a hydroxyl group or with the 3-hydroxyl phenyl substituent, explaining the lower inhibitory potencies of **209** and **210** compared to **208**.

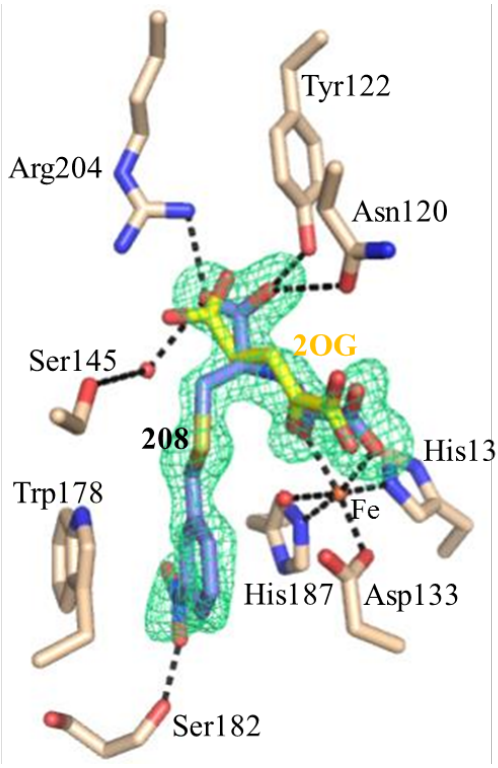

Figure 2. 8 *Superimposition of the crystal structure of AlkB·Fe (beige)·**208** (lilac) with AlkB·Mn·2OG (yellow) (PDB ID: 3I3Q). The image shows the similarity of binding of **208** and 2OG.*[23]

*Crystallographic AlkB analyses with compound **208** were performed by Jerome Ma and Dr. Michael McDonough.*

2.6 Optimisation of inhibitor scaffolds

From analysis of the crystal structure of AlkB with **208** it was proposed that larger hydrophobic substituents could be accommodated in the pocket in place of the 3-nitrobenzene group (Figure 2. 9). Compounds **211** and **212** were identified as potentially improved inhibitors synthesised *via* the same method as the other *N*-oxalyl analogues (Figure 2. 9, Scheme 2. 2). The 1-methylenenaphthalene analogue (**211**) showed very similar activity to **208** (ΔT_m= 3.8 ºC, IC_{50}= 5.4 μM). In contrast, substitution with a 2-methylenenaphthalene (**212**) provided improved inhibitory activity relative to **208**, lowering the IC_{50} tenfold (**212**, ΔT_m= 7.8 ºC, IC_{50}= 0.5 μM, Table 2. 2). The improved binding and inhibition potency of **212**

in comparison with **211** is possibly due to better accommodation of the 2-methylenenaphthalene ring in the hydrophobic active site pocket of AlkB (Figure 2. 9).

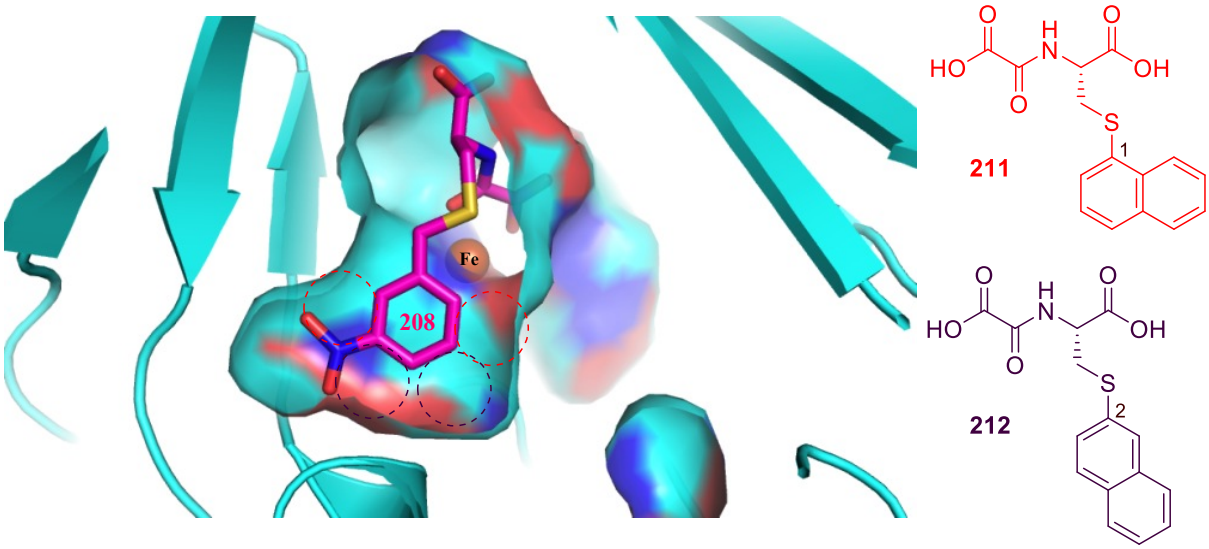

Figure 2. 9 *View of the AlkB·Fe (cyan) ·**208** (pink) structure, showing the hydrophobic pocket area and the filling of this area when expanding with the 2-naphthyl ring **212** (purple dotted circles) and with the 1-naphthyl ring **211** (red dotted circles).*

Overlaying the structures of AlkB with **208** and AlkB with substrate (PDB ID: 2FD8)[23] shows that the binding site of the 3-methylthymidine substrate extends toward the side of the oxalyl group (Figure 2. 10). To occupy this site, compounds with the oxalyl group replaced by bulkier iron chealators were synthesized. Pyridyl (**217-220**, **228-234**, Scheme 2. 3) and quinolinyl (**239-241**, Scheme 2. 4) inhibitors with the 2-methylenaphthyl and other amino acid side-chains were synthesized and tested against AlkB.

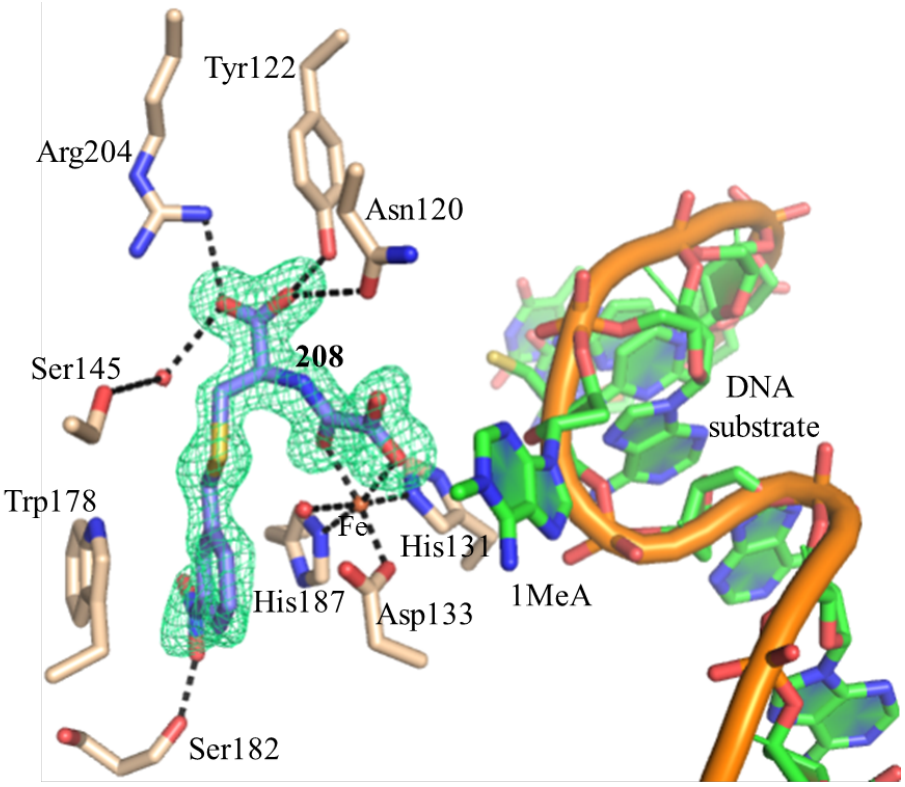

Figure 2. 10 *Superimposition of crystal structures of AlkB·Fe (beige)·**208** (lilac) with that of AlkB·Fe·**202b**·ssDNA (orange) (PDB ID: 2FD8). The image shows the area between **208** and 1MeA of the substrate which may result in improved inhibition if occupied.*[23]

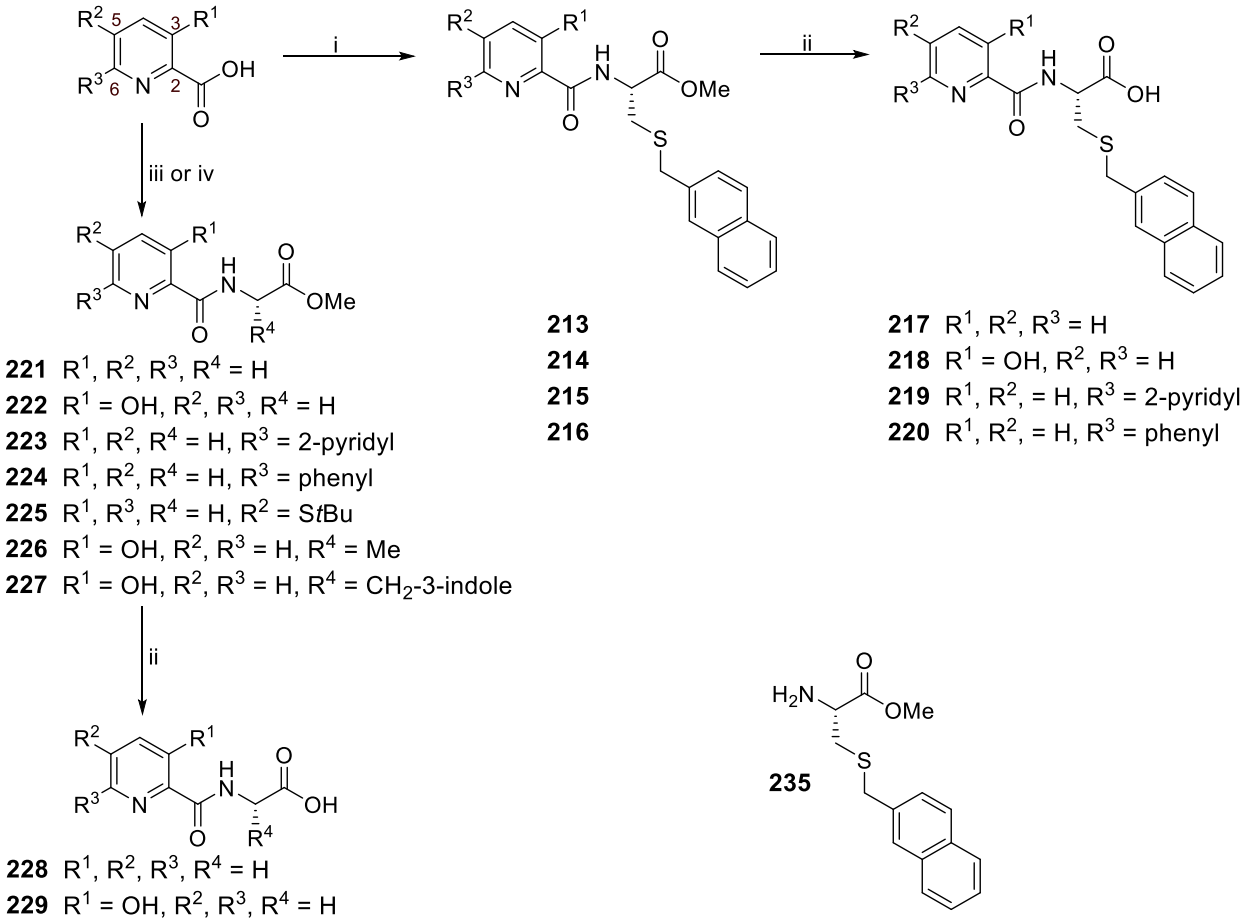

Scheme 2. 3 *Syntheses of pyridyl inhibitors.*

Reagents and Conditions: i) **235**, DIPEA, HOBT, EDCI, CH_2Cl_2, r.t; ii) 1 M LiOH, 1,4-dioxane, r.t; iii) glycine methyl ester hydrochloride, DIPEA, HOBT, EDCI, CH_2Cl_2, r.t; iv) L-alanine methyl ester hydrochloride or L-tryptophan methyl ester hydrochloride for compounds **226** and **227**, respectively, DIPEA, HOBT, EDCI, CH_2Cl_2, r.t.

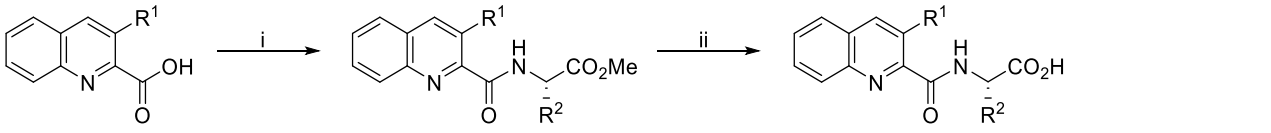

Scheme 2. 4 *Syntheses of quinolinyl inhibitors.*

Reagents and *Conditions*: i) glycine methyl ester hydrochloride (**235** for compound **237**), DIPEA, HOBT, EDCI, CH_2Cl_2; ii) 1 M LiOH, 1,4-dioaxane.

2.7 Inhibition of AlkB by heteroaromatic inhibitors

The inhibition and binding efficiencies of all compounds to AlkB were obtained. While the parent unsubstituted pyridine compound **228** is not an inhibitor of AlkB (IC_{50} > 1 mM), the compound with a substituted ring at C-6 and C-5 displayed reasonable inhibition activity (Table 2. 2). The aryl 6-substituted pyridyl compounds **230** and **231** inhibited the enzyme better than the 5-*tert*butylthio substituted pyridyl **232** (IC_{50}= 51.3 μM, IC_{50}= 54.1 μM and IC_{50}= 121 μM respectively). A substantial improvement in the potency of the pyridine-scaffold was achieved by introducing a hydroxyl-group in position C-3 of the ring **229** (ΔT_m= 8.3 ºC, IC_{50}= 3.4 μM). Surprisingly, the combination of the 3-hydroxy pyridyl scaffold with the 2-methylenenaphthyl side-chain (**218**) that provided the best *N*-oxalyl inhibitor did not result in an inhibitor as potent as either **212** or **229** (**218**, ΔT_m= 10.6 ºC, IC_{50}= 7.9 μM). However, **218** displayed better activity than the alanine- and tryptophan- substituted 3-hydroxypyridyl analogues (**233**, IC_{50}= 9.5 μM; **234**, IC_{50}= 14.1 μM). Moreover the cysteine-2-methylenenaphthyl analogues of the unsubstituted and C-6 substituted pyridines showed significantly improved IC_{50} values (**217**, IC_{50}= 17.8 μM; **219**, IC_{50}= 16.7 μM; **220**, IC_{50}= 14.7 μM) in comparison with the corresponding glycine analogues (**228**, IC_{50}> 1mM; **230**, IC_{50}= 51.3 μM; **231**, IC_{50}= 54.1 μM).

Similar trends were observed with the quinolinyl inhibitors (Scheme 2. 4). Even though the unsubstituted quinoline **239** was not a good inhibitor of AlkB (IC_{50}= 165 μM), the addition of the 2-methylenenaphthyl side chain or a C-3 hydroxyl group improved the activity (**240**, IC_{50}= 22.3 μM; **241**, IC_{50}= 42.5 μM) more than 4 fold. The higher IC_{50} values of the quinolinyl compared to pyridyl inhibitors together with the finding that the C-3 hydroxyl group with the cysteine-2-methylenenaphthyl did not improve activity in pyridyl inhibitors dissuaded us from investigating this scaffold any further.

Table 2. 2 *Melting temperatures of AlkB and inhibition results.*

Compound	ΔTm (˚C)	IC_{50} (μM)	Compound	ΔTm (˚C)	IC_{50} (μM)
208	4.0	5.2	**229**	8.3	3.4
209	1.3	50.4	**230**	0.3	51.3
210	1.8	48	**231**	-0.6	54.1
211	3.8	5.4	**232**	0.6	121
212	7.8	0.5	**233**	10.0	9.5
217	3.1	17.8	**234**	3.7	14.1
218	10.6	7.9	**239**	1.1	165
219	0.4	16.7	**240**	2.0	22.3
220	1.7	14.7	**241**	5.8	42.5
228	0.7	>1000			

To investigate the selectivity of the AlkB inhibitors developed in this study, the three most potent inhibitors (**208**, **212**, and **229**) were tested for inhibition against three other physiologically important human 2OG oxygenases: Prolyl Hydroxylase Domain 2 (PHD2), Plant Homeo Domain finger protein 8 (mutations of which are linked to midline defects[28]), and an AlkB human homologue, Fat-mass and obesity associated (FTO, see Chapter 4).[29, 30] All three compounds displayed no inhibition (IC_{50}> 1 mM) for all three enzymes investigated (except for **229** with FTO, see Chapter 4) showing a >200 fold selectivity towards AlkB.

AlkB inhibition measurements were carried out by Dr. Svetlana M. Krylova; also PHF8 and PHD2 inhibition assays were performed by Louse J. Walport and Andrew Mun Chiang Chan, respectively.

2.8 Further crystallographic analyses of AlkB inhibitors

A crystal structure of the most potent compound **212** (IC_{50}= 0.5 μM) in complex with AlkB was obtained (PDB ID 3T4V). The oxalyl-group of **212** is observed to coordinate with the active site iron in an analogous manner to that of **208** as well as the *N*-oxalyl and main chain amino acid, salt bridge interactions and hydrogen bonding (Figure 2. 11). The cysteinyl linker of **212**, however, adopts a different conformation from that of the 3-nitrobenzyl group, likely in order to preserve the π-stacking interactions of the 2-methylenenaphthalene side-chain of **212** with the side chains of His187 and Trp178 (as in the case of **208**). Analysis of the AlkB·Fe·**212** complex structure suggests that the 1-methylenenaphthalene side-chain of **211** is less able to fit into the hydrophobic sub-pocket due to steric constraints, accounting for its lower inhibitory activity (IC_{50}= 5.4 μM) compared to **212**.

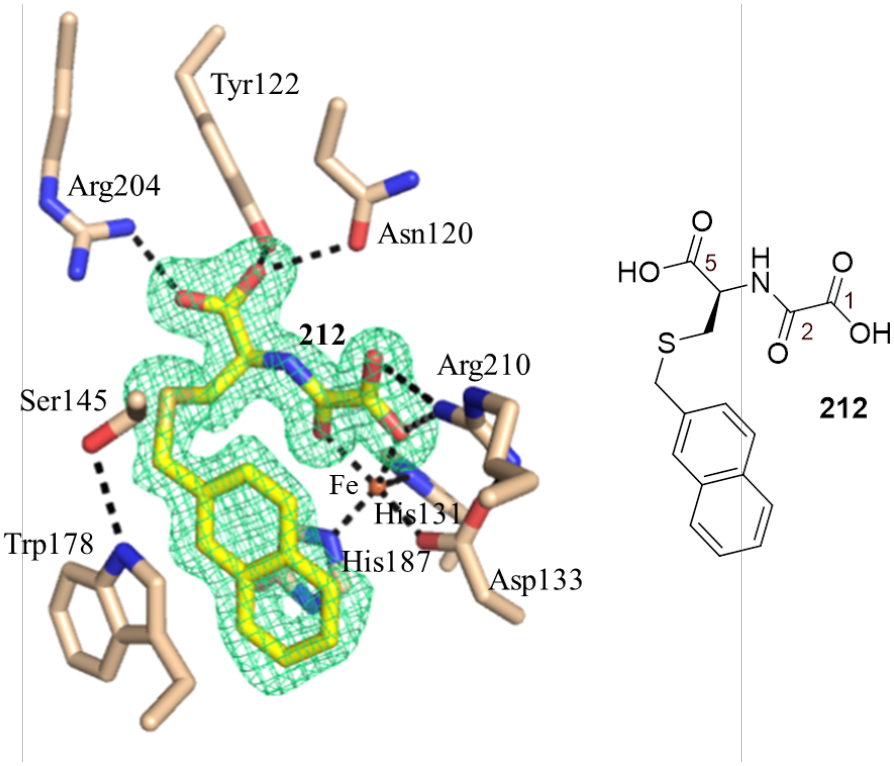

Figure 2. 11 *View from the crystal structure of AlkB·Fe (beige) complexed with* ***212*** *(yellow). The image shows the salt bridge and hydrogen bonds of the carbonyl groups of* ***212*** *with amino acids side-*

chains and the π-π stacking of the 2-methylenaphthyl group in the hydrophobic pocket (contoured to 1.5σ).

A crystal structure of AlkB in complex with the pyridyl inhibitor **229** (PDB ID: 3T3Y) was also obtained. This interestingly revealed a different mode of binding from those of the *N*-oxalyl inhibitors (**208** and **212**), where the pyridine ring, instead of occupying the same metal coordinating position as the oxalyl groups, is "flipped" with the pyridyl nitrogen (2.2 Å) *trans* to His131 and the carboxamide oxygen *trans* to Asp133 (Figure 2. 12). The different orientation of **229** resulted in partial occupation of the hydrophobic subpocket by the pyridine ring. This, may account for the difference in the AlkB inhibition potency between the heteroaromatic and *N*-oxalyl cysteinyl analogues, consistent with the decrease in potency of **218**. The side chain of Trp178 is rotated (approximately 90° about the Cα−Cβ bond and approximately 180° about the Cβ−Cγ bond) to form π-stacking interactions with the pyridine ring. The 3-hydroxyl group of **229** is positioned to participate in a hydrogen bond with the side chain hydroxyl group of Ser145 (2.1 Å), possibly accounting for the greater potencies of **229** (IC_{50}= 3.4 μM), **218** (IC_{50}= 7.9 μM), and **241** (IC_{50}= 42.5 μM) as compared to analogues without the 3-hydroxyl group (**228**, IC_{50} > 1 mM; **217**, (IC_{50}= 17.8 μM; **239**, IC_{50}= 165 μM respectively).

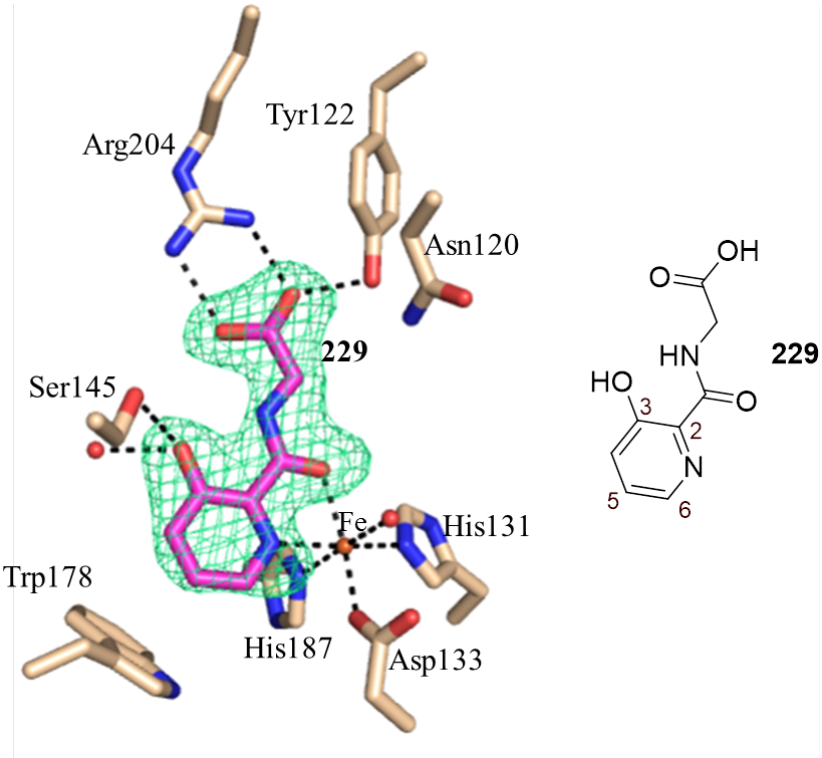

Figure 2. 12 *View from the crystal structure of AlkB·Fe (beige) complexed with* ***229*** *(pink). The image shows the salt bridge and hydrogen bonds of* ***229*** *with amino acid side-chains and rotation of the pyridine ring chelating the iron differently from the oxalyl analogues which results in partial occupation of the hydrophobic pocket (contoured to 1.5σ).*

Crystals were grown and crystal structures were obtained and processed by Wei Shen Aik.

2.9 Conclusions

Dynamic combinatorial mass spectrometry (DCMS) with thiol/disulphide interchange has been successfully used for the identification of lead compounds for the inhibition of AlkB. The results using ESI-MS in the gas phase correlated well with the solution phase binding DSF assay results and with inhibitory potency.[31] Inhibitors functionalised with L-amino acids have provided the first selective inhibitors for AlkB; for some oxygenases, inhibitors containing D-amino acids have been shown to be more selective.[20, 32] Overall the inhibitors identified in this study as well as the crystallographic studies shall be useful starting points

for the development of even more potent inhibitors of human AlkB (AlkBH 1-8) homologues.

2.10 Acknowledgements

Many thanks to Dr. Svetlana M. Krylova under the supervision of Dr. Sergey N. Krylov from York University in Torondo for the electrophoresis AlkB inhibition measurement, also Louise J. Walport and Andrew Mun Chiang Chan for the inhibition studies on PHF8 and PHD2. Special thanks to Dr. Esther Woon for the initial ESI-MS binding of the *N*-oxalyl amino acids, the DCMS of **202b** with thiols, and the synthesis of the initial *N*-oxalyl inhibitors. Also thanks to Dr. Eleanor Bagg for providing AlkB and carrying out DSF experiments. Finally, many thanks to Wei Shen Aik and Jerome Ma for the crystallographic studies and analyses.

2.11 Experimental details

AlkB expression and purification

AlkB and ΔN11 AlkB proteins were expressed and purified as described.[23, 33] BL21 (DE3) *E. coli* transformed with pET24a AlkB or ΔN11 AlkB were grown at 37 ºC and 220 rpm to an OD_{600} of 0.6. Protein expression was induced by addition of 0.2 mM IPTG (Melford Laboratories Ltd). Growth was continued at 28 ºC for 4 h (AlkB) or 15 ºC for 16 h (ΔN11 AlkB), then cells were harvested by centrifugation. The resulting cell pellet was stored at -80ºC. Cell pellets were resuspended to homogeneity in 0.1 M MES, pH 5.8, 1 mM $MgCl_2$, 1x Roche complete EDTA-free protease inhibitor cocktail. Cells were lysed on ice by sonication, and the lysate cleared by centrifugation and filtration. AlkB was purified from the crude cell lysate by cation exchange chromatography using a 50 mL S sepharose column, with elution achieved by application of a gradient to 1 M NaCl. Further purification was achieved by gel

filtration using a 300 mL Superdex 75 column (Pharmacia) in a buffer of 50 mM HEPES pH 7.5.

Non-denaturing ESI-MS studies

All 37 thiols used for DCL generation were from Sigma-Aldrich or Alfa Aesar. AlkB was desalted using a Bio-Spin 6 Column (Bio-Rad, Hemel Hempstead, U.K.) in 15 mM ammonium acetate (pH 7.5). The stock solution was diluted with the same buffer to a final concentration of 100 μM. $Fe(NH_4SO_4)_2 \cdot 6H_2O$ was dissolved in 20 mM HCl at a concentration of 100 mM. This was then diluted with Milli-Q water to give final working concentrations of 500 μM. The protein was mixed with Fe(II) and an inhibitor to give final concentrations of 15 μM AlkB, 75 μM Fe(II), and 15 μM inhibitor. The solution was then incubated for 30 min at room temperature prior to ESI-MS analysis.

Mass spectrometric data were acquired using a Q-TOF mass spectrometer (Q-TOF micro, Micromass, Altrincham, U.K.) interfaced with a NanoMate (Advion Biosciences, Ithaca, NY) with a chip voltage of 1.70 kV and a delivery pressure of 0.25 psi. The sample cone voltage was typically 80 V with a source temperature of 40 ºC and with an acquisition/scan time of 10 s/1 s. Calibration and sample acquisition were performed in the positive ion mode in the range of 500-5000 m/z. The pressure at the interface between the atmospheric source and the high vacuum region was fixed at 6.40 mbar. External instrument calibration was achieved using sodium iodide. Data were processed with the MassLynx 4.0 (Waters).

Differential Scanning Fluorimetry (DSF)[22]

DSF was performed using a MiniOpticon™ Real-Time PCR Detection System (Bio-Rad), monitoring protein unfolding using SYPRO orange (Invitrogen) according to reported method. [22] FAM (492 nm) and ROX (610 nm) filters were used for excitation and emission respectively. Reaction mixes contained 2 μM protein, 50 μM Mn(II), 200 μM compounds, 1x SYPRO orange in a final volume of 50 μL. Reagents were prepared in HEPES buffer except metals, which were dissolved as 100 mM stocks in 20 mM HCl, then further diluted in MilliQ

water. Compounds tested were prepared in 100% DMSO and added such that the final concentration of DMSO was 5 % (v/v).

Fluorescence readings were taken every 1 ºC in the range 25-95 ºC, with the temperature increased linearly by 1 ºC min^{-1}. The software provided was used to perform global minimum subtraction. The inflection point, representing T_m, was calculated by fitting the Boltzmann equation to the sigmoidal curves obtained; data were processed using GraphPad Prism 5.0™. The T_m shift caused by the addition of small molecules/ fragments was determined by subtraction of the "reference" T_m (protein incubated with metal and 5 % DMSO) from the T_m obtained in the presence of the compound.[35] Conditions were tested in triplicate, with standard deviations typically < 1 ºC.

Inhibition assays for AlkB[24, 25]

Synthetic fluorescently labeled DNA substrate (5'-TTC$_m$TTTTTTTTTTT-3'-fluorescein), and product (5'-TTCTTTTTTTTTTT-3'-fluorescein) were produced by ATDBio (University of Southampton, UK). All other chemicals were purchased from Sigma-Aldrich (Toronto, ON). An uncoated fused-silica capillary was purchased from Polymicro Technologies (Phoenix, AZ). All solutions were made using deionized water filtered through a 0.22 μm filter (Millipore, Nepean, ON).

All experiments were conducted using an uncoated fused silica capillary with a total length of 50 cm (40 cm to the detection window), inner diameter of 75 μm and outer diameter of 365 μm. The capillary was mounted on a P/ACE MDQ capillary electrophoresis (CE) instrument (Beckman Coulter, Fullerton, CA) with temperature control to keep the capillary at 15 ºC. A sample was introduced into the capillary by a pressure pulse of 0.5 psi for 5 s. The reaction product (P) and substrate (S) were then separated by CE at 20 kV and quantitated with laser-induced fluorescence (LIF) detection (fluorescence excitation at 488 nm and fluorescence detection at 520 nm). The CE run buffer for kinetic and inhibition studies was 20 mM Borax, 60 mM SDS at pH 8.0.

The enzymatic reaction was initiated by the addition of AlkB protein to a mixture containing the incubation buffer (50 mM Tris-HCl pH 7.5), 4 mM AA, 160 μM 2OG, 80 μM $Fe(NH_4SO_4)_2 \cdot 6H_2O$, 100 nM 5'-$TTC_m$TTTTTTTTTTTT-3'-fluorescein, and 2154 units of catalase. The relative activity of AlkB was measured using 5 nM AlkB, and 100 nM oligonucleotide substrate, while varying the inhibitor concentration in the range 1 to 1000 μM. The enzymatic reactions were incubated for 4.5 min at room temperature and stopped by adding a pre-chilled EDTA solution (5 mM final concentration). The demethylated DNA product formed was separated from the unreacted substrate by CE and quantified with LIF. The relative activity of AlkB at different inhibitor concentrations was plotted against the inhibitor concentration, and the IC_{50} values were calculated as the concentration of inhibitor reducing the enzymatic activity to half its maximal level, using the OriginPro 8.0 software.

Inhibition Assays for PHF8[29] and PHD2

Reaction mixtures consisted of PHF8 (2 μM), Fe(II) (10 μM), ascorbate (100 μM), 2OG (20 μM) H3(1-14)K4me3K9me2 peptide (20 μM) and inhibitor (1mM) in 1% DMSO, 500 mM NaCl, 100 mM HEPES (pH 7.5). PHF8, Fe (II), ascorbate and inhibitors were preincubated at 37 ºC for 15 min before addition of 2OG and peptide. Reactions were incubated at 37ºC for 20 min prior to 1:1 quenching with methanol. Product formation was assessed by MALDI-TOF; 1 μL quenched reaction was mixed with 1 μL α-cyano-4-hydroxycinnamic acid and spotted onto a MALDI-TOF plate for analysis.[29] Inhibition levels were measured relative to an inhibitor free reaction. Inhibition assay methods for PHD2 will be reported elsewhere. Details of the *N*-terminally truncated PHD2 was prepared as reported.[21]

Protein crystallography

Crystals of AlkB in complex with **208**, **212**, and **229** were grown in sitting drops at 293K using vapor diffusion methods. The ratio of protein to reservoir solution for the AlkB·**208** and AlkB·**212** co-crystallization drops was 2:1 (300 nL total drop volume) and for AlkB·**229** was 1:1 (200 nL total drop volume) and the reservoir volume was 80 μL. The AlkB protein

solution contained 10.1 mg/mL protein, 50 mM HEPES pH 7.5, 2.2 mM ammonium iron (II) sulfate, and 5.7 mM **208** or 1 mM **212**. The protein solution for the AlkB·**229** complex contained the same except the ammonium iron (II) sulfate concentration was 0.44 mM and **229** was 1 mM. The reservoir solution for AlkB·**208** contained 0.2 M sodium chloride, 0.1 M HEPES pH 7.5 and 25% w/v polyethylene glycol (PEG) 3350; for AlkB:**212**, 0.2 M ammonium sulfate, 0.1 M tris-hydrochloride pH 8.5 and 25% w/v PEG 3350; for AlkB:**229**, 0.1 M bis-tris pH6.5 and 25% w/v PEG 3350. The crystals were cryocooled using well solution diluted to 25% v/v glycerol and flash cooled in an Oxford Cryosystems nitrogen gas stream. Data were collected from a single crystal at 100K using a Rigaku FR E+ Superbright diffractometer equipped with a copper rotating anode, Osmic HF optics, and a Saturn 944+ CCD detector. The data were indexed, integrated, and scaled using HKL2000[34] and the structure was determined by molecular replacement using the AutoMR (PHASER) [35] subroutine in PHENIX[36] with PDB ID 2FDJ [23] as a search model for AlkB·**208** and 3T4H (PDB ID) as a search model for AlkB·**212** and AlkB·**229**. Iterative rounds of model building and refinement using COOT[37] and PHENIX[37] were performed until the decreasing R and R_{free} no longer converged. The final R-factors for the models were; AlkB·**208**, R = 15.9% and R_{free}=18.7%; AlkB·**212**, R = 16.1% and R_{free} = 20.2%; AlkB·**229**, R = 18.2% and R_{free} = 22.1%.

Table 2. 3 *Crystallographic data collection and refinement statistics.*

	AlkB·208	**AlkB·212**	**AlkB·229**
PDB ID	3T4H	3T4V	3T3Y
Resolution Range (Å) [#]	21.14 - 1.60 (1.66 - 1.60)	22.99 - 1.70 (1.76 - 1.70)	22.91 - 2.00 (2.07 - 2.00)
Space Group	*P*1	*P*1	*P*1
Unit Cell Dimensions (*a* Å, *b* Å, *c* Å, α°, β°, γ°)	36.661, 38.830, 40.274, 77.640, 75.440, 66.420	37.070, 39.234, 40.261, 76.330, 74.560, 65.280	36.813, 38.594, 40.487, 71.250, 72.210, 66.700
Total Number of Reflections Observed	89589	90015	46973
Number of Unique Reflections[#]	24608 (2161)	20297 (1776)	12688 (1260)
Redundancy[#]	3.6 (2.3)	4.4 (1.9)	3.7 (3.2)
Completeness (%)[#]	95.6 (84.0)	93.2 (81.2)	99.2 (97.9)
I/σ(I) [#]	14.2 (4.5)	9.3 (2.9)	25.2 (4.3)
[§]R_{merge} **(%)**[#]	8.2 (22.6)	10.7 (28.2)	4.3 (21.8)
[*]R_{cryst} **(%)**	15.9	16.1	18.2
[†] R_{free} **(%)**	18.7	20.2	22.1
[¶]**RMS Deviation**	0.010 (1.44°)	0.011 (1.49°)	0.010 (1.25°)
[‡]**Average *B* Factor (Å^2)**	26.4 (31.6)	27.7 (22.5)	37.8 (31.6)
Number of Water Molecules	226	282	129

Chemical synthesis

Reagents and solvents were from Aldrich or Alfa Aesar. Reactions were monitored by TLC, which was performed on precoated aluminum-backed plates (Merck, silica 60 F254). Melting points were determined using a Leica Galen III hot-stage melting point apparatus and microscope. Specific rotation was measured in a Perkin Elmer 341 Polarimeter at 20 ºC in

$deg dm^{-1} cm^3 g^{-1}$. Infrared spectra were recorded from KBr discs or neat, on a Bruker Tensor 27 FT-IR spectrometer. NMR spectra were acquired using a Bruker DPX500 NMR spectrometer. Chemical shifts (δ) are given in ppm, and the multiplicities are given as singlet (s), doublet (d), triplet (t), quartet (q), multiplet (m), broad (br). Coupling constants *J* are given in Hz (± 0.5 Hz). High resolution mass spectra (HRMS) were recorded using Bruker MicroTOF. The purity of all compounds synthesized were ≥95% as determined by analytical reverse-phase HPLC (Ultimate 3000). The synthesis and characterization of compound **241** and **239** were as reported in [38] and, [39] respectively.

General procedure A

To a solution of the methyl ester (1 equiv.) in MeOH/EtOAc (1:1), 1M sodium hydroxide (6 equiv.) was added dropwise at 0 ºC. The mixture was stirred for 1 h, then allowed to warm to room temperature overnight, after which, it was evaporated *in vacuo*. The resulting residue was resuspended in H_2O, acidified with aqueous 1 M HCl to pH 2 and extracted with EtOAc. The organic layer was washed (saturated $NaHCO_3$, H_2O, brine), dried over Na_2SO_4 and evaporated *in vacuo*.

General procedure B

To a stirred solution of aromatic acid (1 equiv.) in dry CH_2Cl_2 (20mL) under N_2, hyrdoxybenzotriazole (HOBT, 1.2 equiv.), 1-ethyl-3-(3-dimethylaminopropyl) carbodiimide (EDCI, 1.2 equiv.) and diisopropylethylamine (DIPEA, 2 equiv.) were added. The mixture was stirred for 10 min and glycine methyl ester hydrochloride (1.1 equiv.) was added. The reaction mixture was stirred until consumption of starting material. The mixture was washed with water and the organic layer was dried over $MgSO_4$ and concentrated *in vacuo*. The crude oil was chromatographed (Hexane/ EtOAc 7:3 to 5:5).

General procedure C

To a solution of the methyl ester (1 equiv.) in 1,4-dioxane (5 mL), 1M lithium hydroxide (2 equiv.) was added. The mixture was stirred at room temperature for 24 h until consumption of starting material and then acidified with acetic acid to pH 3 and diluted with CH_2Cl_2. The solution was washed with water, dried over $MgSO_4$ and concentrated *in vacuo*.

Methyl-*N*-(3-methoxy-3-oxopropanoyl)-L-cysteinate 201b

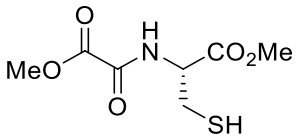

Monomethyl oxalyl chloride (2.94 mL, 32.0 mmol) was added dropwise to a mixture of *L*-cysteine methyl ester hydrochloride (5.00 g, 29.1 mmol) and Et_3N (8.9 mL, 64.0 mmol) in anhydrous CH_2Cl_2 (100 mL) at 0 ºC. The mixture was then stirred at room temperature for overnight, after which it was evaporated *in vacuo*. The resulting residue was dissolved in EtOAc, washed (sat. $NaHCO_3$, H_2O, brine), dried over Na_2SO_4 and evaporated *in vacuo*. Chromatography (hexane/EtOAc 1:1) afforded **201b** (6.43 g, 100 %) as a pale yellow oil. R_f = 0.4. IR (neat) ν/cm^{-1}: 3346 (NH), 1743 (MeOC=O), 1615 (NHC=O); ^{1}H NMR (500 MHz, $CDCl_3$) δ 7.88 (1H, br. s, N*H*), 4.75-4.70 (1H, m, C*H*), 3.93 (3H, s, $COCO_2CH_3$), 3.82 (3H, s, CO_2CH_3), 2.95 (1H, dd, *J*= 14.0 5.0, CH_2SH), 2.90 (1H, dd, *J*= 14.0 5.0, CH_2SH); ^{13}C NMR (125 MHz, $CDCl_3$) δ 169.3 (*C*=O), 160.2 (*C*=O), 155.9 ($COCO_2CH_3$), 54.1 ($COCO_2CH_3$), 53.8 (CO_2CH_3), 53.1 (*C*H), 26.3 (CH_2SH); HRMS (ESI$^+$) calcd. for $C_7H_{11}NNaO_5S$ $[M+Na]^+$ 244.0250; Found 244.0253.

***N*-(carboxyacetyl)-L-cysteine 202b**

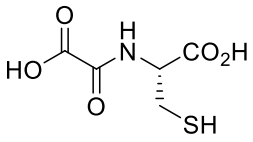

Following general procedure A, to a mixture of **201b** (0.57 g, 1.7 mmol) in MeOH (20 mL), 1 M NaOH (10.00 mL, 10.0 mmol) was added dropwise at 0 ºC. This afforded **202b** (0.38 g, 73%) as a white solid, mp 159-160 ºC. IR (neat) ν/cm^{-1} 3010-3364 (NH and OH), 1645 (NHC=O), 1524 (C=O); ^{1}H NMR (500 MHz, MeOD-*d*$_4$) *δ* 4.67 (1H, dd, *J*= 6.5 4.5, C*H*), 3.09 (1H, dd, *J*= 14.0 5.0, C*H*$_2$SH), 3.01 (1H, dd, *J*= 14.0 6.5, C*H*$_2$SH); ^{13}C NMR (125 MHz, MeOD-*d*$_4$) *δ* 177.4 (*C*=O), 166.6 (*C*=O), 165.5 (*C*=O), 55.9 (*C*H), 35.4 (*C*H$_2$SH); HRMS (ESI$^-$) calcd. for $C_5H_6NO_5S$ $[M-H]^-$ 191.9972; Found 191.9968.

Methyl *N*-(3-methoxy-3-oxopropanoyl)-*S*-(naphthalen-1-ylmethyl)-L-cysteinate 206

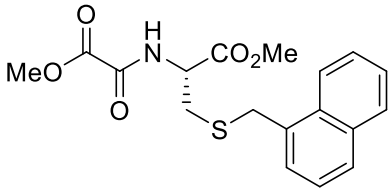

Triethylamine (0.5 mL, 3.39 mmol) was added dropwise to a solution of **201b** (0.5 g, 2.26 mmol) and 1-bromomethylnaphthalene (0.55 g, 3.39 mmol) in anhydrous CH_2Cl_2 (20 mL) at 0 ºC. The mixture was allowed to warm to room temperature overnight, after which, it was washed (H_2O, brine), dried over $MgSO_4$ and evaporated *in vacuo*. Chromatography (hexane /EtOAc 6:4 to 7:3) afforded **206** (0.30 g, 37%) as a white solid, mp 111-113 ^{o}C. R_f = 0.25. $[\alpha]_D$= -174.8 (c= 1.00 x 10^{-3}, MeOH). IR (neat) *ν*/cm^{-1} 3344 (NH), 1743 (MeOC=O), 1708 (MeOC=O), 1618 (NHC=O); ^{1}H NMR (500 MHz, $CDCl_3$) δ 8.09 (1H, d, *J*= 8.5, Ar C*H*), 7.88-7.86 (1H, m, Ar C*H*), 7.80 (1H, dd, *J*= 3.5 2.0, Ar C*H*), 7.71 (1H, d, *J*= 7.5, Ar C*H*), 7.58-7.50 (2H, m, Ar C*H*), 7.43-7.38 (2H, m, Ar C*H*), 4.87-4.83 (1H, m, C*H*), 4.21 (1H, d, *J*= 13.0, C*H*$_2$), 4.17 (1H, d, *J*= 13.0, C*H*$_2$), 3.92 (3H, s, CO_2CH_3), 3.72 (3H, s, CO_2CH_3), 3.02 (1H, dd, *J*= 14.0 5.0, SC*H*$_2$), 2.95 (1H, dd, *J*= 14.0 5.0, SC*H*$_2$); ^{13}C NMR (125 MHz, $CDCl_3$) δ 170.0 (*C*=O), 160.1 (CO_2CH_3), 155.9 (CO_2CH_3), 134.1 (Ar *C*), 132.5 (Ar *C*), 131.2 (Ar *C*),

128.8 (Ar *C*H), 128.5 (Ar *C*H), 127.5 (Ar *C*H), 126.2 (Ar *C*H), 125.9 (Ar *C*H), 125.1 (Ar *C*H), 123.9 (Ar *C*H), 53.8 (CO_2CH_3), 52.9 (CO_2CH_3), 52.2 (*C*H), 34.5 (SCH_2), 33.5 (SCH_2); HRMS (ESI^+) calcd. for $C_{18}H_{19}NNaO_5S$ $[M+Na]^+$ 384.0876; Found 384.0876.

Methyl *N*-(3-methoxy-3-oxopropanoyl)-*S*-(naphthalen-2-ylmethyl)-L-cysteinate 207

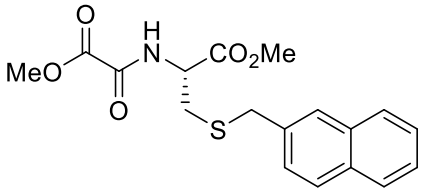

To a solution of **201b** (0.50 g, 2.26 mmol) and 2-bromomethylnaphthalene (0.55 g, 2.49 mmol) in anhydrous CH_2Cl_2 (40 mL) triethylamine (0.4 mL, 2.94 mmol) was added dropwise at room temperature. The mixture was stirred at room temperature for 18 h, washed (H_2O), dried over $MgSO_4$ and evaporated *in vacuo*. Chromatography (hexane/EtOAc 6:4) afforded **207** (0.36 g, 43%) as a white solid, mp 87-90 ºC. R_f= 0.35. $[\alpha]_D$= -67.1 (c= 2.56x10^{-3}). IR (neat) *v*/cm^{-1} 3303 (NH), 1735 (RNHC=O); ^{1}H NMR (500 MHz, $CDCl_3$) δ 7.83-7.81 (3H, m, ArC*H*), 7.71 (1H, d, *J*= 6.5, ArC*H*), 7.51-7.45 (3H, m, ArC*H*), 4.85-4.81 (1H, m, C*H*), 3.90 (3H, s, $COCO_2CH_3$), 3.91-3.88 (2H, m, SCH_2), 3.75 (3H, s, CO_2CH_3), 2.96 (1H, dd, *J*= 14.0 5.0, SCH_2), 2.89 (1H, dd, *J*= 14.0 6.0, SCH_2); ^{13}C NMR (125 MHz, $CDCl_3$) δ 170.0 (*C*=O), 160.2 (*C*=O), 155.9 (*C*=O), 134.6 (Ar *C*), 133.2 (Ar *C*), 132.6 (Ar *C*), 128.6 (Ar CH), 127.7 (Ar *C*H), 127.7 (Ar *C*H), 127.6 (Ar *C*H), 126.8 (Ar *C*H), 126.3 (Ar *C*H), 126.0 (Ar *C*H), 53.8 ($COCO_2CH_3$), 52.9 (CO_2CH_3), 52.0 (*C*H), 36.8 (SCH_2), 32.85 (SCH_2); HRMS (ESI^+) calcd. for $C_{18}H_{19}NNaO_5S$ $[M+Na]^+$ 384.0876; Found 384.0877.

***N*-(carboxyacetyl)-*S*-(naphthalen-1-ylmethyl)-L-cysteine 211**

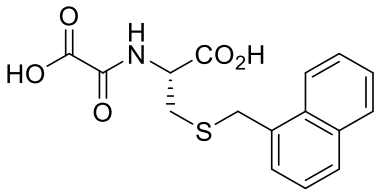

Following general procedure A, to a solution of **206** (0.17 g, 0.47 mmol) in MeOH (10 mL) 1 M NaOH (0.9 mL, 0.9 mmol) was added. Washing with Et_2O (3 mL) afforded **211** (0.10 g, 64%) as a white solid, mp >300 ºC. $[\alpha]_D$= -5.9 (c= 1.10 x 10-3, MeOH). IR (neat) ν/cm^{-1} 3292 (N-H), 3000 (COO-H), 1759 (HOC=O), 1728 (HOC=O), 1663 (NHC=O); ^{1}H NMR (500 MHz, MeOD-*d*$_4$) δ 8.18 (1H, d, *J*= 8.5, Ar C*H*), 7.81 (1H, d, *J*= 8.0, Ar C*H*), 7.89-7.88 (1H, m, Ar C*H*), 7.56-7.40 (4H, m, Ar C*H*), 4.75 (1H, dd, *J*= 8.0 4.5, C*H*), 4.30 (1H, d, *J*= 12.5, SC*H*$_2$), 4.27 (1H, d, *J*= 12.5, SC*H*$_2$), 3.12 (1H, dd, *J*= 14.0 5.0, SC*H*$_2$), 2.96 (1H, dd, *J*= 14.0 5.5, SC*H*$_2$); ^{13}C NMR (125MHz, MeOD-*d*$_4$) δ 172.9 (*C*O_2H), 162.4 (*C*O_2H), 160.1 (*C*ONH), 135.7 (Ar *C*), 134.6 (Ar *C*), 132.8 (Ar *C*), 129.7 (Ar *C*H), 129.3 (Ar *C*H), 128.6 (Ar *C*H), 127.1 (Ar *C*H), 126.9 (Ar *C*H), 126.2 (Ar *C*H), 125.4 (Ar *C*H), 53.6 (*C*H), 34.9 (*C*H_2), 34.0 (*C*H_2); HRMS (ESI$^-$) calcd. for $C_{16}H_{14}NO_5S$ $[M-H]^-$ 332.0598; Found 332.0603.

***N*-(carboxyacetyl)-*S*-(naphthalen-2-ylmethyl)-L-cysteine 212**

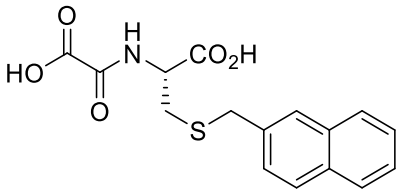

Following general procedure A, to a solution of **207** (0.17 g, 0.47 mmol) in MeOH (10 mL) 1 M NaOH (0.9 mL, 0.9 mmol) was added. Washing with Et_2O afforded **212** (0.07 g, 50%) as a white solid, mp 159-160 ºC. $[\alpha]_D$= -43.6 (c= 1.01x10^{-3}). IR (neat) ν/cm^{-1} 3309 (N-H), 3235 (COO-H), 1748 (HOC=O), 1726 (C=O), 1639 (NHC=O); ^{1}H NMR (500 MHz, MeOD-*d*$_4$) δ 7.84-7.81 (3H, m, Ar C*H*), 7.76 (1H, s, Ar C*H*), 7.51-7.46 (3H, m, Ar C*H*), 4.71-4.68 (1H, m, C*H*), 3.95 (2H, s, C*H*$_2$), 3.04 (1H, dd, *J*= 14.0 4.5, SC*H*$_2$), 2.92 (1H, dd, *J*= 14.0 5.0, SC*H*$_2$); ^{13}C NMR (125MHz, MeOD-*d*$_4$) δ 172.6 (*C*=O), 136.6 (Ar *C*), 134.7 (Ar *C*), 134.1 (Ar *C*),

129.5 (Ar *C*H), 129.3 (Ar *C*H), 128.7 (Ar *C*H), 128.2 (Ar *C*H), 127.3 (Ar *C*H), 127.1 (Ar *C*H), 126.9 (Ar *C*H), 53.9 (*C*H), 37.2 (S*C*H_2), 33.1 (S*C*H_2); HRMS (ESI^-) calcd. for $C_{16}H_{14}NO_5S$ $[M-H]^-$ 332.0598; Found 332.0595.

(*R*)-Methyl *S*-(naphthalen-2-ylmethyl)-*N*-(pyridin-2-ylcarbonyl)cysteinate 213

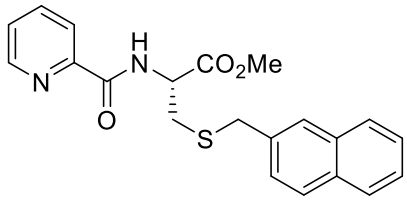

Following general procedure B, picolinic acid (0.09 g, 0.73 mmol) in anhydrous CH_2Cl_2 (10 mL) under N_2, DIPEA (0.14 mL, 0.80 mmol), HOBT (0.12 g, 0.88 mmol), and EDCI (0.18 mL, 0.88 mmol) were stirred for 10 min and **235** (0.20 g, 0.73 mmol) was added. The reaction mixture was stirred for 3 d until consumption of starting material. Chromatography (hexane/EtOAc 8:2 to 6:4) afforded **213** (0.16 g, 58 %) as yellow oil. R_f = 0.09. $[\alpha]_D$= -51.6 (c= 2.09 x 10^{-3}, MeOH). IR (neat) ν/cm^{-1} 3380 (N-H), 1753 (MeOC=O), 1678 (NHC=O); ^{1}H NMR (500 MHz, $CDCl_3$) δ 8.73 (1H, d, *J*= 8.0, N*H*), 8.62-8.61 (1H, m, ArC*H*), 8.19-8.17 (1H, m, Ar C*H*), 7.86 (1H, td, *J*= 7.5 1.5, Ar C*H*), 7.80-7.76 (3H, m, Ar C*H*), 7.81 (1H, s, Ar C*H*), 7.48-7.44 (4H, m, Ar C*H*), 5.07-5.03 (1H, m, C*H*), 3.93 (2H, s, SCH_2), 3.77 (3H, s, CH_3), 3.03 (1H, dd, *J*= 14.5 5.0, SCH_2), 2.92 (1H, dd, *J*= 14.5 5.0, SCH_2); ^{13}C NMR (125MHz, $CDCl_3$) δ 171.1 (*C*=O), 164.1 (*C*=O), 149.1 (Ar *C*), 148.3 (Ar CH), 137.3 (Ar *C*), 134.8 (Ar *C*H), 133.2 (Ar *C*H), 132.55 (Ar *C*H), 128.5 (Ar *C*H), 127.65 (Ar *C*H), 127.6 (Ar *C*H), 127.0 (Ar *C*H), 126.5 (Ar *C*H), 126.2 (Ar *C*H), 125.8 (Ar *C*), 122.3 (Ar *C*H), 52.7 (O*C*H_3), 52.0 (*C*H), 36.8 (S*C*H_2), 33.2 (S*C*H_2); HRMS (ESI^+) calcd. for $C_{21}H_{20}N_2NaO_3S$ $[M+Na]^+$ 403.1087; Found 403.1072.

(*R*)-Methyl *N*-[(3-hydroxypyridin-2-yl)carbonyl]-*S*-(naphthalen-2-ylmethyl)cysteinate 214

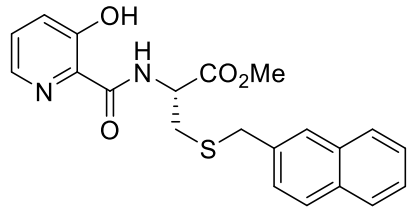

Following general procedure B, 3-hydroxy picolinic acid (0.10 g, 0.73 mmol) in anhydrous CH_2Cl_2 (10 mL) under N_2, DIPEA (0.14 mL, 0.80 mmol), HOBT (0.12 g, 0.88 mmol), and EDCI (0.18 mL, 0.88 mmol) were stirred for 10 min and **235** (0.20 g, 0.73 mmol) was added. The reaction mixture was stirred for 3 d until consumption of starting material. The yellow oil was chromatographed (hexane/EtOAc 8:2 to 6:4). Chromatography afforded **214** (0.06 g, 21 %) as a yellow oil. R_f = 0.19. $[\alpha]_D$= -65.6 (c= 1.17 x 10^{-3}, MeOH). IR (neat) ν/cm^{-1} 3351 (N-H), 1765 (CH_3OC=O), 1676 (NHC=O); ^{1}H NMR (500 MHz, $CDCl_3$) δ 11.78 (1H, s, O*H*), 8.69 (1H, d, *J*= 8.0, N*H*), 8.11 (1H, dd, *J*= 4.5 1.5, Ar C*H*), 7.81-7.76 (3H, m, Ar C*H*), 7.70 (1H, s, Ar C*H*), 7.50-7.44 (3H, m, Ar C*H*), 7.37-7.30 (2H, m, Ar C*H*), 5.00-4.97 (1H, m, C*H*), 3.93 (2H, s, CH_2), 3.78 (3H, s, SCH_3), 3.04 (1H, dd, *J*= 14.0 5.0, SCH_2), 2.95 (1H, dd, *J*= 14.0 5.5, SCH_2); ^{13}C NMR (125MHz, $CDCl_3$) δ 170.6 (*C*=O), 168.6 (*C*=O), 157.8 (Ar *C*), 139.9 (Ar *C*H), 134.6 (Ar *C*), 133.15 (Ar *C*), 132.6 (Ar *C*), 130.9 (Ar *C*), 128.95 (Ar *C*H), 128.6 (Ar *C*H), 127.7 (Ar *C*H), 127.65 (Ar *C*H), 126.9 (Ar *C*H), 126.3 (Ar *C*H), 126.3 (Ar *C*H), 126.1 (Ar *C*H), 125.9 (Ar *C*H), 52.8 (OCH_3), 51.6 (*C*H), 36.8 (SCH_2), 32.9 (SCH_2); HRMS (ESI^+) calcd. for $C_{21}H_{20}N_2NaO_4S$ $[M+Na]^+$ 419.1036; Found 419.1024.

(*R*)-Methyl *N*-(2,2'-bipyridin-6-ylcarbonyl)-*S*-(naphthalen-2-ylmethyl)cysteinate 215

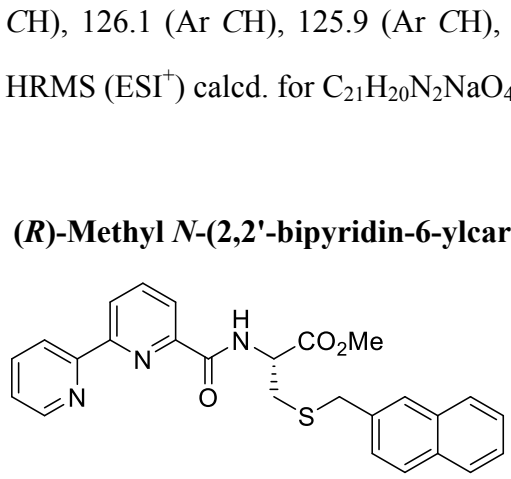

Following general procedure B, [2,2'-bipyridine]-6-carboxylic acid dihydrochloride[40] (0.20g, 0.73 mmol) in anhydrous DMF (10 mL) under N_2, DIPEA (0.34 mL, 2.26 mmol),

HOBT (0.12 g, 0.88 mmol), and EDCI (0.18 mL, 0.88 mmol) were stirred for 10 min and **235** (0.20 g, 0.73 mmol) was added. The reaction mixture was stirred for 3 d until consumption of starting material. DMF was partially evaporated and the solution was further dissolved in EtOAc. The mixture was washed with sat. $NaHCO_3$, brine and the organic layer was dried over $MgSO_4$ and concentrated *in vacuo*. Chromatography (hexane/EtOAc 7:3 to 6:4) afforded compound **215** (0.03 g, 9 %) as a yellow oil. R_f = 0.10. $[\alpha]_D$= -30.3 (c= 1.10 x 10^{-3}, MeOH). IR (neat) ν/cm^{-1} 3377 (N-H), 1744 (CH_3OC=O), 1678 (NHC=O); ^{1}H NMR (400 MHz, $CDCl_3$) δ 8.95 (1H, s, N*H*), 8.74 (1H, d, *J*= 4.5, Ar C*H*), 8.62 (1H, d, *J*= 8.0, Ar C*H*), 8.48 (1H, d, *J*= 8.0, Ar C*H*), 8.20 (1H, d, *J*= 7.5, Ar C*H*), 8.00 (1H, t, *J*= 7.5, Ar C*H*), 7.87 (1H, t, *J*= 7.5, Ar C*H*), 7.76-7.68 (4H, m, Ar C*H*), 7.47-7.36 (4H, m, Ar C*H*), 5.10-5.08 (1H, m, C*H*), 3.97 (1H, d, *J*= 13.5, CH_2), 3.94 (1H, d, *J*= 13.5, CH_2), 3.80 (3H, s, CH_3), 3.08-3.14 (2H, m, SCH_2) 3.04 (1H, dd, *J*= 14.0 4.5, SCH_2), 2.92 (1H, dd, *J*= 14.0 5.0, SCH_2); ^{13}C NMR (100 MHz, $CDCl_3$) δ 171.3 (*C*=O), 164.0 (*C*=O), 154.4 (Ar *C*), 149.1 (Ar *C*H), 138.4 (Ar *C*H), 134.8 (Ar *C*H), 133.1 (Ar *C*), 132.5 (Ar *C*), 128.5 (Ar *C*H), 127.6 (Ar *C*H), 127.6 (Ar *C*H), 126.9 (Ar *C*H), 126.2 (Ar *C*H), 125.8 (Ar *C*H), 124.3 (Ar *C*H), 123.9 (Ar *C*H), 122.5 (Ar *C*), 121.1 (Ar *C*), 52.7 (O*C*H_3), 51.9 (*C*H), 36.9 (S*C*H_2), 33.4 (S*C*H_2); HRMS (ESI^+) calcd. for $C_{26}H_{23}N_3NaO_3S$ $[M+Na]^+$ 480.1352 Found 480.1335.

(*R*)-Methyl *S*-(naphthale-2-ylmethyl)-*N*-[(6-phenylpyridin-2-yl)carbonyl]cysteinate 216

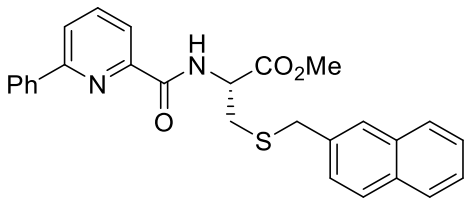

Following general procedure B, 6-phenylpicolinic acid (0.15 g, 0.73 mmol) in anhydrous CH_2Cl_2 (10 mL) under N_2, DIPEA (0.14 mL, 0.80 mmol), HOBT (0.12 g, 0.88 mmol), and EDCI (0.18 mL, 0.88 mmol) were stirred for 10 min and **235** (0.20 g, 0.73 mmol) was added. The reaction mixture was stirred for 3 d. Chromatography (hexane/EtOAc 8:2 to 6:4) afforded compound **216** (0.10 g, 33 %) as a yellow oil. R_f = 0.09. $[\alpha]_D$= -38.4 (c= 1.15 x 10^{-3}, MeOH). IR (neat) ν/cm^{-1} 3386 (N-H), 1743 (CH_3OC=O), 1677 (NHC=O); ^{1}H NMR (500

MHz, $CDCl_3$) δ 8.94 (1H, d, *J*= 8.5, N*H*), 8.13 (1H, dd, *J*= 6.5 2.0, Ar C*H*), 8.11-8.07 (2H, m, Ar C*H*), 7.95-7.90 (2H, m, Ar C*H*), 7.77-7.68 (4H, m, Ar C*H*), 7.55-7.42 (6H, m, Ar C*H*), 5.10-5.06 (1H, m, C*H*), 3.97 (1H, d, *J*= 13.5, CH_2), 3.93 (1H, d, *J*= 13.5, CH_2), 3.79 (3H, s, CH_3), 3.07 (1H, dd, *J*= 14.0 5.0, SCH_2), 3.03 (1H, dd, *J*= 14.0 5.5, SCH_2); ^{13}C NMR (125MHz, $CDCl_3$) δ 171.2 (*C*O_2CH_3), 164.2 (*C*ONH), 156.1 (Ar *C*), 148.9 (Ar *C*), 138.2 (Ar *C*), 138.1 (Ar *C*H), 134.8 (Ar *C*), 133.1 (Ar *C*), 132.5 (Ar *C*), 129.5 (Ar *C*H), 128.9 (Ar *C*H), 128.5 (Ar *C*H), 127.6 (Ar *C*H), 127.6 (Ar *C*H), 127.0 (Ar *C*H), 126.9 (Ar *C*H), 126.1 (Ar *C*H), 125.8 (Ar *C*H), 123.2 (Ar *C*H), 120.7 (Ar *C*H), 52.7 (O*C*H_3), 52.0 (*C*H), 36.9 (S*C*H_2), 33.3 (S*C*H_2); HRMS (ESI^+) calcd. for $C_{27}H_{25}N_2O_3S$ $[M+H]^+$ 457.1580; Found 457.1568.

(*R*)- *S*-(naphthalen-2-ylmethyl)-*N*-(pyridin-2-ylcarbonyl)cysteine 217

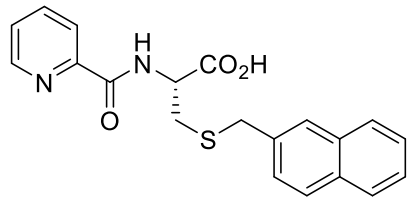

Following general procedure C, **213** (23 mg, 0.06 mmol) in 1,4-dioxane (2 mL), 1 M lithium hydroxide (0.12 mL, 0.12 mmol) was added. Concentration afforded compound **217** (16 mg, 73 %) as a white solid, mp 124-126 ºC. $[\alpha]_D$= -35.2 (c= 1.36 x 10^{-3}, MeOH). IR (neat) ν/cm^{-1} 3285 (N-H), 2917 (COO-H), 1743 (HOC=O), 1651 (NHC=O); ^{1}H NMR (500 MHz, DMSO-d_6) δ 8.95 (1H, d, *J*= 8.5, N*H*), 8.70-8.69 (1H, m, ArC*H*), 8.09-8.02 (2H, m, Ar C*H*), 7.88-7.80 (3H, m, Ar C*H*), 7.76 (1H, s, Ar C*H*), 7.67-7.64 (1H, m, Ar C*H*), 7.50-7.47 (3H, m, Ar C*H*), 4.79-4.75 (1H, m, C*H*), 3.95 (2H, s, SCH_2), 3.06-3.00 (2H, m, SCH_2); ^{13}C NMR (125MHz, DMSO-d_6) δ 171.8 (*C*=O), 163.6 (*C*=O), 149.15 (Ar *C*), 148.6 (Ar *C*H), 138.0 (Ar *C*), 135.6 (Ar *C*), 132.7 (Ar *C*), 132.7 (Ar *C*), 132.0 (Ar *C*H), 128.1 (Ar *C*H), 127.5 (Ar *C*H), 127.45 (Ar *C*H), 127.2 (Ar *C*H), 127.1 (Ar *C*H), 126.9 (Ar *C*H), 126.2 (Ar *C*H), 125.8 (Ar *C*H), 122.0 (Ar *C*H), 51.6 (*C*H), 35.5 (S*C*H_2), 32.2 (S*C*H_2); HRMS (ESI^-) calcd. for $C_{20}H_{17}N_2O_3S$ $[M-H]^-$ 365.0965; Found 365.0955.

(*R*)- *N*-[(3-hydroxypyridin-2-yl)carbonyl]-*S*-(naphthalen-2-ylmethyl)cysteine 218

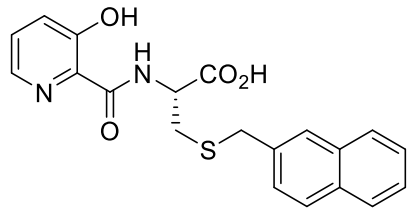

Following general procedure C, **214** (24 mg, 0.06 mmol) in 1,4-dioxane (2 mL) reacted with 1 M lithium hydroxide (0.12mL, 0.12 mmol). Concentration afforded compound **218** (10 mg, 44 %) as off white solid, mp 159-161 ºC. $[\alpha]_D$= -40.6 (c= 1.05 x 10^{-3}, MeOH). IR (neat) ν/cm^{-1} 3368 (ArO-H, N-H), 1724 (HOC=O), 1649 (NHC=O); ^{1}H NMR (500 MHz, DMSO-d_6) δ 12.18 (1H, s, COO*H*), 9.25 (1H, d, *J*= 8.5, N*H*), 8.22 (1H, dd, *J*= 4.5 1.0, Ar C*H*), 7.88-7.81 (3H, m, Ar C*H*), 7.77 (1H, s, Ar C*H*), 7.60-7.57 (1H, m, Ar C*H*), 7.51-7.46 (4H, m, Ar C*H*), 4.75-4.72 (1H, m, C*H*), 3.95 (2H, s, SCH_2), 3.06 (1H, dd, *J*= 14.0 7.0, SCH_2), 2.92 (1H, dd, *J*= 14.0 5.0, SCH_2); ^{13}C NMR (125MHz, DMSO-d_6) δ 171.3 (*C*=O), 168.5 (*C*=O), 157.2 (Ar *C*), 140.1 (Ar *C*H), 135.6 (Ar *C*), 132.7 (Ar *C*), 132.0 (Ar *C*), 130.7 (Ar *C*H), 129.5 (Ar *C*H), 128.1 (Ar *C*H), 127.5 (Ar *C*H), 127.4 (Ar *C*H), 127.2 (Ar *C*H), 127.1 (Ar *C*H), 126.2 (Ar *C*H), 126.1 (Ar *C*H), 125.8 (Ar *C*H), 51.3(*C*H), 35.4 (S*C*H_2) 31.7 (S*C*H_2); HRMS (ESI^-) calcd. for $C_{20}H_{17}N_2O_4S$ $[M-H]^-$ 381.0915; Found 381.0910.

(*R*)- *N*-(2,2'-bipyridin-6-ylcarbonyl)-*S*-(naphthalen-2-ylmethyl)cysteine 219

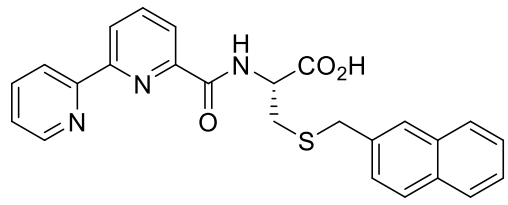

Following general procedure C, to a solution of **215** (23 mg, 0.05 mmol) in 1,4-dioxane (2 mL) 1 M lithium hydroxide (0.15mL, 0.15 mmol) was added. Concentration afforded compound **219** (14 mg, 65 %) as a white solid, mp 119-120 ºC. $[\alpha]_D$= -23.8 (c= 1.13 x 10^{-3}, MeOH). IR (neat) ν/cm^{-1} 3353 (N-H), 2922 (COO-H), 1728 (HOC=O), 1669 (NHC=O); ^{1}H NMR (500 MHz, DMSO-d_6) δ 10.15 (1H, s, CO_2*H*), 9.20 (1H, d, *J*= 8.5, N*H*), 8.73-8.72 (1H, m, Ar*H*), 8.67 (1H, d, *J*= 8.0, Ar C*H*), 8.60 (1H, dd, *J*= 8.0 1.0, Ar C*H*), 8.19-8.16 (1H, m,

Ar C*H*), 8.11-8.10 (1H, m, Ar C*H*), 8.01 (1H, td, *J*= 7.5 2.0, Ar C*H*), 7.88-7.74 (5H, m, Ar C*H*), 7.53-7.45 (4H, m, Ar C*H*), 4.76-4.74 (1H, m, C*H*), 3.95 (2H, s, SCH_2), 3.04-3.06 (2H, m, SCH_2) 3.04 (1H, dd, *J*= 14.0 4.5, SCH_2), 2.92 (1H, dd, *J*= 14.0 5.0, SCH_2); ^{13}C NMR (125MHz, DMSO-d_6) δ 171.9 (*C*=O), 163.6 (*C*=O), 154.3 (Ar *C*), 154.1 (Ar *C*), 149.1 (Ar *C*H), 148.8 (Ar *C*H), 139.2 (Ar *C*H), 137.5 (Ar *C*H), 135.6 (Ar *C*), 132.7 (Ar *C*), 131.9 (Ar *C*), 128.1 (Ar *C*H), 127.6 (Ar *C*H), 127.5(Ar *C*H), 127.4 (Ar *C*H), 127.2 (Ar *C*H), 126.4 (Ar *C*H), 126.3 (Ar *C*H), 124.8 (Ar *C*H), 123.4 (Ar *C*H), 122.3 (Ar *C*H), 121.1 (Ar *C*), 51.9 (*C*H), 35.5 (S*C*H_2), 32.2 (S*C*H_2); HRMS (ESI$^-$) calcd. for $C_{25}H_{20}N_3O_3S$ [M-H]$^-$ 442.1231; Found 442.1215.

(*R*)- *S*-(naphthalen-2-ylmethyl)-*N*-[(6-phenylpyridin-2-yl)carbonyl]cysteine 220

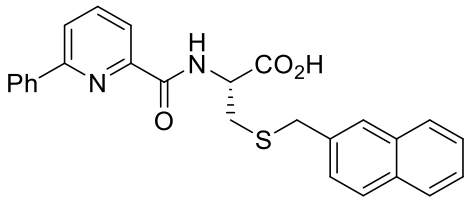

Following general procedure C, to a solution of **216** (0.028 g, 0.09 mmol) in 1,4-dioxane (2 mL) 1 M lithium hydroxide (0.18 mL, 0.18 mmol) was added. Concentration afforded compound **220** (0.01 g, 52 %) as a light yellow solid, mp 260-261 ºC. $[\alpha]_D$= -11.4 (c= 1.22 x 10^{-3}, MeOH). IR (neat) ν/cm^{-1} 3339 (N-H, COO-H), 1721 (HOC=O), 1635 (NHC=O); ^{1}H NMR (500 MHz, DMSO-d_6) δ 9.12 (1H, d, *J*= 8.5, N*H*), 8.31-8.23 (3H, m, ArC*H*), 8.12 (1H, t, *J*= 8.0, Ar C*H*), 8.03 (1H, d, *J*= 7.5, Ar C*H*), 7.87-7.77 (3H, m, Ar C*H*), 7.57-7.47 (7H, m, Ar C*H*), 4.77 (1H, s, C*H*), 3.98 (2H, s, SCH_2), 3.08-3.06 (2H, m, SCH_2); ^{13}C NMR (125MHz, DMSO-d_6) δ 171.9 (*C*=O), 163.6 (*C*=O), 155.0 (Ar *C*), 149.2 (Ar *C*), 139.1 (Ar *C*H), 137.5 (Ar *C*), 135.7 (Ar *C*), 132.7 (Ar *C*), 132.0 (Ar *C*), 129.7 (Ar *C*H), 128.9 (Ar *C*H), 127.5 (Ar *C*H), 127.4 (Ar *C*H), 127.2 (Ar *C*H), 127.1 (Ar *C*H), 126.9 (Ar *C*H), 126.4 (Ar *C*H), 126.2 (Ar *C*H), 125.8 (Ar *C*H), 123.1 (Ar *C*H), 120.7 (Ar *C*H), 51.9 (*C*H), 35.5 (S*C*H_2), 32.3 (S*C*H_2); HRMS (ESI$^-$) calcd. for $C_{26}H_{21}N_2O_3S$ [M-H]$^-$ 441.1278; Found 441.1258.

Methyl *N*-(pyridin-2-yl)carbonylglycinate 221

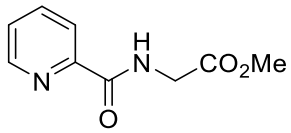

Following general procedure B, picolinic acid (0.44 g, 3.59 mmol) in anhydrous CH_2Cl_2 (20 mL), and HOBT (0.58 g, 4.31 mmol), EDCI (0.76 mL, 4.31 mmol) and DIPEA (1.25 mL, 7.18 mmol) with glycine methyl ester hydrochloride (0.45 g, 3.59 mmol) were stirred for 1 d. Chromatography (hexane/EtOAc 7:3 to 5:5) afforded compound **221** (0.50 g, 72 %) as yellow solid, mp 81-82 ºC. R_f = 0.18. IR (neat) ν/cm^{-1} 3386 (NH), 1749 (MeOC=O), 1672 (NHC=O); ^{1}H NMR (500 MHz, $CDCl_3$) δ 8.58 (1H, d, *J*= 0.5, Ar C*H*), 8.49 (1H, br. s, N*H*), 8.19-8.17 (1H, m, Ar C*H*), 7.85 (1H, td, *J*= 7.5 2.0, Ar C*H*), 7.46-7.43 (1H, m, Ar C*H*), 4.28 (2H, d, *J*= 6.0, CH_2), 3.79 (3H, s, CH_3); ^{13}C NMR (125MHz, $CDCl_3$) δ 170.1 (*C*=O), 164.6 (*C*=O), 149.2 (Ar *C*), 148.25 (Ar *C*H), 137.3 (Ar *C*H), 126.4 (Ar *C*H), 122.3 (Ar *C*H), 52.4 (*C*H_3), 41.2 (*C*H_2); HRMS (ESI$^+$) calcd. for $C_9H_{10}N_2NaO_3$ $[M+Na]^+$ 217.0584; Found 217.0582.

Methyl *N*-[(3-hydroxypyridin-2-yl)carbonyl]glycine 222

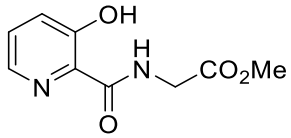

Following general procedure B, picolinic acid (0.50 g, 3.59 mmol) in anhydrous CH_2Cl_2 (20 mL) and HOBT (0.58 g, 4.31 mmol), EDCI (0.76 mL, 4.31 mmol) and DIPEA (1.25 ml, 7.18 mmol) with glycine methyl ester hydrochloride (0.45 g, 3.59 mmol) were stirred for 36 h until consumption of starting material. Chromatography (hexane/ EtOAc 7:3 to 5:5) afforded compound **222** (0.35 g, 47 %) as white needles, mp 54-55 ºC. R_f = 0.36. IR (neat) ν/cm^{-1} 3355 (O-H, N-H), 1749 (MeOC=O), 1651 (NHC=O); ^{1}H NMR (500 MHz, $CDCl_3$) δ 11.76 (1H, s, O*H*), 8.46 (1H, s, N*H*), 8.07 (1H, dd, *J*= 4.0 1.5, Ar C*H*), 7.35-7.28 (2H, m, Ar C*H*), 4.23 (2H, d, *J*= 6.0, CH_2), 3.79 (3H, s, CH_3); ^{13}C NMR (125MHz, $CDCl_3$) δ 169.6 (*C*=O), 169.0 (*C*=O), 157.7 (Ar *C*), 139.8 (Ar *C*H), 131.0 (Ar *C*), 128.9 (Ar *C*H), 126.05 (Ar *C*H), 52.5

(CH_3), 40.7 (CH_2); HRMS (ESI^+) calcd. for $C_9H_{10}N_2NaO_4$ $[M+Na]^+$ 233.0533; Found 233.0525.

Methyl *N*-(2,2'-bipyridin-6-ylcarbonyl)glycinate 223

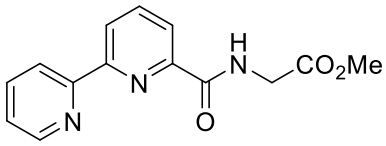

A stirred solution of 2,2'-bipyridine-6-carboxylic acid dihydrochloride[40] (0.20 g, 0.73 mmol) in DMF (10 mL) with DIPEA (0.52 mL, 3.0 mmol), HOBT (0.12 g, 0.88 mmol), and EDCI (0.18 mL, 0.88 mmol) and glycine methyl ester hydrochloride (0.20 g, 0.73 mmol) was stirred for 2 d until consumption of starting material. DMF was partially evaporated and then dissolved in EtOAc. The mixture was washed with sat. $NaHCO_3$ and brine and the organic layer was dried over $MgSO_4$ and concentrated *in vacuo*. Chromatography (hexane/EtOAc 6:4 to 2:8) afforded compound **223** (97 mg, 35 %) as white needles, mp 111-113 ºC. R_f = 0.10. IR (neat) ν/cm^{-1} 3379 (N-H), 1749 (CH_3OC=O), 1672 (NHC=O); ^{1}H NMR (500 MHz, $CDCl_3$) δ 8.67-8.66 (1H, m, Ar C*H*), 8.63 (1H, t, *J*= 5.0, N*H*), 8.54 (1H, dd, *J*= 8.0 1.0, Ar C*H*), 8.40 (1H, d, *J*= 8.0, Ar C*H*), 8.18 (1H, dd, *J*= 7.5 1.0, Ar C*H*), 7.95 (1H, t, *J*= 8.0, Ar C*H*), 7.81 (1H, td, *J*= 8.0 2.0, Ar C*H*), 7.35-7.31 (1H, m, ArC*H*), 4.31 (2H, d, *J*= 5.5, CH_2), 3.79 (3H, s, CH_3); ^{13}C NMR (125MHz, $CDCl_3$) δ 170.4 (*C*=O), 164.5 (*C*=O), 154.9 (Ar *C*), 154.8 (Ar *C*), 149.2 (Ar *C*), 148.6 (Ar *C*H), 138.4 (Ar *C*H), 137.0 (Ar *C*H), 124.2 (Ar *C*H), 123.9 (Ar *C*H), 122.3 (Ar *C*H), 121.0 (Ar *C*H), 52.4 (CH_3), 41.3 (CH_2); HRMS (ESI^+) calcd. for $C_{14}H_{13}N_2NaO_3$ $[M+Na]^+$ 294.0849; Found 294.0842.

Methyl *N*-[(6-phenylpyridin-2-yl)carbonyl]glycinate 224

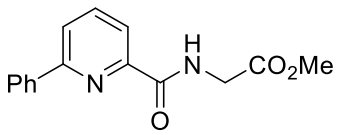

To a stirred solution of glycine methyl ester hydrochloride (0.08 g, 0.60 mmol) and triethylamine (0.18 mL, 1.25 mmol) in anhydrous CH_2Cl_2 (20 mL), 6-phenylpicolinic acid

(0.10 g, 0.5 mmol) and PyBOP (0.29 g, 0.55 mmol) were added. The reaction mixture was stirred at room temperature overnight. The mixture was washed with water and the organic layer was dried over $MgSO_4$ and concentrated *in vacuo*. Chromatography (hexane/ EtOAc 6:4 to 5:5) afforded compound **224** (0.06 g, 44 %) as white needles, mp 106-108 ºC. R_f = 0.29. IR (neat) ν/cm^{-1} 3397 (N-H), 1742 (CH_3OC=O), 1680 (NHC=O); ^{1}H NMR (400 MHz, $CDCl_3$) δ 8.64 (1H, t, *J*= 4.5, N*H*), 8.15 (1H, dd, *J*= 7.0 1.0, Ar C*H*), 8.06-8.04 (2H, m, Ar C*H*), 7.96-7.89 (2H, m, Ar C*H*), 7.54-7.45 (3H, m, Ar C*H*), 4.33 (2H, d, *J*= 5.5, CH_2), 3.82 (3H, s, CH_3); ^{13}C NMR (125MHz, $CDCl_3$) δ 170.3 (*C*=O), 164.7 (*C*=O), 156.1 (Ar *C*), 149.0 (Ar *C*), 138.2 (Ar *C*H), 129.5 (Ar *C*H), 128.9 (Ar *C*H), 126.95 (Ar *C*H), 123.2 (Ar *C*H), 120.7 (Ar *C*H), 52.4 (CH_3), 41.3 (CH_2); HRMS (ESI$^+$) calcd. for $C_{15}H_{14}N_2NaO_3$ $[M+Na]^+$ 293.0897; Found 293.0892.

Methyl *N*-{[5-(tert-butylsulfanyl)pyridin-2-yl]carbonyl}glycinate 225

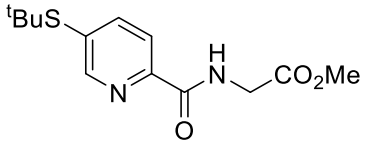

A solution of 5-(*tert*-butylthio)picolinic acid[41] (0.91 g, 4.31 mmol) in $SOCl_2$ (15 mL, excess) was stirred at room temperature for 2 h. The excess $SOCl_2$ was removed *in vacuo* and co-evaporated twice with CH_2Cl_2. The crude product was then diluted (CH_2Cl_2) and glycine methyl ester hydrochloride (0.55 g, 4.32 mmol) was added. Triethylamine (1.20 mL, 8.62 mmol) was then added dropwise over 10min and the mixture was stirred at room temperature for 4 h. The solution was washed with water, dried over $MgSO_4$ and concentrated *in vacuo*. Chromatography (CH_2Cl_2 100%) afforded compound **225** (0.65 g, 52%) as white crystals, mp 108-109 ºC. R_f = 0.30. IR (neat) ν/cm^{-1} 3385 (NH), 1737 (CH_3OC=O), 1676 (NHC=O); ^{1}H NMR (500 MHz, $CDCl_3$) δ 8.66 (1H, d, *J*= 1.5, Ar C*H*), 8.44 (1H, t, *J*= 4.5, N*H*), 8.15 (1H, d, *J*= 8.0, Ar C*H*), 8.00-7.98 (1H, m, Ar C*H*), 4.28 (2H, d, *J*= 5.5, CH_2), 3.81 (3H, s, CH_3), 1.32 (9H, s, $SC(CH_3)_3$); ^{13}C NMR (125MHz, $CDCl_3$) δ 170.0 (*C*=O), 164.2 (*C*=O), 155.0 (Ar *C*H), 148.8 (Ar *C*), 145.5 (Ar *C*H), 133.7 (Ar *C*), 121.9 (Ar *C*H), 52.4 (CH_3), 47.2 ($SC(CH_3)_3$),

41.2 (*C*H_2), 30.9 (*C*H_3); HRMS (ESI$^+$) calcd. for $C_{13}H_{18}N_2NaO_3S$ $[M+Na]^+$ 305.0936; Found 305.0930.

(*S*)-Methyl *N*-[(3-hydroxypyridin-2-yl)carbonyl]alaninate 226

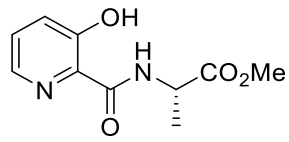

To a stirred solution of 3-hydroxypicolinic acid (0.50 g, 3.59 mmol) in anhydrous CH_2Cl_2 (20 mL) under N_2, HOBT (0.58 g, 4.31 mmol), EDCI (0.76 mL, 4.31 mmol) and DIPEA (1.25 mL, 7.18 mmol) were added at 0 ºC. The mixture was stirred for 10 min and L-alanine methyl ester hydrochloride (0.50 g, 3.59 mmol) was added. The reaction mixture was stirred for 3 d until consumption of starting material. The mixture was washed with water and the organic layer was dried over $MgSO_4$ and concentrated *in vacuo*. Chromatography (hexane/EtOAc 7:3 to 4:6) afforded compound **226** (0.36 g, 45 %) as white needles, mp 60-61 ºC. R_f = 0.5. $[\alpha]_D$= -15.7 (c= 1.27 x 10^{-3}, MeOH). IR (neat) ν/cm^{-1} 3371 (ArO-H, N-H), 1741 (CH_3OC=O), 1647 (NHC=O); ^{1}H NMR (400 MHz, $CDCl_3$) δ 11.80 (1H, s, O*H*), 8.43 (1H, d, *J*= 7.0, N*H*), 7.98-7.97 (1H, m, Ar C*H*), 7.28-7.19 (2H, m, Ar C*H*), 4.72-4.65 (1H, m, C*H*), 3.72 (3H, s, CO_2CH_3), 1.48 (3H, d, *J*= 7.5, CH_3); ^{13}C NMR (101MHz, $CDCl_3$) δ 172.6 (*C*=O), 168.4 (*C*=O), 157.7 (Ar *C*), 139.6 (Ar *C*H), 131.0 (Ar *C*), 128.7 (Ar *C*H), 125.9 (Ar *C*H), 52.5 (CO_2CH_3), 47.6 (*C*H), 18.1 (*C*H_3); HRMS (ESI$^+$) calcd. for $C_{10}H_{12}N_2O_4$ $[M+Na]^+$ 247.0689; Found 247.0687.

(*S*)- Methyl 3-(3a,7a-dihydro-1H-indol-3-yl)-*N*-[(3-hydroxypyridin-2-yl)carbonyl] alaninate 227

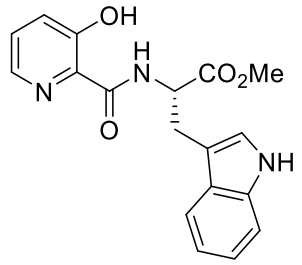

To a stirred solution of 3-hydroxypicolinic acid (0.50 g, 3.59 mmol) in anhydrous CH_2Cl_2 (20 mL) under N_2, HOBT (0.58 g, 4.31 mmol), EDCI (0.76 mL, 4.31 mmol) and DIPEA (1.25 mL, 7.18 mmol) were added at 0 ºC. The mixture was stirred for 10 min and L-tryptophan methyl ester hydrochloride (0.50 g, 3.59 mmol) was added. The reaction mixture was stirred for 2 d until consumption of starting material. The mixture was washed with water and the organic layer was dried over $MgSO_4$ and concentrated *in vacuo*. Chromatography (hexane/EtOAc 7:3 to 4:6) afforded compound **227** (0.66 g, 54 %) as a yellow oil. R_f = 0.25. $[\alpha]_D$= -6.2 (c= 1.27 x 10^{-3}, MeOH). IR (neat) ν/cm^{-1} 3372 (ArO-H, N-H), 1737 (CH_3OC=O), 1648 (NHC=O); ^{1}H NMR (500 MHz, $CDCl_3$) δ 11.94 (1H, s, O*H*), 8.59 (1H, d, *J*= 8.0, N*H*), 8.46 (1H, s, Ar C*H*), 7.99-7.98 (1H, m, Ar C*H*), 7.60 (1H, d, *J*= 8.0, ArC*H*), 7.29-7.27 (2H, m, Ar C*H*), 7.18 (1H, t, *J*= 7.0, Ar C*H*), 7.11 (1H, t, *J*= 7.5, Ar C*H*), 7.02 (1H, d, *J*= 2.0, ArC*H*), 5.13-5.09 (1H, m, C*H*), 3.70 (3H, s, CO_2CH_3), 3.46-3.45 (2H, m, CH_3); ^{13}C NMR (125MHz, $CDCl_3$) δ 171.9 (*C*=O), 168.6 (*C*=O), 157.7 (Ar *C*), 139.8 (Ar *C*H), 136.2 (Ar *C*), 131.0 (Ar *C*), 128.8 (Ar *C*H), 127.3 (Ar *C*H), 126.0 (Ar *C*H), 123.1 (Ar *C*H), 122.2 (Ar *C*H), 119.5 (Ar *C*H), 118.5 (Ar *C*H), 111.4 (Ar *C*H), 109.5 (Ar *C*), 52.6 (CH_3), 52.6 (*C*H), 28.0 (CH_2); HRMS (ESI^-) calcd. for $C_{18}H_{16}N_3O_4$ $[M-H]^-$ 338.1146; Found 338.1149.

***N*-(pyridin-2-ylcarbonyl)glycine 228**

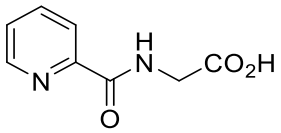

Following general procedure C, to a solution of **221** (0.02 g, 0.10 mmol) in 1,4-dioxane (5 mL) 1 M lithium hydroxide (0.2 mL, 0.2 mmol) was added. Concentration afforded compound **228** (8.07 mg, 45 %) as a white solid, mp 119-121 ºC. IR (neat) ν/cm^{-1} 3354 (N-H), 2933 (COO-H), 1743 (HOC=O), 1670 (NHC=O); ^{1}H NMR (500 MHz, DMSO-d_6) δ 8.99 (1H, t, *J*= 6.0, N*H*), 8.67 (1H, d, *J*= 4.5, Ar C*H*), 8.06-8.00 (2H, m, Ar C*H*), 7.65-7.62 (1H, m, Ar C*H*), 4.00 (2H, d, *J*= 6.0, CH_2); ^{13}C NMR (125MHz, DMSO-d_6) δ 171.05 (*C*=O), 164.1 (*C*=O), 149.4 (Ar *C*), 148.5 (Ar *C*H), 137.85 (Ar *C*H), 126.7 (Ar *C*H), 121.9 (Ar *C*H), 41.0 (*C*H$_2$); HRMS (ESI$^-$) calcd. for $C_8H_7N_2O_3$ [M-H]$^-$ 179.0464; Found 179.0462.

***N*-[(3-hydroxypyridin-2-yl)carbonyl]glycine 229**

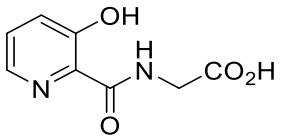

Following general procedure C, to a solution of **222** (0.02 g, 0.095 mmol) in 1,4-dioxane (5 mL) 1 M lithium hydroxide (0.2 mL, 0.2 mmol) was added. Concentration afforded compound **229** (2.0 mg, 20 %) as a white solid, mp 169-170 ºC. IR (neat) ν/cm^{-1} 3354 (O-H, N-H), 2950 (COO-H), 1745 (HOC=O), 1678 (NHC=O); ^{1}H NMR (500 MHz, DMSO-d_6) δ 12.30 (1H, s, O*H*), 9.33 (1H, t, *J*= 6.0, N*H*), 8.20 (1H, dd, *J*= 4.5 1.5, Ar C*H*), 7.56 (1H, q, *J*= 4.0, Ar C*H*), 7.45 (1H, dd, *J*= 8.5 1.5, Ar C*H*), 4.00 (2H, d, *J*= 6.0, CH_2); ^{13}C NMR (125MHz, DMSO-d_6) δ 170.5 (*C*=O), 169.0 (*C*=O), 157.2 (Ar *C*), 140.0 (Ar *C*H), 130.9 (Ar *C*), 129.35 (Ar *C*H), 125.95 (Ar *C*H), 40.6 (*C*H$_2$); HRMS (ESI$^-$) calcd. for $C_8H_7N_2O_4$ [M-H]$^-$ 195.0411; Found 195.0417.

***N*-(2,2'-bipyridin-6-ylcarbonyl)glycine 230**

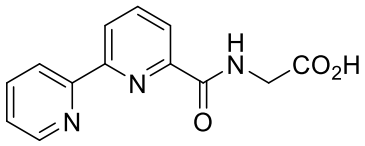

Following general procedure C, to a solution of **223** (16 mg, 0.06 mmol) in 1,4-dioxane (2 mL) 1 M lithium hydroxide (0.12mL, 0.12 mmol) was added. Concentration afforded compound **230** (8 mg, 52 %) as a white solid, mp 175-177 ºC. IR (neat) ν/cm^{-1} 3360 (N-H), 2989 (COO-H), 1743 (HOC=O), 1654 (NHC=O); ^{1}H NMR (500 MHz, DMSO-d_6) δ 12.60 (1H, s, CO_2H), 9.33 (1H, t, J= 6.0, NH), 8.82 (1H, d, J= 8.0, Ar CH), 8.73 (1H, d, J= 4.5, Ar CH), 8.60 (1H, dd, J= 8.0 1.0, Ar CH), 8.16 (1H, t, J= 7.5, Ar CH), 8.10 (1H, dd, J= 7.5 1.0, Ar CH), 8.02 (1H, td, J= 7.5 2.0, Ar CH), 7.53-7.52 (1H, m, Ar CH), 4.06 (2H, d, J= 6.0, CH_2); ^{13}C NMR (125MHz, DMSO-d_6) δ 171.2 (*C*=O), 164.0 (*C*=O), 154.3 (Ar *C*), 154.2 (Ar *C*), 149.3 (Ar *C*), 149.1 (Ar *C*H), 139.0 (Ar *C*H), 137.3 (Ar *C*H), 124.7 (Ar *C*H), 123.0 (Ar *C*H), 122.1 (Ar *C*H), 121.3 (Ar *C*H), 41.1 (*C*H$_2$); HRMS (ESI$^+$) calcd. for $C_{13}H_{10}N_3O_3$ 256.0728; Found 256.0720.

***N*-[(6-phenylpyridin-2-yl)carbonyl]glycine 231**

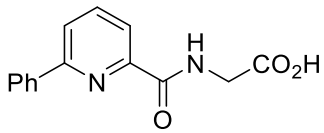

Following general procedure C, to a solution of **224** (20 mg, 0.07 mmol) in 1,4-dioxane (2 mL) 1 M lithium hydroxide (0.14 mL, 0.14 mmol) was added. Concentration afforded compound **231** (15 mg, 82 %) as white solid, mp 132-134 ºC. IR (neat) ν/cm^{-1} 3324 (N-H), 2562 (COO-H), 1757 (HOC=O), 1634 (NHC=O); ^{1}H NMR (500 MHz, MeOD-d_4) δ 8.21-8.19 (2H, m, Ar CH), 8.10-8.01 (3H, m, Ar CH), 7.54-7.46 (3H, m, Ar CH), 4.23 (2H, s, CH_2); ^{13}C NMR (125MHz, MeOD-d_4) δ 173.0 (*C*=O), 167.1 (*C*=O), 157.6 (Ar *C*), 150.4 (Ar *C*), 139.7 (Ar *C*), 139.4 (Ar *C*H), 130.6 (Ar *C*H), 129.9 (Ar *C*H), 128.1 (Ar *C*H), 124.3 (Ar *C*H), 121.6 (Ar *C*H), 42.1 (*C*H$_2$); HRMS (ESI$^-$) calcd. for $C_{14}H_{11}N_2O_3$ [M-H]$^-$ 255.0775; Found 255.0771.

***N*-{[5-(tert-butylsulfanyl)pyridin-2-yl]carbonyl}glycine 232**

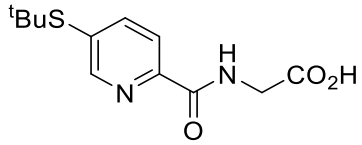

Following general procedure C, to a solution of **225** (0.20 g, 0.78 mmol) in 1,4-dioxane (15 mL) 1 M lithium hydroxide (1.56 mL, 1.56 mmol) was added. Concentration afforded compound **232** (0.18 g, 85 %) as a white solid, mp 143-144 ºC. IR (neat) ν/cm^{-1} 3366 (N-H), 2959 (COO-H), 1748 (HOC=O), 1649 (NHC=O); ^{1}H NMR (500 MHz, MeOD-*d*$_4$) δ 8.66 (1H, d, *J*= 2.0, Ar C*H*), 8.50 (1H, t, *J*= 4.5, N*H*), 8.17 (1H, d, *J*= 8.0, Ar C*H*), 8.01-7.99 (1H, m, Ar C*H*), 4.34 (2H, d, *J*= 5.5, CH_2), 1.32 (9H, s, SC(CH_3)$_3$); ^{13}C NMR (125MHz, MeOD-*d*$_4$) δ 173.7 (*C*=O), 164.6 (*C*=O), 155.0 (Ar *C*H), 148.4 (Ar *C*), 145.6 (Ar *C*H), 134.1 (Ar *C*), 122.1 (Ar *C*H), 47.3 (S*C*(CH$_3$)$_3$), 41.3 (*C*H$_2$), 30.9 (*C*H$_3$); HRMS (ESI$^-$) calcd. for $C_{12}H_{15}N_2O_3S$ [M+Na]$^+$ 267.0809; Found 267.0814.

(*S*)- *N*-[(3-hydroxypyridin-2-yl)carbonyl]alanine 233

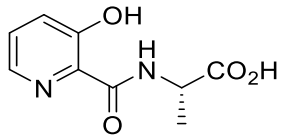

Following general procedure C, to a solution of **226** (20 mg, 0.09 mmol) in 1,4-dioxane (2 mL) 1 M lithium hydroxide (0.18 mL, 0.18 mmol) was added. Concentration afforded compound **233** (14 mg, 74 %) as an off white solid, mp 187-189 ºC. $[\alpha]_D$= -22.6 (c= 1.01 x 10^{-3}, MeOH). IR (neat) ν/cm^{-1} 3354 (N-H), 2925 (COO-H), 1730 (HOC=O), 1628 (NHC=O); ^{1}H NMR (500 MHz, DMSO-*d*$_6$) δ 12.28 (1H, s, O*H*), 9.18 (1H, d, *J*= 8.0, N*H*), 8.20 (1H, dd, *J*= 4.5 1.0, Ar C*H*), 7.57-7.55 (1H, m, Ar C*H*), 7.45 (1H, dd, *J*= 8.5 1.5, Ar C*H*), 4.50 (1H, quin, *J*= 7.5, C*H*), 1.46 (3H, d, *J*= 7.5, CH_3); ^{13}C NMR (125MHz, DMSO-*d*$_6$) δ 173.2 (*C*=O), 168.3 (*C*=O), 157.2 (Ar *C*), 140.0 (Ar *C*H), 130.9 (Ar *C*), 129.4 (Ar *C*H), 126.0 (Ar *C*H), 47.5 (*C*H), 16.9 (*C*H$_3$); HRMS (ESI$^-$) calcd. for $C_9H_9N_2O_4$ [M-H]$^-$ 209.0568; Found 324.0565.

(*S*)-3-(3a,7a-dihydro-1H-indol-3-yl)-*N*-[(3-hydroxypyridin-2-yl)carbonyl]alanine 234

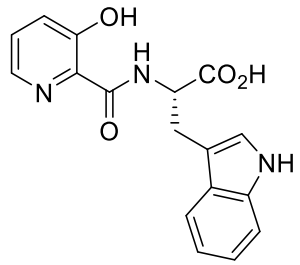

Following general procedure C, to a solution of **227** (20 mg, 0.06 mmol) in 1,4-dioxane (2 mL) 1 M lithium hydroxide (0.12mL, 0.12 mmol) was added. Concentration afforded compound **234** (13 mg, 67 %) as a yellow solid, mp 109-111 ºC. $[\alpha]_D$= -24.7 (c= 1.03 x 10^{-3}, MeOH). IR (neat) ν/cm^{-1} 3279 (ArO-H, N-H), 2949 (COO-H), 1733 (HOC=O), 1647 (NHC=O); ^{1}H NMR (500 MHz, DMSO-d_6) δ 12.17 (1H, s, CO_2H), 10.87 (1H, s, O*H*), 8.94 (1H, d, *J*= 8.0, N*H*), 8.13 (1H, dd, *J*= 4.5 1.0, Ar C*H*), 7.54-7.52 (2H, m, Ar C*H*), 7.42 (1H, dd, *J*= 8.5 1.0, ArC*H*), 7.33 (1H, d, *J*= 8.0, Ar C*H*), 7.16 (1H, d, *J*= 2.0, Ar C*H*), 7.04 (1H, t, *J*= 7.0, Ar C*H*), 6.95 (1H, t, *J*= 7.0, Ar C*H*), 4.79-4.75 (1H, m, C*H*), 3.43-3.35 (2H, m, CH_3); ^{13}C NMR (125MHz, DMSO-d_6) δ 172.4 (*C*=O), 168.3 (*C*=O), 157.1 (Ar *C*), 140.0 (Ar *C*H), 136.1 (Ar *C*), 130.7 (Ar *C*), 129.4 (Ar *C*H), 127.2 (Ar *C*H), 126.0 (Ar *C*H), 123.7 (Ar *C*H), 121.0 (Ar *C*H), 118.4 (Ar *C*H), 118.2 (Ar *C*H), 111.4 (Ar *C*H), 109.4 (Ar *C*), 52.6 (*C*H), 26.4 (*C*H_2); HRMS (ESI$^-$) calcd. for $C_{17}H_{14}N_3O_4$ $[M-H]^-$ 324.0990; Found 324.0984.

(*R*)-methyl *S*-(naphthalen-2-ylmethyl)cysteinate 235

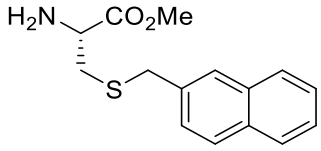

To a solution of L-cysteine methyl ester hydrochloride (2.14 g, 12.14 mmol) and 2-bromomethylnaphthalene (2.50 g, 11.31 mmol) in anhydrous CH_2Cl_2 (60 mL), triethylamine (3.31 mL, 23.75 mmol) was added dropwise at room temperature. The mixture was stirred at room temperature for 2 d, washed (H_2O), dried over $MgSO_4$ and evaporated *in vacuo*. Chromatography (hexane/EtOAc 4:6) afforded **235** (2.50 g, 80%) as a yellow oil. R_f = 0.15. $[\alpha]_D$= -6.0 (c= 1.81 x 10-3, MeOH). IR (neat) ν/cm^{-1} 3347 (NH_2), 1738 (CH_3C=O); ^{1}H NMR

(500 MHz, $CDCl_3$) δ 7.83-7.81 (3H, m, Ar C*H*), 7.71 (1H, s, Ar C*H*), 7.50-7.46 (3H, m, Ar C*H*), 3.89 (2H, s, SCH_2), 3.69 (3H, s, CO_2CH_3), 3.63-3.61 (1H, m, C*H*), 2.84 (1H, dd, *J*= 13.5 5.0, SCH_2), 2.92 (1H, dd, *J*= 13.5 6.0, SCH_2); ^{13}C NMR (125MHz, $CDCl_3$) δ 174.4 (*C*=O), 135.2 (Ar *C*), 133.2 (Ar *C*), 132.6 (Ar *C*), 128.5 (Ar *C*H), 127.7 (Ar *C*H), 127.6 (Ar *C*H), 127.45 (Ar *C*H), 127.0 (Ar *C*H), 126.2 (Ar *C*H), 125.9 (Ar *C*H), 54.1 (CO_2CH_3), 52.2 (*C*H), 36.9 (S*C*H_2), 36.3 (S*C*H_2); HRMS (ESI^+) calcd. for $C_{15}H_{18}NO_2S$ $[M+H]^+$ 276.1053; Found 276.1056.

Methyl *N*-(quinolin-2-ylcarbonyl)glycinate 236

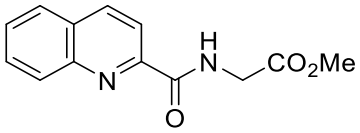

To a solution of glycine methyl ester hydrochloride (0.13 g, 1.04 mmol) and quinaldoyl chloride (0.20 g, 1.04 mmol) in anhydrous CH_2Cl_2 (20 mL), triethylamine (3.31 mL, 23.75 mmol) was added dropwise at room temperature. The mixture was stirred at room temperature for 2 d, washed (H_2O), dried over $MgSO_4$ and evaporated *in vacuo*. Chromatography (hexane /EtOAc 7:3 to 6:4) afforded compound **236** (0.12 g, 50%) as a white solid, mp 98-99 ºC. R_f = 0.36. IR (neat) ν/cm^{-1} 3328 (N-H), 1746 (CH_3OC=O), 1653 (NHC=O); ^{1}H NMR (500 MHz, $CDCl_3$) δ 8.71 (1H, t, *J*= 5.0, N*H*), 8.31 (2H, dd, *J*= 15.0 8.5, Ar C*H*), 8.15 (1H, dd, *J*= 9.0 1.0, Ar C*H*), 7.88 (1H, d, *J*= 4.0, ArC*H*), 7.80-7.76 (1H, m, Ar C*H*), 7.65-7.62 (1H, m, Ar C*H*), 4.35 (2H, d, *J*= 6.0, CH_2), 3.83 (3H, s, CH_3). ^{13}C NMR (125MHz, $CDCl_3$) δ 170.2 (*C*=O), 164.8 (*C*=O), 149.0 (Ar *C*), 146.5 (Ar *C*), 137.5 (Ar *C*), 130.1 (Ar *C*H), 129.8 (Ar *C*H), 129.4 (Ar *C*H), 128.0 (Ar *C*H), 127.7 (Ar *C*H), 118.8 (Ar *C*H), 52.4 (*C*H_3), 41.3 (*C*H_2); HRMS (ESI^-) calcd. for $C_{13}H_{12}N_2O_3$ $[M+Na]^-$ 267.0740; Found 267.0731.

(*R*)- Methyl *S*-(naphthalen-2-ylmethyl)-*N*-(quinolin-2-ylcarbonyl)cysteinate 237

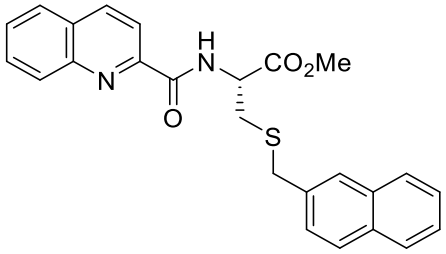

To a stirred solution of quinaldoyl chloride (0.14 g, 0.73 mmol) in anhydrous CH_2Cl_2 (10 mL) under N_2, **235** (0.20 g, 0.73 mmol) was added followed by triethylamine (0.11 mL, 0.80 mmol). The reaction mixture was stirred for 2 d until consumption of starting material. The mixture was washed with water and the organic layer was dried over $MgSO_4$ and concentrated *in vacuo*. Chromatography (hexane/EtOAc 8:2 to 6:4) afforded compound **237** (0.12 g, 37 %) as a yellow oil. R_f = 0.13. $[\alpha]_D$= -88.8 (c= 1.00 x 10^{-3}, MeOH). IR (neat) ν/cm^{-1} 3397 (N-H), 1744 (CH_3OC=O), 1677 (NHC=O); ^{1}H NMR (500 MHz, $CDCl_3$) δ 8.98 (1H, d, *J*= 8.5, N*H*), 8.28-8.25 (2H, m, Ar C*H*), 8.17 (1H, d, *J*= 9.0, ArC*H*), 7.84 (1H, d, *J*= 8.5, ArC*H*), 7.77-7.71 (5H, m, Ar C*H*), 7.60 (1H, t, *J*= 8.0, ArC*H*), 7.49 (1H, dd, *J*= 8.5 2.0, ArC*H*), 7.46-7.40 (2H, m, ArC*H*), 5.15 (1H, d, *J*= 3.5, CH), 3.99 (1H, d, *J*= 13.0, CH_2), 3.96 (1H, d, *J*= 13.0, CH_2), 3.79 (3H, s, CH_3), 3.07 (1H, dd, *J*= 14.0 5.0, SCH_2), 3.04 (1H, dd, *J*= 14.0 6.0, SCH_2); ^{13}C NMR (125MHz, $CDCl_3$) δ 171.2 (*C*=O), 164.3 (*C*=O), 148.9 (Ar *C*), 146.5 (Ar *C*), 137.5 (Ar *C*H), 134.9 (Ar *C*), 133.2 (Ar *C*), 132.5 (Ar *C*), 130.1 (Ar *C*H), 130.0 (Ar *C*H), 129.4 (Ar *C*H), 128.5 (Ar *C*H), 128.1 (Ar *C*H), 127.7 (Ar *C*H), 127.6 (Ar *C*H), 127.6 (Ar *C*H), 127.0 (Ar *C*H), 126.2 (Ar *C*H), 125.8 (Ar *C*H), 118.7 (Ar *C*H), 52.7 (*C*H_3), 52.2 (*C*H), 36.9 (S*C*H_2), 33.25 (*C*H_2); HRMS (ESI^+) calcd. for $C_{25}H_{23}N_2O_3S$ $[M+H]^+$ 431.1424; Found 431.1413.

***N*-(quinolin-2-ylcarbonyl)glycine 239**[39]

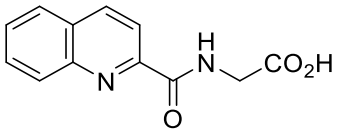

Following general procedure C, to a solution of **236** (25 mg, 0.10 mmol) in 1,4-dioxane (3 mL) 1 M lithium hydroxide (0.20 mL, 0.20 mmol) was added. Concentration afforded compound **239** (15 mg, 66 %) as a white solid, mp 183-184 ºC. IR (neat) ν/cm^{-1} 3357 (N-H), 2915 (COO-H), 1749 (HOC=O), 1624 (NHC=O); ^{1}H NMR (500 MHz, MeOD-*d*$_4$) *δ* 8.47 (1H, d, *J*= 8.5, Ar C*H*), 8.19 (2H, t, *J*= 8.5, Ar C*H*), 8.00 (1H, d, *J*= 8.0, Ar C*H*), 7.85-7.82 (1H, m, Ar C*H*), 7.71-7.68 (1H, m, Ar C*H*), 4.25 (2H, s, C*H*$_2$); ^{13}C NMR (125MHz, MeOD-*d*$_4$) *δ* 172.9 (*C*=O), 167.2 (*C*=O), 150.5 (Ar *C*), 148.1 (Ar *C*), 138.9 (Ar *C*H), 131.5 (Ar *C*H), 130.9 (Ar *C*), 130.8 (Ar *C*H), 129.4 (Ar *C*H), 129.0 (Ar *C*H), 119.5 (Ar *C*H), 42.1 (*C*H$_2$); HRMS (ESI$^-$) calcd. for $C_{12}H_{10}N_2O_3$ [M-H]$^-$ 229.0619; Found 229.0611.

(*R*)- *S*-(naphthalen-2-ylmethyl)-*N*-(quinolin-2-ylcarbonyl)cysteine 240

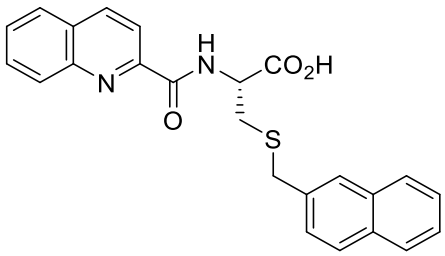

Following general procedure C, to a solution of **237** (26 mg, 0.06 mmol) in 1,4-dioxane (2 mL) 1 M lithium hydroxide (0.12 mL, 0.12 mmol) was added. Concentration afforded compound **240** (10 mg, 40 %) as a yellow solid, mp 225-226 ºC. [α]$_D$= -15.2 (c= 1.05 x 10^{-3}, MeOH). IR (neat) ν/cm^{-1} 3375 (N-H), 2917 (COO-H), 1779 (CH_3OC=O), 1674 (NHC=O); ^{1}H NMR (500 MHz, DMSO-*d*$_6$) *δ* 13.14 (1H, s, CO$_2$*H*), 9.11 (1H, d, *J*= 9.0, N*H*), 8.62 (1H, d, *J*= 9.0, ArC*H*), 8.19 (2H, d, *J*= 8.5, Ar C*H*), 8.13 (1H, d, *J*= 8.0, Ar C*H*), 7.93-7.89 (1H, m, Ar C*H*), 7.86-7.83 (2H, m, Ar C*H*), 7.81-7.75 (3H, m, Ar C*H*), 7.49-7.45 (3H, m, Ar C*H*), 4.85-4.81 (1H, m, C*H*), 3.98 (2H, s, SC*H*$_2$), 3.12-3.03 (2H, m, SC*H*$_2$); ^{13}C NMR (125MHz, DMSO-*d*$_6$) *δ* 171.8 (*C*=O), 163.7 (*C*=O), 149.3 (Ar *C*), 146.0 (Ar *C*), 138.2 (Ar *C*H), 135.6

(Ar *C*), 132.7 (Ar *C*), 132.0 (Ar C), 130.7 (Ar *C*H), 129.2 (Ar *C*H), 129.0 (Ar *C*H), 128.3 (Ar *C*H), 128.2 (Ar *C*H), 128.1 (Ar *C*H), 127.5 (Ar *C*H), 127.4 (Ar *C*H), 127.2 (Ar *C*H), 127.1 (Ar *C*H), 126.2 (Ar *C*H), 125.8 (Ar *C*), 118.6 (Ar *C*H), 51.8(*C*H), 35.5 (S*C*H_2), 32.2 (*C*H_2); HRMS (ESI$^+$) calcd. for $C_{24}H_{20}N_2NaO_3S$ $[M+Na]^+$ 439.1087; Found 439.1081.

2.12 References

1. Falnes, P.O., Bjoras, M., Aas, P.A., Sundheim, O., and Seeberg, E., Substrate specificities of bacterial and human AlkB proteins. *Nucleic Acids Res*, **2004**, 32, 3456-61.

2. Trewick, S.C., Henshaw, T.F., Hausinger, R.P., Lindahl, T., and Sedgwick, B., Oxidative demethylation by Escherichia coli AlkB directly reverts DNA base damage. *Nature*, **2002**, 419, 174-8.

3. Mishina, Y., Duguid, E.M., and He, C., Direct reversal of DNA alkylation damage. *Chem Rev*, **2006**, 106, 215-32.

4. Sedgwick, B., Bates, P.A., Paik, J., Jacobs, S.C., and Lindahl, T., Repair of alkylated DNA: Recent advances. *DNA Repair*, **2007**, 6, 429-42.

5. Yi, C.Q., Yang, C.G., and He, C., A Non-Heme Iron-Mediated Chemical Demethylation in DNA and RNA. *Accounts Chem Res*, **2009**, 42, 519-29.

6. Tsujikawa, K., Koike, K., Kitae, K., Shinkawa, A., Arima, H., Suzuki, T., Tsuchiya, M., Makino, Y., Furukawa, T., Konishi, N., and Yamamoto, H., Expression and sub-cellular localization of human ABH family molecules. *J Cell Mol Med*, **2007**, 11, 1105-16.

7. Aas, P.A., Otterlei, M., Falnes, P.O., Vagbo, C.B., Skorpen, F., Akbari, M., Sundheim, O., Bjoras, M., Slupphaug, G., Seeberg, E., and Krokan, H.E., Human and bacterial oxidative demethylases repair alkylation damage in both RNA and DNA. *Nature*, **2003**, 421, 859-63.

8. Ringvoll, J., Nordstrand, L.M., Vagbo, C.B., Talstad, V., Reite, K., Aas, P.A., Lauritzen, K.H., Liabakk, N.B., Bjork, A., Doughty, R.W., Falnes, P.O., Krokan, H.E., and Klungland, A., Repair deficient mice reveal mABH2 as the primary oxidative demethylase for repairing 1meA and 3meC lesions in DNA. *Embo J*, **2006**, 25, 2189-98.

9. Weber, L., In vitro combinatorial chemistry to create drug candidates. *Drug Discovery Today: Technologies*, **2004**, 1, 261-7.

10. Hochgurtel, M., Biesinger, R., Kroth, H., Piecha, D., Hofmann, M.W., Krause, S., Schaaf, O., Nicolau, C., and Eliseev, A.V., Ketones as building blocks for dynamic

combinatorial libraries: Highly active neuraminidase inhibitors generated via selection pressure of the biological target. *Journal of Medicinal Chemistry*, **2003**, 46, 356-8.

11. Ramstrom, O. and Lehn, J.M., In situ generation and screening of a dynamic combinatorial carbohydrate library against concanavalin A. *Chembiochem*, **2000**, 1, 41-8.

12. Caraballo, R., Dong, H., Ribeiro, J.P., Jimenez-Barbero, J., and Ramstrom, O., Direct STD NMR Identification of beta-Galactosidase Inhibitors from a Virtual Dynamic Hemithioacetal System. *Angew Chem Int Edit*, **2010**, 49, 589-93.

13. Triolo, A., Altamura, M., Cardinali, F., Sisto, A., and Maggi, C.A., Mass spectrometry and combinatorial chemistry: a short outline. *J Mass Spectrom*, **2001**, 36, 1249-59.

14. Poulsen, S.A., Davis, R.A., and Keys, T.G., Screening a natural product-based combinatorial library using FTICR mass spectrometry. *Bioorgan Med Chem*, **2006**, 14, 510-5.

15. Wright, P.A., Rostom, A.A., Robinson, C.V., and Schofield, C.J., Mass spectrometry reveals elastase inhibitors from the reactive centre loop of alpha(1)-antitrypsin. *Bioorg Med Chem Lett*, **2000**, 10, 1219-21.

16. Lienard, B.M.R., Hueting, R., Lassaux, P., Galleni, M., Frere, J.M., and Schofield, C.J., Dynamic combinatorial mass spectrometry leads to metallo-beta-lactamase inhibitors. *Journal of Medicinal Chemistry*, **2008**, 51, 684-8.

17. Mecinovic, J., Loenarz, C., Chowdhury, R., and Schofield, C.J., 2-Oxoglutarate analogue inhibitors of prolyl hydroxylase domain 2. *Bioorg Med Chem Lett*, **2009**, 19, 6192-5.

18. Lienard, B.M.R., Selevsek, N., Oldham, N.J., and Schofield, C.J., Combined mass spectrometry and dynamic chemistry approach to identify metalloenzyme inhibitors. *Chemmedchem*, **2007**, 2, 175-+.

19. Mecinovic, J., Chowdhury, R., Flashman, E., and Schofield, C.J., Use of mass spectrometry to probe the nucleophilicity of cysteinyl residues of prolyl hydroxylase domain 2. *Anal Biochem*, **2009**, 393, 215-21.

20. Rose, N.R., McDonough, M.A., King, O.N.F., Kawamura, A., and Schofield, C.J., Inhibition of 2-oxoglutarate dependent oxygenases. *Chem Soc Rev*, **2011**, 40, 4364-97.

21. McDonough, M.A., Li, V., Flashman, E., Chowdhury, R., Mohr, C., Lienard, B.M.R., Zondlo, J., Oldham, N.J., Clifton, I.J., Lewis, J., McNeill, L.A., Kurzeja, R.J.M., Hewitson, K.S., Yang, E., Jordan, S., Syed, R.S., and Schofield, C.J., Cellular oxygen sensing: Crystal structure of hypoxia-inducible factor prolyl hydroxylase (PHD2). *P Natl Acad Sci USA*, **2006**, 103, 9814-9.

22. Niesen, F.H., Berglund, H., and Vedadi, M., The use of differential scanning fluorimetry to detect ligand interactions that promote protein stability. *Nat Protoc*, **2007**, 2, 2212-21.

23. Yu, B., Edstrom, W.C., Benach, J., Hamuro, Y., Weber, P.C., Gibney, B.R., and Hunt, J.F., Crystal structures of catalytic complexes of the oxidative DNA/RNA repair enzyme AlkB. *Nature*, **2006**, 439, 879-84.

24. Krylova, S.M., Karkhanina, A.A., Musheev, M.U., Bagg, E.A.L., Schofield, C.J., and Krylov, S.N., DNA aptamers for as analytical tools for the quantitative analysis of DNA-dealkylating enzymes. *Anal Biochem*, **2011**, 414, 261-5.

25. Karkhanina, A.A., Mecinovic, J., Musheev, M.U., Krylova, S.M., Petrov, A.P., Hewitson, K.S., Flashman, E., Schofield, C.J., and Krylov, S.N., Direct Analysis of Enzyme-Catalyzed DNA Demethylation. *Anal Chem*, **2009**, 81, 5871-5.

26. Yang, C.G., Yi, C.Q., Duguid, E.M., Sullivan, C.T., Jian, X., Rice, P.A., and He, C., Crystal structures of DNA/RNA repair enzymes AlkB and ABH2 bound to dsDNA. *Nature*, **2008**, 452, 961-U4.

27. Yu, B. and Hunt, J.F., Enzymological and structural studies of the mechanism of promiscuous substrate recognition by the oxidative DNA repair enzyme AlkB. *P Natl Acad Sci USA*, **2009**, 106, 14315-20.

28. Loenarz, C. and Schofield, C.J., Expanding chemical biology of 2-oxoglutarate oxygenases. *Nat Chem Biol*, **2008**, 4, 152-6.

29. Loenarz, C., Ge, W., Coleman, M.L., Rose, N.R., Cooper, C.D.O., Klose, R.J., Ratcliffe, P.J., and Schofield, C.J., PHF8, a gene associated with cleft lip/palate and mental

retardation, encodes for an N-epsilon-dimethyl lysine demethylase. *Hum Mol Genet*, **2010**, 19, 217-22.

30. Schofield, C.J. and Ratcliffe, P.J., Oxygen sensing by HIF hydroxylases. *Nat Rev Mol Cell Bio*, **2004**, 5, 343-54.

31. Daniel, J.M., Friess, S.D., Rajagopalan, S., Wendt, S., and Zenobi, R., Quantitative determination of noncovalent binding interactions using soft ionization mass spectrometry. *Int J Mass Spectrom*, **2002**, 216, 1-27.

32. McDonough, M.A., McNeill, L.A., Tilliet, M., Papamicael, C.A., Chen, Q.Y., Banerji, B., Hewitson, K.S., and Schofield, C.J., Selective inhibition of factor inhibiting hypoxia-inducible factor. *J Am Chem Soc*, **2005**, 127, 7680-1.

33. Welford, R.W.D., Schlemminger, I., McNeill, L.A., Hewitson, K.S., and Schofield, C.J., The selectivity and inhibition of AlkB. *J Biol Chem*, **2003**, 278, 10157-61.

34. Otwinowski, Z. and Minor, W., *Methods in Enzymology*. Vol. 276. 1997: Elsevier.

35. Mccoy, A.J., Grosse-Kunstleve, R.W., Adams, P.D., Winn, M.D., Storoni, L.C., and Read, R.J., Phaser crystallographic software. *J Appl Crystallogr*, **2007**, 40, 658-74.

36. Adams, P.D., Afonine, P.V., Bunkoczi, G., Chen, V.B., Davis, I.W., Echols, N., Headd, J.J., Hung, L.W., Kapral, G.J., Grosse-Kunstleve, R.W., McCoy, A.J., Moriarty, N.W., Oeffner, R., Read, R.J., Richardson, D.C., Richardson, J.S., Terwilliger, T.C., and Zwart, P.H., PHENIX: a comprehensive Python-based system for macromolecular structure solution. *Acta Crystallogr D*, **2010**, 66, 213-21.

37. Emsley, P. and Cowtan, K., Coot: model-building tools for molecular graphics. *Acta Crystallogr D*, **2004**, 60, 2126-32.

38. Baringhaus, K.H., Bickel, M., Tschank, G., and Weidmann, K., 3- hydroxypyridine-2-carboxamidoesters, their preparation and their use as pharmaceuticals., **1997**, EP 765871 A1.

39. Davis, J.W., Studies with Quinolines .1. Synthesis of Quinaldic Acid and Some of Its Amide Derivatives. *J Org Chem*, **1959**, 24, 1691-4.

40. Tse, M.K., Jiao, H., Anilkumar, G., Bitterlich, B., Gelalcha, F.G., and Beller, M., Synthetic, spectral and catalytic activity studies of ruthenium bipyridine and terpyridine complexes: Implications in the mechanism of the ruthenium(pyridine-2,6-

bisoxazoline)(pyridine-2,6-dicarboxylate)-catalyzed asymmetric epoxidation of olefins utilizing H2O2. *J Organomet Chem*, **2006**, 691, 4419-33.

41. Memoli, K.A., A convenient preparation of 3-mercaptopicolinic acid. *Tetrahedron Lett*, **1996**, 37, 3617-8.

Chapter 3. Dynamic Combinatorial Mass Spectrometry for Inhibition of Prolyl Hydroxylase Domain 2

3.1 Introduction

3.1.1 Reversible reactions in dynamic combinatorial mass spectrometry (DCMS)

Of the many reversible reactions that have been used for DCC, only two have found application in DCMS. Disulphide formation is the most used reaction in DCMS and has found application with various protein targets because of the reversibility of this reaction in aqueous solutions at physiological pH and the stability of disulphides under MS conditions.[1, 2] In addition, hydrazone formation, which was the first reaction applied in protein DCMS with carbonic anhydrase (CA),[3, 4] has been used in recent studies to form a dynamic library of pseudo-oligopeptides[5] and to identify γ-aminobutyric acid (GABA) transporter 1 binders.[6] One disadvantage of the hydrazone approach is that libraries have to be composed of electron poor hydrazides in order to enable reversibility of hydrazine formation.[7] Even though both of the thiol/disulphide and hydrazine/hydrazone systems have proved suitable for several enzymes, the slow progression in their application to other biomolecule targets implies limitations in their usability. Thus, there is still a need for a wider range of reversible reactions to be applied in DCMS with biomolecules.

The application of boronate ester formation from boronic acids and alcohols in DCMS was considered because the reaction is reversible in aqueous solution at physiologically relevant pH.[8, 9] Boronic acids react with 1,2- and 1,3-*cis*-diols,[10] α-hydroxy carboxylic acids[11-14] and dicarboxylic acids (Figure 3. 1).[13] They also readily react with sugars[15] and have found application in sugar recognition.[15, 16]

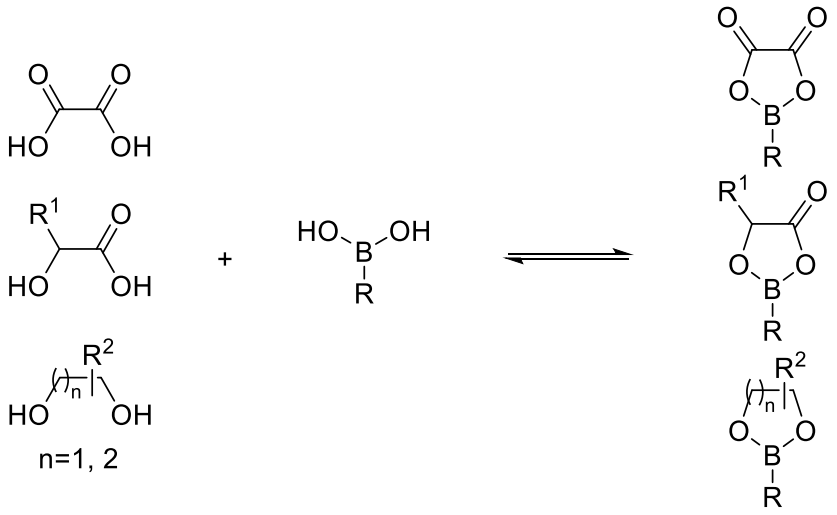

Figure 3. 1 *The reversible reaction of boronic acids with alcohols to form boronate esters.*

Two examples of boronate esters being involved in library formation have been reported. Boronate acid containing libraries were used to identify binders of glycoproteins[17] and DNA.[18] Moreover, a dynamic library based on boronate ester and imine formation has been used for the formation of macrocycles.[19] Proof of principle work with proteases, where boronic acids were shown to react with the nucleophilic serine to form a 'mono' boronate ester that could further react with alcohols, was carried out in our group. [20] This study has revealed that the use of reversibly reacting boronic acid/boronate ester systems for identification of enzyme inhibitors is possible.[20]

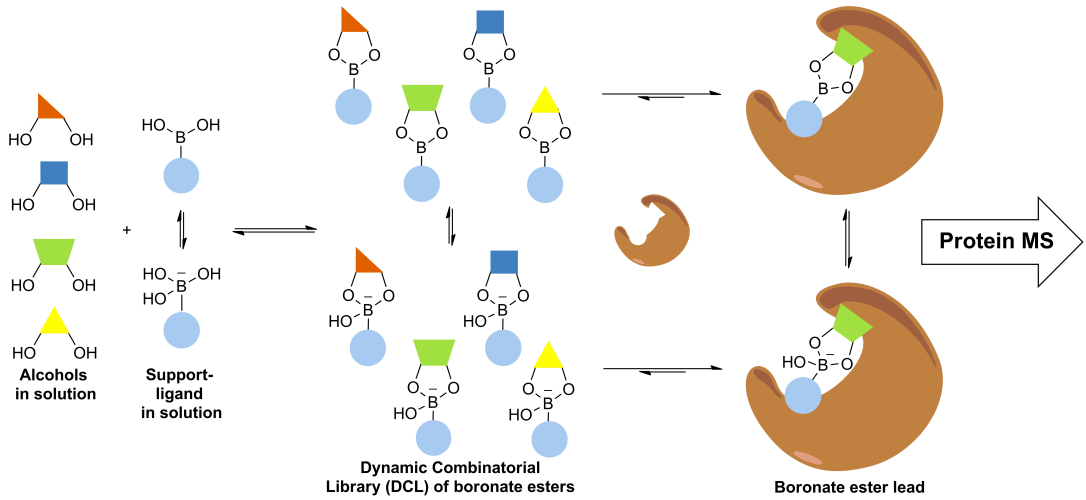

Figure 3. 2 *Dynamic combinatorial chemistry employing the formation of boronate esters and identification of adducts with non-denaturing ESI-mass spectrometry.*

3.1.2 Prolyl Hydroxylase domain 2 (PHD2) inhibitors

The role of the hypoxia inducible factor prolyl-hydroxylase, PHD2, in human oxygen sensing has led to a number of investigations to identify specific inhibitors. Studies with PHD2 inhibition have led to promising results for the treatment of anaemia[21, 22] and ischaemic diseases[23] including heart disease[24, 25] and stroke.[26, 27] Therefore, achieving potent and selective PHD2 inhibitors is a biomedically important objective. Most PHD2 inhibitors that have been reported to date are co-substrate (2OG) analogues which contain iron chelating groups that bind in the active site of the enzyme (Figure 3. 3). Even though some very potent and active *in vivo* PHD2 inhibitors have been identified,[28] their selectivity over other 2OG oxygenases still remains an issue. The importance of developing selective PHD2 inhibitors and the fact that PHD2 has been extensively analysed using ESI-MS,[29-31] led to the selection of PHD2 as a model enzyme for the exploration of the boronic acid/boronate ester DCMS method.

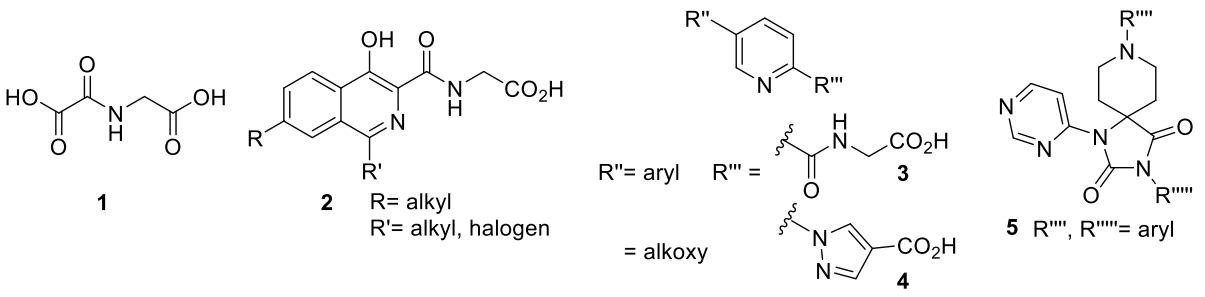

Figure 3. 3 *Examples of reported PHD2 inhibitor classes.*[32]

3.2 Modelling of the scaffold

Firstly, a 'support ligand' that would bind to PHD2 and enable reversible boronate ester formation was proposed. For DCMS, the 'support ligand' compound was required to incorporate both an iron chelating group for binding to the active site bound iron, as well as a boronic acid group to enable the formation of the boronate ester dynamic combinatorial library (DCL). Pyridine based inhibitors with weak inhibitory potency against PHD2 have been recently reported (Figure 3. 3, **3**)[33] and were deemed suitable for this investigation as ligands for DCMS. Manual modelling based on existing crystal structures of PHD2 with inhibitors implied that the C-5 boronic acid (Figure 3. 4 B) would bind in such a way to direct the boronate ester formation into the 'free space' of the substrate binding site. The docking indicates that the C-6 boronic acid (Figure 3. 4 C) may also be able to offer access to the substrate binding site, but with likely less flexibility compared to the C-5 boronic acid as it is positioned very close to the iron chelating aspartic acid (Asp315). The boronic acid of the C-4 substituted pyridine is predicted to make steric clash with the active site so prevent formation of PHD2-binding boronate esters (Figure 3. 4 A).

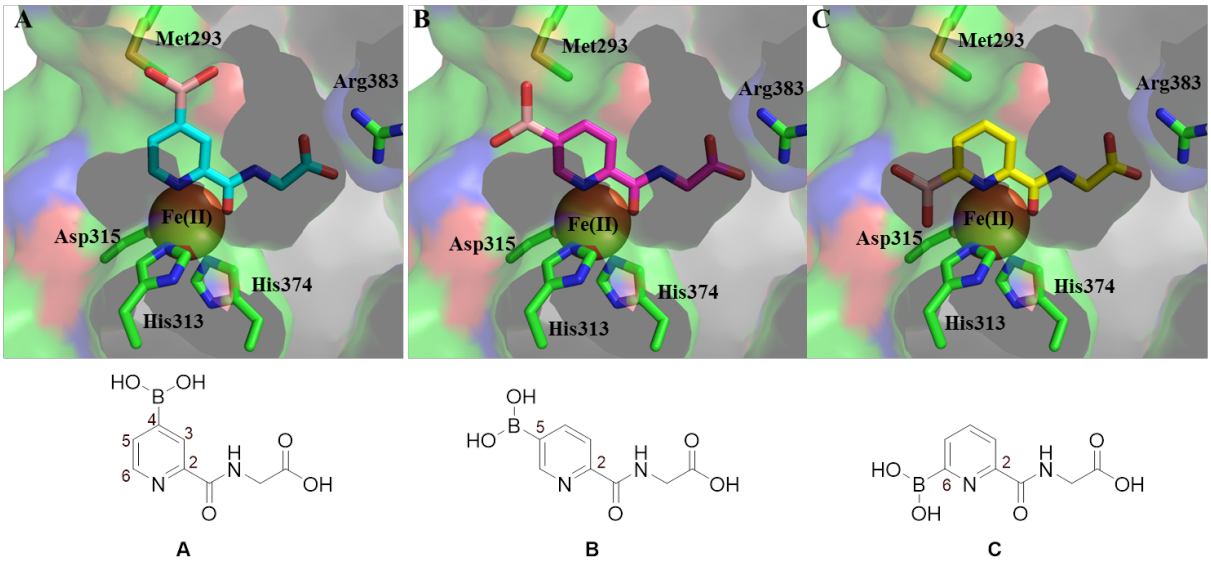

Figure 3. 4 *Modelling of pyridyl-boronate acids (**A-C**) in the active site of PHD2·Fe·**406** (PDB ID: 3HQU).*[34]

3.3 Synthesis of boronic acids

Based on the modelling studies, synthesis of the three pyridyl-boronic acids was attempted (**A-C**, Figure 3. 4). Following optimisation of the syntheses of the bromo-pyridines **301a-c**, boronate esters were synthesised *via* a Suzuki-Miyura coupling by modifying literature conditions.[35] The boronate ester **303** was synthesised to provide the boronate salt **305a**, as the stable pinane boronate esters are readily purified using column chromatography (Scheme 3. 1).[36] However, sufficient hydrolysis of the pinane ester was not successful. Therefore, the pinacol esters **302a-c**, which are less stable than pinane boronate esters, were formed and subsequently deprotected to form the trifluoroborate salts.[37] The borate salts **305** were hydrolysed in the presence of trimethylsilylchloride (TMSCl) to provide the final boronic acids (Scheme 3. 1).[37, 38]

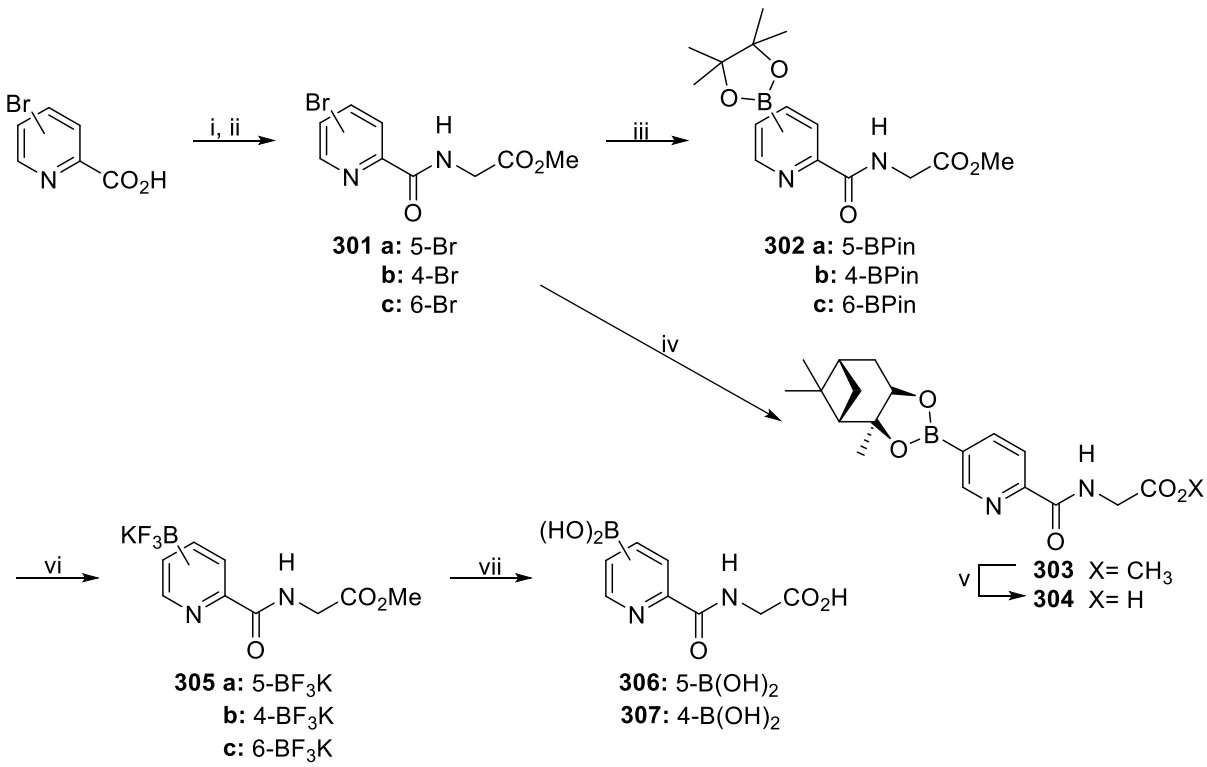

Scheme 3. 1 *Synthesis of boronic acids.*

Reagents and conditions: i) $SOCl_2$ (excess), reflux; ii) glycine methyl ester hydrochloride (1equiv.), NEt_3 (2 equiv.), CH_2Cl_2, r.t; iii) $(PinB)_2$ (1.6 equiv.), KOAc, $Pd(dppf)Cl_2$ (10 mole %); iv) $(PinaneB)_2$ (1.6 equiv.), KOAc, $Pd(dppf)Cl_2$ (10 mole %); v) 1 M LiOH (2 equiv.), 1,4-dioxane, r.t; vi) KHF_2 (10 equiv.), MeOH, r.t; vii) TMSCl (10 equiv.), CH_3CN/ H_2O 2:1, r.t.

Despite some efforts hydrolysis of the boronate salt **305c** to 6-boronic acid was not achieved, presumably because of the known instability of *ortho* substituted pyridine boronic acids.[39, 40] Investigation of the 6-boronate ester-pyridines was therefore abandoned, due to time constraints.

3.4 Binding of boronic acids and esters by ESI-MS

The next step was to investigate the ESI-MS best conditions for boronic acid/boronate ester binding to PHD2. The boronate ester **304** was used in binding optimisation experiments with PHD2 using non-denaturing mass spectrometry. The binding of **304** at different cone voltages was investigated. At cone voltages over 50V the boronate ester was cleaved leaving the

boronic acid, with 34 Da lower mass, being the major species observed bound to PHD2 (Figure 3. 5). Similar observations have been made in studies of boronic acids with α-chymotrypsin by non-denaturing ESI-MS.[41] Calculations have shown that this mass loss is likely due to cleavage of the two hydroxyl groups of the acid to give a trigonal species. The cleavage of the hydroxyl is dependent on the cone voltage, showing that it is a MS induced species formation. Because the boronate ester partially survives at low voltage, these conditions (cone voltage= 30V) were used throughout the study.

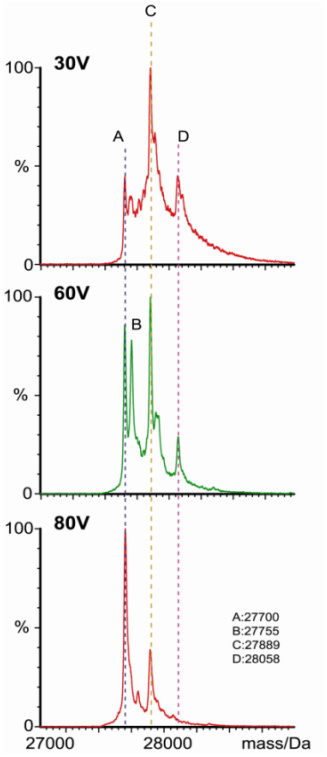

Figure 3. 5 *Mass spectra of* ***304*** *with PHD2·Fe(II) at different cone voltages. A: PHD2·Fe, B: PHD2·2Fe, C: PHD2·Fe·[****304****-pinane diol], D: PHD2·Fe·****304****.*

Before using **306** and **307** in DCMS, their binding to the active site of PHD2 was investigated using the PHD2·Fe(II) complex. **306** and **307** were mixed separately with PHD2·Fe and ESI-MS was used to assess their binding affinity; the affinity was judged by competition with *N*-oxalyl glycine (**202a**, NOG), a generic 2OG oxygenase inhibitor that binds in the active site by iron chelation, to identify the position of binding. Both boronic acids were found to form complexes with PHD2·Fe, confirming their ability to bind to PHD2. Also, the PHD2·Fe·boronate acid peaks disappeared in the presence of **202a**, to give the

PHD2·Fe·**202a** adduct, proving that **306** and **307** bind to PHD2 by chelating the iron in the active site (Figure 3. 6).

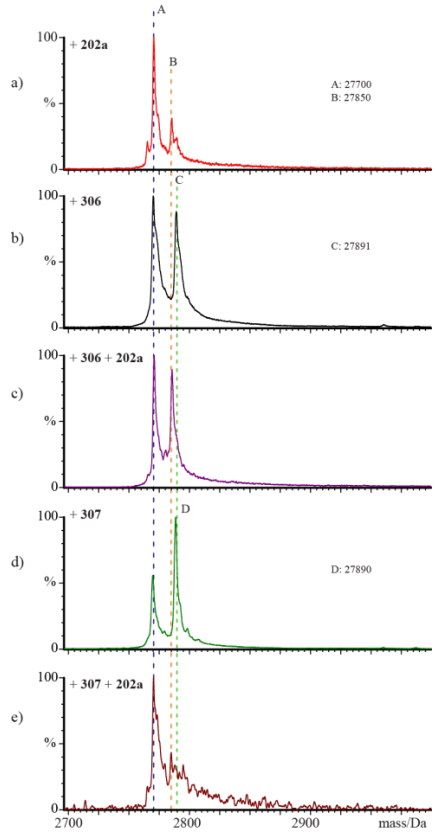

Figure 3. 6 *Mass spectra of* ***306/307*** *in competition with* ***202a*** *for PHD2·Fe(II). A: PHD2·Fe, B: PHD2·Fe·****202a****, C: PHD2·Fe·[****306****-2(OH)], D: PHD2·Fe·[****307****-2(OH)].*

Since the rate of boronate ester formation is increased when the pH of the reaction is higher than the pKa of the boronic acids,[42] the pKa of the two boronic acids was measured by NMR. **306** and **307** were found to have pKa values close (**306**, pKa= 7.4) or lower (**307** pKa= 6.9) than the experimental conditions pH 7.5.

NMR pKa experiments were acquired by Dr. Ivanhoe Leung.

3.5 Dynamic combinatorial library

With the boronic acids in hand a library of diols was assembled to form the dynamic combinatorial library with **306** and **307** (DCL). The library contained alkyl and aromatic diols and aromatic 2-hydroxy carboxylic acids to allow the potential formation of five and six membered boronate esters (Figure 3. 7).

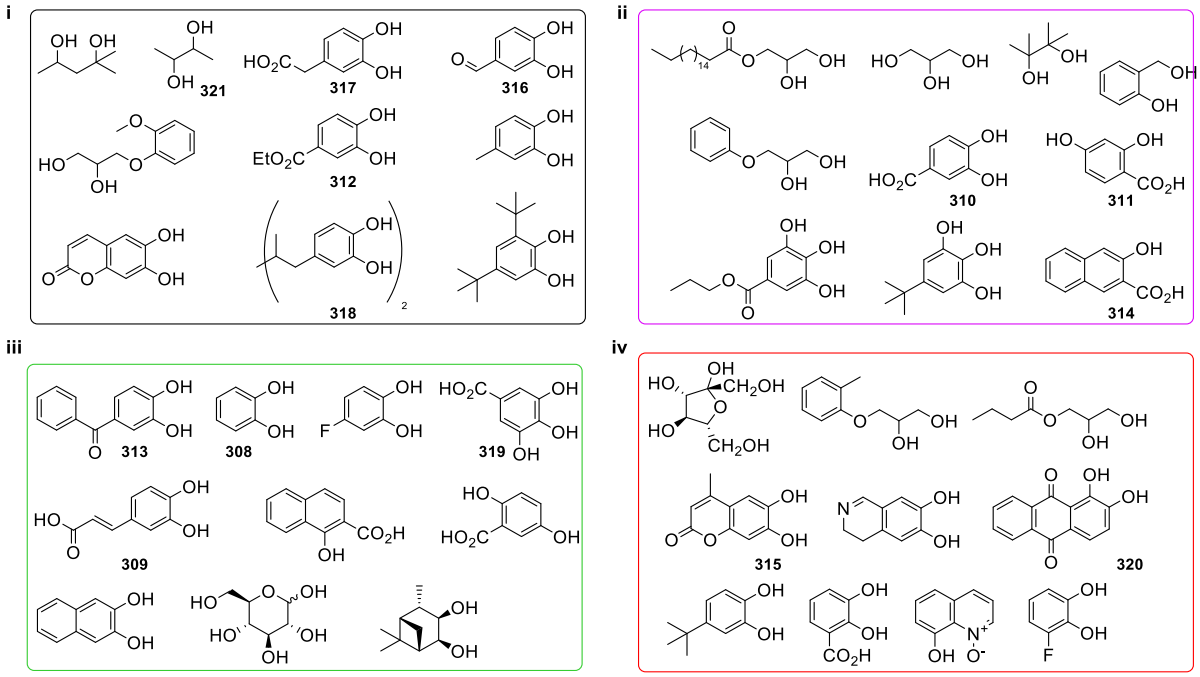

***Figure 3. 7** Library of diols used in this work.*

Many of the diols in the DCL have potential metal chelating functionalities; therefore it was envisaged that they might disrupt the binding of the boronic acid, or even the metal, to the active site of the protein. For this reason, and for analytical reasons, the 40 diols of the library were separated into four groups, in such a way that diols with different molecular weights were in each group (Figure 3. 7).

3.6 Non-denaturing ESI-MS studies on the DCL

As the most promising scavenger from the modelling studies, the 5-boronic acid **306** was used for initial investigations with one of the 10-membered groups of diols (Figure 3. 7, group **ii**). In the first instance, time-course DCC experiments with **306**, **ii** and PHD2 were conducted to determine the time needed for the reaction to reach apparent equilibrium under standard non-denaturing ESI-MS conditions. The standard conditions, use of equimolar reagents and mixing of compounds-binders prior to addition of Fe(II) and enzyme, usually result in immediate observation of PHD2·Fe·compound peaks. In the case of **306** with **ii** the reaction/binding equilibrium was reached after 1 h, as judged by the two boronate ester·PHD2 peaks, that remained constant for at least 5 h (Figure 3. 8). The two rate determining steps were the binding of iron and subsequent binding of **306** in the active site, possibly owing to the iron chelating properties of the diols.

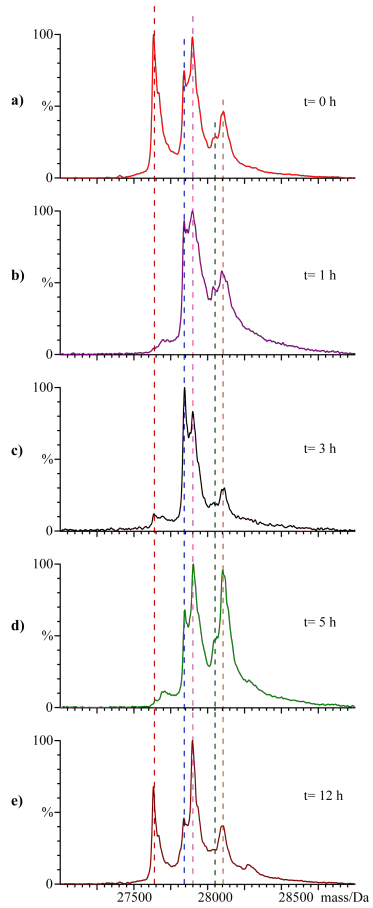

Figure 3. 8 *Deconvoluted non-denaturing ESI-MS of the reaction of PHD2 (1 equiv.) with Fe(II) (1equiv.),* ***306*** *(1 equiv.) and diols* ***ii*** *(1 equiv.) at cone voltage 30Vafter a) no incubation, b) 1 h, c) 3 h, d) 5 h, e) 12 h incubation. Dotted lines; red: ApoPHD2 (27650 ± 1 Da), blue:PHD2·Fe(II)·diol (27859 ± 3Da), pink: PHD2·Fe(II)·****306*** *(27892 ± 2 Da), green: PHD2·Fe(II)·****306-boronate ester1*** *(28047 ± 3 Da), orange: PHD2·Fe(II)·****306-boronate ester2*** *(28081 ± 3 Da).*

To ensure that the active site was saturated with Fe(II), the analyses with **306** and **ii** were repeated with 2 and 5 equivalents of metal. While there was significant improvement in iron binding at 0 min, decrease of apoPHD2 peak (Figure 3. 9), with the use of 2 equivalents of Fe(II), the equilibrium was still not reached before 1 h. In the presence of 5 equivalents of iron the quality of the spectra was reduced; only one peak was observed, believed to correspond to a diol directly binding to PHD2·Fe (Figure 3. 9).

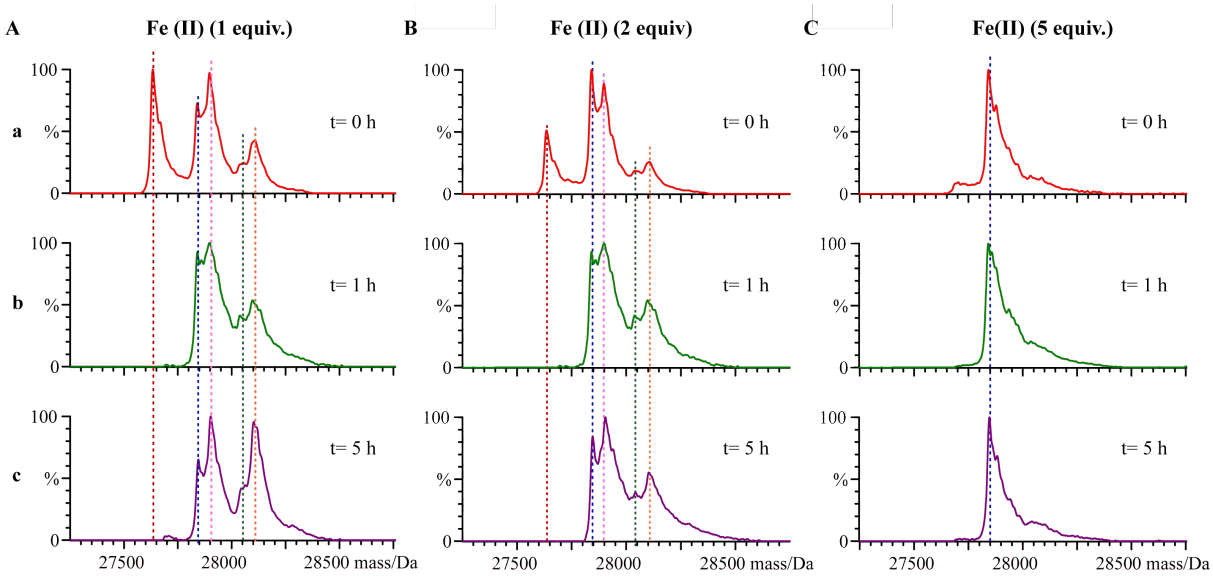

Figure 3. 9 *Deconvoluted non-denaturing ESI-MS of the reaction of PHD2 (1 equiv.) with* ***306*** *(1 equiv.) and diols* ***ii*** *(1 equiv.) and A. Fe(II) (1equiv.), B. Fe(II) (2equiv.) and C. Fe(II) (5equiv.) at cone voltage 30V, after a) no incubation, b) 1 h, c) 5 h incubation. Dotted lines; red: apoPHD2 (27650 ± 1 Da), blue:PHD2·Fe(II)·diol (27859 ± 3Da), pink: PHD2·Fe(II)·****306*** *(27892 ± 2 Da), green: PHD2·Fe(II)·****boronate ester1*** *(28047 ± 3 Da), orange: PHD2·Fe(II)·****boronate ester2*** *(28081 ± 3 Da).*

To enable efficient formation of the PHD2·Fe·boronic acid adduct, the mixture of the three components (i.e. apoPHD2, Fe(II) and **306**) was incubated for 1 min prior to addition of the diols. Indeed, this procedure led to immediate formation of the PHD2·Fe adduct as well as the PHD2·Fe·boronic acid adduct. The addition of diols to the pre-formed mixture of PHD2·Fe·**306** led to observation of the same boronate ester peaks as observed in the previous experiments immediately; the complexes were apparently stable over a period of 2 h. The DCMS analysis was then set up under the same conditions for **306** with the four groups of diols. In total, six boronate ester peaks were observed by ESI-MS from all four groups of diols (Figure 3. 10; peaks D, F, G, J, K, N). In the DCMS with every library, peaks of similar masses as the PHD2·Fe·**306** adduct were also present (Figure 3. 10; peaks C, E, H, I, L, M).

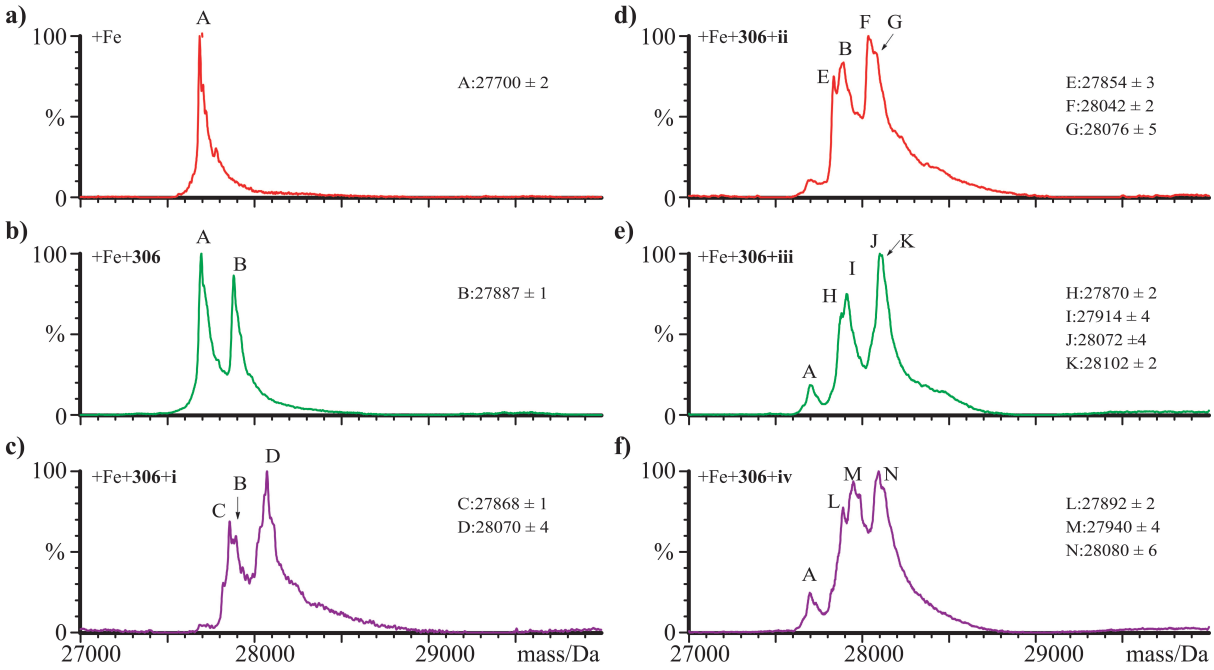

Figure 3. 10 *Deconvoluted non-denaturing ESI-MS of* ***306*** *with PHD2·Fe(II) and diols c)* ***i****, d)* ***ii****, e)* ***iii****, f)* ***iv*** *at cone voltage 30V. A: PHD2·Fe, B: PHD2·Fe·****306****, C,E,H,I,L,M: PHD2·Fe·diols, D,F,G,J,K,N: PHD2·Fe·[boronate esters of* ***306****].*

The DCMS was then carried with **307** under the same conditions as the **306** experiments. No boronate ester hits were revealed, confirming the predicted steric hindrance, for **307** based boronate esters, from the modelling studies (Figure 3. 4, Figure 3. 11). The same peaks (and two more) observed in the case of **306** and diol groups **i-iv** with masses similar to PHD2·Fe·**306,** were also apparent in the DCMS with **307** (Figure 3. 11, peaks C-J). This implies that the species formed are not related with the boronic acid present in the DCMS. These may be peaks of diols directly binding to PHD2 (Figure 3. 10), likely by iron chelation.

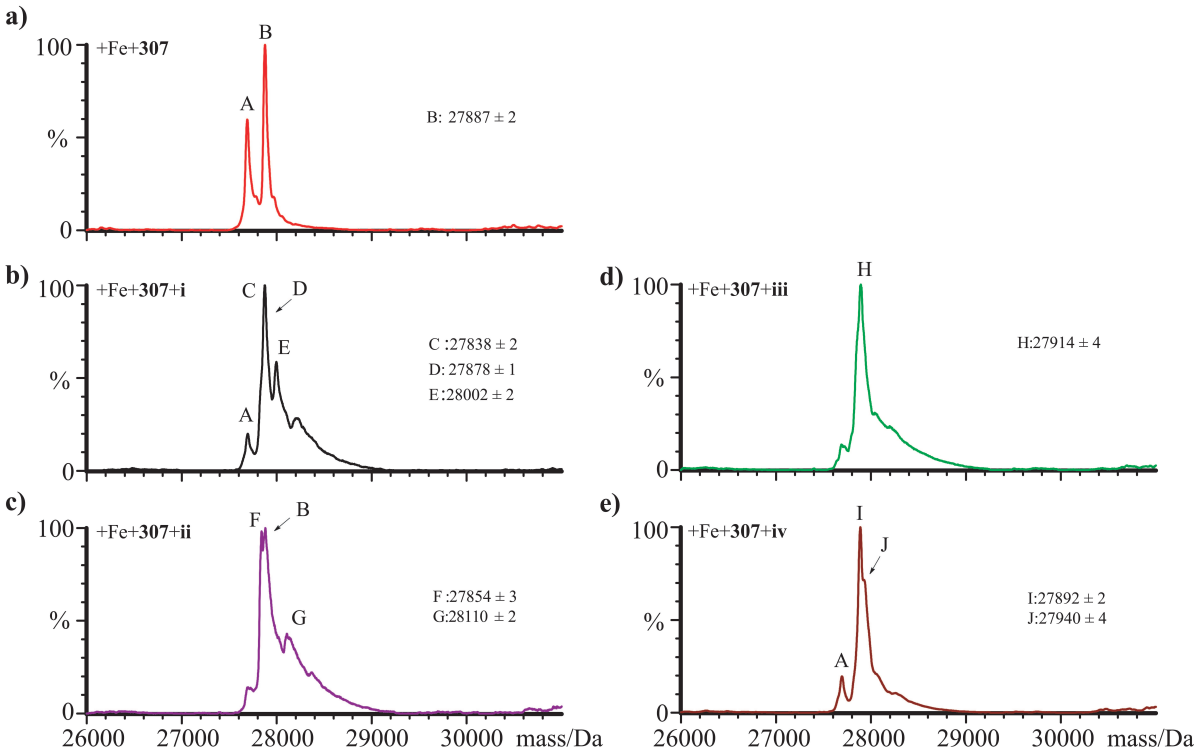

Figure 3. 11 *Deconvoluted non-denaturing ESI-MS of 307 with PHD2·Fe(II) and diols a) i, b) ii, c) iii, d) iv at cone voltage 30V. A: PHD2·Fe, B: PHD2·Fe·**307**, C-J: PHD2·Fe·diols.*

The binding of diols directly to PHD2 was investigated. Diols with masses corresponding to the formation of the PHD2·Fe·diol peak (peak mass – 27705 Da ± 3 Da) were thus tested individually for binding to PHD2·Fe. The same peaks with DCMS were observed when PHD2 was tested with diols **310**, **313**, **315-320** (Figure 3. 12 A).

The next step was to identify which of the boronate esters formed in solution bound to PHD2·Fe. Diols with masses corresponding to the formation of boronate esters were tested with PHD2·Fe·**306**, which identified diols **309-315** as those forming boronate esters with **306** (Figure 3. 12 B). A common structural feature was observed in the DCMS hits; five out of the seven hits were either 4-substituted benzene diols or 4-substituted 2-hydroxybenzoic acid (Figure 3. 13). These diols with **306** formed both five and six membered boronate ester rings, also the boronate esters consisted of two or three fused rings.

It was noticed that some of the hit diols in DCMS were also binding directly to PHD2 (diols **310**, **313** and **315**). To eliminate any suspicions that diols bind at another site of PHD2 at the

same time as boronic acids in the active site, and are responsible for the apparent masses of boronate esters observed, these diols were tested for binding to apoPHD2. No binding of diols was observed to the enzyme in the absence of iron, implying that diols bind directly to the PHD2·Fe complex. Thus it is not possible for both diols and boronic acids to bind to PHD2 together and the peaks observed in DCMS are due to binding of boronate esters formed in solution.

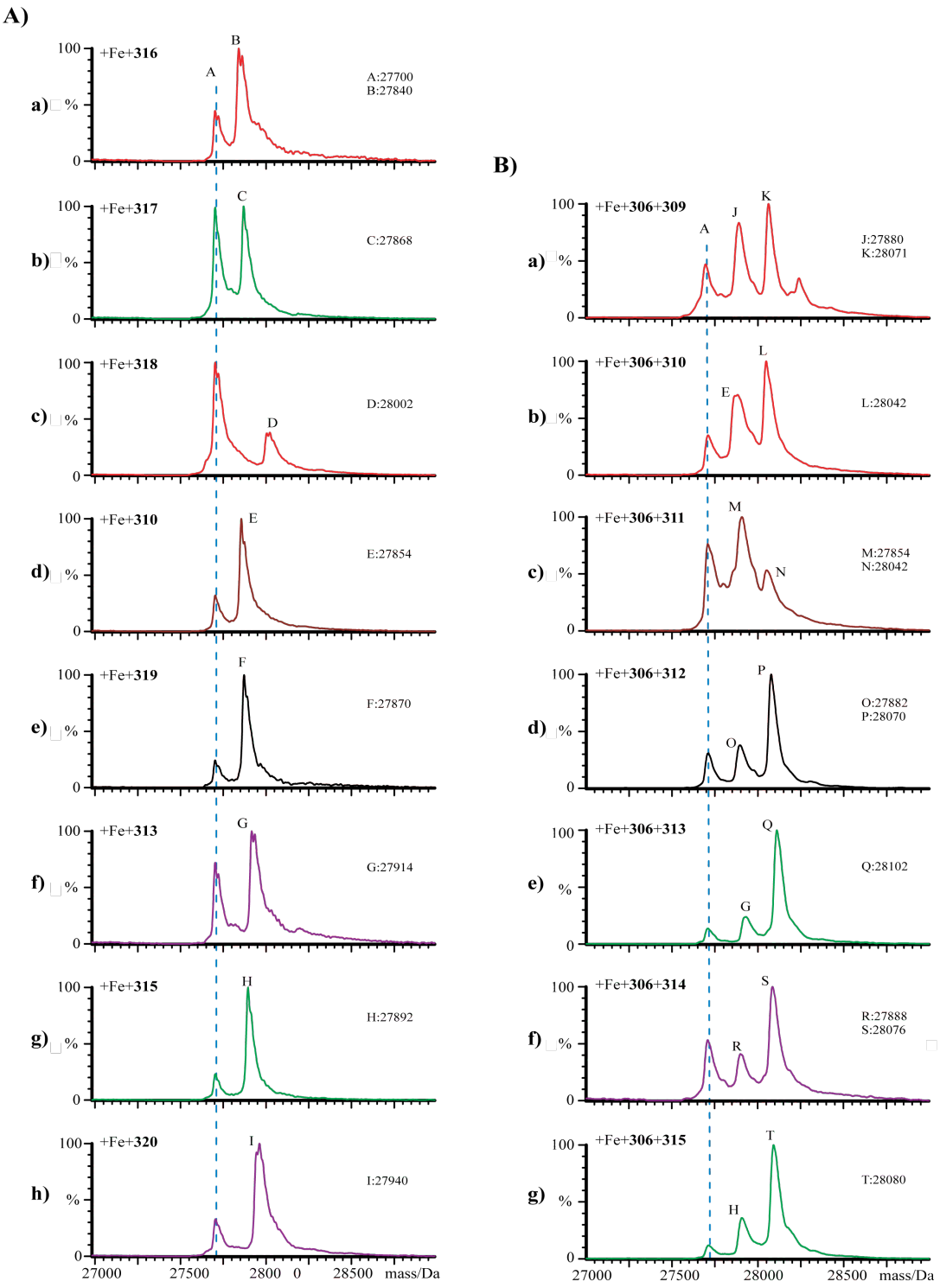

Figure 3. 12 *Mass spectra of PHD2·FeII with A: diols, B:* ***306*** *and diols at cone voltage 30V. E-J, M, O,R: PHD2·Fe·diols, K,L,N,P,Q,S,T: PHD2·Fe·boronate ester.*

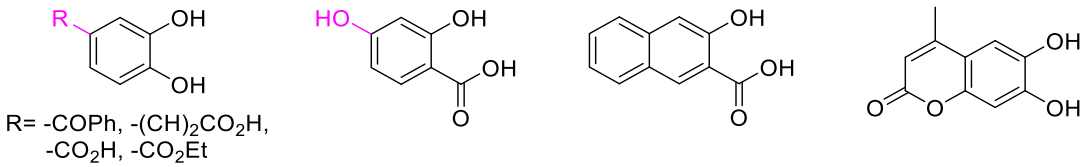

Figure 3. 13 *Diols forming boronate esters with* ***306*** *as identifield by DCMS.*

3.7 NMR binding studies

Since ESI-MS is a gas phase technique, some interactions in solution may not be conserved resulting in false negative or positive results.[43] Thus, the confirmation of the ESI-MS results by a solution phase technique was necessary. Nuclear Magnetic Resonance (NMR) paramagnetic water experiments were carried out to investigate boronate ester formation and binding strengths in solution.[44] These experiments involve the use of paramagnetic Mn(II), substituting for Fe(II) as the active site metal for PHD2. The concentration of water in solution is measured in the absence and at increasing concentrations of ligand. Upon binding of ligands to the active site of the protein the access of water in the active site is restricted increasing the measured concentration of water in solution. Diols **308** and **321** were used as aromatic and aliphatic diol (negative) controls and the apparent binding affinity of the boronate esters, as well as the DCMS hits, formed with **306** were obtained (Table 3. 1). The presence of diol **321** had little impact on the binding affinity of **306** (**306**, $K_{D,app}$= 24.8 μM; **306**+**321**, $K_{D,app}$= 18.2 μM), but the addition of catechol nearly halved the binding constant **306**+**308** ($K_{D,app}$= 13.2 μM). The improvement in binding was significant when hit diols were incubated with **306** ($K_{D,app}$ between 0.6 and 3.0 μM), especially the 4-substituted phenyl alcohols (**306**+**312**, $K_{D,app}$ = 1.3 μM; **306**+**311**, $K_{D,app}$ = 0.8 μM; **306**+**313**, $K_{D,app}$ = 0.6 μM)

Table 3. 1 *Apparent binding constants ($K_{D,app}$) of boronate esters on PHD2*

No.	$K_{D,app}$ (μM)	No.	$K_{D,\ app}$ (μM)
306	24.8 ± 2.4	**306+309**	2.6 ± 0.4
306+321	18.2 ± 0.9	**306+315**	2.2 ± 0.5
306+308	13.2 ± 2.1	**306+312**	1.3 ± 0.1
306+314	3.0 ± 0.4	**306+311**	0.8 ± 0.1
306+310	3.0 ± 0.2	**306+313**	0.6± 0.2

All NMR binding experiments were performed by Dr. Ivanhoe Leung.

3.8 Stable analogue inhibitors

Boronate esters are in equilibrium with their boronic acids and diols in solution; thus they are probably not suitable as inhibitors *in vitro* or *in vivo*. Consequently, compound **301** was reacted with commercial boronic acids in Suzuki couplings to form stable C-C analogues of the lead boronate esters (Scheme 3. 2). Although the stable analogues targeted are not perfect analogues of the boronate esters, boron chemistry enabled the ready preparation of the stable analogues by organo-palladium chemistry.[33]

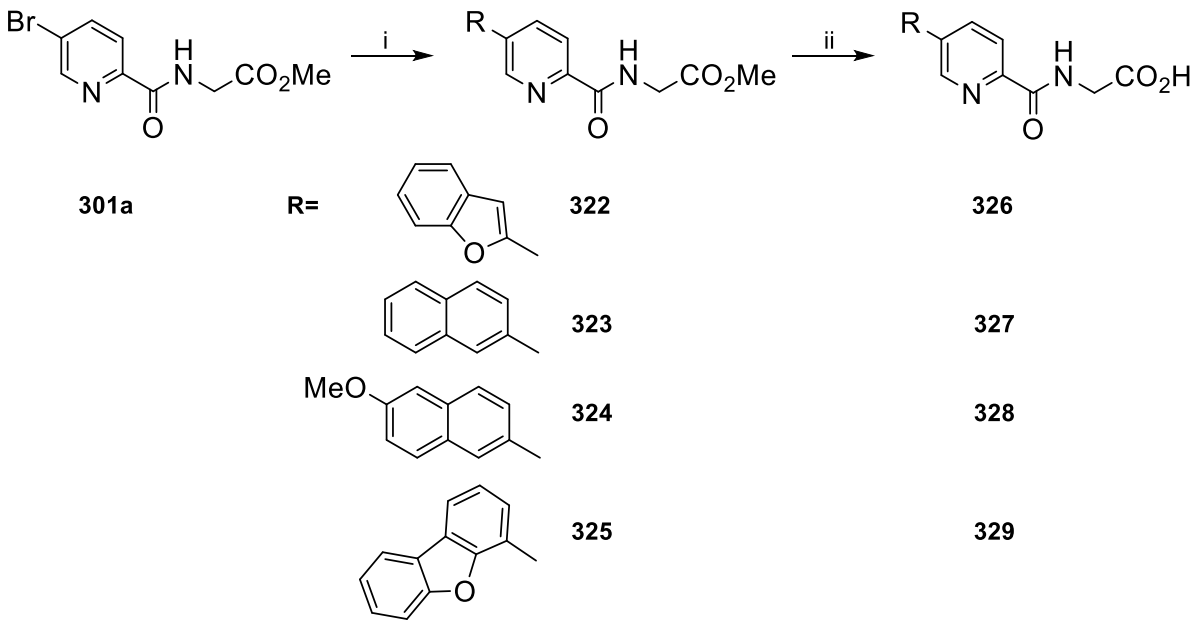

Scheme 3. 2 *Synthesis of stable compounds (analogues of inhibitors identified by DCMS).*

Reagents and conditions: i) $RB(OH)_2$ (1 equiv.), 2 M aq.Na_2CO_3 (3 equiv.), $Pd(PPh_3)_4$ (10 mole %), THF, reflux; ii) 1 M LiOH (2 equiv.), 1,4-dioxane, r.t.

Both five- and six- membered rings were explored as possible mimics of the boronate ester ring. Benzofuran-substituted and naphthalene-substituted compounds (**326** and **327**) were made as analogues of the boronate ester of **306** with **308.** They both displayed negligible PHD2 inhibition (IC_{50}> 500 μM), consistent with the DCMS and NMR binding results (Table 3. 2). The binding constants of **326** and **327**, as determined by NMR, were similar (**326**, K_D= 9.5 μM; **327**, K_D= 7.0 μM) suggesting that both five- and six- membered ring systems can be used as boronate ester mimics. All the 4-substituted benzene hits (**309-313**) were replaced by 6-methoxy-2-naphthalene **328** (IC_{50}= 107 μM, K_D= 1.6 μM), showing significant improvement in the inhibition and binding compared to **326** and **327**, as expected from the DCMS/NMR results.[14] 1-Dibenzofuran was introduced as an analogue of the bicyclic hits (**314**, **315**); the inhibitory activity of **329** (IC_{50}> 200 μM) was better than the catechol analogues **326** and **327** as indicated by DCMS and NMR. **328** was the best inhibitor from the DCMS assay, but its potency was still low. Therefore, improvement of the scaffold was attempted (see below).

Table 3. 2 *Binding constants and PHD2 inhibition of stable analogues.*

No.	K_D (μM)	IC_{50} (μM)
229	3.5	409
306	24.7	126
326	9.5	>500
327	7.0	>500
328	1.6	107
329	8.7	>200

PHD2 inhibition experiments were carried out by Andrew Mun Chan.

3.9 Inhibitor optimisation

Crystallographic studies on known PHD inhibitors suggested that the introduction of a hydroxyl group at position C-3 of the pyridine ring would induce hydrogen bonding of the compounds in the active site of PHD2 (Figure 3. 14).[34] Therefore the synthesis of 3-hydroxy substituted inhibitors was undertaken (Figure 3. 15).

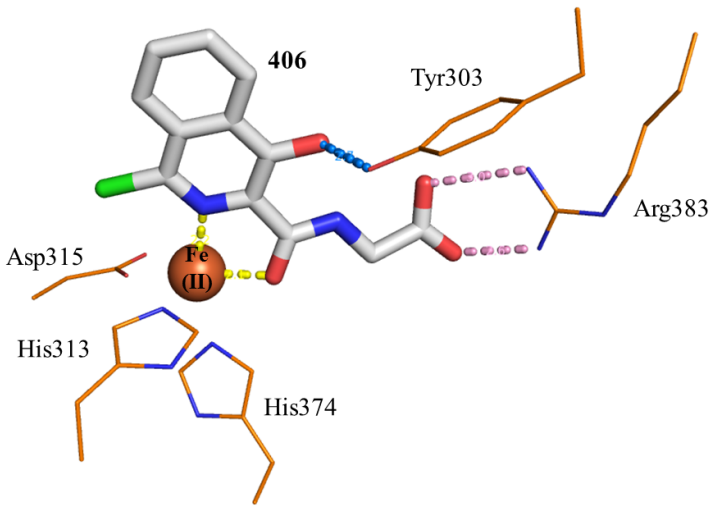

Figure 3. 14 *View from the crystal structure of PHD2 in complex with* ***406*** *(a potent PHD2 inhibitor), showing the hydrogen bonding of the hydroxyl group with Tyr303 (PDB ID: 3HQU).*[34]

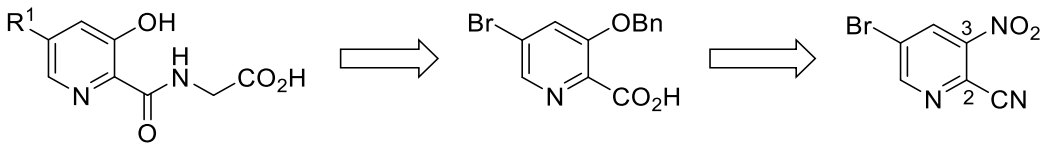

Figure 3. 15 *Retrosynthesis of proposed inhibitors.*

A benzyloxy substituent was introduced on the ring in a nucleophilic substitution of a nitro group at position C-3. This step had to be optimised to ensure selectivity of the reaction to position C-3 over C-2 and also against multi-substitution (Figure 3. 15). Literature conditions[45] for this reaction were initially used with low starting material conversion being observed (Table 3.3), but with a good ratio of the desired product over the side products. Increasing the amount of benzyl alcohol in the mixture, as well as performing the reaction at higher temperatures led to completion of the reaction; however the crude yield was low due to product decomposition. Forming the benzyloxy anion by prestirring at 40 ºC before adding the nitro compound at 20 ºC enabled the reaction to go to completion. By this procedure improved ratio of **330** over **331** and **332** was achieved; even though the yield of the product was still moderate (48 %, Table 3. 3).

Table 3. 3 *Optimisation of nucleophilic substitution on 5-bromo-3-nitropicolinonitrile.*

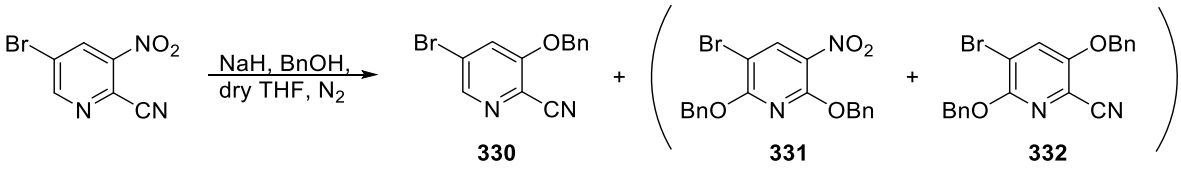

330 **331** **332**

BnOH (equiv.)	**Prestirring T (^{o}C)**	**Time (min)**	**Temperature (^{o}C)**	**Time (h)**	**s.m (%)**	**330 (%)**	**331 (%)**	**332 (%)**
1.1	0	30	5→20	2	50	22	trace	8
1.1	20	30	10→20	2	25	28	trace	9
1.2	20	30	20→40	2.5	-	42	3	12
1.1	40	20	20	1.5	-	48	trace	10

After optimising the nucleophilic substitution reaction, **330** was carried through the following steps, using modified literature conditions in order to achieve preparation of the 5-bromopyridyl compound **334** in moderate yields.[46] Compound **334** was used in Suzuki coupling reactions with substituted naphthalene-2-boronic acids. Deprotection of the products of this reaction **335-337** under palladium hydrogenation afforded the final 3-hydroxy-5-substituted-pyridyl inhibitors (Scheme 3. 3).

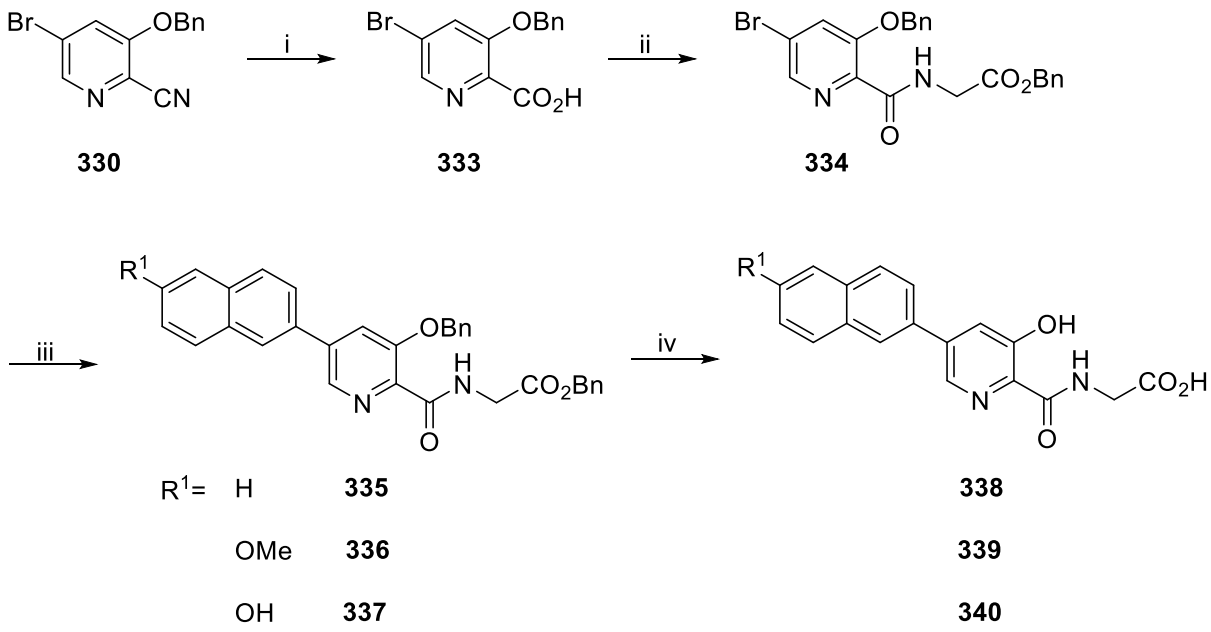

Scheme 3. 3 *Synthesis of stable analogues.*

Reagents and conditions: i) 30 % NaOH, MeOH, reflux; ii) glycine benzyl ester hydrochloride (1 equiv.), EDCI (1.2 equiv.), HOBT (1.5 equiv.), DIPEA (3 equiv.), r.t; iii) R^1naphthylB$(OH)_2$ (1 equiv.), 2 M aq. Na_2CO_3 (3 equiv.), $Pd(PPh_3)_4$ (10 mole %), THF, reflux; iv) Pd/C 10%, H_2, THF, r.t.

Compounds **338**-**339** displayed greatly improved inhibitory potency with PHD2; with their IC_{50} values being in the low nM range, representing a 10000 fold improvement in potency over compound **328** (Table 3. 2, Table 3. 4). The presence of the hydroxyl group reduced the effect of introducing a methoxy group on the naphthalene ring; the naphthalene **338** (IC_{50}= 17 nM) is essentially equipotent with 6-methoxy naphthalene **339** (IC_{50}= 14 nM). To improve the water solubility of the inhibitors, the methoxy group was replaced with a hydroxyl group which resulted in increased inhibition of PHD2 **340** (IC_{50}= 4 nM).

Table 3. 4 *Binding constants and PHD2 inhibition of stable analogues.*

No.	PHD2 K_D (μM)	PHD2 IC_{50} (nM)	FTO IC_{50} (μM)	BBOX IC_{50} (μM)	JMJD2E inhibition @ 20uM (%)
338	0.5	17	43	~50	53
339	0.8	14	>200	>200	58
340	0.9	4	96	~50	4
406	< 1	353	2.8	18	40

These inhibitors, as well as **406**[47] (a PHD2 inhibitor that is currently in clinical trials for the treatment of anaemia), were tested for inhibition against other clinically relevant 2OG oxygenases. Compounds **338**-**340** displayed better IC_{50} values than **406** (IC_{50}= 353 nM) for PHD2, however the opposite is observed for other proteins tested. **406** is a more potent fat mass and obesity-associated protein (FTO) and γ-butyrobetaine hydroxylase (BBOX) inhibitor (FTO IC_{50}= 2.8 μM, BBOX IC_{50}= 18 μM) compared to compounds **338**-**340** (Table 3. 4). For example, compound **339** is 1000 times more selective to PHD2 than **406**. Worth noting is that the inhibition of PHD2 by compound **229**, (IC_{50}= 409 μM, Table 3. 2) a potent AlkB inhibitior, is improved 30000 times with the addition of the 6-methoxy naphthyl group identified by DCMS.

BBOX and JMJD2E inhibition data were obtained by Anna Rydzik and Anthony Tumber respectively.

3.10 Crystallographic studies

To investigate the mode of binding of the highly potent inhibitors developed in this chapter, crystallographic studies were carried out. A crystal structure of PHD2 with Mn(II) (substituting iron) and **339** revealed that **339** binds to the PHD2 active site. **339** complexes the metal in a bidentate manner *via* the pyridyl nitrogen and the amide carbonyl at C-2 of the ring. The carboxylic acid has a salt bridge with Arg383 and the C-3 hydroxy group hydrogen

bonds with the side chain hydroxyl group of Tyr303. The naphthalene group of **339** is twisted relative to the pyridyl ring (torsion angle 53º) directing toward and partially occupying the substrate-binding site (Figure 3. 16).

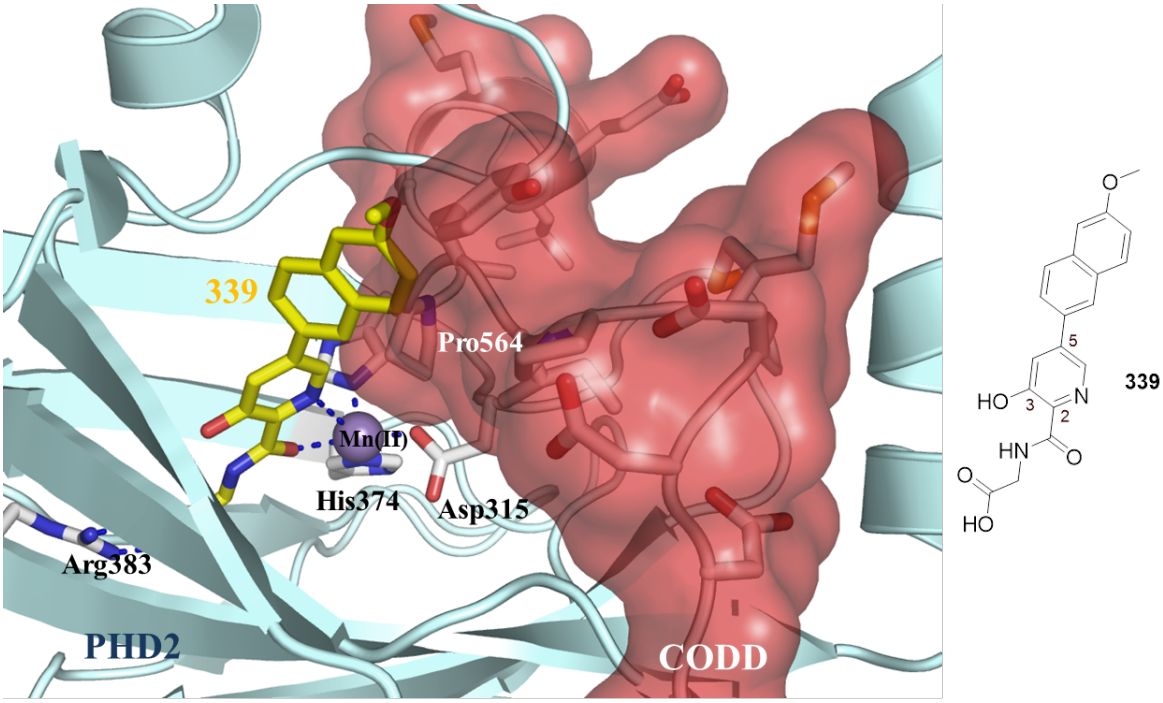

Figure 3. 16 *View from a crystal structure of PHD2·Mn(II) (light blue) complexed with* ***339*** *(yellow) superimposed with a structure of PHD2·Mn(II) in complex with HIF1α residues 558-574 ("CODD": red surface) (PDB ID 3HQR). The image shows the proximity of the C-5 substituent of* ***339*** *(6-methoxynaphthalene) to the substrate binding site. The active site metal is in purple and Pro564 of HIF-1α, is labelled.*[34]

It is likely that the occupation of the substrate binding site combined with the hydrogen bonding for C-3 hydroxyl of **339** results in the high potency of the compound relative to **406** (Figure 3. 17).

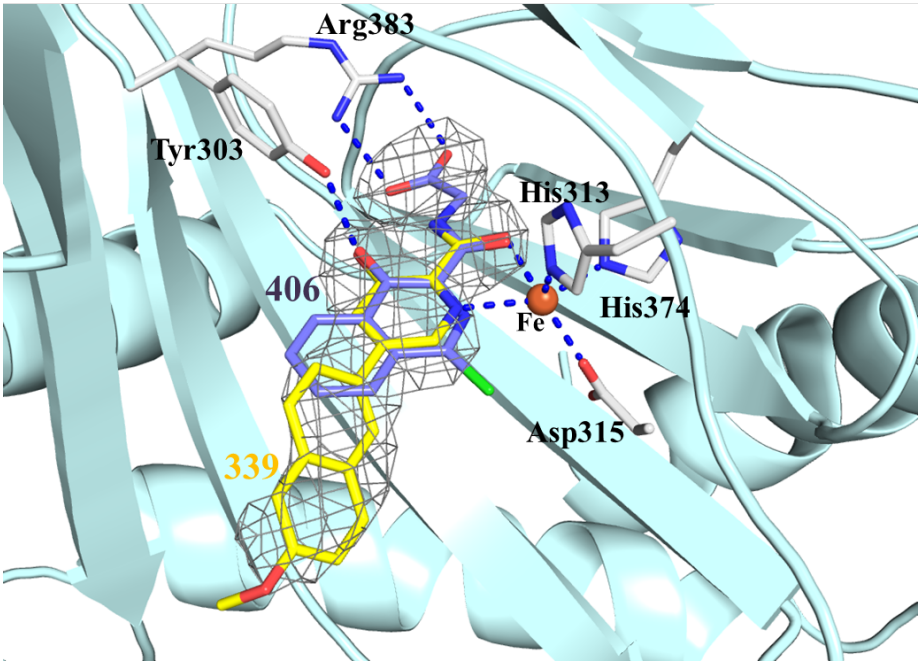

Figure 3. 17 *View from a crystal structure of PHD2·Fe (blue) complexed with* ***406*** *(lilac) (PDB ID: 3HQU) superimposed with a structure of PHD2·Mn(II) in complex with* ***339*** *(yellow) (contoured at 3.0 σ).*[34]

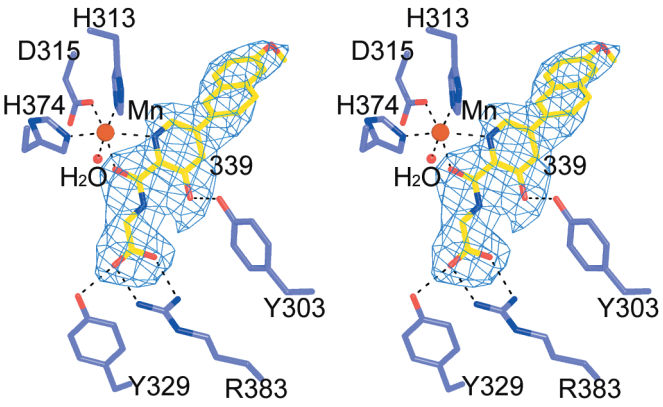

Figure 3. 18 *Stereoviews from the active site of a PHD2·Mn(II)·****339*** *crystal structure showing the Fo-Fc omit map around the ligand (contoured at 3.0 σ).*

Crystal structures were solved by Dr Rasheduzaman Chowdhury

3.11 Conclusions

In this study the application of reversible boronate ester formation, from boronic acids and diols, in dynamic combinatorial chemistry with enzymes under mass spectrometric conditions was achieved. It was shown that the DCMS method can enable the development of selective inhibitors and provide structural insights. The combination of DCMS with previous knowledge of PHD2 SAR and structures made it possible to develop potent and selective PHD2 inhibitors. It was observed that the boronic acids undergo fragmentation under the MS conditions, while the boronate esters are stable. Even though this observation is a drawback of the method, the development of new mild-ionisation MS techniques may overcome this problem. The results from the DCMS assay were further validated by NMR binding experiments and boronate ester formation, demonstrating the utility of NMR as an analytical technique for DCC.

3.12 Acknowledgements

Many thanks to Dr. Ivanhoe Leung for the NMR binding assay and pKa measurments. Special thanks to Dr. Rasheduzzaman Chowdhury for the crystallographic studies and analyses. Finally, thanks to Andrew Chan and Anthony Tumber for the inhibition studies on PHD2 and KDMs respectively.

3.13 Experimental details

Non-Denaturing ESI-MS studies

The 40 diols used for DCL generation were from Sigma-Aldrich, Alfa Aesar or Acros. PHD2 was desalted using a Bio-Spin 6 Column (Bio-Rad, Hemel Hempstead, U.K.) in 15 mM ammonium acetate (pH 7.5). The stock solution was diluted with the same buffer to a final concentration of 100 μM. $Fe(NH_4SO_4)_2 \cdot 6H_2O$ was dissolved in 20 mM HCl at a concentration of 100 mM. This was then diluted with Milli-Q water to give a final working

concentration of 100 μM. The protein was mixed with Fe(II) and boronic acids/diols to give final concentrations of 15 μM PHD2, 15 μM Fe(II), and 15 μM boronic acid and/or 15 μM diol. ESI-MS analysis was performed immediately with no incubation.

Mass spectrometric data were acquired using a Q-TOF mass spectrometer (Q-TOF micro, Micromass, Altrincham, U.K.) interfaced with a NanoMate (Advion Biosciences, Ithaca, NY) with a chip voltage of 1.70 kV and a delivery pressure 0.5 psi. The sample cone voltage was typically 30 V with a source temperature of 100 ºC and with an acquisition/scan time of 1 s/1 s.

Calibration and sample acquisition were performed in the positive ion mode in the range of 2000-4000 m/z. The pressure at the interface between the atmospheric source and the high vacuum region was fixed at 6.30 mbar. External instrument calibration was achieved using sodium formate. Data were processed with the MassLynx 4.0 (Waters).

pK_a NMR measurement

pK_a values were determined at 700 MHz using a Bruker Avance III spectrometer equipped with a 5 mm inverse cryoprobe. Standard 5 mm diameter NMR tubes (Norell, USA) were used. Nine samples containing 1 mM boronic acid at varying pH dissolved in D_2O were measured by standard ^1H experiments. The ^1H chemical shift of the boronic acid/boronate ester was plotted against the solution pH and sigmoid curves were fitted using OriginPro 8.0 (OriginLab, USA).

Binding constant measurements

Apparent binding constants ($K_{D,app}$) and binding constants (K_D) for PHD2 were determined by water relaxation experiments as described.[44] NMR experiments were conducted at 500 MHz using a Bruker Avance II spectrometer equipped with a standard 5 mm TXI probe at 298 K. 3 mm diameter Bruker MATCH tubes (Hilgenberg, Germany) were used. Each sample contained 50 μM apo-PHD2, ~50 μM Mn(II) and 350 μM diols (where applicable). Ligand stock solution of 1 μL or 2 μL was titrated into NMR tubes. Solutions were buffered using 50 mM Tris-D11 (pH 7.5) dissolved in 12.5% H_2O and 87.5% D_2O. Saturation recovery

experiments were performed with 1 transient with a relaxation delay of at least 5 times T_1. K_D curves were fitted using OriginPro 8.0 (OriginLab, USA) using a reported equation.[48]

PHD2 expression and purification

An *N*-terminally truncated form of PHD2 ($PHD2_{181-426}$) was prepared as reported.[49, 50]

Protein purification

Fast Protein Liquid Chromatography: Protein purification using FPLC was carried out using Äkta™ FPLC systems (GE Healthcare) at 4°C. Purification procedures were followed by monitoring absorbance at 280 nm with a UPC-900 monitor on the FPLC and by SDS-PAGE. Sample fractions were collected using a Frac-920 fraction collector.

Cation exchange column chromatography: A cation exchange column (SP Sepharose Fast Flow 50) was equilibrated with Milli-Q water (2CV), 1 M NaCl (2CV) and buffer A (0.1 M MES, pH 5.8) (2CV) prior to loading of the filtered supernatant. The column was washed with buffer A (0.1 M Mes, pH 5.8) until the UV trace returned to its initial level. A gradient of 0-100% buffer B (0.1 Mes, 1 M NaCl, pH 5.8) was then run over a period of 35 mins to elute the protein, and 5 mL fractions were collected. Following use the column was washed with 2CV each of Milli-Q water, 1 M NaOH, water, 1 M NaCl, 1 M AcOH and water. UV trace analysis and SDS PAGE were used to determine fractions containing the required protein which were then combined and concentrated to 2 mL using a 10 kDa MWCO concentrator in an S-4180 rotor in a Beckman Allegra™ 21R bench top centrifuge at 4000 rpm and 4°C.

Gel filtration column chromatography: Prior to use the 320 mL gel filtration Superdex 75 column (Pharmacia) containing S75 gel filtration resin (Amersham Biosciences) was equilibrated by washing with Milli-Q water (1CV), and gel filtration buffer (0.1 M Tris, 0.1 M NaCl, pH 7.5) (1CV). The concentrated protein was then loaded onto the column via a 2 mL injection loop at 0.5 mL min^{-1}, and subsequently run at 1.5 mL min^{-1}. Protein was eluted with gel filtration buffer (1CV), with 5 mL fractions collected when the UV absorption

exceeded 40 mAU. Following use, the column was washed with Milli-Q water (2CV). SDS PAGE was used to identify the protein fractions with highest purity, which were then combined and concentrated. The resulting protein was desalted into 50 mM Tris pH 7.5 by further concentration. The concentration of the desalted protein was determined and stored at -80 °C.

Preparation of apo-PHD2: For non-denaturing ESI-MS and relaxation NMR studies apoPHD2 was obtained by incubation with the iron chelator EDTA. PHD2 after the cation exchange chromatography was dissolved with 0.5 M EDTA pH 8, 20 mM NH_4OAc pH7 to a final concentration of 1 mg/ mL protein, 0.2 M EDTA and 15mM NH_4OAc step and was incubated overnight. The protein solution was concentrated to 2 mL as above prior to gel filtration column.

PHD2 inhibition assays[51]

Inhibition assays were carried out in 384-well white ProxiPlates (PerkinElmer) in 10 μL of reaction volume. Standard reaction mixtures consisted of the compound (in 2% DMSO final concentration), enzyme mix (0.001 μM of PHD2, 10 μM of Fe(II), 100 μM of ascorbate) and peptide mix (0.06 μM of biotinylated *C*-terminal oxygen dependent degradation domain (CODD) peptide, 2 μM of 2OG) in 50 mM HEPES pH 7.5, 0.01% Tween-20 and 0.1% BSA buffer. Compounds were preincubated with the enzyme mix for 15 min before being incubated with peptide mix for 10 min at 22 °C. Each reaction was quenched with 5 μL of 30 mM EDTA. The bead mix containing AlphaScreen beads (AlphaScreen streptavidin-conjugated donor and ProteinA-conjugated acceptor beads; PerkinElmer) was preincubated for 1h with a rabbit monoclonal antibody selective for hydroxy-HIF1α (Pro564) (Cell Signaling, Danvers, MA; 1:8000) and were added to the wells for a further 1 h at 22 °C. The plates were then analyzed with an Envision (PerkinElmer) plate reader. The IC50 values were calculated using nonlinear regression with normalized dose−response fit using GraphPad Prism ($n \geq 3$).

In vitro Demethylation Assays for KDMs (AlphaScreen).

These assays were carried out as described previously.[52]

Protein crystallography

Crystals of PHD2 in complex with **339** were grown in sitting drops at 293K using vapor diffusion methods at a protein to reservoir ratio of 1:1. The PHD2 protein solution contained 19.0 mg/mL protein, 50 mM Tris·HCl pH 7.5, 1.0 mM $MnCl_2$ and 1.2 mM **339**. The reservoir solution contained 1.88 M ammonium sulfate, 0.1 M MES pH 6.5 and 5-7% dioxoane (v/v). The crystals were cryoprotected using well solution that was diluted to 30% v/v glycerol and flash frozen in liguid nitrogen. Data were collected from a single crystal at 100K using a Rigaku FR-E+ Superbright diffractometer equipped with a copper rotating anode, Osmic HF optics, and a Saturn 944+ CCD detector. The data were indexed, integrated, and scaled using HKL2000[53]. The structure was determined by molecular replacement using PHASER [54] and PDB ID: 2g19 as the search model. Iterative rounds of model building and refinement using COOT [55] and CNS [56] were performed until the decreasing R and R_{free} no longer converged.

Table 3. 5 *Crystallographic data processing, refinement statistics and further analysis for tPHD2 in complex with* ***339****.*

Measurement	**tPHD2·Mn^{II}·339**
Data Collection	
Space Group	$P2_12_12_1$
Cell dimensions a,b,c (Å)	84.461
	103.011
	195.981
Resolution (Å)	3.1
No. of unique reflections	36167 (3454)*
Completeness (%)	93.8 (91.3)*
Redundancy	3.8 (3.5)*
R_{sym}**	0.199 (0.826)*
Mean I/σ(I)	7.3 (2.0)*
Refinement	
R_{factor}	0.250
R_{free}	0.291
R.m.s. deviation	
Bond length, Å	0.009
Bond angle, °	1.24

*Highest resolution shell shown in parenthesis.

**$R_{sym} = \sum|I-\langle I\rangle|/\sum I$, where I is the intensity of an individual measurement and $\langle I\rangle$ is the average intensity from multiple observations.

Chemical synthesis

General information

Reagents and solvents were from Aldrich, Alfa Aesar or Acros. Reactions were monitored by TLC, which was performed on precoated aluminum-backed plates (Merck, silica 60 F254). Flash column chromatography was carried out using Biotage SP1 Purification system. Melting points were determined using a Leica Galen III hot-stage melting point apparatus and microscope. Infrared spectra were recorded from neat samples, on a Bruker Tensor 27 FT-IR spectrometer. NMR spectra were acquired using Bruker Avance II 500 MHz spectrometer equipped with a 5mm $^{13}C(^{1}H)$ dual cryoprobe or Avance 400 MHz spectrometer equipped with a 5mm z-gradient $^{1}H/^{13}C/^{19}F/^{31}P$ quad-nucleus probe. Chemical shifts (δ) are given in ppm, and the multiplicities are given as singlet (s), doublet (d), doublet doublet (dd), triplet (t), quartet (q), multiplet (m), broad (br). Coupling constants *J* are given in Hz (± 0.5 Hz). High resolution mass spectra (HRMS) were recorded using Bruker MicroTOF. The purity of all compounds synthesized were ≥98% as determined by analytical reverse-phase LCMS.

General Procedures

General Procedure A

Potassium trifluoro(6-((2-methoxy-2-oxoethyl)carbamoyl)pyridin-3-yl)borates

In a mixture of **302a/b/c** (0.60 g, 1.87 mmol) in MeOH (15 mL), aqueous potassium hydrogen difluoride 4.5 M (4.2 mL, 18.70 mmol) was added and the reaction was stirred at room temperature for 1.5 hours. The solvent was removed *in vacuo*; the crude product was then washed with warm acetone 5 times and filtered.

General procedure B

2-[(Boronopyridin-2-yl)carbonyl]glycines

305a/b (1 equiv.) was dissolved in the minimum volume of a CH_3CN/H_2O 2:1 mixture. Chlorotrimethylsilane (10 equiv.) was added dropwise over 5 min and the mixture was stirred

at room temperature overnight. The solvent was removed, H_2O (1 mL) was added to the crude mixture which was then filtered.

General procedure C

Methyl *N*-2-{[5-(substituted)pyridin-2-yl]carbonyl}glycinates

A mixture of **301** (0.50 g, 1.83 mmol), the boronic acid (1.83 mmol), 2 M sodium carbonate (2.3 mL, 5.49 mmol) and tetrakis(triphenylphosphino)palladium(0) (0.22 g, 0.18 mmol) in THF (40 mL) was heated at reflux until consumption of starting material (TLC). Solvent was removed *in vacuo*. The crude product was then diluted (CH_2Cl_2) and filtered. The filtrate was concentrated and the residue was purified by flash chromatography (hexane/EtOAc, 60: 40) afforded the methyl ester.

General procedure D

2-{[5-(substituted)pyridin-2-yl]carbonyl}glycines

Solid obtained from the filtration (procedure C) was washed first with EtOAc (20mL) and then with water (10 mL). Washing afforded the acids as white solids.

General procedure E

Benzyl *N*-2-{[3-(benzyloxy)-5-(aryl)pyridin-2-yl]carbonyl}glycinates

A mixture of **334** (0.30 g, 0.66 mmol), the boronic acid (1.32 mmol), 2 M sodium carbonate (1.0 mL, 1.97 mmol), triphenylphosphine (17.3 mg, 0.07 mmol) and tetrakis(triphenylphosphino) palladium(0) (76.0 mg, 0.07 mmol) in THF (20 mL) was heated at reflux until consumption of starting material (TLC). The solvent was removed *in vacuo* and the residue redissolved in CH_2Cl_2, washed with water, dried and concentrated. The residue was purified by flash chromatography (hexane/EtOAc 6:4 to 3: 7) afforded the purified product.

General procedure F

2-{[3-hydroxy-5-(aryl)pyridin-2-yl]carbonyl}glycines

To a solution of benzyl *N*-2-{[3-(benzyloxy)-5-(aryl)pyridin-2-yl]carbonyl}glycinates (0.02 g, 0.04mmol) in THF (10 mL), 10% Pd/C (2.0 mg, 0.004 mmol) was added. The mixture was stirred at room temperature under a H_2 atmosphere (1 atm) for 18 h. The suspension was filtered through celite and the filtrate was concentrated *in vacuo*. The oily residue was washed with diethyl ether afforded the desired acids.

Methyl *N*-[(5-bromopyridin-2-yl)carbonyl]glycinate 301a

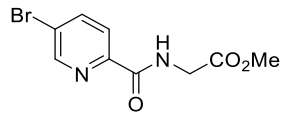

To a solution of 5-bromopicolinic acid (2.46 g, 12.2 mmol) in $SOCl_2$ (20 mL, excess), 2 drops of DMF were added and the solution was stirred under reflux for 17 h. The excess $SOCl_2$ was removed *in vacuo* and co evaporated twice with CH_2Cl_2. The crude product was then diluted in CH_2Cl_2 and glycine methyl ester hydrochloride (1.53g, 12.2 mmol) was added. Triethylamine (3.4 mL, 24.4 mmol) was then added dropwise over 30min and the resultant mixture was stirred at room temperature for 4 h. The solution was then washed with water, dried over $MgSO_4$ and concentrated *in vacuo*. Chromatography (gradient CH_2Cl_2/EtOAc, 9:1 to 8:2) afforded compound **301a** (2.87 g, 86%) as white crystals, mp 88-89 ºC (from hexane). R_f= 0.45. IR (KBr) ν/cm^{-1} 3345 (NH), 1728 (CH_3OC=O), 1667 (NHC=O); ^{1}H NMR (500 MHz, $CDCl_3$) δ 8.29-8.24 (1H, m, Ar C*H*), 7.59-7.53 (1H, app. m, N*H*), 7.49-7.42 (1H, m, Ar C*H*), 6.85 (1H, s, Ar C*H*), 4.97 (2H, d, *J*= 5.5, CH_2), 3.29-3.19 (3H, s, CH_3); ^{13}C NMR (125MHz, $CDCl_3$) δ 170.0 (*C*=O), 163.8 (*C*=O), 149.5 (Ar *C*), 147.7 (Ar *C*), 140.0 (Ar *C*H), 124.3 (Ar *C*H), 123.7 (Ar *C*H), 52.4 (*C*H_3), 41.25 (*C*H_2); MS (ESI$^+$) m/z 273 ([M+H]$^+$, 100%); HRMS calcd. for $C_9H_9BrN_2NaO_3$ [M+Na]$^+$ 294.9689; Found 294.9689.

Methyl *N*-[(4-bromopyridin-2-yl)carbonyl]glycinate 301b

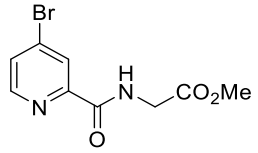

A solution of 4-bromopicolinic acid (1.00 g, 4.95 mmol) in $SOCl_2$ (10mL, excess) was heated at reflux for 2 h. The excess $SOCl_2$ was removed *in vacuo* and co evaporated twice with CH_2Cl_2. The crude product (0.5 g, 2.46 mmol) was diluted with CH_2Cl_2 (10 mL). To the stirred solution a mixture of glycine methyl ester hydrochloride (0.31g, 2.46 mmol), triethylamine (0.65 mL, 4.66 mmol) in CH_2Cl_2 (15 mL) was added dropwise over 20 min and was stirred at room temperature for 1 d. The solution was washed with water, dried over $MgSO_4$ and concentrated *in vacuo*. Chromatography (CH_2Cl_2/EtOAc 9:1) afforded compound **301b** (0.87 g, 64 %) as white crystals, mp 74-75 ºC. R_f= 0.45. IR (neat) ν/cm^{-1} 3348 (NH), 1726 (CH_3OC=O), 1668 (NHC=O); ^{1}H NMR (500 MHz, $CDCl_3$) δ 8.49 (1H, d, *J*= 5.5, Ar C*H*), 8.40 (1H, t, *J*= 5.0, N*H*), 8.20 (1H, d, *J*= 2.0, Ar C*H*), 7.46 (1H, dd, *J*= 5.5 2.0, Ar C*H*), 4.27 (2H, d, *J*= 5.5, CH_2), 3.80 (3H, s, CH_3); ^{13}C NMR (125MHz, $CDCl_3$) δ 169.9 (*C*=O), 163.4 (*C*=O), 150.7 (Ar *C*), 149.2 (Ar *C*), 145.8 (Ar *C*H), 126.6 (Ar *C*H), 122.95 (Ar *C*H), 52.4 (*C*H_3), 41.3 (*C*H_2); MS (FI$^+$) m/z 271 (M^+, 100%).

Methyl *N*-[(6-bromopyridin-2-yl)carbonyl]glycinate 301c

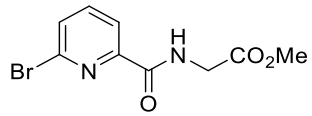

A solution of 6-bromopicolinic acid (5.00 g, 24.75 mmol) in $SOCl_2$ (40mL, excess) was heated at reflux for 3 h. The excess $SOCl_2$ was removed *in vacuo* and co evaporated twice with CH_2Cl_2. The crude product was diluted with CH_2Cl_2 (50 mL). To the stirred solution a mixture of glycine methyl ester hydrochloride (2.60g, 20.66 mmol) and triethylamine (5.80 mL, 41.58 mmol) in CH_2Cl_2 (15 mL) was added dropwise over 20 min and was stirred at room temperature for 14 h. The solution was washed with water, dried over $MgSO_4$ and concentrated *in vacuo*. Chromatography (CH_2Cl_2/EtOAc, 9:1) afforded compound **301c** (3.50 g, 52 %) as pale yellow crystals, mp 80-83 ºC. R_f = 0.45. IR (neat) ν/cm^{-1} 3347 (NH), 1726

(CH_3OC=O), 1668 (NHC=O); ^{1}H NMR (500 MHz, $CDCl_3$) δ 8.25 (1H, br. s, N*H*), 8.18-8.11 (1H, m, Ar C*H*), 7.82 (1H, t, *J*= 8.0, Ar C*H*), 7.59 (1H, d, *J*= 3.0, Ar C*H*), 4.27 (2H, d, *J*= 6.0, CH_2), 3.80 (3H, s, CH_3); ^{13}C NMR (125MHz, $CDCl_3$) δ 169.9 (*C*=O), 163.2 (*C*=O), 150.2 (Ar *C*), 149.7 (Ar *C*), 139.9 (Ar *C*H), 127.3 (Ar *C*H), 121.1 (Ar *C*H), 52.4 (*C*H_3), 41.2 (*C*H_2); MS (FI$^+$) m/z 271 (M^+, 100%).

Methyl *N*-{5-(3a,5,5-trimethylhexahydro-4,6-methanobenzo[d][1,3,2]dioxaborol pyridine-2-yl)carbonyl} glycinate 303

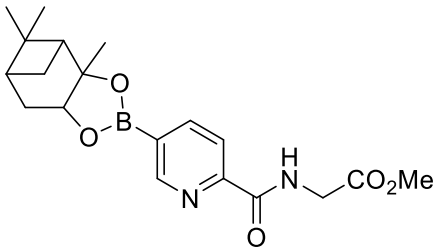

A mixture of **301a** (1.03 g, 3.77 mmol) with bis(pinane)diboron (2.01 g, 6.03 mmol) and anhydrous potassium acetate (1.17 g, 11.31 mmol) was purged with N_2 for 5 min and then 1,1'-bis(diphenylphosphino)ferrocene-palladium(II)dichloride (0.13 g, 0.16 mmol) was added. The mixture was stirred at 80 ^{o}C for 1 d and 1,1'-bis(diphenylphosphino)ferrocene-palladium(II)dichloride (0.12 g, 0.15 mmol) were added. The mixture was stirred at 80 ^{o}C for 18 h until consumption of starting material (TLC). The solvent was removed *in vacuo* and the residue was re dissolved in EtOAc followed by filtration through Celite. The filtrate was washed with brine. The organic phase was dried over $MgSO_4$ and concentrated *in vacuo.* Chromatography (hexane/ EtOAc 4:6 to 3:7) afforded compound **303** (0.96 g, 69 %) as colourless oil. IR (neat) ν/cm^{-1} 3382 (N-H), 1754 (CH_3OC=O), 1675 (NHC=O); ^{1}H NMR (500 MHz, $CDCl_3$) δ 8.91 (1H, s, Ar C*H*), 8.53 (1H, br. s, N*H*), 8.20 (2H, dd, *J*= 8.0 1.5, Ar C*H*), 4.29 (2H, d, *J*= 6.0, CH_2), 3.78 (3H, s, CH_3), 2.47-1.86 (7H, m, pinane CH and CH_2), 1.52 (3H, s, CH_3), 0.90 (6H, s, CH_3); ^{13}C NMR (125MHz, $CDCl_3$) δ 171.0 (*C*=O), 164.7 (*C*=O), 154.0 (Ar*C*), 150.8 (Ar*C*H), 143.8 (Ar*C*H), 126.4 (Ar*C*), 121.3 (Ar*C*H), 69.3 (*C*CH_3), 52.6 (*C*H_3), 51.5-51.3 (multiple peaks, *C*H), 41.3 (*C*H_2), 39.9-39.4 (multiple peaks, *C*H), 35.6-35.3 (multiple peaks, *C*H_2), 28.6-28.4 (multiple peaks, *C*H_3), 27.8-27.0 (multiple peaks, *C*H_2),

26.5-26.3 (multiple peaks, $C(CH_3)_2$), 24.2-24.0 (multiple peaks, $(CH_3)_2$); MS (ESI^+) m/z 395 ($[M+Na]^+$, 90%); HRMS calcd. for $C_{19}H_{25}BN_2NaO_5$ $[M+Na]^+$ 395.1752; Found 395.1735.

_N_-{5-(3a,5,5-trimethylhexahydro-4,6-methanobenzo[d][1,3,2]dioxaborolpyridine-2-yl)carbonyl}glycine 304

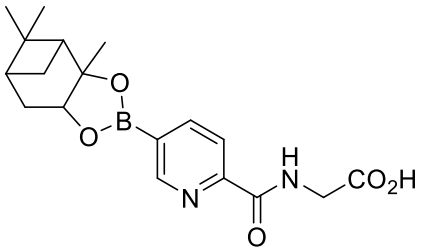

In a solution of **303** (0.28 g, 0.752 mmol) in 1,4-dioxane (5 mL), 1 M lithium hydroxide (1.52 mL, 1.52 mmol) was added. The mixture was stirred at room temperature for 10 h until consumption of starting material. The mixture was acidified with acetic acid to pH 3 and extracted with CH_2Cl_2/H_2O. The solution was washed with water, dried over $MgSO_4$ and concentrated *in vacuo*. Concentration afforded compound **304** (0.16 g, 59 %), as colourless oil. IR (neat) ν/cm^{-1} 3382 (O-H), 3066 (N-H), 1751 (HOC=O), 1663 (NHC=O); ^{1}H NMR (500 MHz, $CDCl_3$) δ 8.91 (1H, s, Ar C*H*), 8.58 (1H, br. s, N*H*), 8.23 (2H, dd, *J*= 7.0 1.5, Ar C*H*), 4.29 (2H, d, *J*= 6.0, CH_2), 2.38-1.83 (7H, m, pinane CH and CH_2), 1.42 (3H, s, CH_3), 0.83 (6H, s, CH_3); ^{13}C NMR (125MHz, $CDCl_3$) δ 173.4 (*C*=O), 164.9 (*C*=O), 153.9 (Ar *C*), 150.8 (Ar *C*H), 143.9 (Ar *C*H), 121.6 (Ar *C*H), 69.3 (*C*CH_3), 51.4-51.2 (multiple peaks, *C*H), 41.2 (*C*H_2), 39.5-39.4 (multiple peaks, *C*H), 35.6-35.3 (multiple peaks, *C*H_2), 29.0-28.4 (multiple peaks, *C*H_3), 27.9-27.3 (multiple peaks, *C*H_2), 26.6-26.3 (multiple peaks, $C(CH_3)_2$), 24.2-23.9 (multiple peaks, $(CH_3)_2$); MS (ESI^-) m/z 357 ($[M-H]^-$, 100%); HRMS calcd. for $C_{18}H_{22}BN_2O_5$ $[M-H]^-$ 357.1631; Found 357.1628.

Methyl 2-[5-(4,4,5,5-tetramethyl-1,3,2-dioxaborolanpyridine-2-yl)carbonyl]glycinate 302a

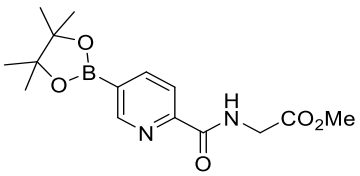

A mixture of **301a** (1.51 g, 5.53 mmol) with bispinacolatodiboron (2.22 g, 8.85 mmol) and potassium acetate (1.74, 16.59 mmol) was purged with N_2 for 5 min and then 1,1'-bis(diphenylphosphino)ferrocene-palladium(II)dichloride (0.20 g, 0.08 mmol) was added. The mixture was stirred at 80 ºC for 3 h and bispinacolatodiboron (1.00 g, 8.85 mmol), 1,1'-bis(diphenylphosphino)ferrocene-palladium(II)dichloride (0.20 g, 0.08 mmol) were added. The mixture was stirred at 80 ºC for 18 h until consumption of starting material (TLC). The solvent was removed *in vacuo* and the crude was redissolved in EtOAc followed by filtration through Celite. The filtrate was washed with brine. The organic phase was dried over $MgSO_4$. Concentration *in vacuo* afforded compound **302a** (1.00 g, 56 %) as a yellow oil. IR (neat) ν/cm^{-1} 3387 (N-H), 1755 (CH_3OC=O), 1680 (NHC=O); ^{1}H NMR (500 MHz, $CDCl_3$) δ 8.87-8.86 (1H, m, Ar C*H*), 8.57 (1H, app. s, N*H*), 8.22-8.19 (1H, m, Ar C*H*), 8.14-8.12 (1H, m, Ar C*H*), 4.26 (2H, d, *J*= 5.5, CH_2), 3.77 (3H, s, CH_3), 1.34 (12H, s, CH_3); ^{13}C NMR (125MHz, $CDCl_3$) δ 170.1 (*C*=O), 164.7 (*C*=O), 153.9 (Ar *C*H), 150.8 (Ar *C*), 143.75 (Ar *C*H), 126.4 (Ar *C*H), 121.3 (Ar *C*H), 52.4 (*C*H_3), 41.2 (*C*H_2), 36.5, 31.4, 25.0-14.1 (multiple peaks, *C*H_3); MS (ESI^+) m/z 243 ($[M+Na]^+$, 70%); HRMS calcd. for $C_{15}H_{21}BN_2NaO_5$ $[M+Na]^+$ 243.1436; Found 243.1443.

Methyl 2-[4-(4,4,5,5-tetramethyl-1,3,2-dioxaborolanpyridine-2-yl)carbonyl]glycinate 302b

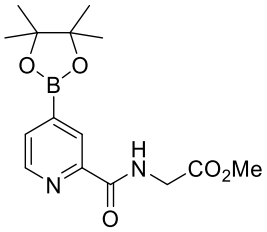

A mixture of **301b** (1.00 g, 3.66 mmol) with bispinacolatodiboron (1.05 g, 4.13 mmol) and potassium acetate (1.08 g, 10.92 mmol) in dry 1,4-dioxane (30 mL) was purged with N_2 for 5 min and then 1,1'-bis(diphenylphosphino)ferrocene-palladium(II)dichloride (0.13 g, 0.16 mmol) was added. The mixture was heated at reflux for 1 h before bispinacolatodiboron (0.50 g, 1.97 mmol) and 1,1'-bis(diphenylphosphino)ferrocene-palladium(II)dichloride (0.10 g, 0.012 mmol) were added. The mixture was heated at reflux for 17 h until consumption of starting material (TLC). The solvent was removed *in vacuo* and the crude was redissolved in EtOAc followed by filtration through Celite. The filtrate was concentrated *in vacuo*. Precipitation with Et_2O (x 2) afforded compound **302b** (0.30 g, 26 %) as white crystals, mp 115-117 ºC. IR (neat) ν/cm^{-1} 3384 (N-H), 1736 (CH_3OC=O), 1673 (NHC=O); ^{1}H NMR (500 MHz, $CDCl_3$) δ 8.60 (1H, d, *J*= 4.5, Ar C*H*), 8.54 (1H, s, Ar C*H*), 8.46 (1H, s, N*H*), 4.28 (2H, d, *J*= 5.5, CH_2), 3.79 (3H, s, CH_3), 1.35 (12H, s, CH_3); ^{13}C NMR (125MHz, $CDCl_3$) δ 170.2 (*C*=O), 164.7 (*C*=O), 148.3 (Ar *C*), 147.65 (Ar *C*), 131.3 (Ar *C*H), 128.3 (Ar *C*H), 83.0 (*C*$(CH_3)_2$), 52.3 (O*C*H_3), 41.25 (*C*H_2), 24.7 (multiple peaks, *C*H_3); MS (FI$^+$) m/z 320 ([M+H]$^+$, 100%); HRMS calcd. for $C_{15}H_{21}BN_2NaO_5$ [M-H]$^-$ 320.1436; Found 320.1436.

Methyl 2-[6-(4,4,5,5-tetramethyl-1,3,2-dioxaborolan pyridine-2-yl)carbonyl]glycinate 302c

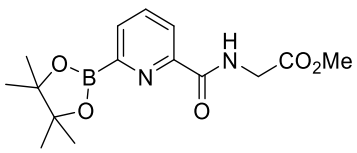

To a solution of **301c** (1.71 g, 6.27 mmol) with bispinacolatodiboron (2.10 g, 8.29 mmol) in anhydrous THF (40 mL), potassium acetate (2.08 g, 18.65 mmol) was added and the mixture

was purged with N_2 for 5 min. Then 1,1'-bis(diphenylphosphino)ferrocene-palladium(II)dichloride (0.20 g, 0.31 mmol) was added. The mixture was heated at reflux for 3 h and bispinacolatodiboron (0.50 g, 1.97 mmol), 1,1'-bis(diphenylphosphino)-ferrocene-palladium(II)dichloride (0.20 g, 0.31 mmol) were added. The mixture was heated at reflux for 1 d until consumption of starting material (TLC). The solvent was removed *in vacuo* and the crude was redissolved in EtOAc followed by filtration through Celite. The filtrate was washed with brine, the organic phase was dried over $MgSO_4$. Concentration *in vacuo* afforded compound **302c** (1.07 g, 53 %) as a yellow oil. IR (neat) ν/cm^{-1} 3387 (N-H), 1755 (CH_3OC=O), 1680 (NHC=O); ^{1}H NMR (500 MHz, $CDCl_3$) δ 8.66 (1H, br. s, N*H*), 8.21 (1H, dd, *J*= 8.0 1.5, Ar C*H*), 7.95 (1H, t, *J*= 1.5, Ar C*H*), 7.85 (1H, t, *J*= 8.0, Ar C*H*), 4.28 (2H, d, *J*= 6.0, CH_2), 3.80 (3H, s, CH_3), 1.42 (12H, s, CH_3); ^{13}C NMR (125MHz, $CDCl_3$) δ 170.2 (*C*=O), 164.9 (*C*=O), 149.7 (Ar *C*), 136.0 (Ar *C*H), 133.2 (Ar *C*H), 123.6 (Ar *C*H), 84.8 (*C*$(CH_3)_2$), 52.3 (*C*H_3), 41.1 (*C*H_2), 24.9 (*C*H_3); MS (ESI$^+$) m/z 243 ([M+Na]$^+$, 70%); HRMS calcd. for $C_{15}H_{21}BN_2NaO_5$ [M+Na]$^+$ 243.1436; Found 243.1443.

Potassium trifluoro(6-(5-(2-methoxy-2-oxoethyl)carbamoyl)pyridin-3-yl)borate 305a

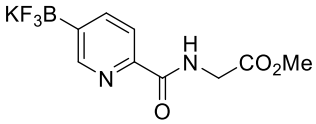

Following procedure A the filtrate was concentrated *in vacuo* to afford compound **305a** (0.20 g, 36 %) as a white solid, mp 202-203 ºC. IR (neat) ν/cm^{-1} 3388 (N-H), 1747 (CH_3OC=O), 1680 (NHC=O); ^{1}H NMR (500 MHz, CD_3COCD_3) δ 8.67-8.64 (2H, m, Ar C*H*), 7.95-7.92 (2H, m, N*H*), 4.21 (2H, d, *J*= 6.0, CH_2), 3.72 (3H, s, CH_3); ^{13}C NMR (125MHz, CD_3COCD_3) δ 171.3 (*C*=O), 166.4 (*C*=O), 152.75 (Ar *C*H), 147.7 (Ar *C*), 141.0 (Ar *C*H), 121.08 (Ar *C*H), 52.2 (*C*H_3), 41.5 (*C*H_2); ^{19}F (470 MHz, CD_3COCD_3) -143.0; MS (ESI$^-$) m/z 261 ([M-K]$^-$, 100%); HRMS calcd. for $C_9H_9BF_3N_2O_3$ [M-K]$^-$ 261.0664; Found 261.0659.

Potassium trifluoro(6-(5-(2-methoxy-2-oxoethyl)carbamoyl)pyridin-3-yl)borate 305b

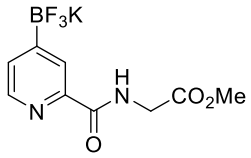

Following procedure A the filtrate was concentrated *in vacuo* to afford compound **305b** (0.45 g, 77 %) as a white solid, mp 243-245 ºC. IR (neat) ν/cm^{-1} 3374 (N-H), 1736 (CH_3OC=O), 1666 (NHC=O); ^{1}H NMR (500 MHz, CD_3COCD_3) δ 8.68 (1H, app. s, N*H*), 8.34 (1H, d, *J*= 4.5, Ar C*H*), 8.28 (1H, s, Ar C*H*), 7.58 (1H, d, *J*= 4.5, Ar C*H*), 4.21 (2H, d, *J*= 6.0, CH_2), 3.72 (3H, s, CH_3); ^{13}C NMR (125MHz, $CDCl_3$) δ 171.3 (*C*=O), 166.7 (*C*=O), 148.2 (Ar *C*), 147.0 (Ar *C*), 130.9 (Ar *C*H), 126.3 (Ar *C*H), 52.2 (*C*H_3), 41.6 (*C*H_2); ^{19}F NMR (470 MHz, CD_3COCD_3) δ -144.7; MS (ESI$^-$) m/z 261 ([M-K]$^-$, 100%); HRMS calcd. for $C_9H_9BF_3N_2O_3$ [M-K]$^-$ 261.0664; Found 261.0657.

Potassium trifluoro(6-(6-(2-methoxy-2-oxoethyl)carbamoyl)pyridin-3-yl)borate 305c

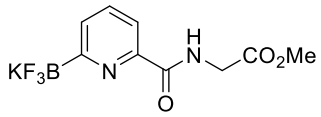

Following procedure A the filtrate was concentrated *in vacuo* to afford compound **305c** (0.35 g, 60 %) as a white solid, mp 247-249 ºC. IR (neat) ν/cm^{-1} 3388 (N-H), 1747 (CH_3OC=O), 1680 (NHC=O); ^{1}H NMR (500 MHz, CD_3COCD_3) δ 8.77 (1H, br. s, N*H*), 7.84-7.81 (1H, m, Ar C*H*), 7.72-7.63 (2H, m, N*H*), 4.20 (2H, d, *J*= 6.0, CH_2), 3.76 (3H, s, CH_3); ^{13}C NMR (125MHz, CD_3COCD_3) δ 170.9 (*C*=O), 166.0 (*C*=O), 148.1 (Ar *C*), 137.7 (Ar *C*), 134.7 (Ar *C*H), 127.7 (Ar *C*H), 118.5 (Ar *C*H), 51.7 (*C*H_3), 40.9 (*C*H_2); ^{19}F (470 MHz, CD_3COCD_3) -140.0; MS (ESI$^-$) m/z 261 ([M-K]$^-$, 100%); HRMS calcd. for $C_9H_9BF_3N_2O_3$ [M-K]$^-$ 261.0664; Found 261.0659.

2-[(5-Boronopyridine-2-yl)carbonyl]glycine 306

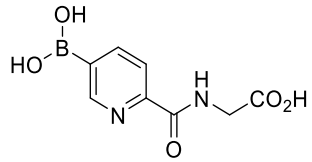

According to procedure B, **305a** (0.65 g, 2.17 mmol) was dissolved in CH_3CN/H_2O (6 mL) and chlorotrimethylsilane (2.8 mL, 21.79 mmol) was added. Washing of the solid with CH_3CN afforded compound **306** (0.25 g, 51 %) as a white solid, mp > 250 ºC. IR (neat) ν/cm^{-1} 3218 (OH), 1724 (CH_3OC=O), 1678 (NHC=O); ^{1}H NMR (500 MHz, DMSO-d_6) δ 8.87 (1H, s, Ar C*H*), 8.63 (1H, t, *J*= 5.0, N*H*), 8.23-8.21 (1H, m, Ar C*H*), 7.97 (1H, d, *J*= 6.0, Ar C*H*), 3.97 (2H, s, O*H*), 3.6 (2H, s, CH_2); ^{13}C NMR (125MHz, DMSO-d_6) δ 174.55 (*C*=O), 172.0 (*C*=O), 163.0 (Ar *C*H), 153.45 (Ar *C*), 150.6 (Ar *C*), 143.1 (Ar *C*H), 120.5 (Ar *C*H), 43.8 (CH_2); MS (ESI$^-$) m/z 223 ([M-H]$^-$, 100%); HRMS calcd. for $C_8H_8BN_2O_3$ [M-H]$^-$ 223.0533; Found 223.0523.

2-[(4-Boronopyridine-2-yl)carbonyl]glycine 307

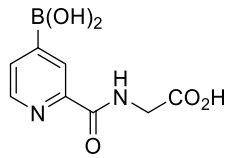

According to procedure B, **305b** (0.20 g, 0.67 mmol) was dissolved in CH_3CN/H_2O (4.5 mL) and chlorotrimethylsilane (1.2 mL, 9.45 mmol) was added. Crystallization (H_2O) afforded compound **307** (0.02 g, 13 %) as white crystals, mp > 300 ºC. IR (neat) ν/cm^{-1} 3071 (OH), 1730 (HOC=O), 1603 (NHC=O); ^{1}H NMR (500 MHz, DMSO-d_6) δ 8.96 (1H, d, *J*= 6.0, Ar C*H*), 8.66 (1H, dd, *J*= 4.5 1.0, N*H*), 8.41 (1H, s, Ar C*H*), 7.90 (1H, dd, *J*= 4.5, 1.0, Ar C*H*), 4.00 (2H, d, *J*= 6.0, CH_2); ^{13}C NMR (125MHz, DMSO-d_6) δ 171.1 (*C*=O), 164.5 (*C*=O), 148.6 (Ar *C*), 147.7 (Ar *C*), 131.3 (Ar *C*H), 126.4 (Ar *C*H), 41.0 (CH_2); MS (FI$^+$) m/z 208 ([M-OH]$^+$, 30%).

Methyl *N*-{[5-(3a,7a-dihydro-1-benzofuran-2-yl)pyridin-2-yl]carbonyl}glycinate 322

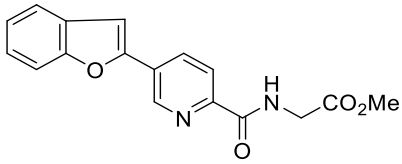

Following general procedure C, the reaction was heated at reflux for 1 d. Chromatography afforded compound **322** (0.33 g, 58 %) as yellow crystals, mp 126-127 ºC. R_f =0.35. IR (KBr) ν/cm^{-1} 3403 (N-H), 1733 (CH_3OC=O), 1681 (NHC=O); ^{1}H NMR (500 MHz, $CDCl_3$) δ 9.06 (1H, s, Ar C*H*), 8.47 (1H, t, *J*= 5.0, N*H*), 8.26-8.25 (2H, m, Ar C*H*), 7.65-7.56 (2H, m, Ar C*H*), 7.38-7.34 (1H, m, Ar C*H*), 7.30-7.27 (2H, m, Ar C*H*), 4.31 (2H, d, *J*= 6.0, CH_2), 3.81 (3H, s, CH_3); ^{13}C NMR (125MHz, $CDCl_3$) δ 170.1 (*C*=O), 164.2 (*C*=O), 155.3 (Ar *C*), 152.1 (Ar *C*), 148.3 (Ar *C*), 144.8 (Ar *C*), 132.8 (Ar *C*H), 128.5 (Ar *C*), 128.4 (Ar *C*H), 125.5 (Ar *C*H), 124.3 (Ar *C*H), 123.7 (Ar *C*H), 121.35 (Ar *C*H), 111.4 (Ar *C*H), 104.3 (Ar *C*H), 52.4 (*C*H_3), 41.3 (*C*H_2); MS (ESI$^+$) m/z 309 ([M+H]$^+$, 100%); HRMS calcd. for $C_{17}H_{14}N_2NaO_4$ [M+Na]$^+$ 333.0846; Found 333.0843.

Methyl *N*-{[5-(naphthalen-2-yl)pyridin-2-yl]carbonyl}glycinate 323

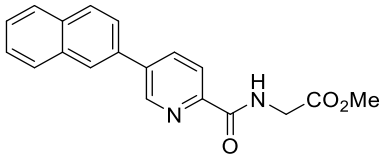

Following general procedure C, the reaction was heated at reflux for 40 h. Chromatography afforded compound **323** (0.15 g, 26 %) as white needles, mp 155-156 ºC. R_f =0.40. IR (KBr) ν/cm^{-1} 3360(NH), 1747 (CH_3OC=O), 1673 (NHC=O); ^{1}H NMR (500 MHz, $CDCl_3$) δ 8.95 (1H, d, *J*= 2.0, Ar C*H*), 8.51 (1H, t, *J*= 5.0, N*H*), 8.30 (1H, d, *J*= 8.0, Ar C*H*), 8.17 (1H, dd, *J*= 6.0 2.0, Ar C*H*), 8.08 (1H, s, Ar C*H*), 7.99 (1H, d, *J*= 9.0, Ar C*H*), 7.96-7.90 (2H, m, Ar C*H*), 7.75 (1H, dd, *J*= 7.0 2.0, Ar C*H*), 7.57-7.55 (2H, m, Ar C*H*),4.33 (2H, d, *J*= 6.0, CH_2), 3.83 (3H, s, CH_3); ^{13}C NMR (125MHz, $CDCl_3$) δ 170.2 (*C*=O), 164.5 (*C*=O), 149.5 (Ar *C*), 147.9 (Ar *C*), 147.1 (Ar *C*), 139.3 (Ar *C*), 135.7 (Ar *C*H), 134.2 (Ar *C*), 133.5 (Ar *C*H), 133.1 (Ar *C*H), 129.1 (Ar *C*H), 128.3 (Ar *C*H), 127.7 (Ar *C*H), 126.8 (Ar *C*H), 126.6 (Ar *C*H),

124.8 (Ar *C*H), 122.4 (Ar *C*H), 52.4 (*C*H_3), 41.3 (*C*H_2); MS (ESI$^+$) m/z 343 ([M+Na]$^+$, 100%); HRMS calcd. for $C_{19}H_{16}N_2NaO_3$ [M+Na]$^+$ 343.1053; Found 343.1051.

Methyl *N*-{[5-(6-methoxynaphthalen-2-yl)pyridin-2-yl]carbonyl}glycinate 324

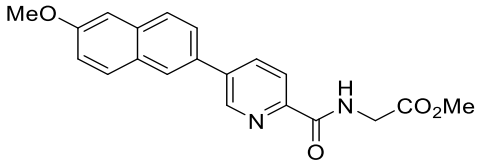

Following general procedure C, after 1 d of reflux, tetrakis(triphenylphosphino)palladium(0) (0.11 g, 0.09 mmol) was added and the reaction was heated at reflux for 2 d more. Chromatography afforded compound **324** (0.13 g, 20 %) as colourless crystals, mp 162-163 ºC. R_f = 0.40. IR (KBr) ν/cm^{-1} 3390(N-H), 1752 (CH_3OC=O), 1659 (NHC=O); ^{1}H NMR (500 MHz, $CDCl_3$) δ 8.93-8.92 (1H, m, Ar C*H*), 8.50 (1H, t, *J*= 5.0, N*H*), 8.29-8.27 (1H, m, Ar C*H*), 8.15-8.135 (1H, m, Ar C*H*), 8.03 (1H, s, Ar C*H*), 7.89-7.83 (2H, m, Ar C*H*), 7.72-7.70 (1H, m, Ar C*H*), 7.24-7.19 (2H, m, Ar C*H*), 4.32 (2H, d, *J*= 6.0, CH_2), 3.97 (3H, s, OCH_3), 3.82 (3H, s, CO_2CH_3); ^{13}C NMR (125MHz, $CDCl_3$) δ 170.2 (*C*=O), 164.6 (*C*=O), 158.4 (Ar *C*), 147.6 (Ar *C*), 146.9 (Ar *C*), 139.4 (Ar *C*), 135.4 (Ar *C*), 134.5 (Ar *C*H), 131.9 (Ar *C*), 129.9 (Ar *C*H), 129.0 (Ar *C*H), 127.9 (Ar *C*H), 126.35 (Ar *C*H), 125.3 (Ar *C*H), 122.4 (Ar *C*H), 119.7 (Ar *C*H), 105.6 (Ar *C*H), 55.4 (*C*H_3), 52.4 (*C*H_3), 41.3 (*C*H_2); MS (ESI$^+$) m/z 373 ([M+Na]$^+$, 60%); HRMS calcd. for $C_{20}H_{18}N_2NaO_4$ [M+Na]$^+$ 373.1159; Found 373.1157.

Methyl *N*-{[5-(dibenzo[*b*,*d*]furan-4-yl)pyridin-2-yl]carbonyl}glycinate 325

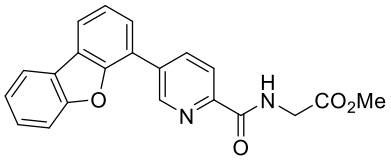

Following general procedure C, reaction was heated at reflux for 1 d. Addition of Et_2O in the colourless oil obtained from chromatography afforded compound **325** (0.20 g, 30 %) as white crystals, mp 143-144 ºC. R_f = 0.35. IR (KBr) ν/cm^{-1} 3392 (N-H), 1734 (CH_3OC=O), 1672 (NHC=O); ^{1}H NMR (500 MHz, $CDCl_3$) δ 9.16-9.16 (1H, m, Ar C*H*), 8.56 (1H, t, *J*= 1.0, N*H*), 8.41-8.34 (2H, m, Ar C*H*), 8.04-8.00 (2H, m, Ar C*H*), 7.66-7.61 (2H, m, Ar C*H*), 7.53-

7.47 (2H, m, Ar C*H*), 7.42-7.385 (1H, m, Ar C*H*), 4.34 (2H, d, *J*= 6.0, CH_2), 3.83 (3H, s, CH_3); ^{13}C NMR (125MHz, $CDCl_3$) δ 170.2 (*C*=O), 164.5 (*C*=O), 156.1 (Ar *C*), 153.3 (Ar *C*), 149.5 (Ar *C*), 148.1 (Ar *C*), 137.0 (Ar *C*), 135.0 (Ar *C*), 127.7 (Ar *C*H), 126.5 (Ar *C*), 125.3 (Ar *C*H), 123.8 (Ar *C*H), 123.7 (Ar *C*H), 123.5 (Ar *C*H), 123.5 (Ar *C*H), 121.4 (Ar *C*H) 121.2 (Ar *C*H), 120.8 (Ar *C*H), 111.9 (Ar *C*H), 52.4 (*C*H_3), 41.3 (*C*H_2); MS (ESI^+) m/z 383 ($[M+Na]^+$, 50%); HRMS calcd. for $C_{21}H_{16}N_2NaO_4$ $[M+Na]^+$ 383.1002; Found 383.0999.

_N_-{[5-(3a,7a-dihydro-1-benzofuran-2-yl)pyridin-2-yl]carbonyl}glycine 326

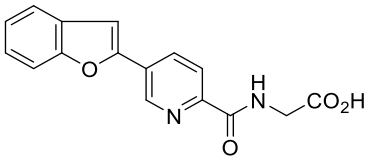

Following general procedure D, washing afforded compound **326** (0.20 g, 36 %) as white crystals, mp > 250 ºC; IR (KBr) ν/cm^{-1} 3385 (O-H), 3307 (N-H), 1659 (NHC=O); ^{1}H NMR (500 MHz, MeOD-d_4) δ 9.18 (1H, s, Ar C*H*), 8.42-8.40 (1H, m, Ar C*H*), 8.20-8.18 (1H, m, Ar C*H*), 7.70-7.60 (2H, m, Ar C*H*), 7.51 (1H, s, Ar C*H*), 7.40-7.31 (2H, m, Ar C*H*), 4.02 (2H, d, *J*= 6.0, CH_2); ^{13}C NMR (125MHz, MeOD-d_4) δ 176.0 (*C*=O), 165.7 (*C*=O), 156.8 (Ar *C*), 153.5 (Ar *C*), 150.3 (Ar *C*), 146.1 (Ar *C*), 141.4 (Ar *C*), 134.0 (Ar *C*H), 130.3 (Ar *C*H), 126.7 (Ar *C*H), 124.6 (Ar *C*H), 124.5 (Ar *C*H), 123.1 (Ar *C*H), 112.3 (Ar *C*H), 105.8 (Ar *C*H), 44.7 (*C*H_2); MS (ESI^-) m/z (ES^-) 295 ($[M-H]^-$, 100%); HRMS calcd. for $C_{16}H_{11}N_2O_4$ $[M-H]^-$ 295.0724; Found 295.0718.

_N_-{[5-(naphthalen-2-yl)pyridin-2-yl]carbonyl}glycine 327

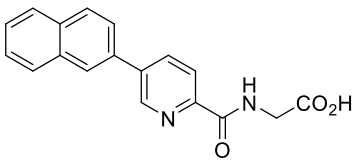

Following general procedure D, washing afforded compound **327** (0.20 g, 36 %) as white crystals, mp >250 ºC. IR (KBr) ν/cm^{-1} 3385 (COO-H), 1660 (NHC=O); ^{1}H NMR (500 MHz, MeOD-d_4) δ 9.06 (1H, d, *J*= 1.0, Ar C*H*), 8.34-8.32 (1H, m, Ar C*H*), 8.25-8.21 (2H, m, Ar C*H*), 8.04-8.00 (2H, m, Ar C*H*), 7.94-7.92 (1H, m, Ar C*H*), 7.87-7.85 (1H, m, Ar C*H*), 7.58-

7.56 (1H, m, Ar C*H*), 4.25 (2H, s, CH_2); ^{13}C NMR (125MHz, MeOD-d_4) δ 176.0 (*C*=O), 166.1 (*C*=O), 149.75 (Ar *C*), 148.4 (Ar *C*), 140.4 (Ar *C*), 136.8 (Ar *C*), 135.4 (Ar *C*), 135.1 (Ar *C*H), 134.7 (Ar *C*H), 130.1 (Ar *C*H), 129.5 (Ar *C*H), 128.75 (Ar *C*H), 127.9 (Ar *C*H), 127.6 (Ar *C*H), 125.8 (Ar *C*H), 123.1 (Ar *C*H), 118.25 (Ar *C*H), 44.8 (*C*H_2); MS (ESI$^-$) m/z 305 ([M-H]$^-$, 100%); HRMS calcd. for $C_{18}H_{13}N_2O_3$ [M-H]$^-$ 305.0932; Found 305.0925.

***N*-{[5-(dibenzo[*b*,*d*]furan-4-yl)pyridin-2-yl]carbonyl}glycine 328**

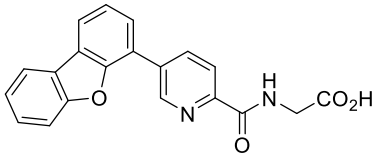

Following general procedure D, washing afforded compound **328** (0.15 g, 23 %) as white powder, mp 181-182 ºC. IR (KBr) ν/cm^{-1} 3518 (O-H), 3353 (N-H), 1672 (NHC=O); ^{1}H NMR (500 MHz, DMSO-d_6) δ 9.25-9.24 (1H, m, Ar C*H*), 8.72 (1H, t, *J*= 4.0, N*H*), 8.53 (1H, dd, *J*= 8.0 2.0, Ar C*H*), 8.27 (1H, dd, *J*= 7.5 1.0, Ar C*H*), 8.24 (1H, d, *J*= 7.5, Ar C*H*), 8.22 (1H, dd, *J*= 8.0 0.5, Ar C*H*), 7.88 (1H, dd, *J*= 7.5 1.0, Ar C*H*), 7.81 (1H, d, *J*= 8.0, Ar C*H*), 7.60-7.56 (2H, m, Ar C*H*), 7.48-7.45 (1H, m, Ar C*H*), 3.51 (2H, d, *J*= 4.0, CH_2); ^{13}C NMR (125MHz, DMSO-d_6) δ 169.4 (*C*=O), 162.1 (*C*=O), 155.5 (Ar *C*), 152.6 (Ar *C*), 149.3 (Ar *C*), 148.0 (Ar *C*), 137.1 (Ar *C*), 133.5 (Ar *C*), 128.0 (Ar *C*), 127.0 (Ar *C*H), 124.6 (Ar *C*H), 123.9 (Ar *C*H), 123.4 (Ar *C*H), 123.3 (Ar *C*H),121.7 (Ar *C*H), 121.45 (Ar *C*H), 121.35 (Ar *C*H), 121.0 (Ar *C*H), 112.0 (Ar *C*H), 44.2 (*C*H_2); MS (ESI$^-$) m/z 345 ([M-H]$^-$, 100%); HRMS calcd. for $C_{20}H_{14}N_2NaO_4$ [M+Na]$^+$ 369.0846; Found 369.0842

***N*-{[5-(6-methoxynaphthalen-2-yl)pyridin-2-yl]carbonyl}glycine 329**

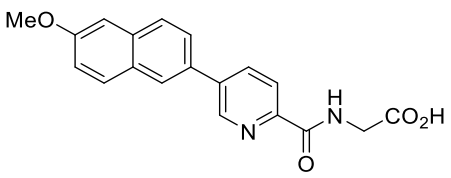

In a solution of **324** (0.02 g, 0.06 mmol) in 1,4-dioxane (1 mL), 1 M lithium hydroxide (0.12 mL, 0.12 mmol) was added. The mixture was stirred at room temperature for 10 h until consumption of starting material. The mixture was acidified with acetic acid to pH 3 and

extracted with CH_2Cl_2/H_2O. The solution was washed with water, dried over $MgSO_4$ and concentrated *in vacuo*. Concentration afforded compound **329** (0.01 g, 52 %), mp 183-184 ºC. IR (KBr) ν/cm^{-1} 3385 (O-H), 3066 (N-H), 1749 (HOC=O), 1664 (NHC=O); ^{1}H NMR (500 MHz, MeOD-*d*$_4$) δ 9.06 (1H, s, Ar C*H*), 8.33 (1H, dd, *J*= 8.5 2.0, Ar C*H*), 8.22-8.19 (2H, m, Ar C*H*), 7.95-7.90 (2H, m, Ar C*H*), 7.83 (1H, dd, *J*= 8.5 2.0, Ar C*H*), 7.32 (1H, d, *J*= 2.5, Ar C*H*), 7.22 (1H, dd, *J*= 9.0 2.5, Ar C*H*), 4.21 (2H, s, CH_2), 3.96 (3H, s, CH_3); ^{13}C NMR (125MHz, MeOD-*d*$_4$) δ 173.3 (*C*=O), 167.0 (*C*=O), 160.0 (Ar *C*), 149.0 (Ar *C*), 148.2 (Ar *C*), 140.9 (Ar *C*), 136.55 (Ar *C*), 136.2 (Ar *C*), 133.0 (Ar *C*H), 131.0 (Ar *C*H), 130.6 (Ar *C*H), 129.1 (Ar *C*H), 127.4 (Ar *C*H), 126.2 (Ar *C*H), 123.3 (Ar *C*H), 120.6 (Ar *C*H), 106.6 (Ar *C*H), 55.9 (*C*H$_3$), 43.5 (*C*H$_2$); MS (ESI$^-$) m/z 335 ([M-H]$^-$, 100%); HRMS calcd. for $C_{19}H_{15}N_2O_4$ [M-H]$^-$ 335.1037; Found 335.1037.

3-(benzyloxy)-5-bromopyridine-2-carbonitrile 330

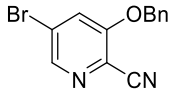

To a mixture of benzyl alcohol (2.95 mL, 28.5 mmol) in dry THF (90 mL) at 0 ºC sodium hydride 60% (1.32 g, 32.9 mmol) was added and the mixture was left to warm to room temperature and then it was warmed to 35 ºC for 20 min. The mixture was added dropwise in a solution of 5-bromo-3-nitropicolinonitrile (5.00 g, 21.9 mmol) in anhydrous THF (60 mL) at room temperature over 20 min and was stirred at this temperature for 1 h. The solvent was removed *in vacuo* and the resulting residue was dissolved in CH_2Cl_2. This was washed with water, dried over $MgSO_4$ and concentrated *in vacuo*. Chromatography (hexane/CH_2Cl_2/EtOAc 80:12:8) afforded compound **330** (3.00 g, 47 %) as white needles, mp 133-134 ºC. R_f = 0.40. IR (neat) ν/cm^{-1} 2300 (C-N); ^{1}H NMR (500 MHz, $CDCl_3$) δ 8.35 (1H, d, *J*= 2.0, Ar C*H*), 7.55 (1H, d, *J*= 1.5, Ar C*H*), 7.46-7.38 (5H, m, Ar C*H*), 5.25 (2H, s, O CH_2); ^{13}C NMR (125MHz, $CDCl_3$) δ 157.5 (*C*N), 144.15 (Ar *C*), 134.0 (Ar *C*), 129.0 (Ar *C*H), 128.9 (Ar *C*H), 127.2 (Ar *C*H), 125.05 (Ar *C*H), 123.7 (Ar *C*H), 122.6 (Ar *C*H), 114.45 (Ar *C*H), 71.4 (*C*H$_2$); MS (ESI$^+$) m/z 311 ([M+Na]$^+$, 30%); HRMS calcd. for $C_{13}H_9BrN_2NaO$ [M+Na]$^+$ 310.9790; Found 310.9788.

2,6-bis(benzyloxy)-3-bromo-5-nitropyridine 331

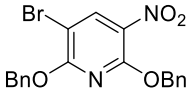

Chromatography afforded **331** (0.02 g, 0.2 %) as yellow needles, mp 126-128 ºC. R_f = 0.48. IR (neat) ν/cm^{-1} 1523, 1366 (NO_2); ^{1}H NMR (500 MHz, $CDCl_3$) δ 8.45 (1H, s, Ar C*H*), 7.46-7.36 (10H, m, Ar C*H*), 5.25 (4H, s, O CH_2); ^{13}C NMR (125MHz, $CDCl_3$) δ 149.3 (Ar *C*H), 131.4 (Ar *C*), 129.2 (Ar *C*H), 129.1 (Ar *C*H), 129.0 (Ar *C*H), 128.8 (Ar *C*H), 128.7 (Ar *C*H), 76.0 (*C*H_2); MS (ESI$^+$) m/z 419 ([M+Na]$^+$, 100%).

3,6-bis(benzyloxy)-5-bromopyridine-2-carbonitrile 332

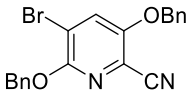

Chromatography afforded **332** (0.12 g, 10 %) as yellow needles, mp 60 ˚C dec.. R_f = 0.46. IR (neat) ν/cm^{-1} 2258 (C-N); ^{1}H NMR (500 MHz, $CDCl_3$) δ 8.60 (1H, s, Ar C*H*), 7.49-7.28 (10H, m, Ar C*H*), 5.55 (2H, s, O CH_2), 5.45 (2H, s, O CH_2); ^{13}C NMR (125MHz, $CDCl_3$) δ 160.5 (*C*N), 155.3 (Ar *C*), 141.0 (Ar *C*H), 135.7 (Ar *C*), 135.5 (Ar *C*), 128.7 (Ar *C*H), 128.7 (Ar *C*H), 128.4 (Ar *C*H), 128.2 (Ar *C*H), 127.4 (Ar *C*H), 127.2 (Ar *C*H), 96.2 (Ar *C*H), 70.2 (*C*H_2), 69.5 (*C*H_2); MS (ESI$^+$) m/z 437 ([M+Na]$^+$, 90%).

3-(benzyloxy)-5-bromopyridine-2-carboxylic acid 333

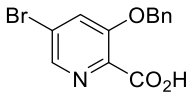

To a stirred suspension of **330** (2.00 g, 6.9 mmol) in methanol (25 mL), 30% w/v NaOH (24.0 mL, 180 mmol) was added and the reaction mixture was heated at reflux overnight. The solvent was removed *in vacuo* and the suspension was acidified with conc. HCl to pH= 2. The resulting precipitate was filtrated and washed with cold water. Filtration afforded compound **333** (1.75 g, 82 %) as pale yellow needles, mp 106-108 ºC. IR (neat) ν/cm^{-1} 3056 (NH), 1716 (HOC=O); ^{1}H NMR (500 MHz, DMSO-d_6) δ 8.31 (1H, s, CO_2H), 8.03 (1H, s, Ar

C*H*), 7.51-7.29 (6H, m, Ar C*H*), 3.90 (2H, s, O CH_2); ^{13}C NMR (125MHz, DMSO-d_6) δ 165.9 (*C*=O), 152.7 (Ar *C*), 141.1 (Ar *C*), 140.4 (Ar *C*), 136.4 (Ar *C*H), 128.5 (Ar *C*), 128.4 (Ar *C*H), 128.1 (Ar *C*H), 127.85 (Ar *C*H), 127.4 (Ar *C*H), 127.3 (Ar *C*H), 124.45 (Ar *C*H), 70.2 (O*C*H$_2$); MS (ESI$^-$) m/z 306 ([M-H]$^-$, 100%); HRMS calcd. for $C_{13}H_9BrNO_3$ [M-H]$^-$ 305.9771; Found 305.9776.

Benzyl *N*-{[3-(benzyloxy)-5-bromopyridin-2-yl]carbonyl}glycinate 334

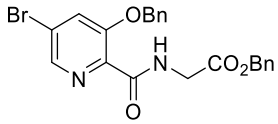

To a stirred suspension of **333** (1.50 g, 4.85 mmol) in anhydrous CH_2Cl_2 (50 mL) under N_2, DIPEA (2.13 mL, 12.18 mmol), HOBT (1.12 g, 7.31 mmol) were added and stirred for 10 min before EDCI (1.39 mL, 7.31 mmol) was added. After 10 min glycine benzyl ester hydrochloride (1.18 g, 5.84 mmol) was added and the reaction mixture was stirred for 3 d until consumption of starting material. The mixture was washed with sat. $NaHCO_3$, brine and H_2O. The organic layer was dried over $MgSO_4$ and concentrated *in vacuo*. Chromatography (hexane/EtOAc 4:6 to 3:7) afforded compound **334** (1.10 g, 50 %) as white needles, mp 107-109 ºC. R_f = 0.35. IR (neat) ν/cm^{-1} 3362 (NH), 1755 (BnOC=O), 1659 (NHC=O); ^{1}H NMR (500 MHz, $CDCl_3$) δ 8.29 (1H, d, *J*= 1.5, Ar C*H*), 8.17 (1H, t, *J*= 5.0, N*H*), 7.56 (1H, d, *J*= 2.0, Ar C*H*), 7.51 (2H, dd, *J*= 7.0 2.5, Ar C*H*), 7.42-7.32 (8H, m, Ar C*H*), 5.24 (2H, s, OCH_2), 5.22 (2H, s, OCH_2), 4.30 (2H, d, *J*= 5.5, CH_2); ^{13}C NMR (125MHz, $CDCl_3$) δ 169.7 (*C*=O), 163.4 (*C*=O), 155.0 (Ar *C*), 141.6 (Ar *C*), 137.2 (Ar *C*), 135.2 (Ar *C*), 135.0 (Ar *C*), 128.8 (Ar *C*H), 128.5 (Ar *C*H), 128.35 (Ar *C*H), 127.1 (Ar *C*H), 125.4 (Ar *C*H), 123.6 (Ar *C*H), 71.4 (O*C*H$_2$), 67.1 (O*C*H$_2$), 65.8 (*C*H$_2$); MS (ESI$^+$) m/z 477 ([M+Na]$^+$, 60%); HRMS calcd. for $C_{22}H_{19}BrN_2NaO_4$ [M+Na]$^+$ 477.0420; Found 477.0408.

Benzyl *N*-{[3-(benzyloxy)-5-(naphthalen-2-yl)pyridin-2-yl]carbonyl}glycinate 335

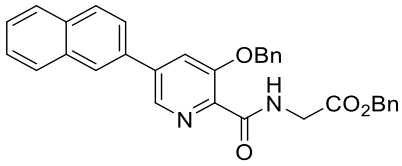

Following general procedure E, the reaction was heated at reflux for 40 h. Chromatography afforded compound **335** (0.15 g, 45 %) as white needles, mp 155-156 ºC. R_f = 0.55. IR (neat) ν/cm^{-1} 3293 (NH), 1749 (BnOC=O), 1659 (NHC=O); ^{1}H NMR (500 MHz, $CDCl_3$) δ 8.61 (1H, d, *J*= 1.5, Ar C*H*), 8.45 (1H, t, *J*= 5.5, N*H*), 7.99-7.83 (2H, m, Ar C*H*), 7.66-7.62 (2H, m, Ar C*H*), 7.57-7.54 (4H, m, Ar C*H*), 7.43-7.34 (8H, m, Ar C*H*), 5.37 (2H, s, CH_2), 5.24 (2H, s, CH_2), 4.36 (2H, d, *J*= 5.5, CH_2); ^{13}C NMR (125MHz, $CDCl_3$) δ 169.8 (*C*=O), 164.1 (*C*=O), 155.0 (Ar *C*), 140.5 (Ar *C*), 139.6 (Ar *C*), 137.0 (Ar *C*), 135.7 (Ar *C*), 135.3 (Ar *C*), 133.75 (Ar *C*), 133.4 (Ar *C*), 133.2 (Ar *C*), 129.1 (Ar *C*H), 128.8 (Ar *C*H), 128.7 (Ar *C*H), 128.6 (Ar *C*H), 128.5 (Ar *C*H), 128.4 (Ar *C*H), 128.35 (Ar *C*H), 128.3 (Ar *C*H), 127.7 (Ar *C*H), 127.3 (Ar *C*H), 126.9 (Ar *C*H), 126.8 (Ar *C*H), 126.7 (Ar *C*H), 126.6 (Ar *C*H), 125.4 (Ar *C*H), 124.7 (Ar *C*H), 121.15 (Ar *C*H), 71.3 (*C*H_2), 67.1 (*C*H_2), 41.6 (*C*H_2); MS (ESI$^+$) m/z 503 ([M+H]$^+$, 100%); HRMS calcd. for $C_{32}H_{26}N_2NaO_4$ [M+Na]$^+$ 525.1785; Found 525.1779.

Benzyl *N*-{[3-(benzyloxy)-5-(6-methoxynaphthalen-2-yl)pyridin-2-yl]carbonyl}glycinate 336

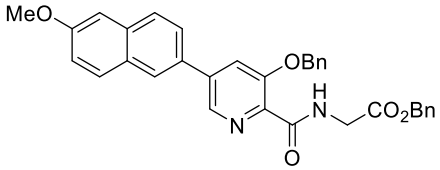

According to general procedure E, after 6 h tetrakis(triphenylphosphino)palladium(0) (60.0 mg, 0.06 mmol) was added and was heated at reflux for further 14 h. Chromatography afforded compound **336** (0.16 g, 46 %) as white needles, mp 104-106 ºC. R_f = 0.25. IR (neat) ν/cm^{-1} 3412 (NH), 1751 (BnOC=O), 1657 (NHC=O); ^{1}H NMR (500 MHz, $CDCl_3$) δ 8.59 (1H, d, *J*= 1.5, Ar C*H*), 8.38 (1H, t, *J*= 5.5, N*H*), 7.93 (1H, d, *J*= 5.0, Ar C*H*), 7.84 (2H, dd, *J*= 16.0 9.0, Ar C*H*), 7.65-7.56 (4H, m, Ar C*H*), 7.43-7.33 (8H, m, Ar C*H*), 7.24-7.18 (2H, m,

Ar C*H*), 5.37 (2H, s, CH_2), 5.24 (2H, s, CH_2), 4.36 (2H, d, *J*= 5.5, CH_2), 3.97 (3H, s, CH_3); ^{13}C NMR (125MHz, $CDCl_3$) δ 169.9 (*C*=O), 164.0 (*C*=O), 158.4 (Ar *C*), 155.1 (Ar *C*), 140.5 (Ar *C*), 139.4 (Ar *C*), 136.9 (Ar *C*), 135.8 (Ar *C*), 135.3 (Ar *C*H), 134.55 (Ar *C*H), 131.6 (Ar *C*), 129.9 (Ar *C*H), 128.9 (Ar *C*H), 128.8 (Ar *C*H), 128.6 (Ar *C*H), 128.4 (Ar *C*H), 128.35 (Ar *C*H), 128.2 (Ar *C*H), 127.85 (Ar *C*H), 127.2 (Ar *C*H), 126.45 (Ar *C*H), 125.2 (Ar *C*H), 121.0 (Ar *C*H), 119.75 (Ar *C*H), 105.6 (Ar *C*H), 71.3 (*C*H_2), 67.1 (*C*H_2), 65.8 (O*C*H_3), 55.4 (*C*H_2); MS (ESI$^+$) m/z 533 ([M+H]$^+$, 20%); HRMS calcd. for $C_{33}H_{29}N_2O_5$ [M+H]$^+$ 533.2071; Found 533.2070.

Benzyl *N*-{[3-(benzyloxy)-5-(6-hydroxynaphthalen-2-yl)pyridin-2-yl]carbonyl}glycinate 337

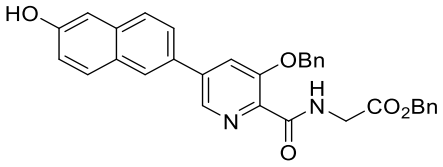

Following general procedure E, the reaction was finished after 12 h. Chromatography afforded compound **337** (65 mg, 29 %) as white needles, mp 146-148 ºC. R_f = 0.15. IR (neat) ν/cm^{-1} 3235 (NH), 1756 (BnOC=O), 1653 (NHC=O); ^{1}H NMR (500 MHz, $CDCl_3$) δ 8.53 (1H, d, *J*= 1.5, Ar C*H*), 8.41 (1H, t, *J*= 5.5, N*H*), 7.85 (1H, s, Ar C*H*), 7.77-7.72 (3H, m, Ar C*H*), 7.57-7.52 (5H, m, Ar C*H*), 7.42-7.33 (8H, m, Ar C*H*), 7.18 (1H, s, Ar C*H*), 7.17-7.17 (1H, m, Ar C*H*), 5.33 (2H, s, CH_2), 5.24 (2H, s, CH_2), 4.36 (2H, d, *J*= 6.0, CH_2); ^{13}C NMR (125MHz, $CDCl_3$) δ 170.1 (*C*=O), 164.2 (*C*=O), 155.0 (Ar *C*), 154.7 (Ar *C*), 140.5 (Ar *C*), 139.4 (Ar *C*), 136.6 (Ar *C*), 135.7 (Ar *C*H), 135.3 (Ar *C*H), 134.6 (Ar *C*H), 132.1 (Ar *C*), 131.3 (Ar *C*H), 130.2 (Ar *C*H), 128.8 (Ar *C*H), 128.7 (Ar *C*H), 128.6 (Ar *C*H), 128.5 (Ar *C*H), 128.5 (Ar *C*H), 128.4 (Ar *C*H), 128.3 (Ar *C*H), 127.5 (Ar *C*H), 127.3 (Ar *C*H), 126.5 (Ar *C*H), 125.2 (Ar *C*H), 120.7 (Ar *C*H), 119.0 (Ar *C*H), 109.4 (Ar *C*H), 71.2 (O*C*H_2), 67.2 (O*C*H_2), 41.6 (*C*H_2); HRMS (ESI$^-$) calcd. for $C_{32}H_{25}N_2O_5$ [M-H]$^-$ 517.1769; Found 517.1759;

***N*-{[3-hydroxy-5-(naphthalen-2-yl)pyridin-2-yl]carbonyl}glycine 338**

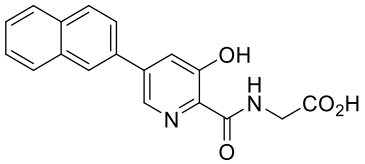

Following general procedure F, washing afforded compound **338** (8.0 mg, 62 %) as white solid, mp > 260 ºC dec. IR (neat) ν/cm^{-1} 3355 (O-H), 2950 (N-H), 1750 (HOC=O), 1665 (NHC=O); ^{1}H NMR (500 MHz, DMSO-d_6) δ 12.47 (1H, s, CO_2H), 9.28 (1H, t, J= 5.5, N*H*), 8.69 (1H, d, J= 2.0, Ar C*H*), 8.45 (1H, s, Ar C*H*), 8.09-8.03 (2H, m, Ar C*H*), 8.01-7.96 (2H, m, Ar C*H*), 7..88 (1H, s, Ar C*H*), 7.62-7.58 (2H, m, Ar C*H*), 3.96 (2H, d, J= 6.0, CH_2); ^{13}C NMR (125MHz, DMSO-d_6) δ 170.3 (*C*=O), 168.5 (*C*=O), 157.3 (Ar *C*), 140.8 (Ar *C*), 138.1 (Ar *C*), 133.1 (Ar *C*), 133.0 (Ar *C*), 132.9 (Ar *C*H), 129.9 (Ar *C*), 128.8 (Ar *C*H), 128.5 (Ar *C*H), 127.6 (Ar *C*H), 126.9 (Ar *C*H), 126.7 (Ar *C*H), 126.65 (Ar *C*H), 124.8 (Ar *C*H), 123.2 (Ar *C*H), 54.9 (CH_2); MS (ESI$^-$) m/z 321 ([M-H]$^-$, 100 %); HRMS calcd. for $C_{18}H_{13}N_2O_4$ [M-H]$^-$ 321.0881; Found 321.08872.

***N*-{[3-hydroxy-5-(6-methoxynaphthalen-2-yl)pyridin-2-yl]carbonyl}glycine 339**

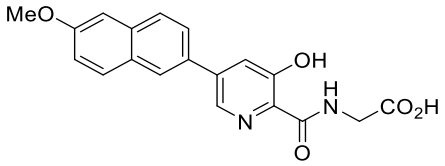

Following general procedure F, washing afforded compound **339** (13.0 mg, 98 %) as white solid, mp >280 ºC dec.. IR (neat) ν/cm^{-1} 3375 (O-H), 3058 (N-H), 1731 (HOC=O), 1652 (NHC=O); ^{1}H NMR (500 MHz, DMSO-d_6) δ 12.67 (1H, s, CO_2H), 8.99 (1H, t, J= 5.5, N*H*), 8.66 (1H, d, J= 2.0, Ar C*H*), 8.37 (1H, s, Ar C*H*), 7.97-7.92 (3H, m, Ar C*H*), 7.81 (1H, d, J= 2.0, Ar C*H*), 7.41 (1H, d, J= 1.5, Ar C*H*), 7.25 (1H, dd, J= 9.0 2.5, Ar C*H*), 3.92 (3H, s, CH_3), 3.70 (2H, d, J= 4.5, CH_2); ^{13}C NMR (125MHz, DMSO-d_6) δ 169.3 (*C*=O), 167.65 (*C*=O), 158.0 (Ar *C*), 157.2 (Ar *C*), 140.7 (Ar *C*), 138.2 (Ar *C*), 134.4 (Ar *C*), 130.7 (Ar *C*H), 130.1 (Ar *C*), 129.9 (Ar *C*), 128.6 (Ar *C*H), 127.65 (Ar *C*H), 126.4 (Ar *C*H), 125.2 (Ar *C*H), 122.6 (Ar *C*H), 119.3 (Ar *C*H), 105.8 (Ar *C*H), 55.3 (CH_3), 54.9 (CH_2); MS (ESI$^-$) m/z 351 ([M-H]$^-$, 100%); HRMS calcd. for $C_{19}H_{15}N_2O_5$ 351.0986; Found 351.0986.

***N*-{[3-hydroxy-5-(6-hydroxynaphthalen-2-yl)pyridin-2-yl]carbonyl}glycine 340**

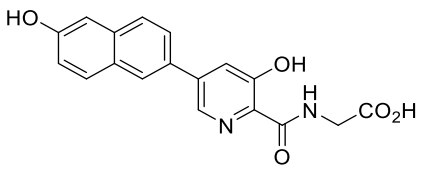

Following general procedure F, washing afforded compound **340** (11.0 mg, 85 %), mp 260 ºC dec.. IR (neat) ν/cm^{-1} 3341 (N-H), 3100 (O-H, COO-H), 1743 (HOC=O), 1645 (NHC=O); ^{1}H NMR (500 MHz, DMSO-d_6) δ 12.54 (1H, s, CO_2H), 10.01 (1H, s, O*H*), 9.14 (1H, t, *J*= 5.0, N*H*), 8.64 (1H, d, *J*= 2.0, Ar C*H*), 8.31 (1H, s, Ar C*H*), 7.90-7.79 (4H, m, Ar C*H*), 7.19-7.15 (2H, m, Ar C*H*), 3.86 (2H, d, *J*= 5.5, CH_2); ^{13}C NMR (125MHz, DMSO-d_6) δ 170.0 (*C*=O), 168.3 (*C*=O), 157.3 (Ar *C*), 157.2 (Ar *C*), 156.3 (Ar *C*), 141.0 (Ar *C*), 138.2 (Ar *C*), 134.7 (Ar *C*H), 130.2 (Ar *C*), 129.7 (Ar *C*), 127.7 (Ar *C*H), 127.0 (Ar *C*H), 126.5 (Ar *C*H), 124.9 (Ar *C*H), 122.5 (Ar *C*H), 119.4 (Ar *C*H), 108.5 (Ar *C*H), 41.7 (CH_2); HRMS (ESI$^-$) calcd. for $C_{18}H_{13}N_2O_5$ $[M-H]^-$ 337.0830; Found 337.0832.

3.14 References

1. Otto, S., Furlan, R.L.E., and Sanders, J.K.M., Dynamic combinatorial libraries of macrocyclic disulfides in water. *J Am Chem Soc*, **2000**, 122, 12063-4.

2. Ramstrom, O. and Lehn, J.M., In situ generation and screening of a dynamic combinatorial carbohydrate library against concanavalin A. *Chembiochem*, **2000**, 1, 41-8.

3. Poulsen, S.A., Direct screening of a dynamic combinatorial library using mass spectrometry. *J Am Soc Mass Spectr*, **2006**, 17, 1074-80.

4. Poulsen, S.A., Gates, P.J., Cousins, G.R.L., and Sanders, J.K.M., Electrospray ionisation Fourier-transform ion cyclotron resonance mass spectrometry of dynamic combinatorial libraries. *Rapid Commun Mass Sp*, **2000**, 14, 44-8.

5. Nour, H.F., Islam, T., Fernandez-Lahore, M., and Kuhnert, N., Probing the dynamic reversibility and generation of dynamic combinatorial libraries in the presence of bacterial model oligopeptides as templating guests of tetra-carbohydrazide macrocycles using electrospray mass spectrometry. *Rapid Commun Mass Sp*, **2012**, 26, 2865-76.

6. Sindelar, M. and Wanner, K.T., Library Screening by Means of Mass Spectrometry (MS) Binding Assays-Exemplarily Demonstrated for a Pseudostatic Library Addressing gamma-Aminobutyric Acid (GABA) Transporter 1 (GAT1). *Chemmedchem*, **2012**, 7, 1678-90.

7. Corbett, P.T., Leclaire, J., Vial, L., West, K.R., Wietor, J.L., Sanders, J.K.M., and Otto, S., Dynamic combinatorial chemistry. *Chem Rev*, **2006**, 106, 3652-711.

8. Springsteen, G. and Wang, B.H., A detailed examination of boronic acid-diol complexation. *Tetrahedron*, **2002**, 58, 5291-300.

9. Ferrier, R.J., Carbohydrate Boronates. *Advances in carbohydrate chemistry and biochemistry*, **1978**, 35, 31-80.

10. Lorand, J.P. and Edwards, J.O., Polyol Complexes and Structure of the Benzeneboronate Ion. *Journal of Organic Chemistry*, **1959**, 24, 769-74.

11. Babcock, L. and Pizer, R., Dynamics of Boron Acid Complexation Reactions - Formation of 1-1 Boron Acid Ligand Complexes. *Inorganic Chemistry*, **1980**, 19, 56-61.

12. Friedman, S., Pace, B., and Pizer, R., Complexation of Phenylboronic Acid with Lactic-Acid - Stability Constant and Reaction-Kinetics. *Journal of the American Chemical Society*, **1974**, 96, 5381-4.

13. Friedman, S. and Pizer, R., Mechanism of Complexation of Phenylboronic Acid with Oxalic-Acid - Reaction Which Requires Ligand Donor Atom Protonation. *Journal of the American Chemical Society*, **1975**, 97, 6059-62.

14. Kustin, K. and Pizer, R., Temperature-Jump Study of Rate and Mechanism of Boric Acid-Tartaric Acid Complexation. *Journal of the American Chemical Society*, **1969**, 91, 317-&.

15. Kuivila, H.G., Keough, A.H., and Soboczenski, E.J., Areneboronates from Diols and Polyols. *Journal of Organic Chemistry*, **1954**, 19, 780-3.

16. Zhao, J.Z., Fyles, T.M., and James, T.D., Chiral binol-bisboronic acid as fluorescence sensor for sugar acids. *Angewandte Chemie-International Edition*, **2004**, 43, 3461-4.

17. Bicker, K.L., Sun, J., Lavigne, J.J., and Thompson, P.R., Boronic Acid Functionalized Peptidyl Synthetic Lectins: Combinatorial Library Design, Peptide Sequencing, and Selective Glycoprotein Recognition. *Acs Comb Sci*, **2011**, 13, 232-43.

18. Martin, A.R., Barvik, I., Luvino, D., Smietana, M., and Vasseur, J.J., Dynamic and Programmable DNA-Templated Boronic Ester Formation. *Angew Chem Int Edit*, **2011**, 50, 4193-6.

19. Christinat, N., Scopelliti, R., and Severin, K., Multicomponent assembly of boronic acid based macrocycles and cages. *Angew Chem Int Edit*, **2008**, 47, 1848-52.

20. Leung, I.K.H., Brown, T., Schofield, C.J., and Claridge, T.D.W., An approach to enzyme inhibition employing reversible boronate ester formation. *Medchemcomm*, **2011**, 2, 390-5.

21. Yan, L., Colandrea, V.J., and Hale, J.J., Prolyl hydroxylase domain-containing protein inhibitors as stabilizers of hypoxia-inducible factor: small molecule-based therapeutics for anemia. *Expert Opinion on Therapeutic Patents*, **2010**, 20, 1219-45.

22. Muchnik, E. and Kaplan, J., HIF prolyl hydroxylase inhibitors for anemia. *Expert Opin Inv Drug*, **2011**, 20, 645-56.

23. Fraisl, P., Aragones, J., and Carmeliet, P., Inhibition of oxygen sensors as a therapeutic strategy for ischaemic and inflammatory disease. *Nat Rev Drug Discov*, **2009**, 8, 139-52.

24. Eckle, T., Kohler, D., Lehmann, R., El Kasmi, K.C., and Eltzschig, H.K., Hypoxia-inducible factor-1 is central to cardioprotection - A new paradigm for ischemic preconditioning. *Circulation*, **2008**, 118, 166-75.

25. Myllyharju, J., HIF Prolyl 4-Hydroxylases and their Potential as Drug Targets. *Curr Pharm Design*, **2009**, 15, 3878-85.

26. Bergeron, M., Gidday, J.M., Yu, A.Y., Semenza, G.L., Ferriero, D.M., and Sharp, F.R., Role of hypoxia-inducible factor-1 in hypoxia-induced ischemic tolerance in neonatal rat brain. *Ann Neurol*, **2000**, 48, 285-96.

27. Prass, K., Ruscher, K., Karsch, M., Isaev, N., Megow, D., Priller, J., Scharff, A., Dirnagl, U., and Meisel, A., Desferrioxamine induces delayed tolerance against cerebral ischemia in vivo and in vitro. *J Cerebr Blood F Met*, **2002**, 22, 520-5.

28. Bishop, T., Talbot, N.P., Turner, P.J., Nicholls, L.G., Pascual, A., Hodson, E.J., Douglas, G., Fielding, J.W., Smith, T.G., Demetriades, M., Schofield, C.J., Robbins, P.A., Pugh, C.W., Buckler, K.J., and Ratcliffe, P.J., Carotid body hyperplasia and enhanced ventilatory responses to hypoxia in mice with heterozygous deficiency of PHD2. *J Physiol-London*, **2013**, 591, 3565-77.

29. Mecinovic, J., Loenarz, C., Chowdhury, R., and Schofield, C.J., 2-Oxoglutarate analogue inhibitors of prolyl hydroxylase domain 2. *Bioorg Med Chem Lett*, **2009**, 19, 6192-5.

30. Mecinovic, J., Chowdhury, R., Flashman, E., and Schofield, C.J., Use of mass spectrometry to probe the nucleophilicity of cysteinyl residues of prolyl hydroxylase domain 2. *Anal Biochem*, **2009**, 393, 215-21.

31. Mecinovic, J., Lienard, B.M.R., Chowdhury, R., and Schofield, C.J., Mass spectrometric studies on an oxygen sensing prolyl hydroxylase. *Proceedings of the 5th Joint Meeting on Medicinal Chemistry*, **2007**, 25-30.

32. Rose, N.R., McDonough, M.A., King, O.N.F., Kawamura, A., and Schofield, C.J., Inhibition of 2-oxoglutarate dependent oxygenases. *Chem Soc Rev*, **2011**, 40, 4364-97.

33. Warshakoon, N.C., Wu, S.D., Boyer, A., Kawamoto, R., Sheville, J., Bhatt, R.T., Renock, S., Xu, K., Pokross, M., Zhou, S.T., Walter, R., Mekel, M., Evdokimov, A.G., and East, S., Design and synthesis of substituted pyridine derivatives as HIF-1 alpha prolyl hydroxylase inhibitors. *Bioorg Med Chem Lett*, **2006**, 16, 5616-20.

34. Chowdhury, R., McDonough, M.A., Mecinovic, J., Loenarz, C., Flashman, E., Hewitson, K.S., Domene, C., and Schofield, C.J., Structural Basis for Binding of Hypoxia-Inducible Factor to the Oxygen-Sensing Prolyl Hydroxylases. *Structure*, **2009**, 17, 981-9.

35. Booker, S., Kim, T.-S., Liao, H., Liu, L.J., Norman, M.H., Peterson, E.A., Stec, M., and Tamayao, N.A., Imidazopyridazine inhibitors of PI3 kinase for cancer treatment, **2007**, WO2007135398.

36. Matteson, D.S., Jesthi, P.K., and Sadhu, K.M., Synthesis and Properties of Pinanediol Alpha-Amido Boronic Esters. *Organometallics*, **1984**, 3, 1284-8.

37. Inglis, S.R., Woon, E.C.Y., Thompson, A.L., and Schofield, C.J., Observations on the Deprotection of Pinanediol and Pinacol Boronate Esters via Fluorinated Intermediates. *J Org Chem*, **2010**, 75, 468-71.

38. Yuen, A.K.L. and Hutton, C.A., Deprotection of pinacolyl boronate esters via hydrolysis of intermediate potassium trifluoroborates. *Tetrahedron Lett*, **2005**, 46, 7899-903.

39. Fuller, A.A., Hester, H.R., Salo, E.V., and Stevens, E.P., In situ formation and reaction of 2-pyridylboronic esters. *Tetrahedron Lett*, **2003**, 44, 2935-8.

40. Tyrrell, E. and Brookes, P., The synthesis and applications of heterocyclic boronic acids. *Synthesis-Stuttgart*, **2003**, 469-83.

41. Brown, T., *Studies on the inhibition of enzymes by boronic acids and lactams*, in *Organic Chemistry*2009, University of Oxford.

42. Bosch, L.I., Fyles, T.M., and James, T.D., Binary and ternary phenylboronic acid complexes with saccharides and Lewis bases. *Tetrahedron*, **2004**, 60, 11175-90.

43. Daniel, J.M., Friess, S.D., Rajagopalan, S., Wendt, S., and Zenobi, R., Quantitative determination of noncovalent binding interactions using soft ionization mass spectrometry. *Int J Mass Spectrom*, **2002**, 216, 1-27.

44. Leung, I.K.H., Flashman, E., Yeoh, K.K., Schofield, C.J., and Claridge, T.D.W., Using NMR Solvent Water Relaxation to Investigate Metalloenzyme-Ligand Binding Interactions. *Journal of Medicinal Chemistry*, **2010**, 53, 867-75.

45. Aicher, T.D., Boyd, S.A., Chicarelli, M.J., Condrowski, K.R., Fell, J.B., Fischer, J.P., Gunawardana, I.W., Hinklin, R.J., Singh, A., Turner, T.M., and Wallace, E.M., Pyridin-2 -yl-amino-i, 2, 4 -thiadiazole derivatives as glucokinase activators for the treatment of diabetes mellitus, **2009**, WO2009042435 A8.

46. Kawamoto, R.M., Prolyl hydroxylase inhibitors and methods of use, **2007**, US20070299086 A1.

47. Arend, M.P., Guenzler-Pukall, V., Ho, W.B., Turtle, E.D., and Du, X., Nitrogen-containing heteroaryl compounds and their use in increasing endogenous erythropoietin, **2004**.

48. Fielding, L., NMR methods for the determination of protein-ligand dissociation constants. *Current Topics in Medicinal Chemistry*, **2003**, 3, 39-53.

49. McDonough, M.A., Li, V., Flashman, E., Chowdhury, R., Mohr, C., Lienard, B.M.R., Zondlo, J., Oldham, N.J., Clifton, I.J., Lewis, J., McNeill, L.A., Kurzeja, R.J.M., Hewitson, K.S., Yang, E., Jordan, S., Syed, R.S., and Schofield, C.J., Cellular oxygen sensing: Crystal structure of hypoxia-inducible factor prolyl hydroxylase (PHD2). *Proceedings of the National Academy of Sciences of the United States of America*, **2006**, 103, 9814-9.

50. McNeill, L.A., Flashman, E., Buck, M.R.G., Hewitson, K.S., Clifton, I.J., Jeschke, G., Claridge, T.D.W., Ehrismann, D., Oldham, N.J., and Schofield, C.J., Hypoxia-inducible factor prolyl hydroxylase 2 has a high affinity for ferrous iron and 2-oxoglutarate. *Mol Biosyst*, **2005**, 1, 321-4.

51. Chowdhury, R., Candela-Lena, J.I., Chan, M.C., Greenald, D.J., Yeoh, K.K., Tian, Y.M., McDonough, M.A., Tumber, A., Rose, N.R., Conejo-Garcia, A., Demetriades, M., Mathavan, S., Kawamura, A., Lee, M.K., van Eeden, F., Pugh, C.W., Ratcliffe, P.J., and

Schofieldt, C.J., Selective Small Molecule Probes for the Hypoxia Inducible Factor (HIF) Prolyl Hydroxylases. *Acs Chem Biol*, **2013**, 8, 1488-96.

52. Rose, N.R., Woon, E.C.Y., Tumber, A., Walport, L.J., Chowdhury, R., Li, X.S., King, O.N.F., Lejeune, C., Ng, S.S., Krojer, T., Chan, M.C., Rydzik, A.M., Hopkinson, R.J., Che, K.H., Daniel, M., Strain-Damerell, C., Gileadi, C., Kochan, G., Leung, I.K.H., Dunford, J., Yeoh, K.K., Ratcliffe, P.J., Burgess-Brown, N., von Delft, F., Muller, S., Marsden, B., Brennan, P.E., McDonough, M.A., Oppermann, U., Klose, R.J., Schofield, C.J., and Kawamura, A., Plant Growth Regulator Daminozide Is a Selective Inhibitor of Human KDM2/7 Histone Demethylases. *Journal of Medicinal Chemistry*, **2012**, 55, 6639-43.

53. Otwinowski, Z. and Minor, W., Processing of X-ray diffraction data collected in oscillation mode. *Macromolecular Crystallography, Pt A*, **1997**, 276, 307-26.

54. Mccoy, A.J., Grosse-Kunstleve, R.W., Adams, P.D., Winn, M.D., Storoni, L.C., and Read, R.J., Phaser crystallographic software. *J Appl Crystallogr*, **2007**, 40, 658-74.

55. Emsley, P. and Cowtan, K., Coot: model-building tools for molecular graphics. *Acta Crystallographica Section D-Biological Crystallography*, **2004**, 60, 2126-32.

56. Brunger, A.T., Adams, P.D., Clore, G.M., DeLano, W.L., Gros, P., Grosse-Kunstleve, R.W., Jiang, J.S., Kuszewski, J., Nilges, M., Pannu, N.S., Read, R.J., Rice, L.M., Simonson, T., and Warren, G.L., Crystallography & NMR system: A new software suite for macromolecular structure determination. *Acta Crystallographica Section D-Biological Crystallography*, **1998**, 54, 905-21.

Chapter 4. Inhibition studies on FTO

4.1 Introduction

The fat mass and obesity associated protein (FTO) is a 2OG and iron dependent oxygenase, which belongs to the subfamily of nucleic acid oxygenses (NAOXs) and which is a homolog of *E.coli* AlkB and the human subfamily AlkBHs1-8.[1-4] Mutations to the fat mass and obesity associated (fto) gene have been linked to increased risk of obesity.[5, 6] It is currently believed that the FTO protein is involved in energy metabolism and homeostasis in mice.[7, 8] FTO was first found to demethylate 3-methylthymidine in ss-DNA and 3-methyluridine in ss-RNA, though the most abundant FTO substrate in RNA probably is 6-methyladenosine (Figure 4. 1).[9, 10] FTO can also demethylate 3-methylthymidine and 6-methyladenosine in isolated forms, although activity on these bases in ds-DNA or ds-RNA is negligible.[2, 3, 10] Mice possessing an inactive FTO variant (single mutation from the wild-type protein) display a lean phenotype, suggesting that selective inhibition of FTO by small molecules might be used to target obesity and related diseases (e.g. heart disease, diabetes).[7]

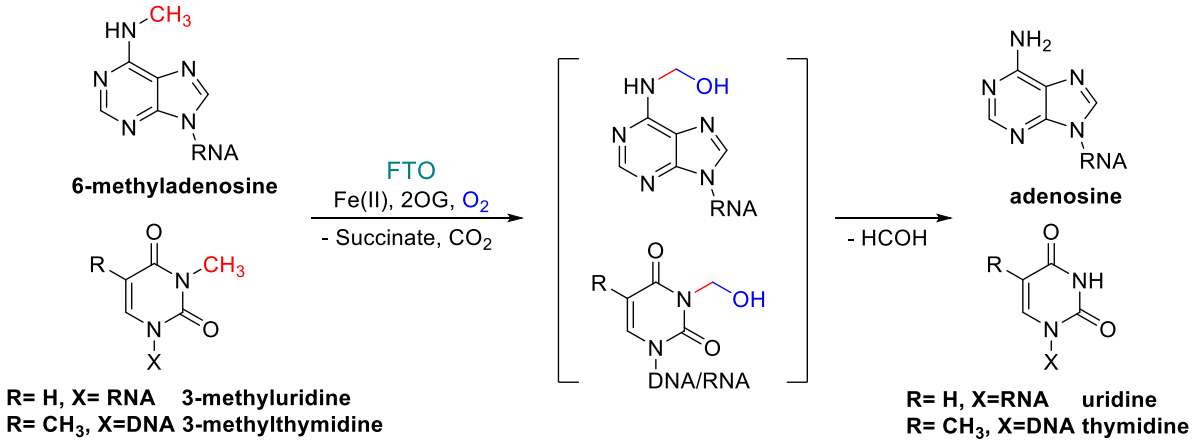

Figure 4. 1 *FTO mediated demethylation of nucleosides.*

Until recently, few inhibitors for FTO have been reported.[2] In 2012, an *in silico* study identified a family of natural product anthraquinones as the first inhibitors of FTO.[11]

However, there is limited structure-activity relation (SAR) data available for this class of FTO inhibitors, or indeed, for any other potential classes. A major hindrance to FTO inhibitor discovery/development has been the lack of suitably robust and high-throughput activity assays; common assays for demethylases used in our laboratory [matrix assisted laser desorption ionisation mass spectrometry (MALDI) assay, formaldehyde dehydrogenase (FDH) assay and NMR assay] are unsuitable due to either the poor activity of FTO, poor detection resolution, or the requirement for expensive oligonucleotide substrates. Therefore, in this study the development of a new activity assay for FTO was required before the inhibition studies could be carried out. It was then envisaged that this assay would be used together with the DSF binding assay for identification of FTO inhibitors. SAR of the identified inhibitors and crystallographic information for FTO in complex with these compounds will be imperative for the rational design of potent and selective FTO inhibitors.

4.2 Development of screening methods

A library of compounds prepared for inhibition of other 2OG oxygenases (*ca.* 150 compounds) was initially tested against FTO in order to identify scaffolds for future development of FTO inhibitors (Figure 4. 2). The compounds were screened either by a differential scanning fluorimetry (DSF) or a liquid chromatography (LC) inhibition assay to identify those with potential to inhibit FTO.

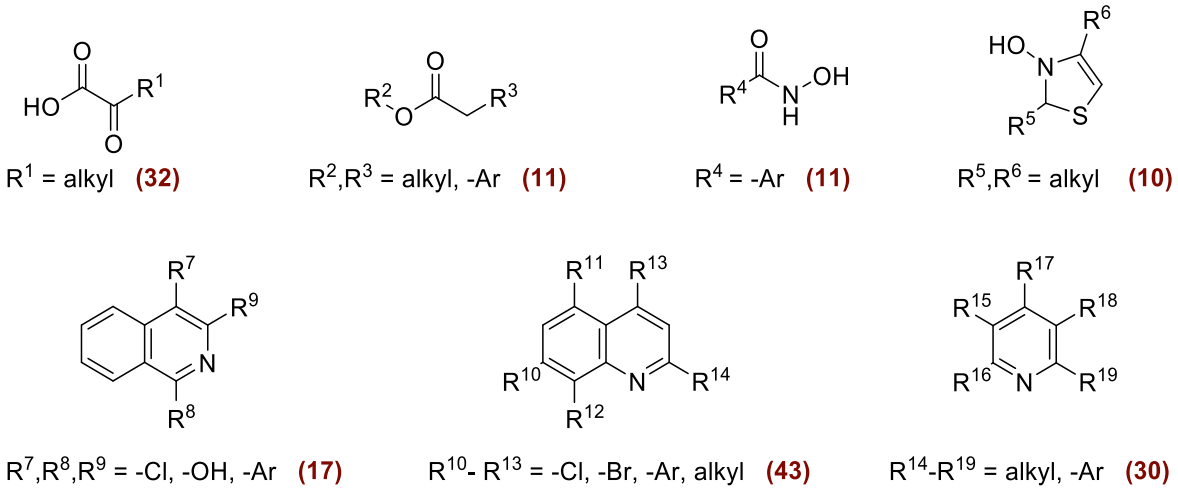

Figure 4. 2 *Library of compounds tested, number of compounds in each family in parentheses.*

4.2.1 Differential scanning fluorimetry (DSF) screening

The DSF assay is based on the fluorescence of a dye with affinity to hydrophobic parts of proteins. With increasing temperature, protein unfolds, allowing for more hydrophobic parts to interact with the dye.[12] The presence of a bound small ligand usually stabilises the protein, therefore increasing the melting temperature (T_m) of the enzyme. The stronger a compound binds to that enzyme the higher the T_m.[13] Hence, the DSF assay can be a useful and efficient method for identifying strong binders that will possibly be good inhibitors of FTO. While the DSF technique is simple and quick, the stabilising ability of a compound does not necessarily translate to inhibition activity. Another drawback of this method is the interference of fluorescent compounds observed during fluorescence read out.[12] Selected isoquinolines, hydroxythiazoles, hydroxamides and 2-oxoglutarate analogue compounds, which display no intrinsic fluorescence, were screened using the DSF-assay prior to the development of an FTO inhibition assay based on catalysis.

4.2.2 Liquid chromatography (LC) inhibition assay

For the quantification and correlation of compound inhibitory potencies, a FTO inhibition assay for the IC_{50} measurement of compounds was developed. The same assay was also used

to determine the activity of the pyridyl and quinolinyl compounds, which were not initially screened using the DSF assay due to their intrinsic fluorescence (see above).

Liquid chromatography (LC) analysis was first optimised to ensure that separation and quantification of the substrate and the product of FTO catalysis would be possible. Separation of oligonucleotide substrates and products was unsuccessful, and therefore attention was focused on nucleoside substrates. After screening a number of different columns, an Ethylene Bridged Hybrid C18 column (Waters ACQUITY UPLC **BEH**) gave the desired resolution of the substrate and product peaks (as determined by UV detection, Figure 4. 3). 3-Methylthymidine (3MeT) was the substrate chosen for the assay since it was better separated from thymidine (T) (Δt= 0.57 mim) compared to 6-*N*-methyladenosine (6MeA) and adenosine (A) (Δt= 0.32 mim). Using samples of known concentrations of 3MeT and T, it was demonstrated that the quantities of the two species in the mixture could be determined by integrating the peak intensities. The reaction conditions used for AlkBH inhibition assays were initially employed, however the conditions were later optimised for FTO (see below).

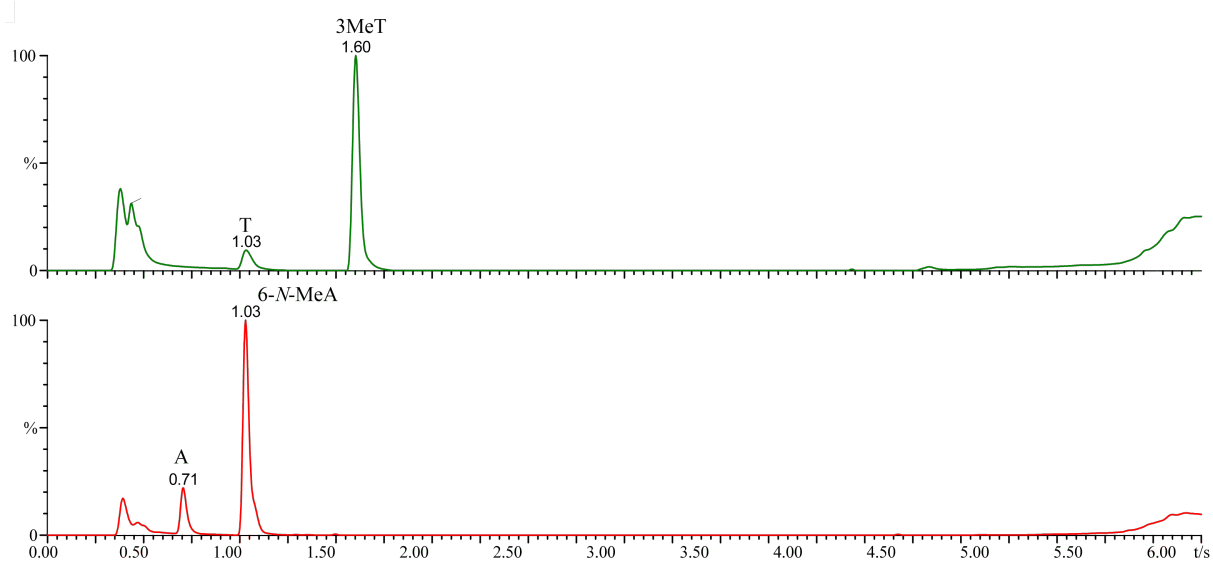

Figure 4. 3 *LC chromatogram of 3-methylthymidine (MeT), thymidine (T), 6-N-methyladenosine (6-N-MeA) and adenosine (A) showing the resolution of the methylated and nonmethylated substrate peaks with a BEH column. UV (λ=266nm).*

To allow for a minimal amount of FTO to be used without losing sensitivity, the concentration of FTO was varied and tested over time at room temperature. In the presence of 1 and 2 µM FTO, insufficient thymidine was formed to enable UV detection. 3 µM and 5µM FTO showed similar thymidine formation rates during initial stages of the assay; consequently, 3 µM of FTO was used in the assay thereafter (Figure 4. 4 a). At this enzyme concentration, the reaction time was set to 1 h to ensure the reaction would be quenched during the linear range (Figure 4. 4 b).

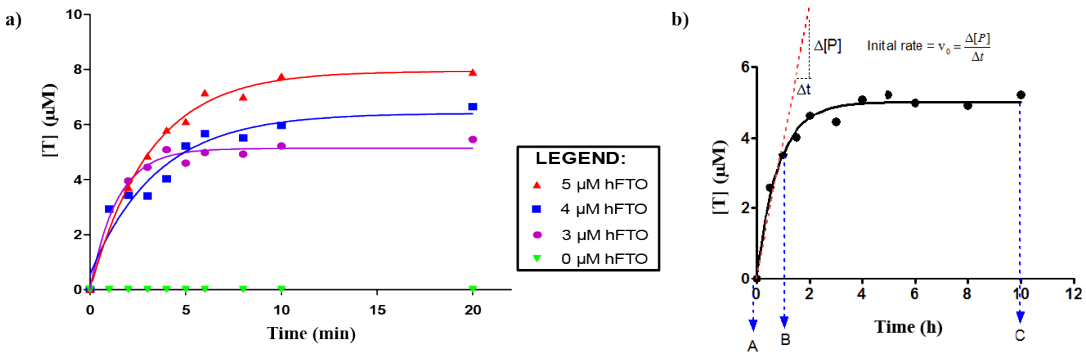

Figure 4. 4 *Thymidine concentration with time at a) varying FTO concentrations and b) 3µM of FTO.*

To estimate the appropriate concentrations of the other reagents, K_M values for the substrate (3MeT) and 2OG for FTO were obtained and the required concentrations of L-ascorbic acid and iron were optimised using 3 µM FTO and a 1 h incubation at 20 ºC (Figure 4. 5).

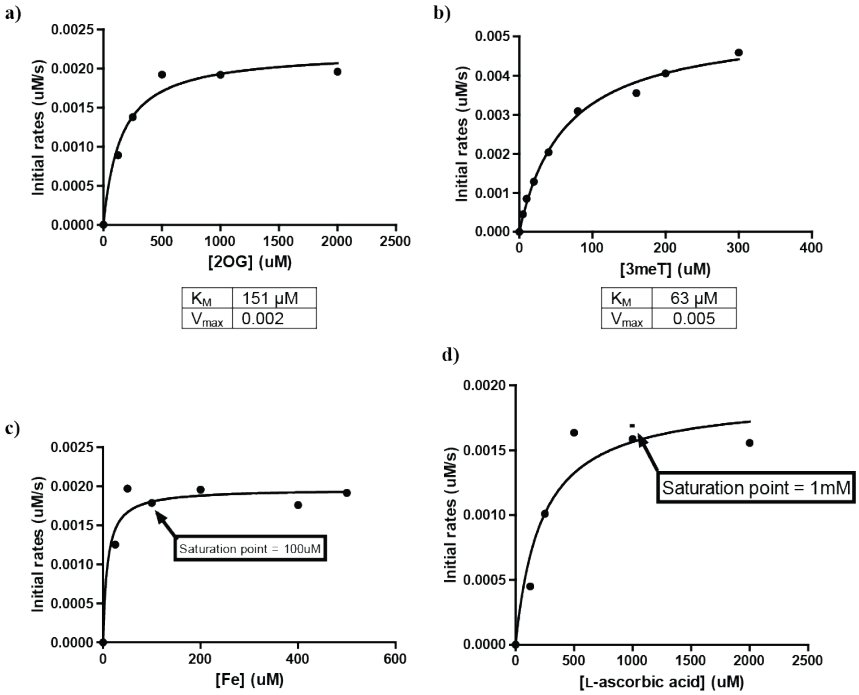

Figure 4. 5 *Rates of 3MeT demethylation at varying concentrations of a) 2OG, b) 3MeT, c) Fe(II), d) L-ascorbic acid with 3 µM of FTO at 20 ºC after 1 h.*

The K_M values for 2OG and 3MeT were calculated as 151 µM and 63 µM respectively (Figure 4. 5). Consequently, the concentrations of 3mT and 2OG in the assays mixture were set to 160 µM and 70 µM respectively, close to the K_M values (Table 4. 1). Accordingly, lower concentrations of iron and L-ascorbic acid (100 µM and 500 µM respectively) were selected for the assay to ensure optimised reaction rates (Figure 4. 5, Table 4. 1).

Table 4. 1 *Optimised conditions of in vitro inhibition assay based on the K_M of reagents.*

Component	K_M (μM)	Optimised conditions
Enzyme		3 μM
3meT nucleoside	63	70 μM
2OG	151	160 μM
L-ascorbate		500 μM
Fe(II)		100 μM
Buffer		50mM MES (pH 6.3)
Incubation time at 20 ˚C		1 h

FTO inhibition assay was originally developed by Muhamad Hamdan, a Part II student in the Chemistry Department.

4.3 IC_{50} measurement of selected compounds

Compounds that displayed less than 25 % remaining FTO activity at 200 μM in the LC assay or higher melting temperature than T_m= 8 ºC in the DSF assay were selected for IC_{50} measurements (Figure 4. 6). The majority of selected compounds were pyridyl and isoquinolinyl inhibitors, which have been previously found to be PHD2 and AlkB inhibitors (Chapter 2 and 3).[14, 15] Compound **406** is a potent PHD2 inhibitor currently in clinical trials for the treatment of anemia; the very high T_m shift of **406** and other isoquinolines with FTO suggested that analogues of **406** may be FTO inhibitors. Compound **413**, which is a structural homologue of **406** that is a PHD2 inhibitor and clinical candidate for anaemia, was also tested using the FTO assay.

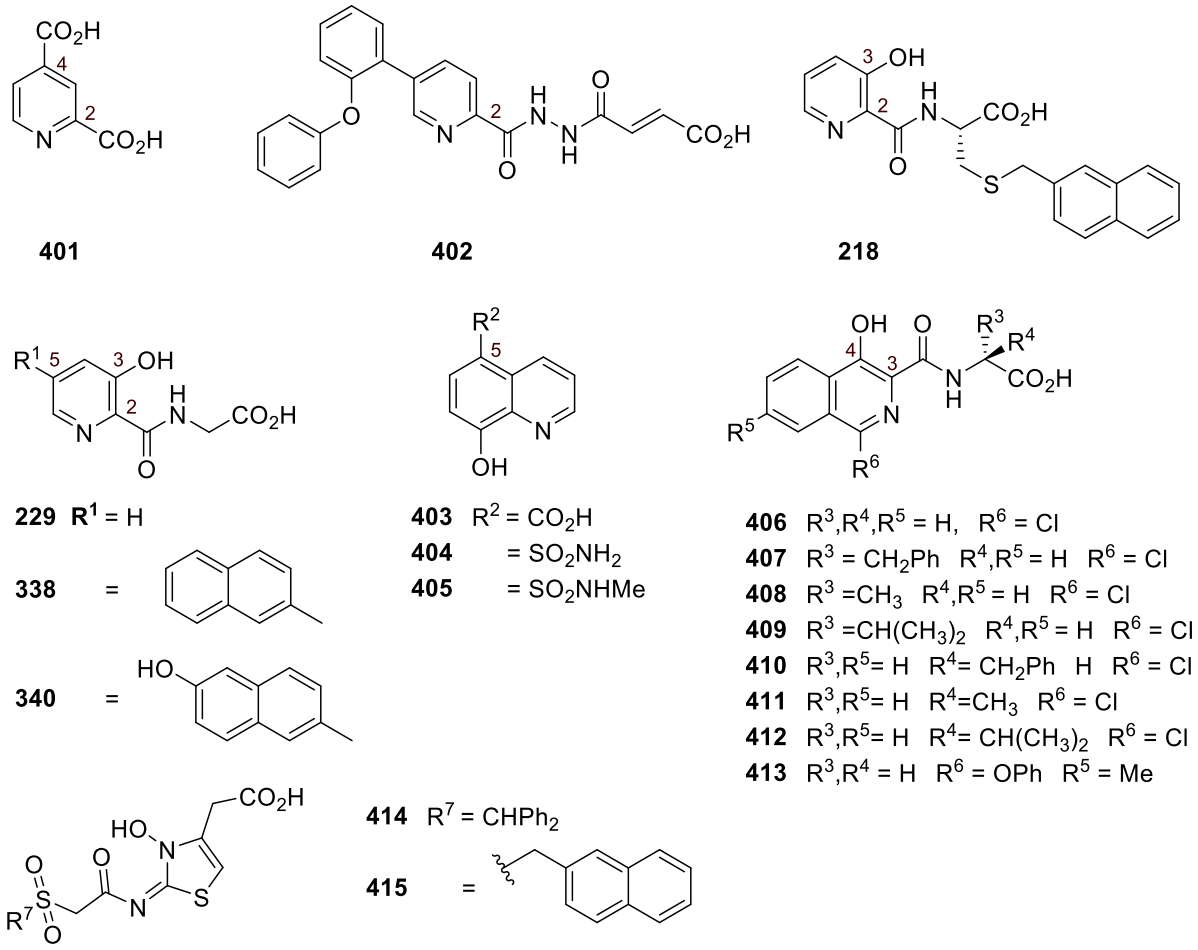

Figure 4. 6 *Lead FTO inhibitors as identified by DSF and end point inhibition screening.*

Further, two of the anthraquinone natural products recently identified as potent and cell permeable inhibitors of FTO (**416** and **417**, Figure 4. 7) were also tested.[11] All the compounds were tested in the range of 1µM-1mM in triplicate (Table 4. 2).

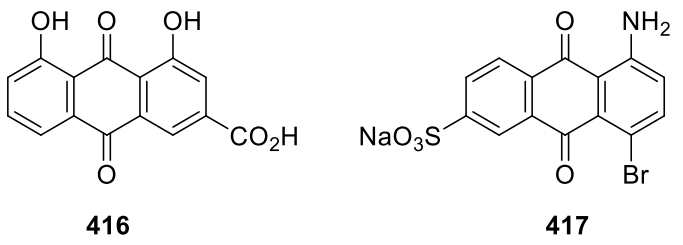

Figure 4. *7 Natural product FTO inhibitors.*

The broad-spectum 2OG oxygenase inhibitors NOG (**202b**) and 2,4-pyridinedicarboxylic acid (**401**) displayed moderate and good potencies for FTO respectively, (**202b**, IC_{50}= 44 μM; **401**, IC_{50}= 8 μM), indicating that the pyridyl scaffold might be favourable for FTO inhibition. The potent AlkB inhibitor **229** (IC_{50}= 8 μM against AlkB) also had a good inhibitory activity against FTO (IC_{50}= 15 μM); however, pyridyl inhibitors substituted at either the pyridine ring or the amino acid side chain, showed moderate to low inhibition of FTO (**218**, IC_{50}= 92 μM; **338**, IC_{50}= 43 μM; **340**, IC_{50}= 96 μM; **402**, IC_{50}= 120 μM). The isoquinolinyl inhibitors[16] behave similarly, displaying relatively high (**409**, IC_{50}= 120 μM; **411**, IC_{50}= 110 μM; **412**, IC_{50}= 160 μM) and moderate (**407**, IC_{50}= 38 μM; **408**, IC_{50}= 60 μM; **410**, IC_{50}= 84 μM) IC_{50} values. The values indicate that the D-amino acid side chain analogues are better inhibitors than the L-amino acid derived substituted isoquinolines. Interestingly, the two clinical (PHD2-inhibiting) candidates (**406**, IC_{50}= 3 μM; **413**, IC_{50}= 10 μM) displayed very good potencies against FTO, implying common features between FTO and PHD2 inhibition.[17, 18] **403**, a potent lysine demethylase inhibitor,[19] gave the lowest IC_{50} value against FTO along with **406** (**403**, **406** IC_{50}= 3 μM), while the sulfonamide derivatives of **403**, were less potent (**404**, IC_{50}= 23 μM; **405**, IC_{50}= 18 μM). The hydroxythiazoles **414** and **415** were also good inhibitors with IC_{50} values of 132 μM and 17 μM respectively. Further, both anthraquinone compounds **416** and **417** appear to inhibit FTO well (**416**, IC_{50}= 9 μM; **417**, IC_{50}= 11 μM), in agreement with previous studies.

Table 4. 2 *DSF, end point screening data for selected compounds and in vitro inhibition of FTO.*

No.	ΔTm/ remaining activity at 200 µM (ºC/%)	IC_{50} (µM)	No.	ΔTm/ remaining activity at 200 µM (ºC/%)	IC_{50} (µM)
202a		44 ± 1	**407**	29 ºC	38 ± 1
218	9 ºC	92 ± 1	**408**	26 ˚C	60 ± 1
229	25 %	15 ± 1	**409**	23 ºC	120 ± 1
338	19 %	43 ±1	**410**	29 ºC	84 ± 1
340	16%	96 ± 1	**411**	23 ºC	110± 1
401		8 ± 1	**412**	17 ºC	160 ± 1
402	25 %	120 ± 1	**413**		10 ± 1
403		3 ± 1	**414**	10 ºC	132 ± 1
404	14 %	23 ± 1	**415**	14 ºC	7 ± 1
405	17 %	18 ± 1	**416**		9 ± 1
406	12 ºC	3 ± 1	**417**		11 ± 1

*Compound **403** was synthesised by Jacob Bush, **404**, **405**, **414** and **415** were prepared by Dr. Clarisse Lejeune and **407-412** by Dr. Kar Kheng Yeoh.*

4.4 Crystallography

Crystals of FTO in the presence of inhibitors were obtained to investigate the observed inhibition profiles and to assist in the design of future potent and selective FTO inhibitors. A structure of **401** in complex with FTO·Zn shows the C-4 carboxylate of **401** positioned to form electrostatic and hydrogen-bonding interactions with the side chains of Arg316, Ser318 and Tyr295. **401** chelates the zinc in a bidentate manner, with the C-2 carboxylate positioned *trans* to the imidazole side chain of His307 and the pyridyl nitrogen *trans* to the Asp233 side chain carboxylate (Figure 4. 8).

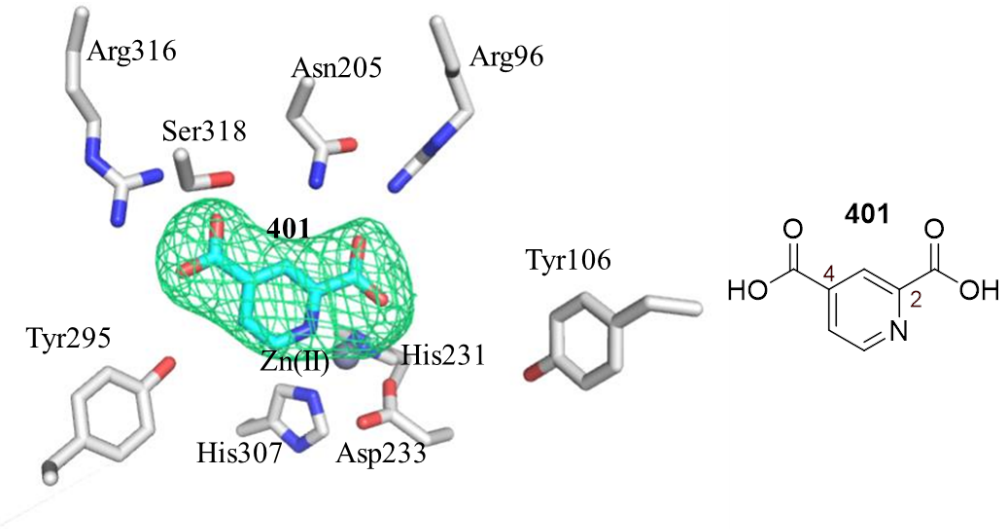

Figure 4. 8 *View from the crystal structure of FTO·Zn (silver) in complex with* ***401*** *(cyan) (contoured to 3.0σ).*

A structure of FTO·Zn in complex with **403** (PDB ID: 4IE4, 2.5Å resolution) reveals the iron chelation to be similar to **401**; the 8-hydroxyl group is positioned *trans* to His307 in place of the carboxylate group (Figure 4. 9). Also the C-5 carboxylate of **403** is placed to interact similarly to the C-4 carboxylate of **401**, rationalising the reduced potencies of **404** and **405**, which lack this interaction.

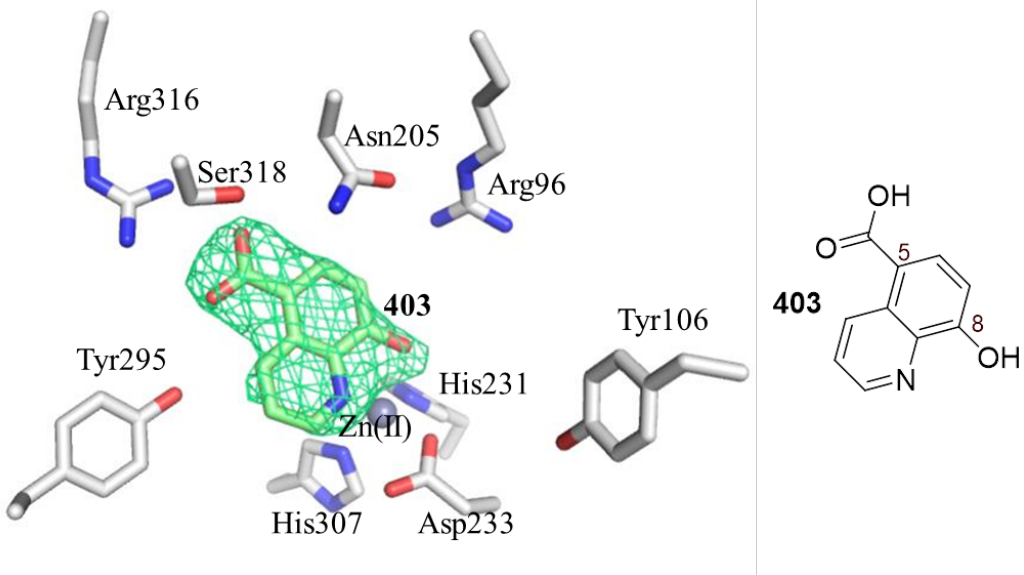

Figure 4. 9 *View from the crystal structure of FTO·Zn (silver) in complex with* ***403*** *(green) (contoured to 3.0σ).*

A structure of FTO·Zn with **229** (PDB ID: 4IE5, 2.0 Å resolution) shows the **229** glycine side chain positioned in the 2OG pocket of FTO with its carboxylate positioned to interact with the side chains of Ser318 and Tyr295 and a salt bridge interaction with Arg316. **229** chelates iron in a similar manner to **401** and forms a hydrogen bond between the 3-hydroxyl oxygen and the side chain of Asn205 (Figure 4. 10). The pyridine ring of **229** is positioned close to the substrate binding site of FTO. Superimposition of the FTO·Zn·**229** and FTO·Fe·NOG·3meT structures shows that the C-5 carbon of the pyridine ring is positioned ~1.4 Å from the position of the 3MeT carbonyl in the FTO·Fe·NOG·3meT structure, suggesting that **229** may sterically hinder binding of the FTO substrate (Figure 4. 11).[20]

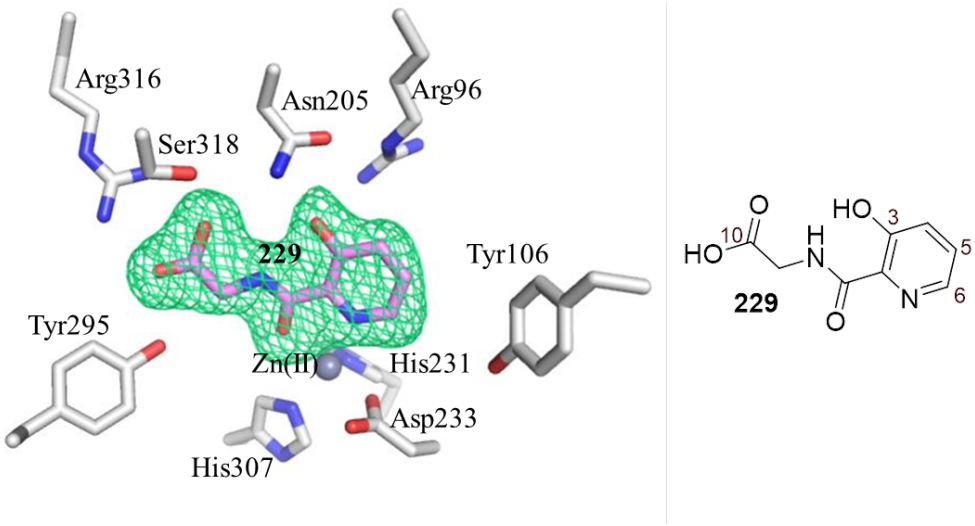

Figure 4. 10 *View from the crystal structure of FTO·Zn (silver) in complex with* ***229*** *(pimk) (contoured to 3.0σ).*

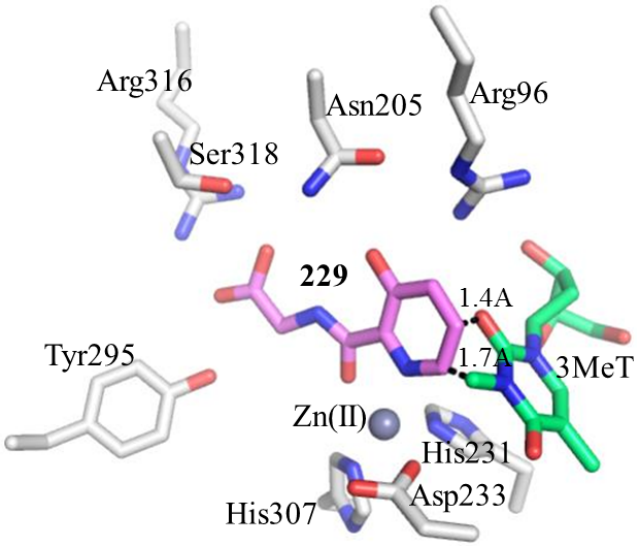

Figure 4. 11 *Superimposition of FTO·Zn·**229** (pink) (PDB ID: 4IE5) and FTO·Fe·NOG·3MeT (green) (PDB ID: 3LFM) showing the proximity of C-5 and C-6 of **229** to the substrate.*[20]

A structure of FTO complexed with the known PHD2 inhibitor **406** was acquired (PDB ID: 4IE6, 2.50 Å resolution). **406** is observed to bind to FTO in a similar manner to **229**; the chlorine of **406** sits in the substrate binding site forming additional hydrophobic and potentially halogen bonding interactions with FTO. The planarity of the isoquinoline relative to the C-4 carbamide is distorted upon metal coordination ($O_{10}C_9C_3N_2$ dihedral angle 60°, Figure 4. 12), presumably resulting in a significant energy cost upon binding. This puckering may be attributed to the proximity of the side chain of Arg96 to the isoquinoline (Figure 4. 12).

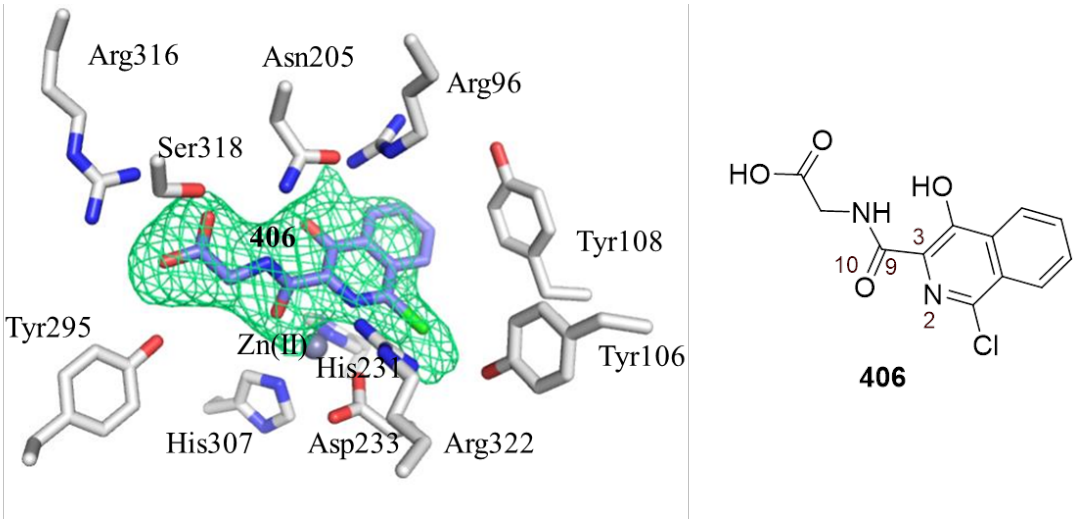

Figure 4. 12 *View from the crystal structure of FTO·Zn (silver) in complex with* ***406*** *(lilac) (contoured to 3.0σ).*

Previous biochemical and modelling studies suggested that **416** binds in the 2OG binding site of FTO, interacting with Arg316.[11] However, without crystallographic or other structural information, it is impossible to be confident of the correct binding mode of these compounds. In order to clarify the nature of **416** binding, an FTO·Zn·**416** complex structure was determined (PDB ID: 4IE7, 2.6 Å resolution). Under the crystallization conditions **416** is observed to bind in the substrate binding site not as predicted, in the 2OG binding pocket.[11] The C-2 carboxylate of **416** is positioned to form a hydrogen bond with the Ser229 side chain hydroxyl group (2.7 Å). One of the rings (ring C, Figure 4. 13) of **416** is positioned to form partial π-π interactions with His231 and **416** is positioned to form hydrogen bonds between the hydroxyl group of the A-ring and the Arg96 side chain (Figure 4. 13). A citrate molecule from the crystallisation buffer is observed in the 2OG binding site. One of the citrate carboxylates is positioned to interact with the active site metal, similar to succinate binding observed in other 2OG oxygenase structures.[21] The second citrate carboxylate is positioned in the 2OG side chain binding pocket, interacting with the side chain of Arg316, whilst the third citrate carboxylate is positioned to form hydrogen bonding interactions with the side chain of Asn205 (Figure 4. 13). Even though citrate binds on the FTO active site, it is not (at least a good) FTO inhibitor (IC_{50}= 297 μM), suggesting that the binding is a result of the high concentration of citrate in the crystallisation buffer (100mM). Other tricarboxylic acid (TCA)

cycle intermediates have shown no inhibition of FTO (IC_{50}> 1mM) with the only exceptions being fumarate (IC_{50}= 154 μM) and L-2-hydroxyglutarate (IC_{50}= 319 μM). While these values are relatively high, the possibility that FTO can be inhibited by endogenous small molecules like TCA cycle intermediates and related compounds may be of physiological or pathophysiological relevance, as proposed for other 2OG oxygenases.[22, 23]

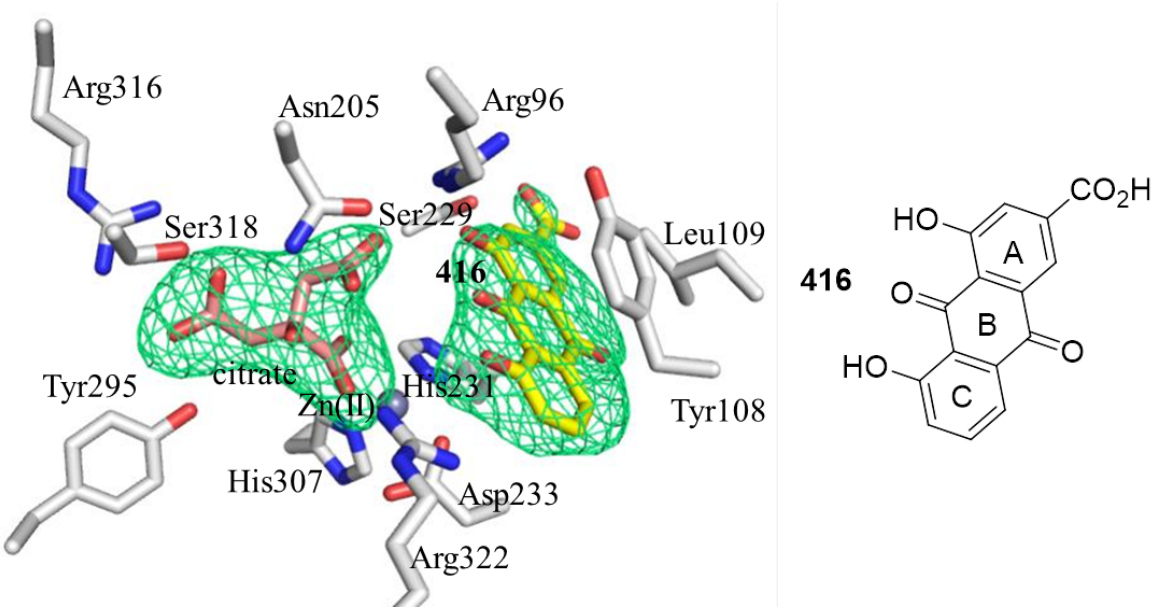

Figure 4. 13 *View from the crystal structure of FTO·Zn (silver) in complex with* ***416*** *(yellow) in the substrate binding site and citrate in the co-substrate binding site (contoured to 3.0σ).*

Crystallisations of FTO with inhibitors and crystallographic data analysis were performed by Wei Shen Aik.

4.5 Structure activity relation studies for the design of new inhibitors

The high potency of the 8-hydroxyquinoline derivative **403**, together with the fact that the glycine analogues of both pyridyl and isoquinolinyl inhibitors (**229** and **406**) displayed the best potencies in their respective structural families imply that future FTO inhibitors could contain simple side-chains at the carbonyl. However, the same compounds (**403**, **406** and

229) are also good inhibitors for other 2OG oxygenases. Therefore, to acquire sufficient selectivity, as well as inhibitory potency, substitution of the aryl ring was deemed necessary. It was envisaged that an inhibitor based on the pyridyl or isoquinolinyl inhibitors that also occupied the substrate binding site may provide good selectivity for FTO over other 2OG oxygenases. To investigate the potential of **406** and/or **229** derivatives to occupy both sites, the crystal structure of **416**, which occupies the substrate binding site, was aligned with the structures of **406** and **229**. As mentioned above (Section 4.4) **406** is not planar when bound in the active site of FTO (Figure 4. 12), something that results in part of the isoquinoline ring to be in the substrate site (Figure 4. 14). The orientation and proximity of **406** to **416** implies that addition of a substituent on **406** that will be directed towards the substrate binding site (Figure 4. 14 A) is not possible. In contrast, the pyridine ring of **229** has a more favourable positioning in the active site of FTO (Figure 4. 14 B). Manual modelling studies in the superimposed structures of **416** and **229** have shown that substitution at the C-6 of **229** may result in partial occupation of the substrate site as well as the 2OG binding pocket (Figure 4. 14 C, D). Therefore the synthesis of 6-aryl substituted analogues of **229** was sought.

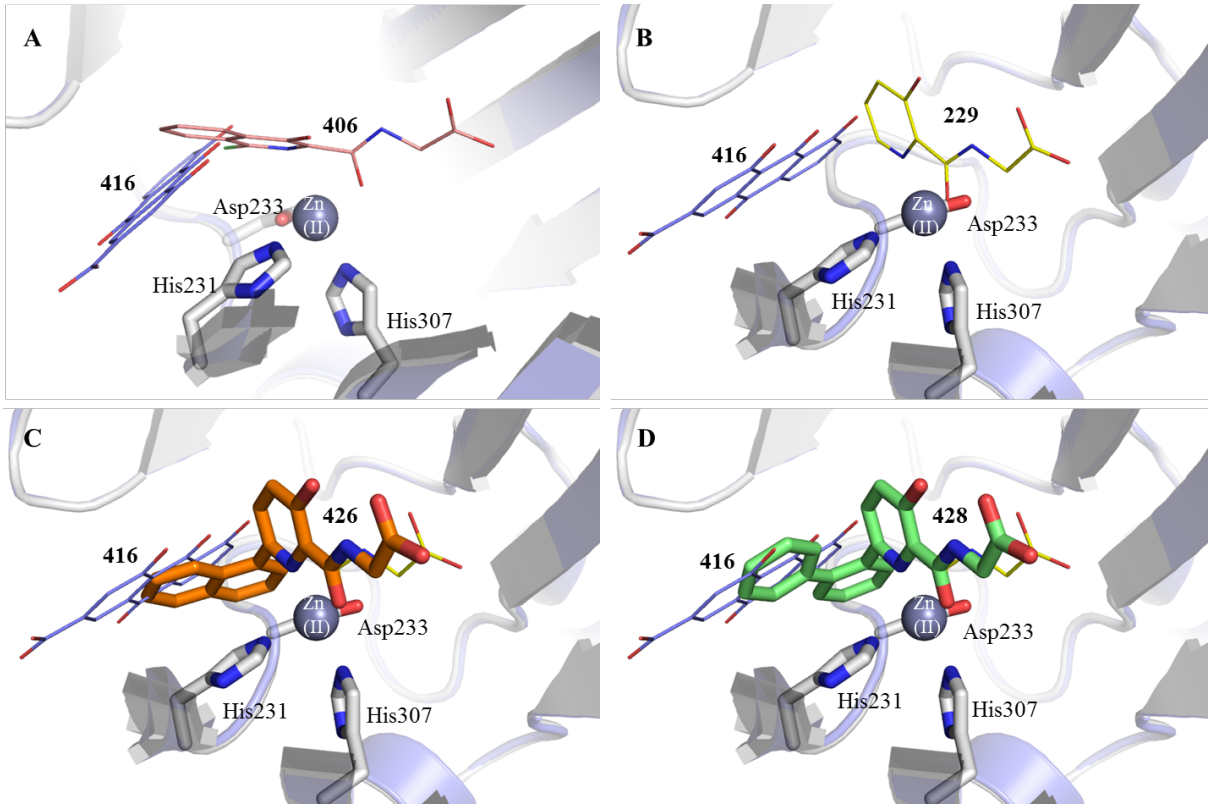

Figure 4. 14 *A) Superimposition of the images of FTO·Zn·**416** (cyan) (PDB ID: 4IE7) and FTO·Zn·**406** (pink) (PDB ID: 4IE6), B) Superimposition of the images of FTO·Zn·**416** (cyan) (PDB ID: 4IE7) and FTO·Zn·**229** (yellow) (PDB ID: 4IE5), C,D) Modelling of novel inhibitors (**426**, **428**) aiming to occupy the co-substrate and substrate binding sites based on FTO·Zn·**416** and FTO·Zn·**229** structures.*

4.6 Synthesis of new inhibitors

The synthesis of 6-substituted 3-hydroxy-pyridyl compounds (**426-429**) was attempted *via* Suzuki coupling;[24] this route required the incorporation of a bromine atom to the pyridine ring. However, following literature conditions,[25] in the bromination reaction (using *N*-bromosuccinimide, NBS) a major side product was observed, i.e. the dibromo substituted compound **419**, as well as unreacted starting material. Single bromination and starting material consumption were achieved by portion-wise addition of NBS and longer reaction times (Table 4. 3).

Table 4. 3 *Optimization for the synthesis of 6-bromo-3-hydroxypicolinonitrile from 3-hydroxypicolinonitrile.*

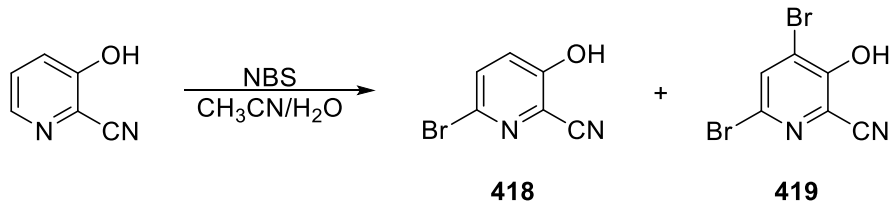

418 **419**

No.	NBS (Equiv.)	Temperature (˚C)	Time (h)	Recovered s.m (%)[a]	Yield 418 (%)[a]	Yield 419 (%)[a]
1	1.6	20	2	20	20	60
2	1.2	0	3	19	42	39
3	1.3	-10-(-2)	9	20	50	30
4	1.1	-30-(-10)	3	15	47	38
5	1.1	-7-3	7	16	46	38
6	1.1	-5-2	7	12	46	42
7	1.1	-5-(-2)	3 d	1	53	46

[a] as identified by LC-MS

For the amide coupling of **420** with glycine, the usual coupling agents HOBT/EDCI (Figure 4. 15) did not give desired product; consequently, other coupling reagents were investigated. HATU gave the desired product in very low yield but T3P (Figure 4. 15) gave sufficient yield (25 %) of **421**. The reaction with T3P was further investigated; it was found that heating in a microwave reactor (mw) and increasing the amount of base (from 3 to 4 equivalents) improved the yield of **421** (42 %, Scheme 4. 1).

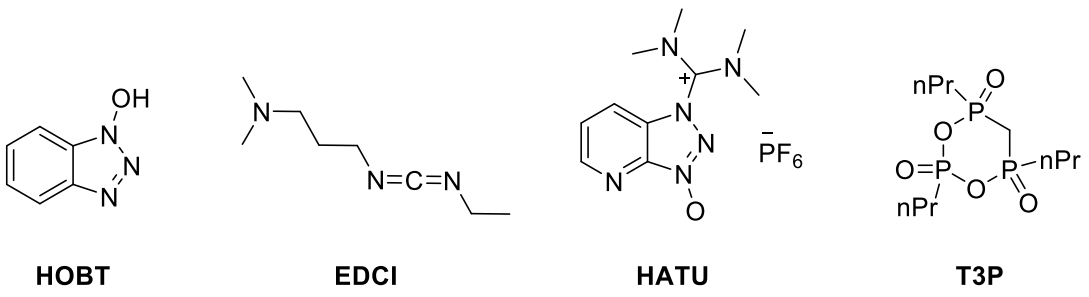

Figure 4. 15 *Coupling reagents used for the reaction of* ***420*** *with glycine tert-butyl hydrochloride.*

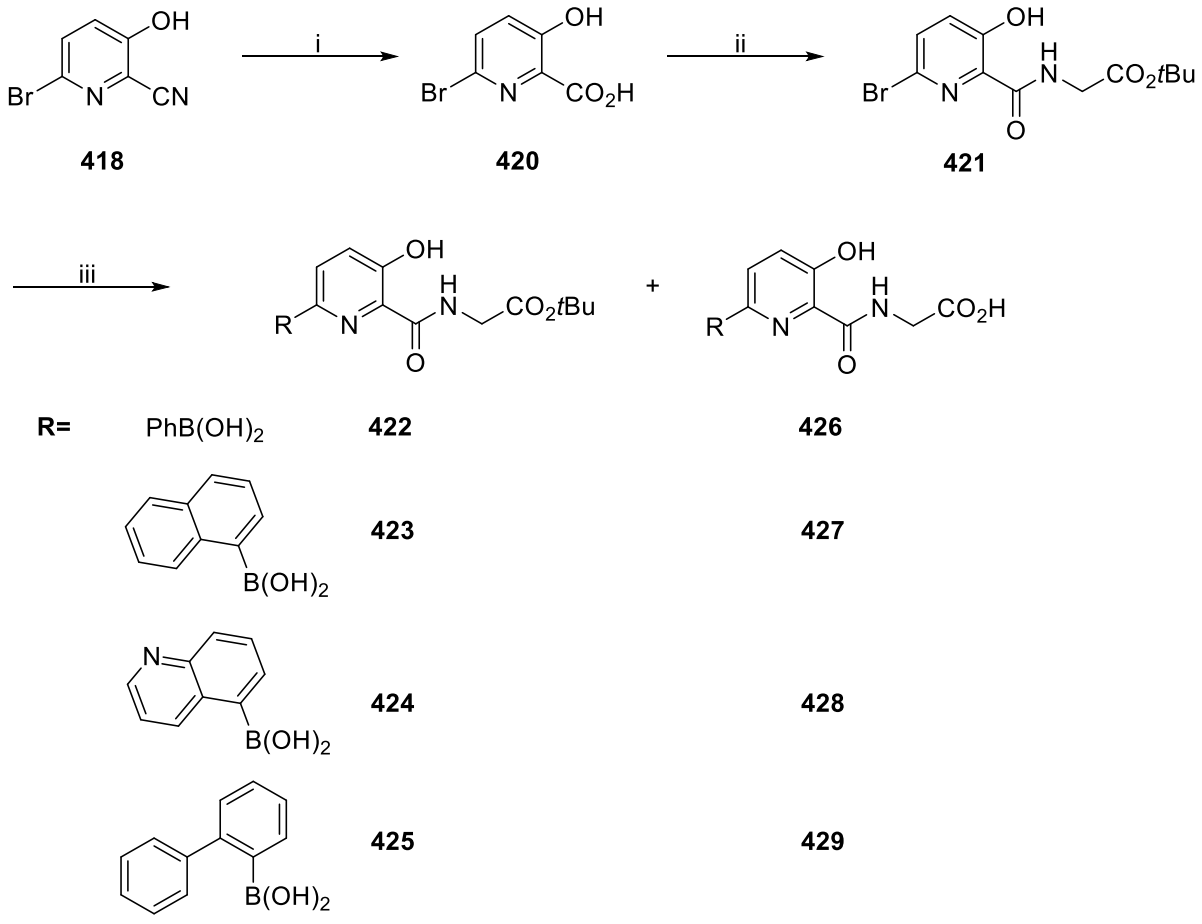

Scheme 4. 1 *Synthesis of inhibitors.*

Reagents and conditions: i) 30 % NaOH, MeOH, reflux; ii) glycine *tert*-butyl ester hydrochloride (1.5 equiv.), T3P (1.5 equiv.), DIPEA (4 equiv.), mw, 150 ºC; iii) $RB(OH)_2$ (1.3 equiv.), K_2CO_3 (4 equiv.), $Pd(PPh_3)_4$ (10 mole %), mw, 130 ºC.

Compounds ***422-429*** *were synthesised by Caitlin Clunie-O'Connor.*

4.7 *In vitro* assays for first generation of FTO inhibitors

The LC assay was used to determine the IC_{50} values of the designed inhibitors for FTO. The most potent FTO inhibitors identified from screening, **403** and **406**, are also potent and cell permeable inhibitors of KDMs and PHD2 respectively. Hence, inhibitors **426-429** were also tested for inhibition against other 2OG oxygenases to determine their relative selectivity for FTO (Table 4. 4).

Table 4. 4 *Inhibition data for inhibitors against FTO, PHD2, JMJD1A, JMJD2C and JMJD3.*

No.	FTO IC_{50} (μM)	PHD2 IC_{50} (μM)	JMJD1A IC_{50} (μM)	JMJD2C IC_{50} (μM)	JMJD3 IC_{50} (μM)
403	3 ± 1	14.3	0.2	0.6	0.1
406	3 ± 1	0.3	>20	>20	>20
426	35 ± 1	> 100	>100	>100	>100
427	4 ± 1	> 100	>100	>100	76
428	25 ± 1	> 100	>100	>100	>100
429	15 ± 1	> 100	13	27	40

The presence of a phenyl group at C-6 resulted in improved inhibitory potency relative to the C-5 substituted and other C-2 carbonyl substituted pyridines discussed above (**426**, IC_{50}= 35 μM); however, compound **229** showed greater inhibitory potency (IC_{50}= 15 μM). The addition of a biphenyl ring (**429**, IC_{50}= 15μM) resulted in very good inhibition. The 1-naphthalene substituted compound **427** (IC_{50}= 4 μM) was a very potent inhibitor ranking very close to the clinical candidate **406** (IC_{50}= 3 μM). Further, the quinoline substituted compound **428** was introduced as a more basic and water soluble analogue of **427**, in order to be used in future cell studies but this resulted in a 6 fold decrease in potency (**428**, IC_{50}= 25 μM).

As anticipated the compounds, with the exception of **429**, displayed no inhibition of the JmjC KDMs, revealing improved selectivity for FTO. Compound **427** is 5 times more selective for

FTO than **406** and 7 times more selective for FTO than **403**. Regarding PHD2, **427** is 5 times more selective for FTO than **403** and 200 times more than **406**.

4.8 Crystallography of FTO with 427

Crystallographic studies of FTO in the presence of **427** were carried out. The structure of **427** complexed with FTO·Zn shows similarity with the observed binding of **229** in the 2OG binding site of FTO (Figure 4. 16). The 1-naphthyl side chain of **427** extends, as predicted, to occupy the substrate binding site. The position of ring B of the naphthyl group enables the formation of partial π-π interactions with His231 as observed with compound **416**. Compound **427** lacks the hydrogen bonding of the ring A hydroxyl of **416** (Figure 4. 13). However, the electrostatic interactions of the 3-hydroxypyridine part of **427** with the side chains of Arg316, Ser318, Tyr295, Asn205 and Arg96, as compound **229**, apparently results in the improved inhibitory activity of **427** (Figure 4. 17).

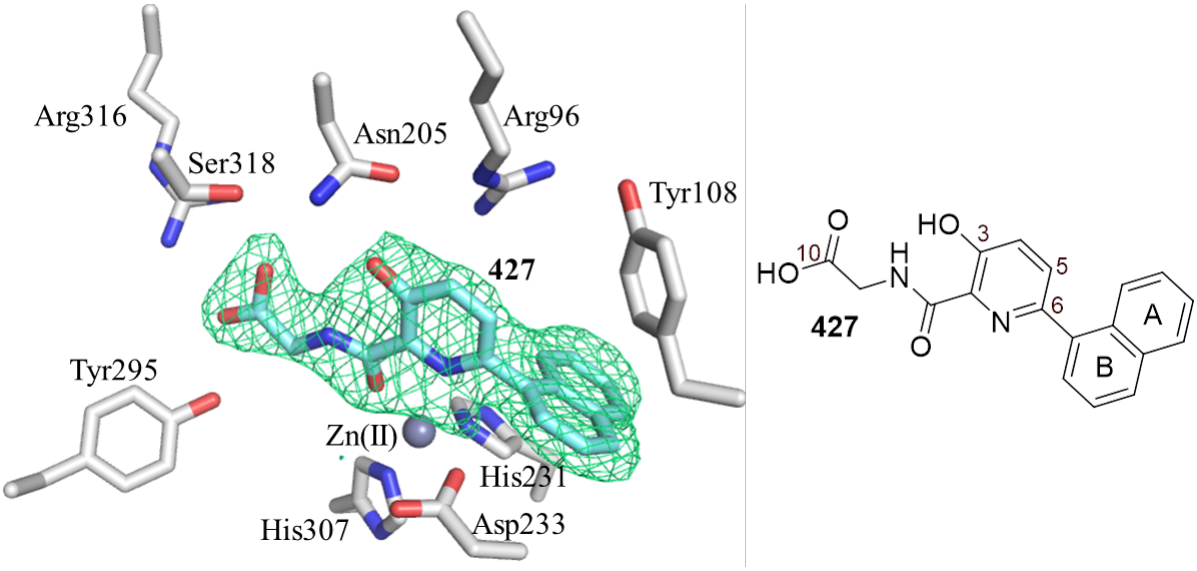

Figure 4. 16 *View from the crystal structure of FTO·Zn (silver) in complex with **427** (cyan).*

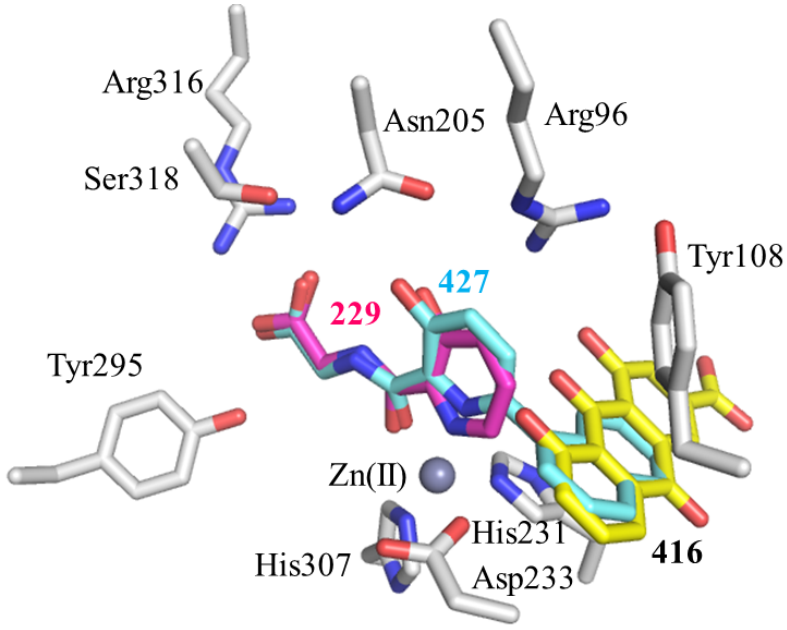

Figure 4. 17 *Superimposition of the images of FTO·Zn·**416** (yellow) (PDB ID: 4IE7), FTO·Zn·**229** (pink) (PDB ID: 4IE5) and FTO·Zn·**427** (cyan) showing **427** occupies both the substrate and co-substrate binding sites of FTO.*

4.9 Conclusions

An assay was developed and used for the assessment of FTO inhibition from a library of compounds. A combination of the inhibition and binding studies has led to the identification of novel inhibitor templates for FTO that display unprecedented properties of inhibitory potency and selectivity. Crystallographic studies also revealed the binding modes of a number of the identified inhibitors, and allowed the rational design of the first generation of FTO inhibitors with improved activities. Inhibitors of FTO with improved selectivity for FTO over other 2OG oxygenases were identified. For example, compound **427** which is a potent inhibitor of FTO displayed ~ 6 times better selectivity for FTO over other 2OG oxygenases compared to **406** and **403**. A crystal structure of **427** with FTO revealed that this compound indeed occupies both substrate and 2OG binding sites of FTO. Notably, two of the most potent FTO inhibitors that were identified are in clinical trials as HIF prolyl-hydroxylase inhibitors. Thus, clinical use of these compounds should take into account their propensity to inhibit FTO.

4.10 Acknowledgements

Many thanks to Kamilin Hamdan for the development of the LC inhibition assay and for carrying out the DSF experiments. Special thanks to Wei Shen Aik for the crystallographic studies and analyses and for providing FTO for inhibition assays and Caitlin Clunie-O'Connor for syntheses of the final inhibitors. Finally, thanks to Tzu-Lan Yeh and Anthony Tumber for the inhibition studies on PHD2 and KDMs respectively.

4.11 Experimental details

Differential scanning fluorimetry (DSF)[13]

DSF was performed using a MiniOpticon™ Real-Time PCR Detection System (Bio-Rad), monitoring protein unfolding using SYPRO orange (Invitrogen) according to reported method. [13] FAM (492 nm) and ROX (610 nm) filters were used for excitation and emission respectively. Reaction mixes contained 2 μM protein, 50 μM Mn(II), 200 μM compounds, 1x SYPRO orange in a final volume of 50 μL. Reagents were prepared in HEPES buffer except metals, which were dissolved as 100 mM stocks in 20 mM HCl, then further diluted in MilliQ water. Compounds tested were prepared in 100% DMSO and added such that the final concentration of DMSO was 5 % (v/v).

Fluorescence readings were taken every 1 °C in the range 25-95 °C, with the temperature increased linearly by 1 °C min^{-1}. The software provided was used to perform global minimum subtraction. The inflection point, representing T_m, was calculated by fitting the Boltzmann equation to the sigmoidal curves obtained; data were processed using GraphPad Prism 5.0™. The T_m shift caused by the addition of small molecules/ fragments was determined by subtraction of the "reference" Tm (protein incubated with metal and 5 % DMSO) from the T_m obtained in the presence of the compound. Conditions were tested in triplicates, with standard deviations from the mean typically < 1 °C.

In vitro demethylation assay

For catalytic assays, a 50 μL reaction mixture containing final concentrations of 3 μM FTO, 70 μM 3meT nucleoside, 160 μM 2OG, 500 μM L-ascorbate, 100 μM diammonium iron(II) sulfate complex, 200 μM test compound (2% DMSO in control reaction) and 50 mM 2-(*N*-morpholino)ethanesulfonic acid (MES), pH 6.3 was incubated at room temperature for 1 h. The reaction was quenched with methanol (50 μL) then centrifuged to remove precipitated protein. The supernatant was then dried using an Eppendorf Speedvac concentrator and reconstituted with (50 μL) water. The product (thymidine) and substrate (3meT) were separated using Waters Acquity Ultra Performance Liquid Chromatography (UPLC) BEH C18 column, 130 Å, 1.7 μm, 2.1 mm x 50 mm with a gradient of 95% A (H_2O with 1% formic acid) to 80% B (methanol with 0.1% formic acid) over 5 min. UV detection wavelength was set to 266 nm room temperature (thymidine) = 0.95 min, room temperature (3meT) = 1.48 min (Liquid chromatography method was modified from previously reported[20]).The peaks were identified using a positive ion mode in the ESI-TOF mass spectrometry (Waters LCT Premier XE machine). Peaks were integrated using MassLynx software (Agilent) and the percentage conversion of 3meT to thymidine was used to quantify the activity of FTO in the presence of inhibitors. For IC_{50} determinations, assays were carried out in triplicate with a range of compound concentration (0 μM, 10 μM, 30 μM, 100 μM, 300 μM, 1 mM, 3 mM, and 10 mM). IC_{50} values were calculated from dose-response curve plotted using GraphPad Prism® 5.

Protein crystallization and X-ray crystallography

Crystals of hFTOΔ31 in complex with **401**, **403**, **229**, **406**, **416** or **427** were grown in hanging drops at 293 K by the vapour diffusion method using 24 well pre-greased VDX plates and round plastic coverslips (HR8-082, Hampton Research). The protein solution and reservoir solution (200 μL) conditions are listed in Table S4 (see below). Hanging drops were set up by adding protein solution to reservoir solution with 2:1 ratio (total volume 3 uL). The resultant crystals were cryo-protected using the well-solution diluted with 15%-20% $^{v}/_{v}$ glycerol

(cryoprotectant solution for the FTO·**418** crystal contains an additional 1mM **418**) then flash cooled in liquid nitrogen. Data were collected at 100 K for single crystals of FTO:**403** and FTO·**406** complexes using a Rigaku FR-E+ Superbright diffractometer equipped with a copper rotating anode, osmic HF optics, and a Saturn 944+ CCD detector. Data were collected at 100 K for FTO·**401**, FTO·**229**, and FTO·**418** using a single crystal at Diamond Beamline I03 equipped with a Pilatus 6M-F detector. All data were indexed, integrated, and scaled using HKL2000.[26] The structures were solved by molecular replacement using the MR-PHASER[27] subroutine in PHENIX[28] using FTO·Ni^{+2}·**202b**·3meT (PDB ID: 3LFM) as a search model. Iterative cycles of model building and refinement were performed using COOT[29] and PHENIX until decreasing R and R_{free} no longer converged.

Table 4. 5 *Crystallisation conditions for protein and reservoir solution.*

	FTO·**401**	FTO·**403**	FTO·**229**	FTO·**406**	FTO·**416**	FTO·**427**
PDB ID	4IE0	4IE4	4IE5	4IE6	4IE7	
Protein Solution Conditions	~8 mg/mL hFTOΔ31, 1 mM $ZnSO_4$, 1 mM **401**	~8 mg/mL hFTOΔ31, 1 mM $ZnSO_4$, 2 mM **403**	~8 mg/mL hFTOΔ31, 1 mM $ZnSO_4$, 1 mM **229**	~8 mg/mL hFTOΔ31, 1 mM $ZnSO_4$, 1.5 mM **406**	~8 mg/mL hFTOΔ31, 1 mM $ZnSO_4$, 2 mM **416**	~8 mg/mL hFTOΔ31, 1 mM $ZnSO_4$, 2 mM **427**
Reservoir Solution Conditions	100 mM trisodium citrate pH 5.6, 11% PEG3350, 4% tert-butanol	100 mM trisodium citrate pH 5.6, 13% PEG3350, 4% tert-butanol	100 mM trisodium citrate pH 5.6, 9% PEG3350, 4% tert-butanol	100 mM trisodium citrate pH 5.6, 11.5% PEG3350, 4% tert-butanol	100 mM trisodium citrate pH 5.6, 11.5% PEG3350, 4% tert-butanol	100 mM trisodium citrate pH 5.6, 11.5% PEG3350, 4% tert-butanol

6meA – N^6-methyladenosine

PEG3350 – polyethylene glycol 3350

Chemical Synthesis

General information

Reagents and solvents were from Aldrich, Alfa Aesar or Acros. Compound **401** was purchased from Sigma Aldrich and **413** was purchased from Selleckbio; compounds **416**, **417** and 1-chloro-4-hydroxyisoquinoline-3-carboxylic acid were purchased from TCI UK and from Reddy Chemtech respectively. Reactions were monitored by TLC, which was performed on precoated aluminum-backed plates (Merck, silica 60 F254). Flash column chromatography was carried out using Biotage SP1 Purification system. Melting points were determined using a Stuart automatic melting point apparatus (SMP40). Infrared spectra were recorded from neat samples, on a Bruker Tensor 27 FT-IR spectrometer. NMR spectra were acquired using Bruker Avance II 500 MHz spectrometer equipped with a 5mm $^{13}C(^{1}H)$ dual cryoprobe or Avance 400 MHz spectrometer equipped with a 5mm z-gradient $^{1}H/^{13}C/^{19}F/^{31}P$ quad-nucleus probe. Chemical shifts (δ) are given in ppm, and the multiplicities are given as singlet (s), doublet (d), doublet doublet (dd), triplet (t), quartet (q), multiplet (m), broad (br). Coupling constants *J* are given in Hz (± 0.5 Hz). High resolution mass spectra (HRMS) were recorded using Bruker MicroTOF. The purity of all compounds synthesized were ≥98% as determined by analytical reverse-phase LCMS.

General procedure A

tert-butyl glycinates 422-425

To a stirred mixture of **421** (1 equiv.), K_2CO_3 (3 equiv.) and the requisite boronic acid (1.2 equiv.) in CH_3CN/H_2O (3:1), purged with N_2 for 5 min, $Pd(PPh_3)_4$ (10 % mole) was added. The mixture was heated at 135 ºC under microwave radiation for 3 h and basified with 1 M NaOH. The mixture was washed with EtOAc (3 x 10 mL), the combined organics were dried over $MgSO_4$ and concentrated *in vacuo*. The crude mixture was chromatographed (C_6H_{12}/EtOAc 8:2 to 7:3) to provide pure *tert*-butyl glycinates.

General procedure B

Purification of glycines 426-429

The basic aqueous layer (procedure A) was acidified with 1 M HCl to pH 3 and washed with EtOAc (3 x 10 mL). The organic layers were combined, dried over $MgSO_4$ and concentrated *in vacuo* to provide the aryl glycines.

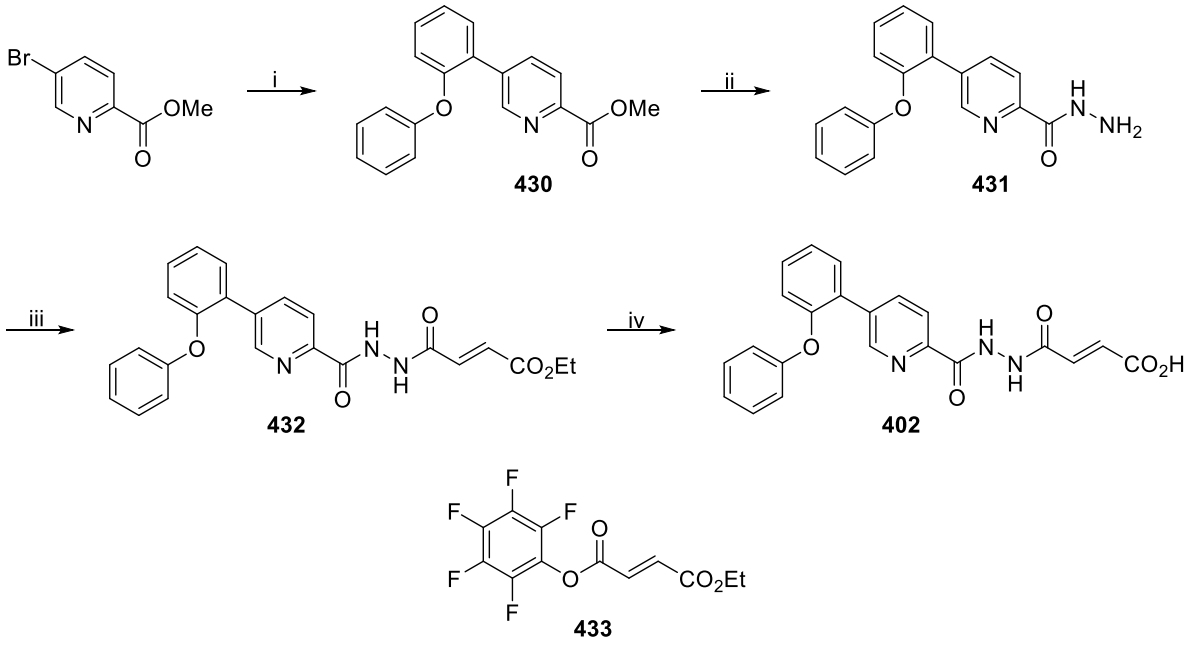

Scheme 4. 2 *Synthesis of* ***402****.*

Reagents and conditions: i) $RB(OH)_2$ (1.5 equiv.), 2 M Na_2CO_3 (4 equiv.), $Pd(PPh_3)_4$ (10 mole %), THF, reflux; ii) $NH_2NH_2 \cdot H_2O$, (3 equiv.), MeOH, reflux; iii) 433 (1.1 equiv.), EtOAc/THF 1:1, iv) 1 M NaOH (3 equiv.), MeOH.

Methyl 5-(2-phenoxyphenyl)picolinate 430

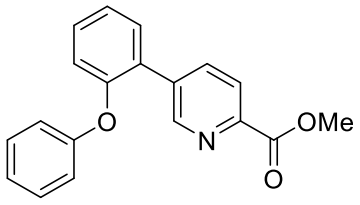

To a solution of 5-bromo-pyridine-2-carboxylic acid methyl ester[30] (0.50 g, 2.29 mmol) in THF, 2-phenoxyphenyl boronic acid (0.73 g, 3.43 mmol), 2 M Na_2CO_3 (2.3 mL, 4.60 mmol) and $Pd(PPh_3)_4$ (0.22 g, 0.23 mmol) was added. The reaction was refluxed for 14 h; the solvent

was then removed *in vacuo*. The crude was dissolved in EtOAc and washed with water. The organic phase was dried over $MgSO_4$ and concentrated *in vacuo*. Chromatography (CH_2Cl_2/ EtOAc 9:1) afforded compound **430** (0.55 g, 72 %) as yellow solid, mp 60-61 ºC. R_f = 0.45. IR (KBr) ν/cm^{-1} 1677 (MeOC=O); ^{1}H NMR (500 MHz, $CDCl_3$) δ 8.95 (1H, s, Ar C*H*), 8.04 (2H, dd, *J*= 1 0.5, Ar C*H*), 7.49 (1H, d, *J*= 0.5, Ar C*H*), 7.47-7.37 (1H, m, Ar C*H*), 7.29-7.25 (3H, m, Ar C*H*), 7.06-7.03 (2H, m, Ar C*H*), 6.92-6.90 (2H, m, Ar C*H*), 4.00 (3H, s, CH_3); ^{13}C NMR (500MHz, $CDCl_3$) δ 165.6 (*C*=O), 156.95 (Ar*C*), 153.95 (Ar*C*), 149.9 (Ar*C*), 146.1 (Ar*C*H), 137.35 (Ar*C*H), 136.9 (Ar*C*H), 130.9 (Ar*C*), 130.4 (Ar*C*H), 129.8 (Ar*C*H), 128.8 (Ar*C*H), 124.6 (Ar*C*H), 124.3 (Ar*C*H), 123.3 (Ar*C*H), 120.0 (Ar*C*H), 118.2 (Ar*C*H), 52.8 (*C*H_3); HRMS calcd. for $C_{19}H_{15}NNaO_3$ $[M+Na]^+$ 328.0944; Found 328.0946.

5-(2-phenoxyphenyl)picolinohydrazide 431

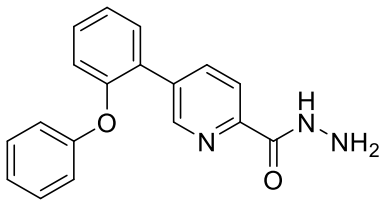

To a solution of **430** (0.55 g, 1.80 mmol) in MeOH, hydrazine monohydrade (0.26 mL, 5.40 mmol) was added. The reaction was stirred at 65 ºC until consumption of starting material. After 9 h the reaction was allowed to cool and the desired product crystallised. Sanction filtration afforded compound **431** (0.44 g, 80 %) as yellow needles, m.p 127-128 ºC. IR (KBr) ν/cm^{-1} 1673 (NHC=O); ^{1}H NMR (500 MHz, MeOD-d_4) δ 8.80-8.79 (1H, m, ArC*H*), 8.13-8.05 (2H, m, Ar C*H*), 7.57 (1H, dd, *J*= 1.0, 0.5, Ar C*H*), 7.48-7.45 (1H, m, Ar C*H*), 7.35-7.28 (3H, m, Ar C*H*), 7.08-7.04 (2H, m, Ar C*H*), 6.91-6.89 (2H, m, Ar C*H*), 4.61 (2H, s, NH_2); ^{13}C NMR (125MHz, MeOD-d_4) δ 165.5 (*C*=O), 158.7 (Ar *C*), 155.1 (Ar *C*), 150.05 (Ar *C*H), 149.0 (Ar *C*), 138.0 (Ar *C*H), 137.85 (Ar *C*H), 132.2 (Ar *C*H), 131.6 (Ar *C*H), 130.9 (Ar *C*), 130.7 (Ar *C*H), 125.8 (Ar *C*H), 124.2 (Ar *C*H), 122.6 (Ar *C*H), 121.4 (Ar *C*H), 118.9 (Ar *C*H); HRMS calcd. for $C_{18}H_{15}N_3NaO_2$ $[M+Na]^+$ 328.1060; Found 328.1056.

(*E*)-ethyl 4-oxo-4-(2-(5-(2-phenoxyphenyl)picolinoyl)hydrazinyl)but-2-enoate 432

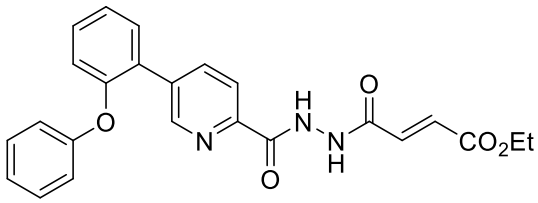

To a stirred suspension of **431** (0.50 g, 3.6 mmol) in THF: EtOAc (1:1) (50 mL), compound **433**[31] (1.24 g, 4.0 mmol) was added and the reaction mixture was stirred at room temperature overnight. The organic solvents were removed *in vacuo*, the resulting solid residue was washed with EtOAc (50 mL). Concentration of the filtrate *in vacuo* and co-evaporation with Et_2O afforded **432** (0.10 g, 28 %) as a white solid, mp 170-172 °C. IR (KBr) ν/cm^{-1} 3374 (CON-H), 3204 (COO-H), 1719 (EtOC=O), 1622 (NHC=O); ^{1}H NMR (500 MHz, $CDCl_3$) δ 8.83 (1H, d, *J*= 0.5, Ar C*H*), 8.33 (1H, d, *J*= 1.0, Ar C*H*), 8.16 (1H, dd, *J*= 1.0 0.5, Ar C*H*), 7.49 (1H, dd, *J*= 1.0 0.5, Ar C*H*), 7.42-7.37 (2H, m, Ar C*H*), 7.32-7.26 (3H, m, Ar C*H*), 7.09-7.04 (2H, m, Ar C*H*), 7.005-6.93 (3H, m, Ar C*H*), 4.24 (2H, q, *J*= 1.0, CH_2), 1.28 (3H, t, *J*= 1.0, CH_3); ^{13}C NMR (125MHz, $CDCl_3$) δ 165.3 (*C*=O), 159.2 (*C*=O), 159.05 (*C*=O), 156.8 (Ar *C*), 154.1 (Ar *C*), 148.4 (Ar *C*), 145.45 (Ar *C*H), 138.4 (Ar *C*H), 137.3 (Ar *C*H), 133.2 (Ar *C*H), 131.7 (Ar *C*H), 130.9 (Ar *C*), 130.5 (Ar *C*H), 129.9 (*C*H=CH), 128.5 (*C*H=CH), 124.25 (Ar *C*H), 123.5 (Ar *C*H), 122.55 (Ar *C*H), 119.75 (Ar *C*H), 118.4 (Ar *C*H), 61.2 (*C*H_2CH$_3$), 14.1 (*C*H$_3$); HRMS calcd. for $C_{24}H_{21}N_3NaO_5$ $[M+Na]^+$ 454.1373; Found 454.1383.

(*E*)-4-oxo-4-(2-(5-(2-phenoxyphenyl)picolinoyl)hydrazinyl)but-2-enoic acid 402

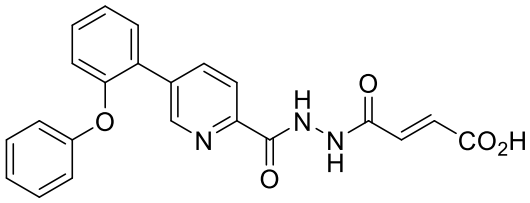

A mixture of **432** (0.06 g, 0.15 mmol) with LiOH·H_2O (0.02 g, 0.44 mmol) in THF/H_2O 2:1 (1 mL) was stirred at room temperature for 3 h. The reaction mixture was then washed with EtOAc (3 x 10 mL). The aqueous layer was acidified with 1 M HCl to pH 3. The white precipitate was filtered and washed with H_2O. Drying afforded compound **402** (0.04 g, 71 %) as off white needles, mp 274-275 ºC. IR (KBr) ν/cm^{-1} 3365 (CON-H), 3218 (COO-H), 1709

(HOC=O), 1632 (NHC=O); ^{1}H NMR (500 MHz, DMSO-d_6) δ 10.75 (1H, s, CO_2H), 8.84 (1H, d, J= 0.5, Ar C*H*), 8.21-8.19 (1H, m, Ar C*H*), 8.07 (1H, d, J= 1.0, Ar C*H*), 7.65 (1H, dd, J= 1.0 0.5, Ar C*H*), 7.52-7.48 (1H, m, Ar C*H*), 7.38-7.33 (3H, m, Ar C*H*), 7.11-7.01 (5H, m, Ar C*H*), 6.97-6.64 (1H, m, Ar C*H*); ^{13}C NMR (125MHz, DMSO-d_6) δ 166.1 (*C*=O), 162.3 (*C*=O), 161.9 (*C*=O), 156.7 (Ar *C*), 153.2 (Ar *C*), 148.4 (Ar *C*), 147.4 (Ar *C*H), 137.9 (Ar *C*H), 136.0 (Ar *C*H), 134.2 (Ar *C*H), 131.3 (Ar *C*H), 131.2 (Ar *C*H), 130.7 (Ar *C*), 130.1 (*C*H=CH), 128.6 (*C*H=CH), 124.7 (Ar *C*H), 123.3 (Ar *C*H), 122.1 (Ar *C*H), 119.9 (Ar *C*H), 118.0 (Ar *C*H), 117.9 (Ar *C*H); HRMS calcd. for $C_{22}H_{17}N_3NaO_5$ $[M+Na]^+$ 426.1060; Found 426.1058.

6-bromo-3-hydroxypyridine-2-carbonitrile 418

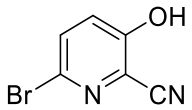

To a solution of 2-cyano-3-hydroxypyridine (2.40 g, 20 mmol) in CH_3CN/H_2O (60mL / 10mL), NBS (3.9 g, 22 mmol) was added portion-wise over 3 d at -4 ºC. The mixture was washed with 5 % sodium bisulfate (50 mL), H_2O (20 mL), dried over $MgSO_4$ and concentrated *in vacuo*. The crude was chromatographed (C_6H_{12}/CH_2Cl_2/ EtOAc 7:2:1 to 5:3:2). Recrystallisation (EtOAc) afforded **418** (1.10 g, 28 %) as off white crystals, mp 135 ºC dec.. R_f= 0.19. IR (neat) ν/cm^{-1} 3150 (b, ArO-H), 2290 (C-N); ^{1}H NMR (400 MHz, CD_3CN) δ 7.60 (1H, appt. d, J= 9.0, Ar C*H*), 7.37 (1H, appt. d, J= 9.0, Ar C*H*); ^{13}C NMR (125MHz, CD_3CN) δ 156.6 (*C*N), 142.5 (Ar*C*), 132.9 (Ar*C*H), 130.4 (Ar*C*), 128.15 (Ar*C*), 127.5 (Ar*C*H), 123.9; MS (ESI$^-$) m/z 197 ([M-H]$^-$, 80%); HRMS (ESI$^-$) calcd. for $C_6H_2BrN_2O$ $[M-H]^-$ 196.9356; Found 196.9350.

6-bromo-3-hydroxypyridine-2-carbonitrile 419

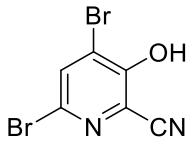

Chromatography of crude from above (CH_2Cl_2/ EtOAc 7:3 to 6:4) afforded **419** (2.00 g, 36 %) as white solid, mp >200 ºC. R_f= 0.16. IR (neat) ν/cm^{-1} 3133 (b, ArO-H), 2298 (C-N); ^{1}H NMR (400 MHz, $CDCl_3$) δ 9.09 (1 H, br. s, Ar O*H*), 7.77 (1 H, s, Ar C*H*); ^{13}C NMR (101MHz, $CDCl_3$) δ 157.4 (*C*N), 154.6 (Ar *C*), 135.4 (Ar *C*H), 131.5 (Ar*C*), 124.4 (Ar *C*), 120.9 (Ar *C*); MS (ESI$^-$) m/z 275 ([M-H]$^-$, 60%); HRMS (ESI$^-$) calc. for $C_6H_2Br_2N_2O$ [M-H]$^-$ 274.8461; Found 274.8458.

6-bromo-3-hydroxypyridine-2-carboxylic acid 420

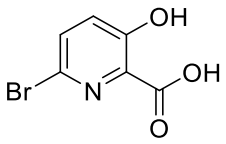

To a stirred suspension of **418** (2.80 g, 14.07 mmol) in methanol (50 mL), 30% w/v NaOH (44.0 mL, 351.8 mmol) was added and the reaction mixture was heated at reflux overnight. The solvent was removed under reduced pressure and the suspension was acidified with conc. HCl to pH 2. The resulting precipitate was filtrated and washed with cold water (5mL). Filtration afforded compound **420** (3.10 g, 100 %) as white needles, mp 122-124 ºC. IR (neat) ν/cm^{-1} 3100 (b, ArO-H), 2850 (b, COO-H), 1716 (HOC=O); ^{1}H NMR (400 MHz, DMSO-*d*$_6$) δ 7.75-7.33 (1H, m, Ar C*H*), 7.10-7.05 (1H, m, Ar C*H*); ^{13}C NMR (125MHz, DMSO-*d*$_6$) δ 169.1 (*C*=O), 160.2 (*C*=O), 143.3 (Ar *C*), 137.9 (Ar *C*), 135.8 (Ar *C*H), 133.7 (Ar *C*H), 131.2 (Ar *C*); MS (ESI$^-$) m/z 216 ([M-H]$^-$, 50%); HRMS calcd. for $C_6H_3BrNO_3$ [M-H]$^-$ 215.9302; Found 215.9298.

***tert*-butyl *N*-[(6-bromo-3-hydroxypyridin-2-yl)carbonyl]glycinate 421**

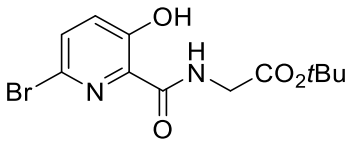

To a mixture of 6-bromo-3-hydroxypicolinic acid (0.20 g, 0.917 mmol), DIPEA (0.48 mL, 2.75 mmol) and T3P (0.71 mL, 1.19 mmol) in EtOAc (2 mL) was added glycine *tert*-butyl ester hydrochloride (0.2 g, 1.20 mmol). The reaction was heated under microwave irradiation at 150 ºC for 45 min. H_2O (10 mL) was added to the mixture and was washed with EtOAc (2 x 10 mL). Organics were combined, dried over $MgSO_4$ and concentrated *in vacuo*. Chromatography (C_6H_{12}/EtOAc, 9:1 to 6:4) afforded (0.13 g, 42 %) as a pale yellow solid, mp 105-106 ºC. R_f = 0.42. IR (neat) ν/cm^{-1} 3349 (NH), 1748 (*t*BuOC=O), 1675 (NHC=O); ^{1}H NMR (500 MHz, $CDCl_3$) δ 11.83 (1 H, s, Ar O*H*) 8.10 (1 H, br. s., N*H*), 7.40 (1 H, d, *J*= 8.5, Ar C*H*) 7.13 (1 H, d, *J*= 9.0, Ar C*H*), 4.04 (2 H, d, *J*= 5.5, CH_2), 1.44 (9 H, s, C(CH_3)$_3$); ^{13}C NMR (125MHz, $CDCl_3$) δ 168.0 (*C*=O), 167.7 (*C*=O), 157.3 (Ar *C*), 133.2 (Ar *C*H), 131.3 (Ar *C*), 129.4 (Ar *C*H), 129.0 (Ar *C*), 82.7 (*C*(CH$_3$)$_3$), 41.5 (*C*H$_2$), 28.0 (C(*C*H$_3$)$_3$); MS (ESI$^+$) m/z 353 ([M+Na]$^+$, 100%); HRMS calcd. for $C_{12}H_{15}BrN_2NaO_4$ [M+Na]$^+$ 353.0107; Found 353.0095.

***tert*-butyl *N*-[(3-hydroxy-6-phenylpyridin-2-yl)carbonyl]glycinate 422**

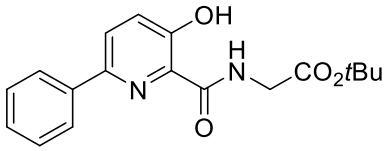

Following general procedure A, **421** (0.20 g, 0.604 mmol) was reacted with phenylboronic acid (88 mg, 0.725 mmol), K_2CO_3 (0.25 g, 1.18 mmol) in CH_3CN/H_2O (4 mL) with $Pd(PPh_3)_4$ (70 mg, 0.060 mmol). Chromatography afforded compound **422** (35 mg, 21 %) as a colourless oil. IR (neat) ν/cm^{-1} 3400 (N-H), 3090 (C-H), 1737 (*t*BuOC=O), 1652 (NHC=O); ^{1}H NMR (400 MHz, $CDCl_3$) δ 11.95 (1H, s, O*H*), 8.59 (1H, t, *J*= 5.0, N*H*), 7.97-7.94 (2H, m, Ar C*H*), 7.84 (1H, d, *J*= 9.0, Ar C*H*), 7.52-7.47 (2H, m, Ar C*H*), 7.45-7.40 (2H, m, Ar C*H*), 4.19 (2H, d, *J*= 5.5, CH_2), 1.56 (9H, s, C(CH_3)$_3$); ^{13}C NMR (101MHz, $CDCl_3$) δ 168.2

(C=O), 160.9 (C=O), 156.9 (Ar *C*), 147.7 (Ar *C*), 138.1 (Ar *C*), 130.3 (Ar *C*), 128.8 (2 Ar *C*H), 128.6 (2Ar *C*H), 127.1 (Ar *C*H), 126.3 (2 Ar *C*H), 126.0 (Ar *C*H), 82.6 (*C*$(CH_3)_3$), 41.6 (*C*H_2), 28.1 (C(*C*$H_3)_3$); MS (ESI^+) m/z 329 ($[M+H]^+$, 100 %); HRMS calcd. for $C_{18}H_{20}N_2NaO_4$ $[M+Na]^+$ 351.1321; Found 351.1315.

***tert*-butyl *N*-{[3-hydroxy-6-(naphthalen-1-yl)pyridin-2-yl]carbonyl}glycinate 423**

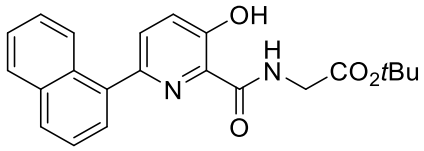

Following general procedure A **421** (0.20 g, 0.604 mmol) was reacted with, naphthalen-1-ylboronic acid (0.13 g, 0.725 mmol), K_2CO_3 (0.25 g, 1.18 mmol) in CH_3CN/H_2O (4 mL) with $Pd(PPh_3)_4$ (70 mg, 0.060 mmol). Chromatography afforded compound **423** (61 mg, 27 %) as a yellow oil. IR (neat) ν/cm^{-1} 3400 (N-H), 2978 (C-H), 1740 (*t*BuOC=O), 1652 (NHC=O); ^{1}H NMR (400 MHz, $CDCl_3$) δ 12.03 (1H, s, O*H*), 8.42 (1H, t, *J*= 6.0, N*H*), 8.09-8.06 (1H, m, Ar *H*), 7.96-7.93 (2H, m, Ar *H*), 7.67 (1H, d, *J*= 8.5, Ar *H*), 7.60-7.50 (4H, m, Ar *H*), 7.49 (1H, d, *J*8.5, Ar *H*), 4.14 (2H, d, *J*6.0, CH_2), 1.52 (9H, s, C(C*H*$_3)_3$); ^{13}C NMR (101MHz, $CDCl_3$) δ 169.1 (C=O), 168.1 (C=O), 156.7 (Ar *C*), 149.2 (Ar *C*), 137.3 (Ar *C*), 133.9 (Ar *C*), 131.5 (Ar *C*), 130.5 (Ar *C*H), 130.4 (Ar *C*), 128.9 (Ar *C*H), 128.5 (Ar *C*H), 127.4 (Ar *C*H), 126.6, (Ar *C*H), 126.6 (Ar *C*H), 125.9 (Ar *C*H), 125.4 (Ar *C*H), 125.3 (Ar *C*H), 82.5 (*C*$(CH_3)_3$), 41.5 (*C*H_2), 28.0 (C(*C*$H_3)_3$); MS (ESI^+) m/z 379 ($[M+H]^+$, 100 %); HRMS calcd. for $C_{22}H_{22}N_2N_2NaO_4$ $[M+Na]^+$ 401.1472; Found 401.1462.

***tert*-butyl *N*-{[3-hydroxy-6-(quinolin-5-yl)pyridin-2-yl]carbonyl}glycinate 424**

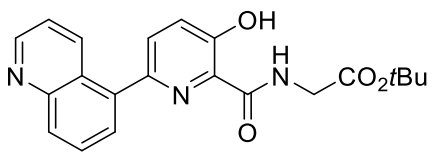

Following general procedure A **421** (0.25 g, 0.757 mmol) was reacted with, quinolin-5-ylboronic acid (0.156 g, 0.906 mmol), K_2CO_3 (0.313 g, 2.27 mmol) in CH_3CN/H_20 (4 mL) with $Pd(PPh_3)_4$ (87 mg, 0.076 mmol). Chromatography afforded compound **424** (70 mg, 24

%) as a white solid, mp 197-200 °C. IR (neat) ν/cm^{-1} 3200 (N-H), 1749 (*t*BuOC=O), 1646 (NHC=O); ^{1}H NMR (400 MHz, $CDCl_3$) δ 12.05 (1H, s, O*H*), 8.94-8.89 (1H, m, Ar *H*), 8.51-8.47 (2H, m, Ar *H* and N*H*), 8.16 (1H, d, *J*= 8.5, Ar *H*), 7.74-7.78 (1H, m, Ar *H*), 7.64-7.68 (2H, m, Ar *H*), 7.52-7.56 (1H, m, Ar *H*), 7.40 (1H, dd, *J*= 8.5, 4.0, Ar *H*), 4.12 (2H, d, *J*= 6.0, CH_2), 1.46 (9H, s, C(C*H*$_3$)$_3$); ^{13}C NMR (101MHz, $CDCl_3$) δ 168.9 (*C*=O), 168.1 (*C*=O), 157.0 (Ar *C*), 150.4 (Ar *C*H), 148.5 (Ar *C*), 147.9 (Ar *C*), 137.35 (Ar *C*H), 134.1 (Ar *C*H), 132.9 (Ar *C*), 130.3 (Ar *C*H), 130.2 (Ar *C*H), 128.8 (Ar *C*H), 127.6 (Ar *C*H), 127.1 (Ar *C*H), 121.5 (Ar *C*H), 82.6 (*C*(CH$_3$)$_3$), 41.4 (*C*H$_2$), 28.0 (C(*C*H$_3$)$_3$); MS (ESI$^+$) m/z 380 ([M+H]$^+$ 100 %); HRMS calcd. for $C_{21}H_{22}N_3O_4$ [M+H]$^+$ 380.1605; Found 380.1603.

tert-butyl _N_-{[6-(biphenyl-2-yl)-3-hydroxypyridin-2-yl]carbonyl}glycinate 425

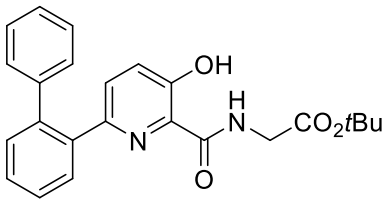

Following general procedure A **421** (0.20 g, 0.604 mmol) was reacted with, [1,1'-biphenyl]-2-ylboronic acid (0.10 g, 0.725 mmol), K_2CO_3 (0.25 g, 1.18 mmol) in CH_3CN/H_2O (4 mL) with $Pd(PPh_3)_4$ (70 mg, 0.0604 mmol). Chromatography afforded compound **425** (66 mg, 27 %) as a yellow oil. IR (neat) ν/cm^{-1} 3400 (N-H), 2978 (Ar C-H), 1743 (*t*BuOC=O), 1653 (NHC=O); ^{1}H NMR (400 MHz, $CDCl_3$) δ 11.89 (1H, s, O*H*), 8.18 (1H, t, *J*= 6.0, N*H*), 7.73-7.69 (1H, m, Ar C*H*), 7.49-7.46 (3H, m, Ar *H*), 7.38-7.26 (4H, m, Ar *H*), 7.22-7.12 (3H, m, Ar *H*), 4.07 (2H, d, *J*= 6.0, CH_2), 1.55 (9H, s, (C(C*H*$_3$)$_3$); ^{13}C NMR (101MHz, $CDCl_3$) δ 160.1 (*C*=O), 168.7 (*C*=O), 168.1 (Ar *C*), 156.2 (Ar *C*), 148.1 (Ar *C*), 141.6 (Ar *C*), 140.8 (Ar *C*), 167.6 (Ar *C*), 137.1 (Ar *C*), 133.8 (Ar *C*H), 130.65 (Ar *C*H), 130.8 (Ar *C*H), 130.2 (Ar *C*H), 130.2 (Ar *C*H), 129.5 (Ar *C*H), 128.8 (Ar *C*H), 128.5 (Ar *C*H), 128.2 (Ar *C*H), 127.7 (Ar *C*H), 126.75 (Ar *C*H), 82.45 (*C*(CH$_3$)$_3$), 41.47 (*C*H$_2$), 28.1 (C(*C*H$_3$)$_3$); MS (ESI$^+$) m/z 405 ([M+H]$^+$, 100 %), 427 ([M+Na]$^+$ 50%), HRMS calcd. for $C_{24}H_{24}N_2NaO_4$ [M+Na]$^+$ 427.1634; Found 426.1628.

***tert*-butyl *N*-[(3-hydroxy-6-phenylpyridin-2-yl)carbonyl]glycinate 426**

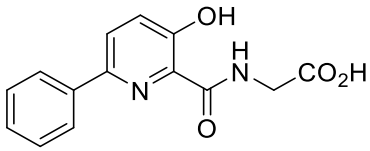

Following general procedure B, concentration *in vacuo* afforded compound **426** (50 mg, 30 %) as a white solid, mp 141-145 ºC. IR (neat) ν/cm^{-1} 3400 (O-H), 3200 (N-H), 3070 (C-H) 1708 (HOC=O), 1652 (NHC=O); ^{1}H NMR (400 MHz, DMSO-d_6) δ 12.38 (1H, s, O*H*), 9.48 (1H, t, *J*= 6.0, N*H*), 8.25-8.23 (2H, m, Ar *H*), 8.18 (1H, d, *J*= 9.0, Ar *H*), 7.59-7.54 (3H, m, Ar *H*), 7.46-7.41 (1H, m, Ar *H*), 4.07 (2H, d, *J*= 6.0, CH_2); ^{13}C NMR (101MHz, DMSO-d_6) δ 171.1 (*C*=O), 169.5 (*C*=O), 156.9 (Ar *C*), 147.0 (Ar *C*), 137.7 (Ar *C*), 134.5 (Ar *C*), 130.5 (Ar *C*H), 129.2 (Ar *C*H), 129.1 (Ar *C*H), 127.8 (Ar *C*H), 127.5 (Ar *C*H), 126.7 (Ar *C*H), 126.3 (Ar *C*H), 41.2 (*C*H_2); MS (ESI$^-$) m/z 271 ([M-H]$^-$ 100 %); HRMS calcd. for $C_{14}H_{11}N_2O_4$ [M−H]$^-$ 271.0719; Found 271.0719.

***N*-{[3-hydroxy-6-(naphthalen-1-yl)pyridin-2-yl]carbonyl}glycine 427**

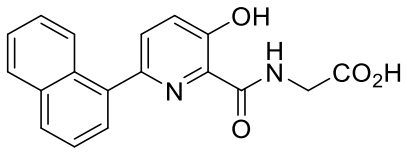

Following general procedure B, concentration *in vacuo* afforded compound **427** (67 mg, 34 %) as a white solid, mp 179-182 ºC. IR (neat) ν/cm^{-1} 3361 (O-H), 3200 (N-H), 1749 (HOC=O), 1658 (NHC=O); ^{1}H NMR (400 MHz, DMSO-d_6) δ 12.44 (1H, s, O*H*), 9.17 (1H, t, *J*= 6.0, N*H*), 8.04 (2H, dd, *J*= 8.0 1.0, Ar *H*), 7.96-7.94 (1H, m, Ar H), 7.80 (1H, d, *J*= 8.5, Ar *H*), 7.67-7.54 (5H, m, Ar *H*), 4.02 (2H, d, *J*= 6.0, CH_2); ^{13}C NMR (101MHz, DMSO-d_6) δ 170.9 (*C*=O), 169.4 (*C*=O), 156.7 (Ar *C*), 149.2 (Ar *C*), 137.5 (Ar *C*), 133.8 (Ar *C*), 121.15 (Ar *C*), 131.1 (Ar *C*H), 130.8 (Ar *C*), 129.1 (Ar *C*H), 128.8 (Ar *C*H), 127.95 (Ar *C*H), 127.2 (Ar *C*H), 127.1 (Ar *C*H), 126.5 (Ar *C*H), 125.85 (Ar *C*H), 125.6 (Ar *C*H), 41.2 (*C*H_2); MS (ESI$^-$) m/z 321 ([M-H]$^-$, 100 %), HRMS calcd. for $C_{18}H_{13}N_2O_4$ [M−H]$^-$ 321.0881; Found 321.0877.

***N*-{[3-hydroxy-6-(quinolin-5-yl)pyridin-2-yl]carbonyl}glycine 428**

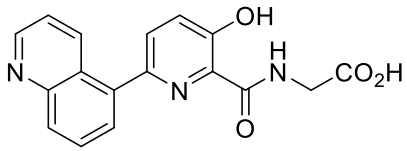

Following general procedure B, concentration *in vacuo* afforded compound **428** (114 mg, 47 %) as an off white oil. IR (neat) ν/cm^{-1} 3376 (N-H), 1730 (HOC=O), 1654 (NHC=O); ^{1}H NMR (400 MHz, DMSO-d_6) δ 12.45 (1H, s, O*H*), 9.20 (1H, t, *J*= 6.0, N*H*), 8.95 (1H, dd, *J*= 4.0 1.5, Ar *H*), 8.43 (1H, ddd, *J*= 8.5 1.5 1.0, Ar *H*), 8.13-8.11 (1H, m, Ar *H*), 7.90-7.84 (2H, m, Ar *H*), 7.78 (1H, dd, *J*= 7.0 1.0, Ar *H*), 7.63 (1H, dd, *J*= 8.5 2.0 Ar H), 7.54 (1H, dd, *J*= 8.5 4.0 Ar *H*), 4.00 (2H, d, *J*= 6.0, CH_2); ^{13}C NMR (101MHz, DMSO-d_6) δ 172.6 (*C*=O), 171.0 (*C*=O), 169.40 (Ar *C*), 156.9 (Ar *C*), 151.0 (Ar *C*H), 148.3 (Ar *C*), 148.0 (Ar *C*), 137.75 (Ar *C*), 134.3 (Ar *C*H), 131.2 (Ar *C*H), 130.8 (Ar *C*H), 130.1 (Ar *C*H), 128.2 (Ar *C*H), 127.5 (Ar *C*H), 126.3 (Ar *C*), 122.5 (Ar *C*H), 41.9 (*C*H$_2$); MS (ESI$^-$) m/z 322 ([M-H]$^-$ 100 %), HRMS calcd. for $C_{17}H_{12}N_3O_4$ [M–H]$^-$ 322.0833; Found 322.0828.

***N*-{[6-(biphenyl-2-yl)-3-hydroxypyridin-2-yl]carbonyl}glycine 429**

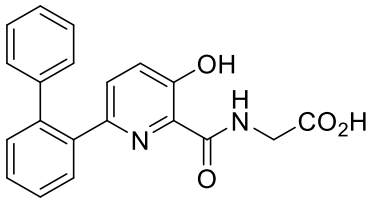

Following general procedure B, concentration *in vacuo* afforded compound **429** (16 mg, 8 %) as an off white oil. IR (neat) ν/cm^{-1} 3402 (N-H), 2913 (Ar C-H), 1750 (HOC=O), 1657 (HNC=O); ^{1}H NMR (400 MHz, DMSO-d_6) δ 4.09 (2H, s, CH_2), 7.09-7.15 (4H, m, Ar *H*), 7.24-7.30 (3H, m Ar *H*), 7.40-7.43 (1H, m, Ar *H*), 7.45-7.49 (2H, m, Ar *H*), 7.71 (1H, dd, *J*= 6.0, 3.0, Ar *H*); ^{13}C NMR (101MHz, DMSO-d_6) δ 171.1 (Ar *C*), 169.2 (Ar *C*), 155.9 (Ar *C*), 149.5 (Ar *C*), 141.8 (Ar *C*), 140.9 (Ar *C*), 138.0 (Ar *C*), 132.4 (Ar *C*), 131.7 (Ar *C*H), 130.2 (Ar *C*H), 130.0 (Ar *C*H), 129.9 (Ar *C*H), 129.2 (Ar *C*H), 128.6 (Ar *C*H), 128.2 (Ar *C*H), 127.9 (Ar *C*H), 127.3 (Ar *C*H), 126.4 (Ar *C*H), 125.3 (Ar *C*H), 39.9 (*C*H$_2$); MS (ESI$^-$) m/z 347 ([M-H]$^-$, 100 %); HRMS calcd. for $C_{20}H_{15}N_2O_4^-$ [M-H]$^-$ 347.1037; Found 347.1023.

4.12 References

1. Falnes, P.O., Johansen, R.F., and Seeberg, E., AlkB-mediated oxidative demethylation reverses DNA damage in Escherichia coli. *Nature*, **2002**, 419, 178-82.

2. Gerken, T., Girard, C.A., Tung, Y.C.L., Webby, C.J., Saudek, V., Hewitson, K.S., Yeo, G.S.H., McDonough, M.A., Cunliffe, S., McNeill, L.A., Galvanovskis, J., Rorsman, P., Robins, P., Prieur, X., Coll, A.P., Ma, M., Jovanovic, Z., Farooqi, I.S., Sedgwick, B., Barroso, I., Lindahl, T., Ponting, C.P., Ashcroft, F.M., O'Rahilly, S., and Schofield, C.J., The obesity-associated FTO gene encodes a 2-oxoglutarate-dependent nucleic acid demethylase. *Science*, **2007**, 318, 1469-72.

3. Jia, G.F., Yang, C.G., Yang, S.D., Jian, X., Yi, C.Q., Zhou, Z.Q., and He, C., Oxidative demethylation of 3-methylthymine and 3-methyluracil in single-stranded DNA and RNA by mouse and human FTO. *Febs Lett*, **2008**, 582, 3313-9.

4. Trewick, S.C., Henshaw, T.F., Hausinger, R.P., Lindahl, T., and Sedgwick, B., Oxidative demethylation by Escherichia coli AlkB directly reverts DNA base damage. *Nature*, **2002**, 419, 174-8.

5. Dina, C., Meyre, D., Gallina, S., Durand, E., Korner, A., Jacobson, P., Carlsson, L.M.S., Kiess, W., Vatin, V., Lecoeur, C., Delplanque, J., Vaillant, E., Pattou, F., Ruiz, J., Weill, J., Levy-Marchal, C., Horber, F., Potoczna, N., Hercberg, S., Le Stunff, C., Bougneres, P., Kovacs, P., Marre, M., Balkau, B., Cauchi, S., Chevre, J.C., and Froguel, P., Variation in FTO contributes to childhood obesity and severe adult obesity. *Nat Genet*, **2007**, 39, 724-6.

6. Frayling, T.M., Timpson, N.J., Weedon, M.N., Zeggini, E., Freathy, R.M., Lindgren, C.M., Perry, J.R.B., Elliott, K.S., Lango, H., Rayner, N.W., Shields, B., Harries, L.W., Barrett, J.C., Ellard, S., Groves, C.J., Knight, B., Patch, A.M., Ness, A.R., Ebrahim, S., Lawlor, D.A., Ring, S.M., Ben-Shlomo, Y., Jarvelin, M.R., Sovio, U., Bennett, A.J., Melzer, D., Ferrucci, L., Loos, R.J.F., Barroso, I., Wareham, N.J., Karpe, F., Owen, K.R., Cardon, L.R., Walker, M., Hitman, G.A., Palmer, C.N.A., Doney, A.S.F., Morris, A.D., Smith, G.D., Hattersley, A.T., and McCarthy, M.I., A common variant in the FTO gene is associated with body mass index and predisposes to childhood and adult obesity. *Science*, **2007**, 316, 889-94.

7. Church, C., Lee, S., Bagg, E.A.L., McTaggart, J.S., Deacon, R., Gerken, T., Lee, A., Moir, L., Mecinovic, J., Quwailid, M.M., Schofield, C.J., Ashcroft, F.M., and Cox, R.D., A Mouse Model for the Metabolic Effects of the Human Fat Mass and Obesity Associated FTO Gene. *Plos Genet*, **2009**, 5.

8. Fischer, J., Koch, L., Emmerling, C., Vierkotten, J., Peters, T., Bruning, J.C., and Ruther, U., Inactivation of the Fto gene protects from obesity. *Nature*, **2009**, 458, 894-U10.

9. Fu, Y., Jia, G.F., Pang, X.Q., Wang, R.N., Wang, X., Li, C.J., Smemo, S., Dai, Q., Bailey, K.A., Nobrega, M.A., Han, K.L., Cui, Q., and He, C., FTO-mediated formation of N-6-hydroxymethyladenosine and N-6-formyladenosine in mammalian RNA. *Nat Commun*, **2013**, 4.

10. Jia, G.F., Fu, Y., Zhao, X., Dai, Q., Zheng, G.Q., Yang, Y., Yi, C.Q., Lindahl, T., Pan, T., Yang, Y.G., and He, C., N6-Methyladenosine in nuclear RNA is a major substrate of the obesity-associated FTO. *Nat Chem Biol*, **2011**, 7, 885-7.

11. Chen, B.E., Ye, F., Yu, L., Jia, G.F., Huang, X.T., Zhang, X.J., Peng, S.Y., Chen, K., Wang, M.N., Gong, S.Z., Zhang, R.H., Yin, J.Y., Li, H.Y., Yang, Y.M., Liu, H., Zhang, J.W., Zhang, H.Y., Zhang, A., Jiang, H.L., Luo, C., and Yang, C.G., Development of Cell-Active N-6-Methyladenosine RNA Demethylase FTO Inhibitor. *J Am Chem Soc*, **2012**, 134, 17963-71.

12. Epps, D.E., Sarver, R.W., Rogers, J.M., Herberg, J.T., and Tomich, P.K., The ligand affinity of proteins measured by isothermal denaturation kinetics. *Anal Biochem*, **2001**, 292, 40-50.

13. Niesen, F.H., Berglund, H., and Vedadi, M., The use of differential scanning fluorimetry to detect ligand interactions that promote protein stability. *Nat Protoc*, **2007**, 2, 2212-21.

14. Woon, E.C.Y., Demetriades, M., Bagg, E.A.L., Aik, W., Krylova, S.M., Ma, J.H.Y., Chan, M.C., Walport, L.J., Wegman, D.W., Dack, K.N., McDonough, M.A., Krylov, S.N., and Schofield, C.J., Dynamic Combinatorial Mass Spectrometry Leads to Inhibitors of a 2-Oxoglutarate-Dependent Nucleic Acid Demethylase. *Journal of Medicinal Chemistry*, **2012**, 55, 2173-84.

15. Demetriades, M., Leung, I.K.H., Chowdhury, R., Chan, M.C., McDonough, M.A., Yeoh, K.K., Tian, Y.M., Claridge, T.D.W., Ratcliffe, P.J., Woon, E.C.Y., and Schofield, C.J., Dynamic Combinatorial Chemistry Employing Boronic Acids/Boronate Esters Leads to Potent Oxygenase Inhibitors. *Angew Chem Int Edit*, **2012**, 51, 6672-5.

16. Arend, M.P., Guenzler-Pukall, V., Ho, W.B., Turtle, E.D., and Du, X., Nitrogen-containing heteroaryl compounds and their use in increasing endogenous erythropoietin, **2004**.

17. Rose, N.R., McDonough, M.A., King, O.N.F., Kawamura, A., and Schofield, C.J., Inhibition of 2-oxoglutarate dependent oxygenases. *Chem Soc Rev*, **2011**, 40, 4364-97.

18. Yan, L., Colandrea, V.J., and Hale, J.J., Prolyl hydroxylase domain-containing protein inhibitors as stabilizers of hypoxia-inducible factor: small molecule-based therapeutics for anemia. *Expert Opinion on Therapeutic Patents*, **2010**, 20, 1219-45.

19. King, O.N.F., Li, X.S., Sakurai, M., Kawamura, A., Rose, N.R., Ng, S.S., Quinn, A.M., Rai, G., Mott, B.T., Beswick, P., Klose, R.J., Oppermann, U., Jadhav, A., Heightman, T.D., Maloney, D.J., Schofield, C.J., and Simeonov, A., Quantitative High-Throughput Screening Identifies 8-Hydroxyquinolines as Cell-Active Histone Demethylase Inhibitors. *Plos One*, **2010**, 5.

20. Han, Z.F., Niu, T.H., Chang, J.B., Lei, X.G., Zhao, M.Y., Wang, Q., Cheng, W., Wang, J.J., Feng, Y., and Chai, J.J., Crystal structure of the FTO protein reveals basis for its substrate specificity. *Nature*, **2010**, 464, 1205-U129.

21. Hausinger, R.P., Fe(II)/alpha-ketoglutarate-dependent hydroxylases and related enzymes. *Crit Rev Biochem Mol*, **2004**, 39, 21-68.

22. Chowdhury, R., Yeoh, K.K., Tian, Y.M., Hillringhaus, L., Bagg, E.A., Rose, N.R., Leung, I.K.H., Li, X.S., Woon, E.C.Y., Yang, M., McDonough, M.A., King, O.N., Clifton, I.J., Klose, R.J., Claridge, T.D.W., Ratcliffe, P.J., Schofield, C.J., and Kawamura, A., The oncometabolite 2-hydroxyglutarate inhibits histone lysine demethylases. *Embo Rep*, **2011**, 12, 463-9.

23. Frezza, C., Pollard, P.J., and Gottlieb, E., Inborn and acquired metabolic defects in cancer. *J Mol Med*, **2011**, 89, 213-20.

24. Warshakoon, N.C., Wu, S.D., Boyer, A., Kawamoto, R., Sheville, J., Bhatt, R.T., Renock, S., Xu, K., Pokross, M., Zhou, S.T., Walter, R., Mekel, M., Evdokimov, A.G., and East, S., Design and synthesis of substituted pyridine derivatives as HIF-1 alpha prolyl hydroxylase inhibitors. *Bioorg Med Chem Lett*, **2006**, 16, 5616-20.

25. Kawaguchi, T., Akatsuka, H., Iijima, T., Watanabe, T., Murakami, J., and Mitsui, T., Fused furan compound, **2006**, US 2006/0094724 A1.

26. Otwinowski, Z. and Minor, W., Processing of X-ray diffraction data collected in oscillation mode. *Macromolecular Crystallography, Pt A*, **1997**, 276, 307-26.

27. Mccoy, A.J., Grosse-Kunstleve, R.W., Adams, P.D., Winn, M.D., Storoni, L.C., and Read, R.J., Phaser crystallographic software. *J Appl Crystallogr*, **2007**, 40, 658-74.

28. Adams, P.D., Afonine, P.V., Bunkoczi, G., Chen, V.B., Davis, I.W., Echols, N., Headd, J.J., Hung, L.W., Kapral, G.J., Grosse-Kunstleve, R.W., McCoy, A.J., Moriarty, N.W., Oeffner, R., Read, R.J., Richardson, D.C., Richardson, J.S., Terwilliger, T.C., and Zwart, P.H., PHENIX: a comprehensive Python-based system for macromolecular structure solution. *Acta Crystallogr D*, **2010**, 66, 213-21.

29. Emsley, P., Lohkamp, B., Scott, W.G., and Cowtan, K., Features and development of Coot. *Acta Crystallogr D*, **2010**, 66, 486-501.

30. Keith, J.M., Letavic, M.A., Ly, K.S., Mani, N.S., Mills, J.E., Pandit, C.R., Villani, F.J., and Zhong, H., Substituted pyridyl amide compounds as modulators of the histamine H3 receptor **2007**, 753607.

31. Yeoh, K.K., Chan, M.C., Thalhammer, A., Demetriades, M., Chowdhury, R., Tian, Y.M., Stolze, I., McNeill, L.A., Lee, M.K., Woon, E.C.Y., Mackeen, M.M., Kawamura, A., Ratcliffe, P.J., Mecinovic, J., and Schofield, C.J., Dual-action inhibitors of HIF prolyl hydroxylases that induce binding of a second iron ion. *Org Biomol Chem*, **2013**, 11, 732-45.

Overall conclusions

As described in Chapter 1, 2OG oxygenases are a large superfamily of human enzymes that are involved in important biological processes. A number of 2OG oxygenases are linked to disease onset and progression, and are consequently considered therapeutic targets. Work in this thesis describes studies to identify inhibitors of three 2OG oxygenases; dynamic combinatorial chemistry methods using mass spectrometric detection (DCMS) were optimised and applied for the discovery of AlkB and PHD2 inhibitors. Work on FTO inhibition resulted in the development of a new inhibition assay, which led to the development of the first designed selective inhibitors of FTO.

For studies with AlkB, DCMS was applied using a library of thiols. *N*-oxalyl-L-cysteine was selected as the 'support ligand' and was used in conjunction with a library of 37 thiols to provide a dynamic combinatorial library (DCL). The DCL, which contained thiols and disulphides in dynamic equilibrium, was analysed using non-denaturing ESI-MS. The MS studies identified three AlkB binders, of which all three contained disulphide bonds (Figure 2. 6). Synthesis of structural analogues of the three binders, which lack the labile disulphide group, resulted in the identification of stable inhibitors. One of the identified inhibitors was successfully crystallised with AlkB, which enabled structure based design of a fourth AlkB inhibitor with improved inhibitory activity (sub-micromolar IC_{50}, Table 2. 2). Changing the iron chelating group from oxalyl- to pyridyl- and quinolinyl- did not yield better AlkB inhibitors, although one pyridyl- inhibitor displayed good potency against AlkB. No inhibition was observed for the three most potent AlkB inhibitors against three other 2OG oxygenases (PHD2, FTO and PHF8), revealing selectivity for AlkB.

Hydroxylation of hypoxia inducible factor (HIF1α) by 2OG oxygenases (PHD1-3 and FIH) promotes HIF1α degradation under normal levels of oxygen. Inhibition of prolyl hydroxylase domain 2 (PHD2), at low oxygen levels, leads to survival of HIF1α and transcription of hypoxia response elements (HREs). Transcription of HREs promotes increased vasculature which results in cardioprotection and erythropoiesis. Therefore inhibition of PHD2 under

normal oxygen levels has a potential to be used for the treatment of conditions such as anaemia. For studies with PHD2, a novel reversible reaction was applied for the development of a DCL; the formation of boronate esters from boronic acids and alcohols/diols occurs in aqueous solution at physiological pH and is therefore biomolecule compatible. Two boronic acid substituted pyridyl compounds with iron chelating properties were identified as suitable 'support ligands' for DCMS. Optimisation of the boronic acid/diol reaction for DCMS analysis showed that the diol library should be reacted with the PHD2·Fe·boronic acid complex to enable rapid formation of a DCL. Incubation of a 5-substituted pyridyl boronic acid with the library of diols resulted in the identification of seven 'hit' structures for development of PHD2 inhibitors (Figure 3. 10). NMR binding experiments confirmed the DCMS results showing the stronger binding of the 7 boronate esters to PHD2 compared to the parent boronic acid and boronate esters formed with other diols from the library. Synthesis of stable carbon analogues of the boronate ester hits, that were active PHD2 inhibitors, validated the boronate ester DCMS approach. These pyridyl inhibitors were modified in order to introduce a hydrogen bond with PHD2 active site residues and hence improve their binding strength. The new inhibitors were highly potent against PHD2; their activity over PHD2 was improved 10000 times compared to the lead compounds. Moreover, the improved inhibitor derived from the DCMS hit structure was found to be roughly 1000 times more selective for PHD2 over other 2OG oxygenases compared to a PHD2 inhibitor used in clinical trials against anaemia. The use of boronic acids/esters for DCMS studies has proved to be a powerful tool for the identification of selective inhibitors for PHD2. In the future this method may be applied to inhibition studies with other enzymes, including other 2OG oxygenases (Table 3. 4).

Taken together, the work in this thesis demonstrates the applicability of DCMS for inhibitor design. Moreover, boronic acid/boronate ester formation has been successfully used for the first time in protein DCMS. Limitations of this method, such as the cleavage of boronate esters during MS analysis and direct binding of alcohols to PHD2 were identified and solved. New MS techniques which will allow milder sample ionisation/desolvation may be used without significant ester cleavage.

The fat mass and obesity associated (FTO) protein belongs in the same subfamily as the AlkBHs (human homologues of AlkB). Mice studies have linked FTO levels with risk of obesity; inhibition of FTO can prevent obesity related diseases such as diabetes and heart disease. Small molecule induced inhibition of FTO is therefore desirable for prevention of diet related obesity and diseases. An inhibition assay for FTO was developed and used with a DSF binding assay to enable the screening of a library of ~150 compounds against FTO, including inhibitors identified in the DCMS studies of AlkB and PHD2 (Figure 4. 2). 21 compounds were selected for IC_{50} determination, with 8 library members displaying good potency. Out of these 8 inhibitors, 4 compounds were found to be potent inhibitors of other 2OG oxygenases including PHD2 and lysine demethylases. Crystal structures were obtained for 5 of the 8 inhibitors with FTO (Figure 4. 8-13). Information from the inhibition assay was used in an SAR study and, in combination with the crystallographic data, enabled the design of more potent FTO inhibitors. One of these inhibitors displayed great potency against FTO; crystallographic studies revealed that the high potency of this compound is likely due to partial occupation of the substrate binding site. Inhibition studies of this compound with other 2OG oxygenases revealed that it has improved selectivity for FTO compared to the initially screened compounds (Table 4. 4). Overall, the combined inhibition and crystallographic studies have led to the formation of the first designed FTO inhibitors, and will hopefully result in the development of analogues to provide even more potent and selective inhibitors.

Overall, this thesis describes studies to identify selective inhibitors of three 2OG oxygenases, which was achieved with the use of DCMS, SAR and crystallographic analyses. The DCMS method was enriched with the development of a novel DCL using the reversible reaction between boronic acids and diols, which may be applied for future DCC studies with multiple templates.

Publications

1. Woon, E.C.Y., Demetriades, M., Bagg, E.A.L., Aik, W., Krylova, S.M., Ma, J.H.Y., Chan, M.C., Walport, L.J., Wegman, D.W., Dack, K.N., McDonough, M.A., Krylov, S.N., and Schofield, C.J., Dynamic Combinatorial Mass Spectrometry Leads to Inhibitors of a 2-Oxoglutarate-Dependent Nucleic Acid Demethylase. *J Med Chem*, 2012, 55, 2173-84.

2. Demetriades, M., Leung, I.K.H., Chowdhury, R., Chan, M.C., McDonough, M.A., Yeoh, K.K., Tian, Y.M., Claridge, T.D.W., Ratcliffe, P.J., Woon, E.C.Y., and Schofield, C.J., Dynamic Combinatorial Chemistry Employing Boronic Acids/Boronate Esters Leads to Potent Oxygenase Inhibitors. *Angew Chem Int Edit*, 2012, 51, 6672-5.

3. Catto, M., Berezin, A.A., Lo Re, D., Loizou, G., Demetriades, M., De Stradis, A., Campagna, F., Koutentis, P.A., and Carotti, A., Design, synthesis and biological evaluation of benzo[e][1,2,4]triazin-7(1H)-one and [1,2,4]-triazino[5,6,1-jk]carbazol-6-one derivatives as dual inhibitors of beta-amyloid aggregation and acetyl/butyryl cholinesterase. *Eur J Med Chem*, 2012, 58, 84-97.

4. Yeoh, K.K., Chan, M.C., Thalhammer, A., Demetriades, M., Chowdhury, R., Tian, Y.M., Stolze, I., McNeill, L.A., Lee, M.K., Woon, E.C.Y., Mackeen, M.M., Kawamura, A., Ratcliffe, P.J., Mecinovic, J., and Schofield, C.J., Dual-action inhibitors of HIF prolyl hydroxylases that induce binding of a second iron ion. *Org Biomol Chem*, 2013, 11, 732-45.

5. Leung, I.K.H., Demetriades, M., Hardy, A.P., Lejeune, C., Smart, T.J., Szollossi, A., Kawamura, A., Schofield, C.J., and Claridge, T.D.W., Reporter Ligand NMR Screening Method for 2-Oxoglutarate Oxygenase Inhibitors. *J Med Chem*, 2013, 56, 547-55.

6. Chowdhury, R., Candela-Lena, J.I., Chan, M.C., Greenald, D.J., Yeoh, K.K., Tian, Y.M., McDonough, M.A., Tumber, A., Rose, N.R., Conejo-Garcia, A., Demetriades, M., Mathavan, S., Kawamura, A., Lee, M.K., van Eeden, F., Pugh, C.W., Ratciffe, P.J., and Schofieldt, C.J., Selective Small Molecule Probes for the Hypoxia Inducible Factor (HIF) Prolyl Hydroxylases. *Acs Chem Biol*, 2013, 8, 1488-96.

7. Bishop, T., Talbot, N.P., Turner, P.J., Nicholls, L.G., Pascual, A., Hodson, E.J., Douglas, G., Fielding, J.W., Smith, T.G., Demetriades, M., Schofield, C.J., Robbins, P.A., Pugh, C.W., Buckler, K.J., and Ratcliffe, P.J., Carotid body hyperplasia and enhanced ventilatory responses to hypoxia in mice with heterozygous deficiency of PHD2. *J Physiol-London*, 2013, 591, 3565-77.

8. Aik, W., Demetriades, M., Hamdan, M.K.K., Bagg, E.A.L., Yeoh, K.K., Lejeune, C., Zhang, Z.H., McDonough, M.A., and Schofield, C.J., Structural Basis for Inhibition of the Fat Mass and Obesity Associated Protein (FTO). *J Med Chem*, 2013, 56, 3680-8.

9. Valegard, K., Iqbal, A., Kershaw, N.J., Ivison, D., Genereux, C., Dubus, A., Blikstad, C., Demetriades, M., Hopkinson, R.J., Lloyd, A.J., Roper, D.I., Schofield, C.J., Andersson, I., and McDonough, M.A., Structural and mechanistic studies of the orf12 gene product from the clavulanic acid biosynthesis pathway. *Acta Crystallogr D*, 2013, 69, 1567-79.

10. Cherblanc, F.L., Chapman, K.L., Reid, J., Borg, A.J., Sundriyal, S., Alcazar-Fuoli, L., Bignell, E., Demetriades, M., Schofield, C.J., Dimaggio, P.A.J., Brown, R., and Fuchter, M.J., On the Histone Lysine Methyltransferase Activity of Fungal Metabolite Chaetocin. *J Med Chem*, 2013.

Appendix. Syntheses of modified aminoacids

Chemical synthesis

Reagents and solvents were from Aldrich or Alfa Aesar. Reactions were monitored by TLC, which was performed on precoated aluminum-backed plates (Merck, silica 60 F254). Melting points were determined using a Leica Galen III hot-stage melting point apparatus and microscope. Specific rotation was measured in a Perkin Elmer 341 Polarimeter at 20 ºC in $degdm^{-1}cm^3g^{-1}$. Infrared spectra were recorded from neat samples, on a Bruker Tensor 27 FT-IR spectrometer. NMR spectra were acquired using a Bruker DPX500 NMR spectrometer. Chemical shifts (δ) are given in ppm, and the multiplicities are given as singlet (s), doublet (d), triplet (t), quartet (q), multiplet (m), broad (br). Coupling constants *J* are given in Hz (± 0.5 Hz). High resolution mass spectra (HRMS) were recorded using Bruker MicroTOF. The purity of all compounds synthesized were ≥95% as determined by analytical reverse-phase HPLC (Ultimate 3000).

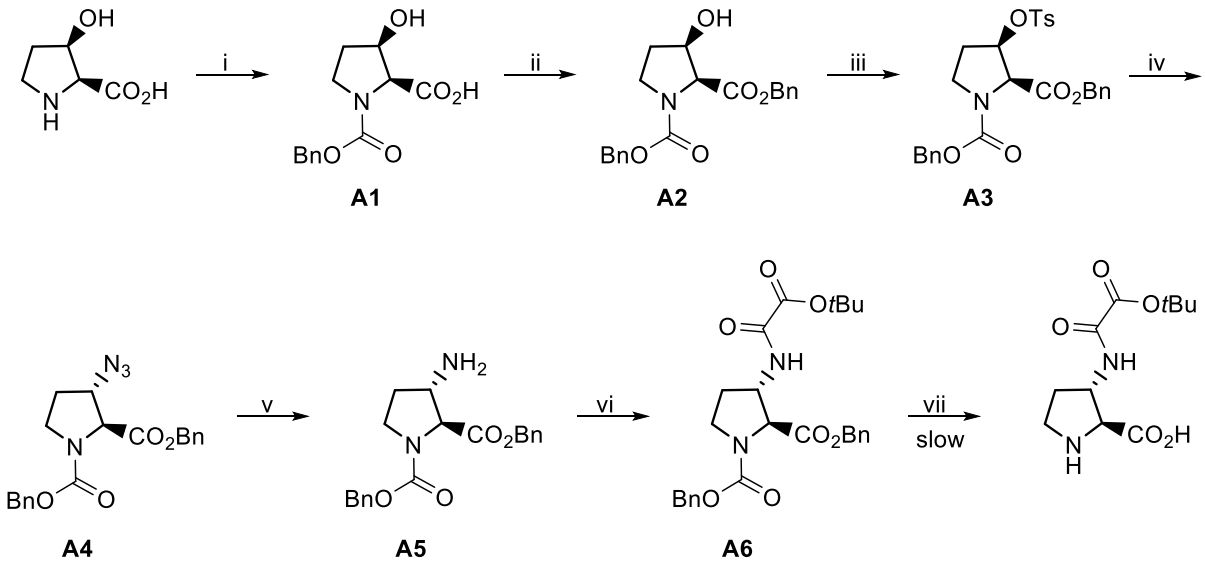

Scheme A. 1 *Synthesis of 3-substituted L-proline.*

Reagents and conditions: i) benzyl chloroformate, sat. $NaHCO_3$, THF, r.t; ii) benzyl bromide, tetrabutyl ammonium iodide, NEt_3, THF; iii) tosyl chloride, py, r.t; iv) NaN_3, DMF; v) PPh_3, H_2O, THF, reflux; vi) PPh_3, H_2O, CH_2Cl_2, r.t; vii) Pd/C, H_2, THF, r.t.

(2*S*,3*R*)- 1-[(benzyloxy)carbonyl]-3-hydroxyproline A1

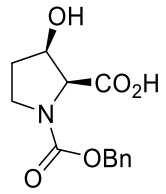

To a stirred suspension of cis-3-hydroxy-L-proline (1.50 g, 11.4 mmol) in sat. $NaHCO_3$/THF 3:2 (70 mL), benzyl chloroformate (2.13 mL, 14.91 mmol) was added dropwise over 10 min at 0 ºC and the reaction mixture was at room temperature. After 3 h Et_2O was added and removed. The mixture was acidified with 3 M HCl and washed with EtOAc. The solvent was removed *in vacuo* to afford compound (3.5 g, quantitative) as yellow oil. $[\alpha]_D$= -38.6 (c= 1.36 x 10^{-3}, CH_2Cl_2). IR (neat) ν/cm^{-1} 3400 (OH), 3035 (NH), 1678 (HOC=O), 1735 (BnOC=O); ^{1}H NMR (500 MHz; $CDCl_3$) δ 7.33-7.28 (5H, m, Ar C*H*), 5.18-5.09 (2H, m, OCH_2Bn), 4.58 (1H, q, *J* = 7.0, C*H*), 4.45-4.39 (1H, m, C*H*), 3.68-3.49 (2H, m, NCH_2), 2.22-1.96 (2H, m, CH_2); ^{13}C NMR (125MHz, $CDCl_3$) δ 173.7 (*C*=O), 173.1 (*C*=O), 155.6, 136.7, 128.6, 128.2, 127.9, 127.1, 71.2 (*C*H), 67.6 (O*C*H_2), 63.9 (*C*H), 44.6 (*C*H_2), 31.9 (*C*H_2); MS (ESI^-) m/z 288 ($[M+Na]^+$, 100%); HRMS calcd. for $C_{13}H_{15}NNaO_5$ $[M+Na]^+$ 288.0842; Found 288.0841.

(2S,3R)- dibenzyl 3-hydroxypyrrolidine-1,2-dicarboxylate A2

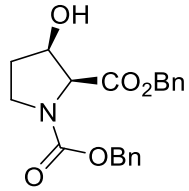

To a solution of (2.9 g, 10.93 mmol) in anhydrous THF (40 mL) under N_2, NEt_3 (5.7 mL, 40.89 mmol), tetrabutylammonium iodide (4.80 g, 13.2 mmol) were added and stirred for 10 min before benzyl bromide (2.0 mL, 16.4 mmol) was added. After 1 d tetrabutylammonium iodide (2.50 g, 6.88 mmol) and benzyl bromide (1.8 mL, 14.76 mmol) was added and the mixture was stirred for further 2 d until consumption of starting material. The mixture was washed with water; the organic layer was dried over $MgSO_4$ and concentrated *in vacuo*. Chromatography (hexane/EtOAc 2:8 to 5:5) gave compound **A2** (2.47 g, 64 %) as colourless

oil. R_f = 0.13. $[\alpha]_D$= -35.4 (c= 2.56 x 10^{-3}, CH_2Cl_2). IR (neat) ν/cm^{-1} 3435 (NH), 1749 (BnOC=O), 1706 (HNC=O); ^{1}H NMR (400 MHz; $CDCl_3$) δ 7.24-7.15 (2H, dd, J = 7.0 2.5, Ar C*H*), 5.18-4.91 (4H, m, O CH_2), 4.53-4.51 (1H, m, C*H*), 4.49-4.37 (1H, m, C*H*), 3.66-3.41 (2H, m, CH_2), 3.66-3.41 (2H, m, CH_2) 2.03-1.92 (2H, m, CH_2); ^{13}C NMR (101MHz, $CDCl_3$) δ 170.0 (*C*=O), 169.2 (*C*=O), 154.9 (Ar *C*), 154.0 (Ar *C*), 136.4 (Ar *C*H), 135.5 (Ar *C*H), 128.5 (Ar *C*H), 128.4 (Ar *C*H), 128.3 (Ar *C*H), 128.2 (Ar *C*H), 128.1 (Ar *C*H), 128.0 (Ar *C*H), 127.9 (Ar *C*H), 127.8 (Ar *C*H), 82.2 (*C*H), 72.0 (O*C*H_2), 67.2 (O*C*H_2), 63.9 (*C*H), 44.3 (*C*H_2), 32.1 (*C*H_2); MS (ESI^+) m/z 378 ($[M+Na]^+$, 100%); HRMS calcd. for $C_{20}H_{21}NNaO_5$ $[M+Na]^+$ 378.1312; Found 378.1313.

(2S,3R)- dibenzyl 3-{[(4-methylphenyl)sulfonyl]oxy}pyrrolidine-1,2-dicarboxylate A3

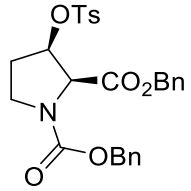

To a solution of **A2** (0.98 g, 2.76 mmol) in pyridine (5 mL), tosyl chloride (0.74 mL, 3.86 mmol) was added at room temperature and stirred for 1d. The mixture was washed with 1M HCl, the organic layer was dried over $MgSO_4$ and concentrated *in vacuo*. Chromatography (hexane/EtOAc 1:9 to 4:6) gave compound **A3** (0.95 g, 64 %) as light yellow oil. R_f = 0.60. IR (neat) ν/cm^{-1} 3060 (NH), 1747 (BnOC=O), 1708 (HNC=O); $[\alpha]_D$= 2.95 (c= 11.2 x 10^{-3}, CH_2Cl_2). ^{1}H NMR (500 MHz; $CDCl_3$) δ 7.74-7.68 (1 H, m, Ar C*H*), 7.68-7.62 (1 H, m, Ar C*H*), 7.40-7.27 (9 H, m, Ar C*H*), 7.26-7.20 (3 H, m, Ar C*H*), 5.21-5.14 (2H, m, O CH_2), 5.21-5.01 (4 H, m, O CH_2), 4.96-4.85 (1 H, m, C*H*), 4.54 (1 H, t, J = 7.5, C*H*), 3.76-3.64 (1 H, m, CH_2), 3.57 (1 H, dq, J = 10.5, 7.0, CH_2), 2.42 (3H, d, J = 9.0, CH_3), 2.34-2.26 (2H, m, CH_2); ^{13}C NMR (125MHz, $CDCl_3$) δ 167.8 (*C*=O), 167.6 (*C*=O), 154.5 (Ar *C*), 153.8 (Ar *C*), 145.3 (Ar *C*), 145.2 (Ar *C*), 136.2 (Ar *C*H), 136.0 (Ar *C*H), 135.1 (Ar *C*H), 133.1 (Ar *C*H), 133.0 (Ar *C*H), 129.9 (Ar *C*H), 128.5 (Ar *C*H), 128.4 (Ar *C*H), 128.3 (Ar *C*H), 128.3 (Ar *C*H), 128.2 (Ar *C*H), 128.1 (Ar *C*H), 128.0 (Ar *C*H), 127.8 (Ar *C*H), 78.7 (*C*H), 78.0 (O*C*H_2),

67.4 (O*C*H$_2$), 61.8 (*C*H), 44.0 (*C*H$_2$), 30.1 (*C*H$_2$), 21.4 (C*H*$_3$); MS (ESI$^+$) m/z 532 ([M+Na]$^+$, 100%); HRMS calcd. for $C_{27}H_{27}NNaO_7S$ [M+Na]$^+$ 532.1400; Found 532.1417.

(2S,3S)- dibenzyl 3-azidopyrrolidine-1,2-dicarboxylate A4

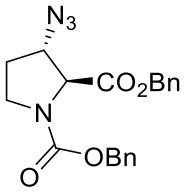

To a solution of above (1.10 g, 2.16 mmol) in DMF (6 mL), sodium azide (0.56 g, 8.64 mmol) was added and the mixture was heated at 61 ºC for 18 h. The mixture was diluted with EtOAc and was washed with water, the organic layer was dried over $MgSO_4$ and concentrated *in vacuo*. Chromatography (hexane/EtOAc 1:9 to 2:8) gave compound **A4** (0.68 g, 83 %) as oil. R_f = 0.86. $[\alpha]_D$= 24.3 (c= 6.07 x 10^{-3}, CH_2Cl_2). IR (neat) ν/cm^{-1} 3081 (NH), 2106 (N_3), 1735 (BnOC=O), 1705 (HNC=O); ^{1}H NMR (500 MHz; $CDCl_3$) δ 7.37-7.24 (10H, m, Ar C*H*), 5.26-5.04 (4H, m, O C*H*$_2$), 4.42 (1H, d, *J*= 57.0, C*H*), 4.19-4.17 (1H, m, C*H*), 3.75-3.57 (2H, m, C*H*$_2$), 2.20-2.00 (2H, m, C*H*$_2$); ^{13}C NMR (125MHz, $CDCl_3$) δ 169.9 (*C*=O), 169.7 (*C*=O), 154.8 (Ar *C*), 154.1 (Ar *C*H), 128.7 (Ar *C*H), 128.6 (Ar *C*H), 128.5 (Ar *C*H), 128.4 (Ar *C*H), 128.3 (Ar *C*H), 128.2 (Ar *C*H), 128.1 (Ar *C*H), 128.1 (Ar *C*H), 127.9 (Ar *C*H), 120.5 (Ar *C*H), 67.7 (*C*H), 67.3 (O*C*H$_2$), 64.7 (O*C*H$_2$), 63.4 (*C*H), 44.4 (*C*H$_2$), 30.1 (*C*H$_2$); MS (ESI$^+$) m/z 403 ([M+Na]$^+$, 100%); HRMS calcd. for $C_{20}H_{20}N_4NaO_4$ [M+Na]$^+$ 403.1377; Found 403.1373.

(2S,3S)- dibenzyl 3-aminopyrrolidine-1,2-dicarboxylate A5

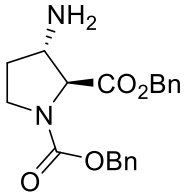

A solution of **A4** (0.68 g, 1.79 mmol) with triphenylphosphine (0.94 g, 3.58 mmol) in THF (8 mL) was refluxed for 3 h before water (130 μL, 7.15 mmol) was added. After 6 h water (130 μL, 7.15 mmol) and refluxed for 14 h. The solvent was removed and the crude diluted in

Et_2O and was washed with 0.1 M HCl. The aqueous layer was neutralized with 10 % Na_2CO_3 and washed with CH_2Cl_2, the organic layer was dried over $MgSO_4$ and concentrated *in vacuo*. Chromatography (EtOAc/MeOH 10:1 to 8:2) gave compound **A5** (0.30 g, 47 %) as yellow oil. R_f = 0.33. $[\alpha]_D$= -10.0 (c= 0.41 x 10^{-3}, CH_2Cl_2). IR (neat) ν/cm^{-1} 2954 (d. NH_2), 1743 (BnOC=O), 1700 (HNC=O); ^{1}H NMR (500 MHz; $CDCl_3$) δ 7.46-7.17 (10 H, m, Ar C*H*), 5.30-5.15 (2 H, m, O CH_2), 5.14-5.01 (2 H, m, O CH_2), 4.20-4.04 (1 H, m, C*H*), 3.81-3.70 (1 H, m, C*H*), 3.67-3.58 (2 H, m, CH_2), 2.27-1.65 (2 H, m, CH_2); ^{13}C NMR (125MHz, $CDCl_3$) δ 171.3 (*C*=O), 171.1 (*C*=O), 155.0 (Ar C), 154.4 (Ar C), 135.4 (Ar C*H*), 128.6 (Ar C*H*), 128.4 (Ar C*H*), 128.4 (Ar C*H*), 128.3 (Ar C*H*), 128.1 (Ar C*H*), 128.1 (Ar C*H*), 128.0 (Ar C*H*), 127.9 (Ar C*H*), 127.8 (Ar C*H*), 68.2 (*C*H), 67.0 (O*C*H_2), 66.8 (O*C*H_2), 55.8 (*C*H), 44.7 (*C*H_2), 32.6 (*C*H_2); MS (ESI^+) m/z 355 ($[M+H]^+$, 100%); HRMS calcd. for $C_{20}H_{23}N_2O_4$ $[M+Na]^+$ 355.1652; Found 355.1639.

(2*S*,3*S*)-dibenzyl 3-{[*tert*-butoxy(oxo)acetyl]amino}pyrrolidine-1,2-dicarboxylate A6

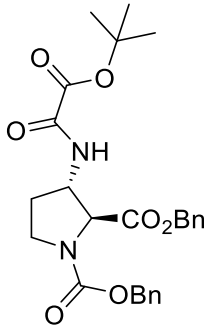

To a solution of **A5** (0.30 g, 0.85 mmol) with triethylamine (0.30 mL, 2.12 mmol) in CH_2Cl_2 (10 mL), tertbotoxy oxalyl chloride (0.17 g, 1.02 mmol) was added dropwise at room temperature under N_2. After 20 h the mixture was washed with water the organic layer was dried over $MgSO_4$ and concentrated *in vacuo*. Chromatography (C_6H_{12}/EtOAc 9:1 to 5:5) gave compound **A6** (0.42 g, 90 %) as colourless oil. R_f = 0.22. $[\alpha]_D$= 2.53 (c= 1.01 x 10^{-3}, CH_2Cl_2). IR (neat) ν/cm^{-1} 3350 (NH), 1749 (MeOC=O), 1678 (HNC=O); ^{1}H NMR (500 MHz; $CDCl_3$) δ 7.51-7.74 (1 H, m, N*H*) 7.32 (6 H, m, Ar C*H*), 7.22 (4 H, m, Ar C*H*), 5.15 (2 H, d, *J* = 16.0, O CH_2), 4.92-5.09 (2 H, m, O CH_2) 4.55 (1 H, br. s., C*H*), 4.48-4.24 (1 H, m, C*H*), 3.76-3.51 (2 H, m, CH_2), 2.30-1.82 (3 H, m, CH_2), 1.60-1.41 (9 H, m, C(CH_3)$_3$); ^{13}C

NMR (125MHz, $CDCl_3$) δ 170.1 (*C*=O), 169.8 (*C*=O), 159.0 (*C*=O), 157.0 (*C*=O), 154.5 (Ar C), 153.9 (Ar C), 136.0 (Ar CH), 135.8 (Ar CH), 134.9 (Ar C*H*), 128.3 (Ar C*H*), 128.2 (Ar C*H*), 128.1 (Ar C*H*), 128.0 (Ar C*H*), 127.8 (Ar C*H*), 127.6 (Ar C*H*), 127.5 (Ar C*H*), 84.5 ($C(CH_3)_3$)), 67.1 (O CH_2), 64.3 (O CH_2), 64.0 (*C*H), 54.1 (s), 53.1 (*C*H), 44.7 (s), 44.2 (CH_2), 30.1 (s), 29.2 (CH_2), 27.4 ($C(CH_3)_3$); HRMS calcd. for $C_{26}H_{30}N_2NaO_7$ $[M+Na]^+$ 505.1945; Found 505.1942.

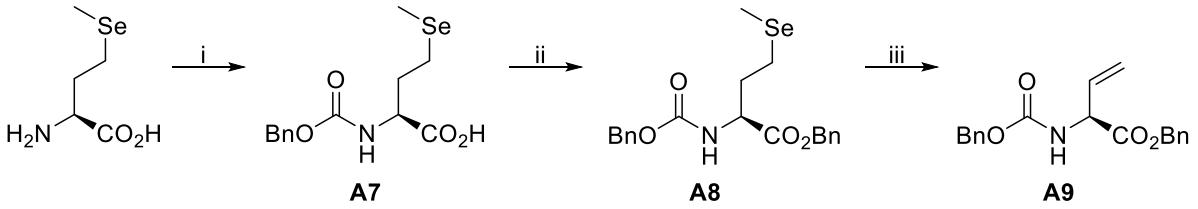

Scheme A. 2 *Synthesis of L-vinyl glycine.*

Reagents and Conditions: i) benzyl chloroformate, sat. $NaHCO_3$, THF, r.t; ii) BBDI, benzyl alcohol, Boc_2O, CH_2Cl_2; iii) H2O2, py, CH_2Cl_2, reflux.

(*S*)- *N*-[(benzyloxy)carbonyl]selenomethionine A7

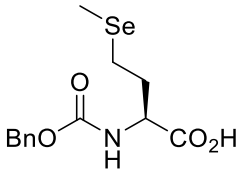

To a stirred suspension of L-selenomethionine (2.50 g, 12.75 mmol) in 1M $NaHCO_3$/THF 20:1 (55 mL), benzyl chloroformate (2.0 mL, 14.02 mmol) was added dropwise over 10 min at 0 ºC and the reaction mixture was warmed to room temperature. After 6 h the mixture was washed with Et_2O and then was acidified with 3 M HCl and washed with EtOAc. The solvent was removed *in vacuo* to afford compound (3.6 g, 85 %) as yellow oil. $[\alpha]_D$= -2.0 (c= 1.36 x 10^{-3}, MeOH). IR (neat) ν/cm^{-1} 2928 (NH), 1710 (HOC=O); ^{1}H NMR (400 MHz; DMSO-d_6) δ 8.43 (1H, b, COO*H*), 7.37-7.29 (5H, m, Ar C*H*), 5.60 (1H, m, Ar C*H*), 5.16-5.08 (2H, m, OCH_2), 4.52-4.43 (1H, m, OCH_2), 2.58-2.55 (2H, m, CH_2), 2.27-2.01 (2H, m, CH_2), 1.98 (3H, s, CH_3); ^{13}C NMR (101MHz, DMSO-d_6) δ 175.5 (*C*=O), 163.6 (*C*=O), 156.2 (Ar C), 136.1 (Ar C*H*), 128.5 (Ar C*H*), 128.2 (Ar C*H*), 128.1 (Ar C*H*), 128.0 (Ar C*H*), 67.2 (CH_2),

53.9 (O*C*H_2), 32.9 (*C*H_2), 20.4 (*C*H_3); MS (ESI^-) m/z 330 ($[M-H]^-$, 100%); HRMS calcd. for $C_{13}H_{16}NO_4Se$ $[M-H]^-$ 330.0250; Found 330.0239.

(*S*)- benzyl *N*-[(benzyloxy)carbonyl]selenomethioninate A8

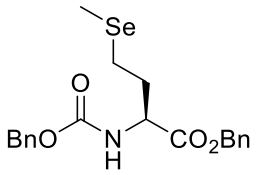

To a solution of above (3.5 g, 10.51 mmol) in CH_2Cl_2 (50mL) Boc_2O (2.75 mL, 12.62 mmol), BBDI (0.48 g, 1.58 mmol) were added and stirred for 15 min before benzyl alcohol (1.3 mL, 12.62 mmol) was added and left to stir for 1 d until consumption of starting material. The mixture was washed with water, the organic layer was dried over $MgSO_4$ and concentrated *in vacuo* to give compound **A8** (4.64 g, quantitative) as yellow oil. $[\alpha]_D$= -0.9 (c= 1.36 x 10^{-3}, MeOH). IR (neat) ν/cm^{-1} 2929 (NH), 1714 (BnOC=O), 1659 (HNC=O); ^{1}H NMR (500 MHz; $CDCl_3$) δ 7.40-7.29 (10H, m, Ar C*H*), 5.50 (1H, b, N*H*), 5.25-5.14 (2H, m, OCH_2), 5.12 (2H, s, OCH_2), 4.59-4.54 (1H, m, C*H*), 2.55-2.45 (2H, m, CH_2), 2.27-2.02 (2H, m, CH_2), 1.95 (3H, s, CH_3); ^{13}C NMR (125MHz, $CDCl_3$) δ 155.9 (*C*=O), 146.8 (*C*=O), 141.0 (Ar C), 136.2 (Ar C*H*), 135.2 (Ar C), 128.7 (Ar C*H*), 128.6 (Ar C*H*), 128.6 (Ar C*H*), 128.4 (Ar C*H*), 128.3 (Ar C*H*), 128.2 (Ar C*H*), 127.6 (Ar C*H*), 127.0 (Ar C*H*), 85.2 (O*C*H_2), 67.4 (O*C*H_2), 67.1 (*C*H), 54.1 (*C*H_2), 33.1 (*C*H_2), 27.4 (*C*H_3); MS (ESI^+) m/z 444.1 ($[M+Na]^+$, 40%); HRMS calcd. for $C_{20}H_{23}NNaO_4Se$ $[M+Na]^+$ 444.0685; Found 444.0690.

(*S*)-benzyl 2-{[(benzyloxy)carbonyl]amino}but-3-enoate A9

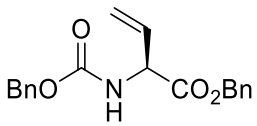

To a solution of **A8** (1.56 g, 3.70 mmol) in CH_2Cl_2 (130 mL), 30% hydrogen peroxide (9.5 mL, 92.20 mmol) and pyridine (9.5 mL, 117.70 mmol) were added and refluxed for 1 d until consumption of starting material. The mixture was washed with water, sat. $CuSO_4$, 2 M HCl and sat. $NaHCO_3$, the organic layer was dried over $MgSO_4$ and concentrated *in vacuo*. Chromatography (hexane/EtOAc 85:15 to 6:4) gave compound **A9** (1.00 g, 78 %) as white

solid, mp 61-64 ^{o}C. R_f= 0.60. $[\alpha]_D$= -3.4 (c= 5.9 x 10^{-3}, CH_2Cl_2). IR (neat) ν/cm^{-1} 3329 (NH), 2980 (br, COO-H) 1721 (BnOC=O); ^{1}H NMR (500 MHz; $CDCl_3$) δ 7.39-7.34 (10H, m, Ar C*H*), 5.97-5.90 (1H, m, CH_2=C*H*), 5.52 (1H, b, N*H*), 5.37 (1H, dd, *J*= 5.0 , HC=CH_2), 5.37 (1H, dd, *J*= 5.0, HC=CH_2), 5.21-5.11 (4H, m, OCH_2), 5.01 (1H, appt t, *J*= 5.5, C*H*); ^{13}C NMR (125MHz, $CDCl_3$) δ 171.7 (*C*=O), 170.3 (*C*=O), 155.6 (Ar *C*), 153.5 (Ar C*H*), 136.1 (Ar *C*), 135.6 (Ar C*H*), 135.1 (Ar C*H*), 132.2 (Ar C*H*), 128.7 (Ar C*H*), 128.6 (Ar C*H*), 128.5 (Ar C*H*), 128.4 (Ar C*H*), 128.3 (Ar C*H*), 117.8 (H*C*=CH_2), 82.3 (HC=*C*H_2), 68.7 (O*C*H_2), 67.1 (O*C*H_2), 56.2 (*C*H_2); MS (ESI^+) m/z 348 ($[M+Na]^+$, 100%); HRMS calcd. for $C_{19}H_{19}NNaO_4$ $[M+Na]^+$ 348.1206; Found 348.1216.